Report No. FHWA-RD-76-20

PB259237

DEVELOPMENT AND TESTING OF INCIDENT DETECTION ALGORITHMS

Vol. 2. Research Methodology and Detailed Results

H. J. Payne, E. D. Helfenbein and H. C. Knobel

April 1976

Final Report

This document is available to the public through the National Technical Information Service, Springfield, Virginia 22161

REPRODUCED BY
U.S. DEPARTMENT OF COMMERCE
NATIONAL TECHNICAL
INFORMATION SERVICE
SPRINGFIELD, VA 22161

Prepared for

FEDERAL HIGHWAY ADMINISTRATION

Offices of Research & Development

Washington, D.C. 20590

NOTICE

This document is disseminated under the sponsorship of the Department of Transportation in the interest of information exchange. The United States Government assumes no liability for its contents or use thereof.

The contents of this report reflect the views of the contracting organization, which is responsible for the facts and the accuracy of the data presented herein. The contents do not necessarily reflect the official views or policy of the Department of Transportation. This report does not constitute a standard, specification, or regulation.

The United States Government does not endorse products or manufacturers. Trade or manufacturers' names appear herein only because they are considered essential to the object of this document.

FHWA DISTRIBUTION NOTICE

This report is being distributed by FHWA memorandum to interested researchers. A limited number of additional copies are available upon request from the Systems Requirements and Evaluation Group of the Traffic Systems Division, Office of Research.

Technical Report Documentation Page

1. Report No. FHWA-RD-76-20	2. Government Accession No.	3. Recipient's Catalog No.
4. Title and Subtitle: Development and Testing of Incident Detection Algorithms, Volume 2: Research Methodology and Detailed Results		5. Report Date: April 1976
		6. Performing Organization Code
7. Author(s): H. J. Payne, E. D. Helfenbein and H. C. Knobel		8. Performing Organization Report No.
9. Performing Organization Name and Address: Technology Service Corporation, 2811 Wilshire Boulevard, Santa Monica, California 90403		10. Work Unit No. (TRAIS): 31C3-502
		11. Contract or Grant No.: DOT-FH-11-8278
12. Sponsoring Agency Name and Address: Offices of Research and Development, Federal Highway Administration, U.S. Department of Transportation, Washington, D.C. 20590		13. Type of Report and Period Covered: Final Report, Jan 1974 - Feb 1976
		14. Sponsoring Agency Code: T-0165

15. Supplementary Notes

FHWA Contract Manager: S. C. Tignor (HRS-33)

16. Abstract

The development and testing of incident detection algorithms was based on Los Angeles and Minneapolis freeway surveillance data. Algorithms considered were based on times series and pattern recognition techniques. Attention was given to the effects of geometrics, sensor configuration and weather, and methods were developed for detecting malfunctioning sensors and for identifying the lane of an incident.

The second volume describes the methodology used for evaluating and calibrating incident detection algorithms, the specific time series techniques examined (exponential smoothing and traffic correlation) and the decision tree structure for algorithms. Detailed results and discussions pertaining to all aspects of this study are presented here.

This volume is the second of four. The others are:

Vol. No.	FHWA No.	Title
1	RD-76-19	Summary of Results
3	RD-76-21	User Guidelines
4	RD-76-22	Program Documentation for Evaluation, Calbration and Implementation

17. Key Words: Incident detection, freeway surveillance	18. Distribution Statement: Unlimited

19. Security Classif. (of this report): Unclassified	20. Security Classif. (of this page): Unclassified	21. No. of Pages	22. Price

Form DOT F 1700.7 (8-72) Reproduction of completed page authorized

TABLE OF CONTENTS

Section		Page
	LIST OF FIGURES	v
	LIST OF TABLES	xi
	ACKNOWLEDGEMENTS	xix
	OVERVIEW	xx
1.	INTRODUCTION	1
2.	PATTERNS IN TRAFFIC DATA	13
	2.1 INCIDENT PATTERNS	14
	2.2 PATTERNS IN INCIDENT-FREE TRAFFIC THAT TEND TO PRODUCE FALSE ALARMS	15
	2.3 CONSEQUENCES FOR ALGORITHM DEVELOPMENT	15
3.	STRUCTURES FOR INCIDENT DETECTION ALGORITHMS	23
	3.1 FEATURES	23
	3.1.1 Simple Features	23
	3.1.2 Time-Series Features	24
	3.1.2.1 Double Exponential Smoothing	27
	3.1.2.2 Traffic Stream Correlation	28
	3.2 BINARY DECISION TREES	31
	3.2.1 Binary Decision Trees without States	31
	3.2.2 Binary Decision Trees with States	36
	3.2.3 Validity Checks for Coding Algorithms	37
4.	EVALUATION CRITERIA AND CALIBRATION METHODOLOGY	41
	4.1 EVALUATION CRITERIA	41
	4.2 THRESHOLD CALIBRATION METHODOLOGY	45
	4.3 EVALUATION AND CALIBRATION SOFTWARE AND RELATED DATA REQUIREMENTS	51
	4.3.1 Evaluation and Calibration Software	51
	4.3.2 Data Requirements	51
	4.4 PAIRWISE COMPARISON OF ALGORITHMS	55
	4.5 DEPENDENCE OF PERFORMANCE MEASURES ON THE DATA BASE	58

TABLE OF CONTENTS (Continued)

Section		Page
5.	BASIC ALGORITHM DEVELOPMENT WITH THE LOS ANGELES DATA BASE	59
5.1	GENERAL ANALYSIS PROCEDURE	59
5.1.1	The Los Angeles Data Base	59
5.1.2	Coding the Algorithm	67
5.1.3	Culling the Data	67
5.1.4	Calibration	69
5.1.5	Evaluation	69
5.1.6	Time-to-Detect Statistics	69
5.2	THE CALIFORNIA ALGORITHM AND SIMPLE VARIANTS	73
5.3	ALGORITHMS WITH A PERSISTENCE REQUIREMENT	78
5.4	AN ALGORITHM THAT SUPPRESSES COMPRESSION WAVES	82
5.5	AN ALGORITHM BASED ON A SPEED FEATURE	90
5.6	COMPARISONS OF THE ALGORITHMS	90
6.	FURTHER ALGORITHM DEVELOPMENT AND EVALUATION WITH THE LOS ANGELES DATA BASE	99
6.1	EFFECTS OF GEOMETRICS	99
6.1.1	Geometric Anomalies in the Los Angeles System	99
6.1.2	Adjusting Features for Geometric Anomalies	101
6.2	EFFECTS OF SENSOR CONFIGURATION	104
6.2.1	Sensor Configurations	107
6.2.2	Data Bases	107
6.2.3	Algorithm Performance	107
6.3	FREQUENCY OF ALGORITHM EXECUTION	116
6.4	ALGORITHMS FOR LANE CLASSIFICATION OF FREEWAY INCIDENTS	118
6.4.1	The Evaluation Data Base	119
6.4.2	Algorithms Employing Upstream Station Data	120
6.4.3	Algorithms Employing Downstream Station Data	120
6.4.4	An Algorithm Employing Both Upstream and Downstream Data	128
6.4.5	Testing the Algorithm	132
6.4.6	Interpretation and Accuracy of the Performance Evaluation	139
6.4.7	Practical Evaluation and Recommendations	139

TABLE OF CONTENTS (Continued)

Section		Page
6.5	SENSOR MALFUNCTION DETECTION ALGORITHMS	140
6.5.1	Types of Malfunctions	140
6.5.2	Types of malfunction detection algorithms	152
6.5.2.1	Single-sensor algorithms . .	152
6.5.2.2	Neighbor comparison malfunction algorithms	156
7.	EVALUATION WITH THE MINNEAPOLIS DATA BASE	163
7.1	THE MINNEAPOLIS DATA BASE	163
7.2	ALGORITHM EVALUATIONS	163
7.3	EFFECTS OF WEATHER	172
8.	RECOMMENDATIONS FOR FURTHER RESEARCH	177
APPENDICES		
A.	TRAFFIC STREAM CORRELATION	181
B.	ALGORITHM DEFINITIONS, CALIBRATION AND EVALUATION RESULTS	203
C.	TESTING STATISTICAL SIGNIFICANCE OF DIFFERENCES IN FALSE ALARMS	293

LIST OF FIGURES

Figure		Page
1.	The California algorithm for incident detection	5
2.	The California algorithm with a test for termination	7
3.	A refined California algorithm with a persistence requirement	9
4.	Schematic of the geometry at a freeway-to-freeway interchange in Los Angeles--San Diego freeway northbound to the Santa Monica freeway	18
5.	Lane sensor notation	25
6.	The wave speed in a traffic stream	29
7.	Elementary building block of a binary decision tree	32
8.	The California algorithm considered as a binary decision tree	33
9.	Coding the California algorithm as a binary decision tree	35
10.	Coding of a version of the California algorithm as a binary decision tree with a state	38
11.	Cumulative distribution of detection rate versus time to detect for the California algorithm (figure 8)	46
12.	Detection rate and false alarm rate pairs for an incident detection algorithm	48
13.	Performance pairs for Algorithm 7	49
14.	Decision tree for Algorithn 7	50
15.	Structure of calibration program	52
16.	Significance of pairwise differences in false alarm rates, N_F = 45,000	56
17.	Significance of pairwise differences in false alarm rates, N_F = 100,000	57

LIST OF FIGURES (Continued)

Figure		Page
18.	Los Angeles data collection site	60
19.	Decision tree used to cull data for calibration	68
20.	Decision tree for Algorithm 1	74
21.	Decision tree for Algorithm 2	75
22.	Decision tree for Algorithm 3	76
23.	Decision tree for Algorithm 4	77
24.	Comparison of performance of Algorithms 2, 3, and 4	80
25.	Decision tree for Algorithm 5	81
26.	Decision tree for Algorithm 6	83
27.	Decision tree for Algorithm 7	84
28.	Comparison of performance of Algorithms 5, 6, and 7	85
29.	Test for presence of a compression wave	86
30.	Decision tree for Algorithm 8	87
31	Comparison of performance for Algorithms 8 and 9	89
32.	Decision tree for Algorithm 10	91
33.	Comparison of performance of Algorithms 2, 9, and 11	94
34.	Comparison of performance of Algorithms 2, 7, and 8, (based on full Los Angeles data base)	96
35.	Scattergram of station 31 occupancy versus station 32 occupancy, San Diego freeway northbound, Los Angeles data base	102
36.	Comparison of performance for Algorithm 7, with and without geometric adjustments	106
37.	Sensor configuration A	108
38.	Sensor configuration B	109

LIST OF FIGURES (Continued)

Figure		Page
39.	Sensor configuration C	110
40.	Comparison of performance of Algorithm 2 for three sensor configurations	112
41.	Comparison of performance of Algorithm 7 for three sensor configurations	113
42.	Comparison of performance of Algorithm 8 for three sensor configurations	114
43.	Comparison of performance of Algorithm 7 recalibrated for three sensor configurations	115
44.	Algorithm 7 modified for testing at 20-second intervals	117
45.	An algorithm employing upstream and downstream occupancy data for lane identification of an incident	133
46.	Preliminary data processor to detect stuck ON or OFF sensors without affecting incident detection	149
47.	Caltrans malfunction routine	153
48.	Chicago malfunction routine	155
49.	Single-sensor malfunction algorithm	157
50.	Decision tree and coding for single-sensor malfunction algorithm	158
51.	A mean comparison malfunction algorithm for detection of intermittent operation and hanging on	162
52.	Minneapolis data collection site	164
53.	Comparison of performance of Algorithm 2 on Los Angeles and Minneapolis data base	169
54.	Comparison of performance of Algorithm 7 on Los Angeles and Minneapolis data bases	170
55.	Comparison of performance of Algorithm 8 on Los Angeles and Minneapolis data bases	171

LIST OF FIGURES (Continued)

Figure		Page
56.	Comparison of performance of Algorithm 7 on Minneapolis clear weather data base	174
57.	Comparison of performance of Algorithm 7 on Minneapolis snowy weather data base	175
58.	Suggested refinement to Algorithm 7	178
59.	Decision tree for Algorithm 1	207
60.	Distribution of times-to-detect for Algorithm 1 Los Angeles data base	210
61.	Decision tree for Algorithm 2	211
62.	Distribution of times-to-detect for Algorithm 2, Los Angeles data base	215
63.	Distribution of times-to-detect for Algorithm 2, Minneapolis data base	220
64.	Decision tree for Algorithm 3	222
65.	Distribution of times-to-detect for Algorithm 3, Los Angeles data base	225
66.	Decision tree for Algorithm 4	226
67.	Distribution of times-to-detect for Algorithm 4, Los Angeles data base	229
68.	Distribution of times-to-detect for Algorithm 4, geometrically adjusted Los Angeles data base	231
69.	Decision tree for Algorithm 5	232
70.	Distribution of times-to-detect for Algorithm 5, Los Angeles data base	235
71.	Decision tree for Algorithm 6	236
72.	Distribution of times-to-detect for Algorithm 6, Los Angeles data base	239
73.	Decision tree for Algorithm 7	240

LIST OF FIGURES (Continued)

Figure		Page
74.	Decision tree for twenty-second update version of Algorithm 7	242
75.	Distribution of times-to-detect for Algorithm 7, Los Angeles data	245
76.	Distribution of times-to-detect for Algorithm 7, geometrically adjusted to Los Angeles data base	250
77.	Distribution of times-to-detect for Algorithm 7, Los Angeles, sensor configuration A data base	252
78.	Distribution of times-to-detect for Algorithm 7, Los Angeles, sensor configuration B data base	254
79.	Distribution of times-to-detect for Algorithm 7, Los Angeles, sensor configuration C data base	256
80.	Distribution of times-to-detect for Algorithm 7, Minneapolis data base	258
81.	Distribution of times-to-detect for Algorithm 7, Minneapolis clear weather data base	261
82.	Distribution of times-to-detect for Algorithm 7, Minneapolis snowy weather data base	263
83.	Decision tree for Algorithm 8	264
84.	Decision tree for an equivalent form of Algorithm 8	267
85.	Distribution of times-to-detect for Algorithm 8, Los Angeles data base	270
86.	Distribution of times-to-detect for Algorithm 8, Los Angeles data base (T_2= -.300)	275
87.	Distribution of times-to-detect for Algorithm 8, geometrically adjusted Los Angeles data base	277
88.	Distribution of times-to-detect for Algorithm 8, Minneapolis data base	279

LIST OF FIGURES (Continued)

Figure		Page
89.	Decision tree for Algorithm 9	281
90.	Distribution of times-to-detect for Algorithm 9, Los Angeles data base	285
91.	Distribution of times-to-detect for Algorithm 9, geometrically adjusted Los Angeles data base	287
92.	Decision tree for Algorithm 10	288
93.	Distribution of times-to-detect for Algorithm 10, Los Angeles data base	291

LIST OF TABLES

Table		Page
1.	Occupancy values for incident data set 74051501 Santa Monica eastbound	2
2.	Occupancy values for incident-free data set 74090454, San Diego southbound	3
3.	Occupancy data for incident data set 74032203, Santa Monica eastbound	16
4.	Occupancy data for incident data set 74032901, Santa Monica westbound	17
5.	Occupancy data for incident-free data set 74042368, San Diego northbound	19
6.	Occupancy data for incident-free data set 74090463, Santa Monica eastbound	20
7.	Definitions of simple features	26
8.	State values produced by the California algorithm for the incident free data set 74090454	43
9.	State values produced by the California algorithm for the incident data set 74051501, Santa Monica eastbound	44
10.	Parameters for confidence limits	53
11.	95% confidence limits for false alarm rates	54
12.	95% confidence limits for detection rates	54
13.	Incident data sets in the Los Angeles data base	61
14.	Incident data set characteristics definitions	65
15.	Incident-free data sets in the Los Angeles data base	66
16.	Input data for the program CALB	70
17.	Sample calibration output from the program CALB	71
18.	Sample case labels produced by the program CALB	72

LIST OF TABLES (continued)

Table		Page
19.	Partial label printout of Algorithm 2, T_1 = 4.99, T_2 = .563, T_3 = .013	79
20.	Noninferior algorithms	92
21.	Calibration results for Algorithm 11	95
22.	Characteristics of the ten new incident detection algorithms	97
23.	A partial listing of false alarms for Algorithm 7, T_1=8.1, T_2=.313, T_3=16.81	100
24.	Slopes obtained from regressing upstream occupancy against downstream occupancy	103
25.	A partial listing of false alarms for algorithm 7, T_1-8.1, T_2=.313, T_3=16.8, using normalized features	105
26.	Occupancy dominance, lane 3	121
27.	Volume dominance, lane 1	122
28.	Speed dominance, lane 4	123
29.	No volume dominance	124
30.	OCC at upstream station, one-minute interval following alarm	125
31.	OCC at upstream station, two-minute interval following alarm	125
32.	OCC at upstream station, five-minute interval following alarm	125
33.	SPD at upstream station, one-minute interval following alarm	126
34.	SPD at upstream station, two-minute interval following alarm	126
35.	SPD at upstream station, five-minute interval following alarm	126

LIST OF TABLES (Continued)

Table		Page
36.	OCC at downstream station, two-minute interval following alarm	127
37.	Sudden drop in downstream lane occupancy	129
38.	Sudden drop to zero of downstream lane occupancy	130
39.	Sudden rise in upstream lane occupancy	131
40.	OCC at downstream (threshold = 0.0), one-minute interval before alarm--overall performance	134
41.	OCC at downstream station (threshold = 0.0), one-minute interval before alarm--cases where data existed for actual lane	134
42.	OCC at downstream station (threshold = 0.0), one-minute interval before alarm--cases with no data for actual lane	134
43.	OCC at upstream or downstream station determined by deviation feature (threshold = .10), one minute interval before alarm--overall performance	135
44.	OCC at upstream or downstream station determined by deviation feature (threshold = .10), one-minute interval before alarm--cases where data existed for actual lane	135
45.	OCC at upstream or downstream station determined by deviation feature (threshold = .10), one-minute interval before alarm--overall performance	135
46.	OCC at upstream and downstream station determined by deviation feature (threshold = .15), one-minute interval before alarm--overall performance	136
47.	OCC at upstream and downstream station determined by deviation feature (threshold = .15), one-minute interval before alarm--cases where data existed for actual lane	136

LIST OF TABLES (Continued)

Table		Page
48.	OCC at upstream and downstream station determined by deviation feature (threshold = .15), one-minute interval before alarm--cases with no data for actual lane	136
49.	OCC at upstream and downstream station determined by deviation feature (threshold = .20), one-minute interval before alarm--overall performance .	137
50.	OCC at upstream and downstream station determined by deviation feature (threshold = .20), one-minute interval before alarm--cases where data existed for actual lane	137
51.	OCC at upstream and downstream station determined by deviation feature (threshold = .20), one-minute interval before alarm--cases with no data for actual lane	137
52.	OCC at upstream station (threshold = 1.00), one-minute interval before alarm--overall performance	138
53.	Zero occupancies due to an incident at 6:12, sta 27, lane 4	141
54.	Ninety-nine percent occupancies due to an incident at 8:36, sta 19, lane 1	142
55.	Scan data from a chattering sensor, lane 4	143
56.	Five-minute OCC map of chattering sensor (sta 18, lane 4) and intermittent hanging on (sta 14, lane 1) .	144
57.	Five-minute VOL map of chattering sensor (sta 18, lane 4) and hanging on (sta 14, lane 1)	145
58.	Five-minute SPD map of chattering sensor (sta 18, lane 4) and hanging on (sta 14, lane 1)	146
59.	Scan data from sensor hanging on (lane 1).	148
60.	Scan data of intermittent hanging <u>on</u> (lane 1)	151
61.	Erratic 20-second OCC's from intermittent hanging on (lane 1)	159

LIST OF TABLES (Continued)

Table		Page
62.	Feature computation	161
63.	Minneapolis station labeling	165
64.	Upstream-downstream pointers for Minneapolis stations	166
65.	Incident-free data sets in the Minneapolis data base	167
66.	Incident data sets in the Minneapolis data base	168
67.	Single Exponential Smoothing, Data Set 74042354, Santa Monica Westbound, Station 9, Lane 2, Twenty-Second Occupancy	192
68.	Double Exponential Smoothing, Data Set 74042354, Santa Monica Westbound, Station 9, Lane 2, Twenty-Second Occupancy	193
69.	Upstream-to-Downstream Correlation with Single Exponential Smoothing, Data Set 74042354, Santa Monica Westbound, Station 10 (Upstream), Station 9 (Downstream), Lane 2, Twenty-Second Occupancy	194
70.	Upstream-to-Downstream Correlation with Double Exponential Smoothing, Data Set 74042354, Santa Monica Westbound, Station 10 (Upstream), Station 9 (Downstream), Lane 2, Twenty-Second Occupancy	195
71.	One-minute occupancy map, data set 74090454, San Diego southbound	197
72.	Single-Exponential Smoothing, Data Set 74090454, San Diego Northbound, Station 30, All Lanes, One-Minute Occupancy	198
73.	Downstream-to-Upstream Correlation with Single Exponential Smoothing, Data Set 74090454, San Diego Southbound, Station 30 (Upstream), Station 29 (Downstream), All Lanes, One-Minute Occupancy	199
74.	Operation Count for Elements of the Correlation Feature Computation	200

LIST OF TABLES (Continued)

Table		Page
75.	Storage Requirements for the Correlation Feature . .	201
76.	Coding for Algorithm 1	208
77.	Calibration and evaluation of Algorithm 1 on Los Angeles data base	209
78.	Coding for Algorithm 2	212
79.	Evaluation of Algorithm 2 for thresholds determined for Algorithm 1 from Los Angeles data base (see Table 76)	213
80.	Calibration and evaluation of Algorithm 2 on Los ngeles data base	214
81.	Evaluation of Algorithm 2 for thresholds determined from Los Angeles data base (see Table 78)	216
82.	Calibration and evaluation of Algorithm 2 on Minneapolis data base	219
83.	Evaluation of Algorithm 2 for thresholds determined from Minneapolis data base (see Table 81).	221
84.	Coding for Algorithm 3	223
85.	Calibration and evaluation of Algorithm 3 on Los Angeles data base	224
86.	Coding for Algorithm 4	227
87.	Calibration and evaluation of Algorithm 4 on Los Angeles data base	228
88.	Calibration and evaluation of Algorithm 4 on geometrically adjusted Los Angeles data base	230
89.	Coding for Algorithm 5	233
90.	Calibration and evaluation of Algorithm 5 on Los Angeles data base	234

LIST OF TABLES (Continued)

Table		Page
91.	Coding for Algorithm 6	237
92.	Calibration and evaluation of Algorithm 6 on Los Angeles data base	238
93.	Coding for Algorithm 7	241
94.	Coding for twenty-second update version of Algorithm 7	243
95.	Calibration and evaluation of Algorithm 7 on Los Angeles data base	244
96.	Evaluation of Algorithm 7 for thresholds determined from Los Angeles data base (see Table 94)	246
97.	Calibration and evaluation of Algorithm 7 on geometrically adjusted Los Angeles data base	249
98.	Calibration and evaluation of Algorithm 7 on Los Angeles sensor configuration A data base	251
99.	Calibration and evaluation of Algorithm 7 on Los Angeles sensor configuration B data base	253
100.	Calibration and evaluation of Algorithm 7 on Los Angeles sensor configuration C data base	255
101.	Calibration and evaluation of Algorithm 7 on Minneapolis data base	257
102.	Evaluation of Algorithm 7 for thresholds determined from Minneapolis data base (see Table 100)	259
103.	Calibration and evaluation of Algorithm 7 on Minneapolis clear weather data base	260
104.	Calibration and evaluation of Algorithm 7 on Minneapolis snowy weather data base	262
105.	Coding for Algorithm 8	265
106.	Coding for alternative configuration of Algorithm 8	268

LIST OF TABLES (Continued)

Table		Page
107.	Calibration and evaluation of Algorithm 8 on Los Angeles data base	269
108.	Evaluation of Algorithm 8 for thresholds determined from Los Angeles data base (see Table 106)	271
109.	Calibration and evaluation of Algorithm 8 on Los Angeles data base (T_2 = -.300)	274
110.	Calibration and evaluation of Algorithm 8 on geometrically adjusted Los Angeles data base	276
111.	Calibration and evaluation of Algorithm 8 on Minneapolis data base	278
112.	Evaluation of Algorithm 8 for thresholds determined from Minneapolis data base (see Table 111)	280
113.	Coding for Algorithm 9	282
114.	Calibration and evaluation of Algorithm 9 on Los Angeles data base	284
115.	Calibration and evaluation of Algorithm 9 on geometrically adjusted Los Angeles data base	286
116.	Coding for Algorithm 10	289
117.	Calibration and evaluation of Algorithm 10 on Los Angeles data base	290

ACKNOWLEDGEMENTS

While the expression of the research results presented in this report was the work of the three authors, the following individuals also contributed to a significant degree in obtaining these results: Diane Goodwin, Wesley Lum and Michael Teener, members of the Technology Service Corporation technical staff and Leo Breiman, a consultant.

OVERVIEW

This is the final report pertaining to the research study "Development and Testing of Incident Detection Algorithms." This study entailed an empirical, data analytic approach based on data obtained from the Los Angeles and Minneapolis freeway surveillance systems. Results include new incident detection algorithms with significantly improved performance, algorithms for detecting malfunctioning sensors and an algorithm for detecting the lane location of an incident. This report is in four volumes, whose contents are briefly described as follows:

Volume 1: Summary of Results - This volume provides a brief discussion of the role and nature of electronic incident detection systems, and a summary of the research methodology and results obtained in this study.

Volume 2: Research Methodology and Detailed Results - This volume provides a thorough description of the methodological tools and a detailed discussion of analyses pertaining to algorithm development and testing. The binary decision tree structure is introduced as a basis for algorithms. An optimization procedure is identified for automating the calibration of algorithms. Ten incident detection algorithms are introduced and compared. Effects of geometrics, sensor configuration, and frequency of algorithm execution are addressed and corresponding modifications to algorithms are identified. These analyses were performed entirely on data taken from the Los Angeles system. Finally, comparative evaluations were performed using data from the Minneapolis system, including tests pertaining to snowy-weather. Additional study was made of malfunctioning sensors and the lane location of incidents.

Volume 3: User Guidelines - In this volume, the research results are used as a basis for developing guidelines to users for implementing the sensor malfunction, incident detection, and incident lane location algorithms. Procedures for calibration of algorithms, and for modifications pertaining to geometrics, sensor configuration and frequency of algorithm tests are described.

Volume 4: Program Documentation for Evaluation, Calibration and Implementation - This volume contains documentation for computer programs which are necessary for evaluation, calibration and implementation of the incident detection algorithms. These include NTREE and CTREE, needed for implementation. In addition, four routines pertaining to time series analyses are included. When using Volume 4, it is particulary helpful to also have Volume 3.

1. INTRODUCTION

This is the second of four volumes constituting the Final Report of the research study "Development and Testing of Incident Detection Algorithms," sponsored by the Federal Highway Administration.

The purpose of this research effort was to develop and evaluate computer algorithms which can, from surveillance data, detect the presence of traffic incidents, e.g., disabled vehicles in the travelled lanes. This volume delineates the methodology used in the research and provides details of the analyses which have led to recommended algorithms and practices.

The development of incident detection algorithms undertaken in this research effort is constrained by the nature of the data which are available for processing. While more detailed forms of the data were available for this study, the aggregated forms--occupancy and volume[1]--typically used in present freeway surveillance systems[2] have been found to provide a satisfactory basis for incident detection algorithms.

Certain incidents in the traffic stream generate patterns in surveillance data that differ from most patterns occurring in incident-free traffic. It is this difference in patterns that is exploited by the algorithms we have developed.

Consider the two patterns of occupancy data displayed in Tables 1 and 2. Both tables contain entries each of which is the average occupancy, expressed as a percentage, during the one-minute time interval ending at the time indicated. For example, in Table 1, 15 is the one-minute average occupancy of station 21 during the minute ending at 705. This table illustrates an incident; Table 2 illustrates heavy traffic conditions which are incident-free.

In Table 1, the pattern is seen to include a difference in occupancy values between stations 25 and 26 beginning at 718 which is considerably larger than differences observed elsewhere in the pattern. This feature or function of surveillance data has been found to be useful in incident detection algorithms. However, we have found no single feature which is, by itself, sufficient to define an algorithm with acceptable performance. In the case of the feature described above, incident-free, but heavy

---

[1] Definitions of these variables are provided in Section 2.

[2] H.J. Payne, D.N. Goodwin, and M.D. Teener, "Evaluation of Existing Incident Detection Algorithms," Report No. FHWA-RD-75-39, February 1975, prepared for the Federal Highway Administration (PB No. 241-883/AS).

Table 1. Occupancy values for incident data set 74051501, Santa Monica eastbound.[1]

Entries are one-minute occupancies. Incident occurred at 7:15:40 between stations 25 (upstream) and 26 (downstream).

Direction of Travel →

Time \ Stations	21	22	23	24	25	26	27
705	15	17	15	16	16	17	15
706	15	18	13	13	15	16	15
707	16	16	15	15	15	15	14
708	14	17	17	15	17	15	15
709	15	17	17	16	16	15	16
710	16	18	18	19	15	15	14
711	17	17	19	17	16	16	15
712	18	19	15	17	18	15	15
713	15	19	17	16	20	18	20
714	16	17	17	17	18	18	25
715	18	19	18	16	17	20	21
716	18	17	17	18	19	15	23
717	17	21	17	19	21	14	17
718	14	20	19	17	43	10	19
719	15	21	20	30	33	10	11
720	14	18	18	47	32	10	13
721	14	16	34	30	29	9	11
722	16	14	30	38	37	12	10
723	15	19	21	37	32	10	10
724	15	27	20	46	33	11	9
725	17	37	27	35	36	11	11
726	25	32	43	30	32	12	11
727	26	20	26	33	40	11	12
728	44	20	20	42	44	12	10
729	37	38	20	40	30	15	11
730	27	42	28	41	25	14	14
731	26	32	37	30	27	14	14
732	34	25	29	29	37	11	12
733	30	22	33	43	27	14	12
734	28	35	37	32	24	13	13
735	26	44	38	32	22	12	12
736	35	28	28	29	22	14	13
737	54	33	27	30	29	12	14
738	35	42	23	29	30	12	13
739	30	37	21	41	29	13	13
740	49	31	24	36	40	14	13

[1]Data sets are described in Sections 5 and 7.

Table 2. Occupancy values for incident-free data set 74090454, San Diego southbound.

Entries are one-minute occupancies.

Direction of Travel →

Time \ Stations	32	31	30	29	28	27	26
710	15	20	20	18	22	26	22
711	13	21	19	18	22	28	26
712	16	19	20	19	21	32	26
713	13	18	16	18	30	25	25
714	14	22	17	18	25	23	24
715	14	20	20	26	44	29	26
716	14	18	18	25	34	26	24
717	13	21	19	36	26	21	25
718	14	24	21	48	29	25	21
719	16	26	32	28	31	26	25
720	21	24	47	19	26	39	23
721	14	26	32	27	26	21	22
722	14	52	32	22	29	19	23
723	14	27	23	20	50	18	24
724	13	26	21	21	30	22	26
725	24	21	22	62	23	26	24
726	39	20	23	38	23	28	23
727	23	21	65	29	22	30	23
728	26	24	43	28	23	23	25
729	31	26	26	29	22	30	23
730	30	60	22	35	22	24	23
731	31	41	21	30	17	26	24
732	37	29	27	26	23	18	26
733	50	26	35	22	37	22	24
734	53	22	31	21	29	26	26
735	48	21	32	21	25	22	23
736	29	28	33	39	21	24	23
737	37	33	28	26	22	30	27
738	38	29	44	21	20	23	24
739	40	25	38	21	21	20	27
740	53	23	43	19	30	23	24
741	37	47	44	22	36	26	23
742	41	30	42	23	38	28	26
743	38	26	38	21	31	22	25
744	56	24	29	33	29	23	22
745	64	25	24	38	27	27	24

traffic patterns can also be seen to include large differences in occupancy values between adjacent stations. In Table 2 such large differences are observed at 723 between stations 28 and 27, at 725 between stations 29 and 28, and at many other times and places. In this pattern, the large differences in occupancy values are associated with the passage of a compression or shock wave in a direction counter to the direction of travel. Boxes isolate particularly large occupancy values associated with one such shock wave.

This and other features of these patterns serve to (imperfectly) distinguish between incident and incident-free conditions. The algorithms that are discussed here involve the use of several features which, in combination, distinguish more clearly between incident and incident-free conditions than algorithms based on any one feature. Three steps in the development of good multiple-feature algorithms are:

(1) the identification of features which tend to take on different values under incident and incident-free conditions.

(2) the identification of effective combinations of features.

(3) the calibration of thresholds.

Our investigations have indicated that simple features based upon occupancy data are consistently among the most useful features that we have examined. More complex features, e.g., those based upon exponential smoothing and traffic correlation[1] have not been found to lead to algorithms with superior performance. As a consequence all but one of the algorithms that we discuss in detail here are based entirely on functions of occupancy.

As a convenient approach for combining features, we have adopted a generalization of the structure of the California algorithm, illustrated in Figure 1. The essential characteristic of this algorithm is the sequence of binary decisions, each of which involves the comparison of a feature to a threshold. Our generalized structure is that of a <u>binary decision tree</u>, which involves a tree-like arrangement of binary decisions. This subject is discussed in Section 3.

It can be seen that algorithms based on a binary decision tree structure will involve, in addition to several features, several thresholds. The process of calibrating thresholds requires a careful statement of measures of performance for an incident detection algorithm and the use of a substantial quantity of data pertaining to both incident and incident-free conditions. The methodology we have developed for calibration is described in Section 4.

---

[1] See Section 3.

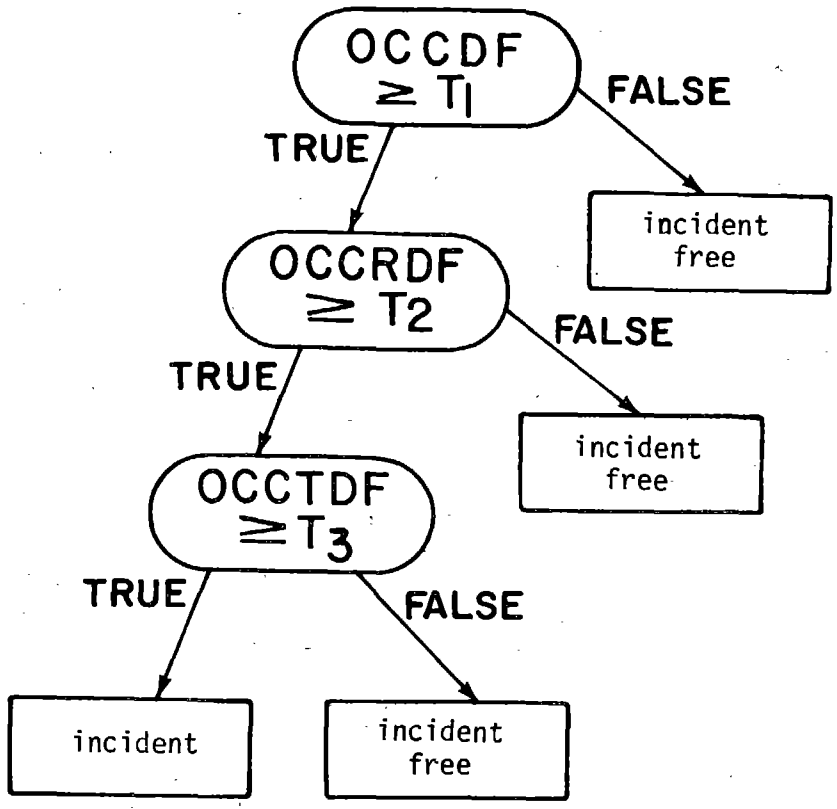

OCC = minute average occupancy (expressed as a percentage)

OCCDF = OCC (upstream) - OCC (downstream)

$$\text{OCCRDF} = \frac{\text{OCCDF}}{\text{OCC(upstream)}}$$

OCCTDF = [OCC(downstream, two minutes ago) - OCC(downstream, now)]/ OCC(downstream, two minutes ago)

T_1, T_2, T_3 = Thresholds

Figure 1. The California algorithm for incident detection.

In addition to using algorithms to detect the occurrence of an incident, it is desirable to have them signal the continuation and termination of the incident. This could be achieved by using two algorithms, one to detect the occurrence and the second to detect the termination. Functioning of the second algorithm, of course, is conditional upon a signal from the first algorithm; that is, one looks for termination only after an incident has been detected.

We have found that accommodation of this desideratum can be nicely achieved by associating a state with the traffic condition for each station. For example, let

State	Designate
0	Incident-free conditions
1	Incident has occurred
2	Incident is continuing

The state '1' would be set at the time that an incident was detected. Subsequently, the state for that station would be set equal to 2 until the termination algorithm indicated an end to the incident. A revised California algorithm with a state feature is illustrated in Figure 2. Note that the algorithm assigns a state which is indicated by the number in the box to which the feature comparison leads. This state is saved and used in the subsequent test for that station.

For example, suppose we take

$$T_1 = 8$$
$$T_2 = .50$$
$$T_3 = .15$$
$$T_4 = .50$$

(The first three values are those most generally used in Los Angeles.) For station 25 in Table 1, we get the following states from the algorithm:

Time	State
715	0
716	0
717	0
718	1
719	2
720	2
⋮	
729	2
730	0

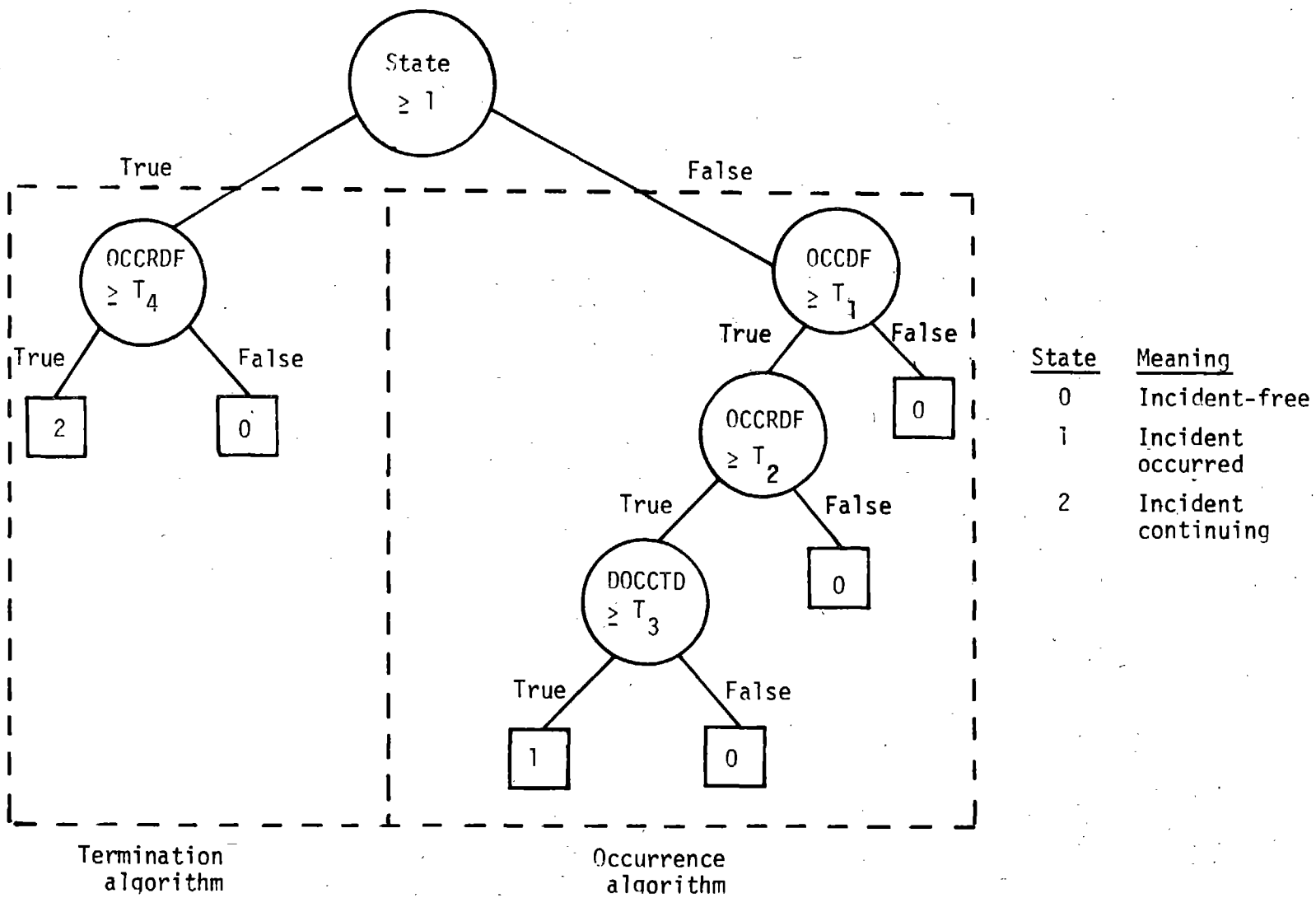

Figure 2. The California algorithm with a test for termination.

which is interpreted to mean that the incident is detected at 718 and a termination signal is produced at 730.

The algorithm of Figure 2 is an example of a binary decision tree with a state, a structure we have adopted for virtually all of our algorithm development. A discussion of this subject is presented in Section 3.

At this point, we would like to note other capabilities which an algorithm structured as a binary decision tree with a state may have. Observe in Tables 1 and 2 that the differences in occupancy values persist in the incident pattern but do not always persist in the incident-free, heavy traffic pattern. We can achieve improved discrimination then by requiring that the difference in occupancy values (e.g., as measured by OCCRDF) persists for two consecutive tests. To do this, we define states as follows:

State	Designates
0	Incident-free conditions
1	Tentative incident
2	Incident has occurred
3	Incident is continuing

A refined California algorithm embodying this device is illustrated in Figure 3. With this algorithm and the thresholds specified earlier, the sequence of states determined for station 25 in Table 1 is

Time	State
715	0
716	0
717	0
718	1
719	2
720	3
721	3
.	
.	
.	
729	3
730	0

The sequence of states determined for station 28 in Table 2 is

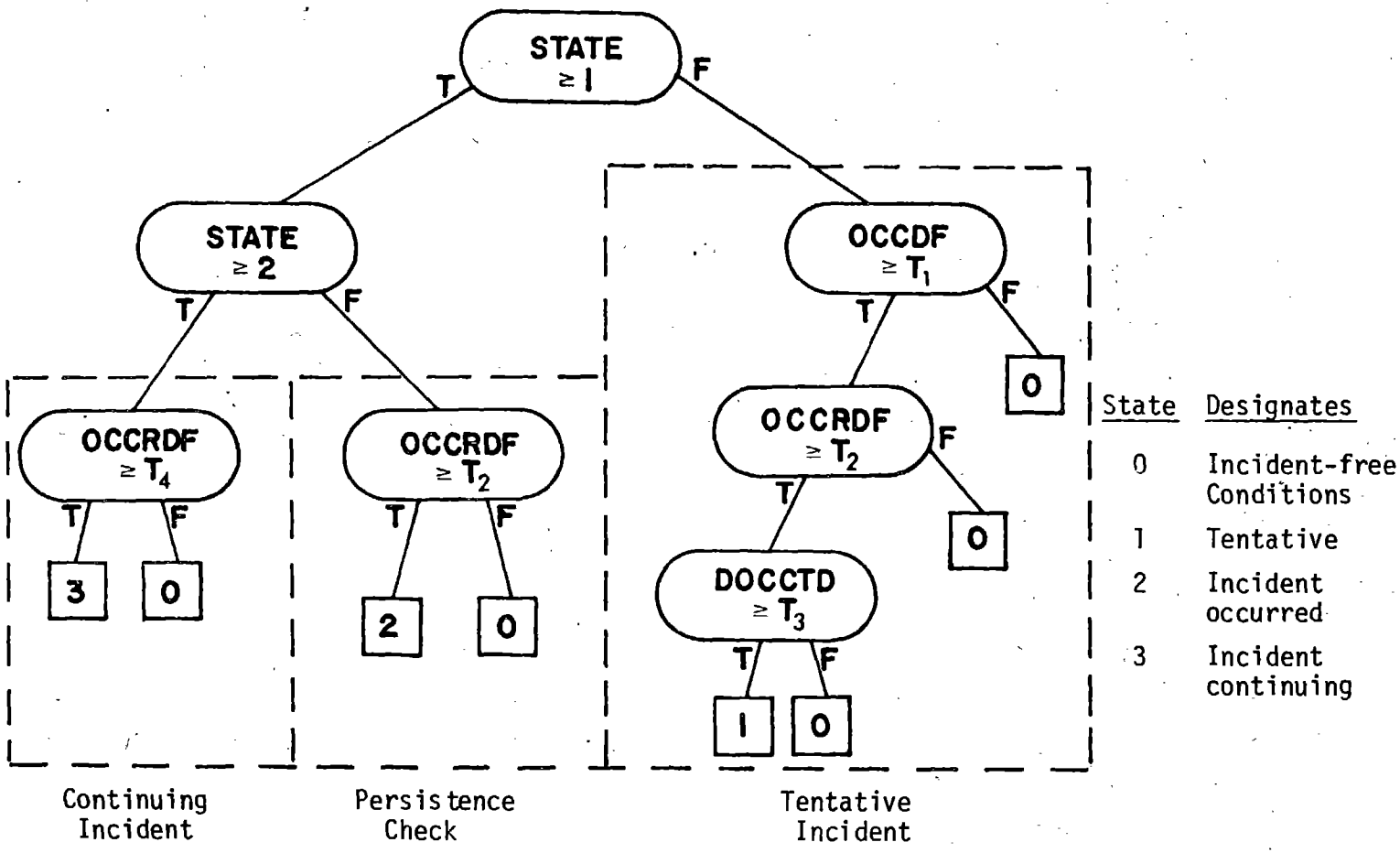

Figure 3. A refined California algorithm with a persistence requirement.

Time	State
720	0
721	0
722	0
723	1
724	0

Note that, as compared to the algorithm of Figure 2 which does not involve a check for persistence, the time of detection is delayed by one minute and the false indication of an incident for station 28 is eliminated. Not all such false indications are eliminated, however, as can be seen by examining Table 2 for station 32 over the interval 733-735.

Our development of incident detection algorithms was carried out with the use of data obtained from the Los Angeles area, representing 118 incidents and an average of 18 hours of incident-free conditions for each of 144 sensor stations. These developments are described in Sections 5 and 6. In Section 5, a series of algorithms are introduced that are designed to provide increasingly better discrimination in traffic patterns, i.e., better algorithm performance. These developments were guided by close examination of algorithm performance to reveal consistent sources of false alarms, which we then attempted to eliminate by refining the algorithm structure. The result of these developments is the identification of several new incident detection algorithms with considerably improved performance relative to that for algorithms previously identified.

Implementation of an incident detection algorithm requires attention to a number of issues which were the subject of limited studies reported in Section 6. These issues include parameters of the surveillance system (i.e., the configuration of sensors), the frequency of algorithm executions, adjustments for certain geometric conditions, and related algorithms for the detection of malfunctioning surveillance hardware and the identification of the lane of an incident. Results pertaining to these issues can be summarized as follows:

- Full count stations at one-half mile intervals yield better performance, i.e., fewer false alarms while detecting the same fraction of incidents, than partial count stations at one-half mile intervals or full count stations at one-mile intervals.
- Modifications to the algorithms we have identified to make tests for incident conditions at other than one-minute intervals are easily made; such modifications have minor effects on algorithm performance.
- A procedure of adjusting algorithms to accommodate anomalous geometric conditions has been defined but its efficacy is in doubt.

- Candidate algorithms for detecting malfunctioning sensors are defined, with elements of these algorithms being associated with specific types of malfunctions.

- A lane identification algorithm has been identified which is both simple and quite effective.

As all of our algorithm developments were carried out with data from a single freeway surveillance system, there can be a question of the universality of the results. To address this, several of the more promising algorithms that were developed were evaluated using data from the freeway surveillance system in the Minneapolis area. These data pertain to 36 incidents and approximately 15 hours of incident-free conditions for each of 72 sensor stations. Both clear weather and snowy weather conditions were involved. The general conclusions to be drawn from the discussion of Section 7 is that

- performance of a given algorithm will differ between facilities

- the algorithms we have developed provide a satisfactory range of performance for systems both with and without TV surveillance

- use of thresholds determined by calibration on the Los Angeles data base provides satisfactory performance, but significantly better performance is obtained by calibration on data from the implementing facility

- it is not necessary to use different thresholds for different weather conditions.

This report is concluded with a discussion in Section 8 of areas of research which we feel merit further attention. These areas are the detection of incidents in light traffic, the use of lane-specific occupancy data, and further study of the effects of sensor configuration.

2. PATTERNS IN TRAFFIC DATA

The development of incident detection algorithms undertaken in this research effort is constrained by the nature of the data that are available for processing. The purpose of this section is to delineate the nature of available data and to describe typical patterns in these data that pertain to both incident and incident-free conditions.

In the course of developing and evaluating incident detection algorithms, we have discovered that certain types of patterns in the traffic data appear repeatedly and we have developed an understanding of traffic conditions which provides rational explanations for the appearance of such patterns. In this section we describe and rationalize these patterns so that the directions we took in algorithm development can be more easily understood.

The freeway surveillance data available for this study are typical of data generally available in freeway surveillance systems for the purpose of incident detection. The sensors which were the source of the data are induction loops with associated electronics. Good descriptions of this and other hardware available for freeway surveillance are given by Everall.[1] Characteristics of present freeway surveillance systems in the United States are described in the first interim report of this research.[2]

While data made available for this study from Los Angeles were in the form of records pertaining to each activation and deactivation of individual loop detectors, our developments were based entirely on aggregated forms of these data typically used in freeway software systems--specifically, occupancy and volume. Occupancy is defined as the mean activation time computed over a specified interval of time (e.g., twenty seconds, thirty seconds, or one minute) and is generally expressed as a percentage. For purposes of incident detection, occupancies computed as averages over all lanes at a given location were used exclusively. Lane-specific occupancies were used in lane identification and techniques for detecting malfunctioning detectors. Volume is defined as the number of vehicle crossings of a loop in a specified interval of time (e.g., twenty seconds, thirty seconds, or one minute) and is generally expressed as vehicles per lane per hour. These aggregated forms of the data can be conveniently displayed in tabular form, as in Table 1. We will find

---

[1] P. Everall, "Urban Freeway Surveillance and Control: The State of the Art," U.S. Department of Transportation, Federal Highway Administration, June 1973. (Available through U.S. Government Printing Office, Stock Number 5001-00058).

[2] H.J. Payne, D.N. Goodwin, and M.D. Teener, "Evaluation of Existing Incident Detection Algorithms," Report No. FHWA-RD-75-39, February 1975, prepared for the Federal Highway Administration (PB No. 241-883/AS).

Preceding page blank

repeated use of tabular forms in this report to identify and discuss patterns in traffic data.

2.1 INCIDENT PATTERNS

Depending upon the nature of an incident and upon the traffic conditions prevailing at the time, the pattern that develops in traffic data in the presence of that incident may be one of five types.

The first type is the most distinctive in that it is most easily discriminated from patterns associated with incident-free conditions. This pattern occurs when the capacity at the incident site is less than the volume of oncoming traffic so that a queue develops upstream of the incident site. Simultaneously, a region of light traffic develops downstream of the incident site. An example of this pattern is illustrated by the occupancy data of Table 1, pertaining to incident data set no. 74051501. This pattern is clearest when traffic is freely flowing prior to the incident as is the case here.

The second type occurs when the prevailing traffic condition is freely flowing but the impact of the incident is less severe, for example, as might result from a lane blockage which yields a capacity at the site of the incident which is greater than the volume of oncoming traffic. Table 3, for data set 74032203, illustrates the situation. This situation is more difficult to distinguish from certain incident-free patterns and, therefore, may not result in a detection.

The third type of pattern occurs, again, in freely flowing traffic but the impact of the incident is not noticeable in the traffic data. This may occur when the incident is a disabled vehicle in the median. Incident detection algorithms cannot be expected to detect incidents of this sort.

The fourth pattern is one which occurs in heavy traffic where the capacity at the incident site is less than the volume of traffic downstream of the site. This difference leads, generally, to a clearance in the region downstream of the incident. An example of this is illustrated in Table 4 for incident data set 74032901. Here the traffic pattern evolves rather slowly so that a distinguishable pattern develops only after several minutes. Obviously, a very severe incident with several lanes blocked would result in rapid development of the pattern but the more typical situation is that illustrated by this table.

The fifth pattern occurs in heavy traffic in which the capacity at the site of the incident is not less than the downstream volume. The effects are then localized and are not noticeable in the traffic data. Incident detection algorithms cannot be expected to detect incidents of this sort.

2.2 PATTERNS IN INCIDENT-FREE TRAFFIC THAT TEND TO PRODUCE FALSE ALARMS

Four types of patterns occur under incident-free conditions which are similar to incident patterns and therefore tend to produce false alarms. The first of these is that related to malfunctioning detectors, a subject we address in Section 6.

The second arises in heavy traffic in which individual vehicles experience significant speed variations. This phenomenon shows up in traffic data in the form of compression waves that propagate in a direction counter to the flow of traffic. Several such waves can be seen in the occupancy data of Table 2. An examination of these data reveals significant station-to-station differences in occupancies of the same magnitude as seen in patterns related to incidents. This pattern is the most significant contributor to false alarms for algorithms identified prior to our development (at least as measured with respect to the Los Angeles data).

The third type of pattern is associated with abnormal geometrics, for example, that which is found at freeway-to-freeway interchanges. One geometric situation which is particularly troublesome for algorithms in the Los Angeles area is depicted in Figure 4. The volume of traffic at station 31 is split between traffic proceeding northbound on the San Diego freeway and that using the connectors to the Santa Monica freeway. A frequent consequence is that the volume per lane at station 32 is less than the volume per lane at station 31 and a resultant difference in occupancies, as illustrated in Table 5 for data set no. 74042368.

The fourth pattern is associated with bottlenecks, for example, at locations with a substantial volume of on-ramp traffic. These bottleneck locations are such that the total demand exceeds the capacity of the freeway. The result is a pattern as illustrated in Table 6 for data set no. 74090462. Note the discontinuity between stations 18 and 19 until 730 and between stations 19 and 20 thereafter.

2.3 CONSEQUENCES FOR ALGORITHM DEVELOPMENT

It should be evident from this discussion that effective incident detection algorithms require more than an identification of a discontinuity in the traffic data--there are numerous such occurrences in incident-free data. The algorithms we have developed explicitly account for the differences in the detailed nature of the discontinuities found in the traffic stream under incident and incident-free conditions. Our developments have led to algorithms that can always detect the first incident pattern and can sometimes detect the second and fourth incident patterns. At the same time, certain algorithms have been developed that are invulnerable to compression waves.

A means for largely eliminating the false alarms due to geometric anomalies has been identified and is discussed in more detail in

Table 3. Occupancy data for incident data set 74032203, Santa Monica eastbound.

Entries are one-minute occupancies. Incident occurred at 18:16 between stations 23 (upstream) and 24 (downstream).

Direction of Travel →

Time \ Stations	19	20	21	22	23	24	25
1810	11	8	10	9	8	10	9
1811	10	10	8	9	8	8	9
1812	11	10	9	10	8	9	8
1813	10	11	9	10	9	8	9
1814	10	10	10	11	9	8	9
1815	10	10	10	8	10	10	8
1816	9	10	8	11	10	7	9
1817	11	9	8	10	13	7	6
1818	11	12	10	8	15	7	6
1819	12	11	12	11	15	7	9
1820	7	8	9	11	15	8	9
1821	11	9	7	7	16	7	8
1822	12	13	9	9	16	7	8
1823	11	9	10	11	15	8	7
1824	9	12	10	10	16	6	7
1825	10	11	10	11	17	9	8
1826	8	10	8	9	18	9	5
1827	8	8	7	9	16	10	10
1828	10	9	8	8	17	9	9
1829	9	9	8	9	16	8	9
1830	9	11	9	8	15	6	8
1831	9	8	9	11	14	6	8
1832	10	12	7	7	20	7	6
1833	10	8	9	12	15	6	8
1834	11	10	8	9	19	7	5
1835	11	10	8	9	18	8	8
1836	9	12	9	10	14	9	10
1837	10	9	9	12	16	8	8
1838	9	9	10	12	20	12	11
1839	9	12	7	11	22	12	11
1840	10	9	8	11	27	12	9
1841	11	8	8	8	22	12	13
1842	10	9	8	8	21	10	12
1843	10	10	8	10	19	11	9
1844	9	10	9	10	18	10	9
1845	10	6	7	8	23	11	10
1846	11	13	9	6	18	11	10
1847	8	8	10	11	7	9	11
1848	11	11	9	8	11	8	7
1849	7	11	10	10	8	10	9
1850	9	8	8	10	10	8	8

Table 4. Occupancy data for incident data set 74032901, Santa Monica westbound.

Entries are one-minute occupancies. Incident occurred at 17:27 between stations 27 (upstream) and 26 (downstream).

Direction of Travel →

Time \ Stations	28	27	26	25	24
1720	25	30	27	22	17
1721	25	40	28	21	19
1722	18	38	25	24	16
1723	18	35	27	20	20
1724	39	33	27	22	29
1725	43	31	28	34	20
1726	25	36	28	34	18
1727	22	34	26	22	15
1728	24	35	29	21	16
1729	19	31	43	21	15
1730	12	40	28	20	19
1731	22	43	21	22	16
1732	15	44	17	24	19
1733	18	41	9	24	20
1734	36	45	9	23	21
1735	29	45	10	20	21
1736	49	43	10	12	19
1737	36	40	10	12	19
1738	29	36	9	12	14
1739	30	39	9	11	15
1740	30	36	8	11	15
1741	39	40	10	11	12
1742	49	40	4	10	10
1743	29	43	13	8	7
1744	35	35	13	13	10
1745	25	31	14	14	12
1746	40	27	13	15	13
1747	39	19	13	15	12
1748	39	21	12	14	15
1749	22	38	16	12	14
1750	19	29	14	15	11
1751	15	28	14	14	13
1752	19	30	15	16	12
1753	15	37	18	15	15
1754	11	20	18	18	13
1755	15	27	15	19	14
1756	14	25	15	15	14
1757	14	29	15	18	18
1758	11	26	15	16	18
1759	10	28	13	16	18
1800	6	14	15	15	24

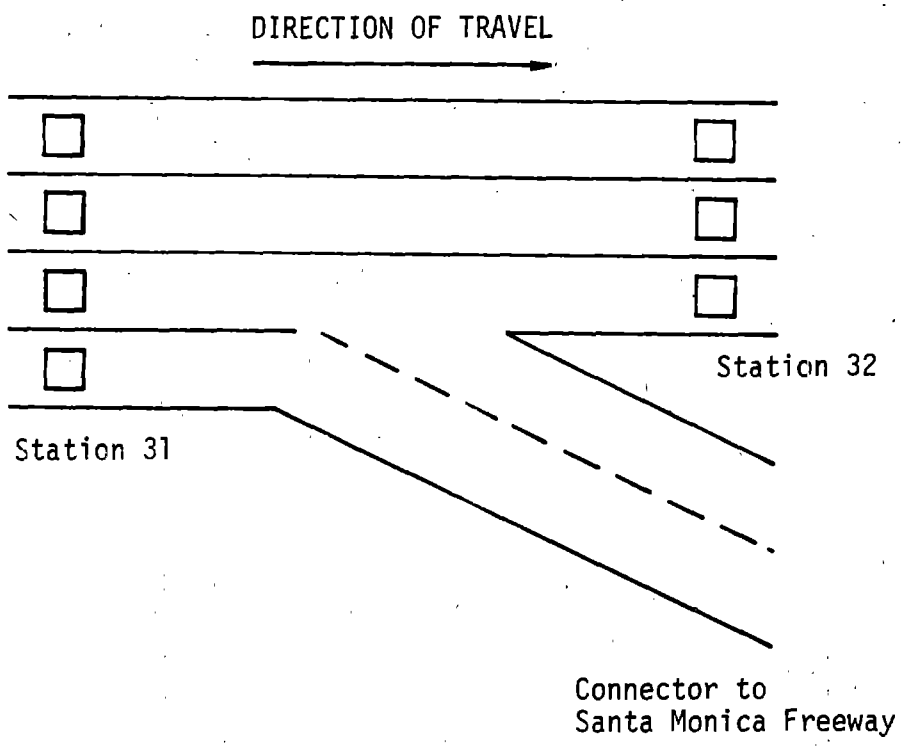

Figure 4. Schematic of the geometry at a freeway-to-freeway interchange in Los Angeles--San Diego freeway northbound to the Santa Monica freeway.

Table 5. Occupancy data for incident-free data set 74042368, San Diego northbound.

Entries are for one-minute occupancies.

Direction of Travel →

Time \ Stations	28	29	30	31	32
1640	10	14	16	17	15
1641	14	14	13	26	17
1642	15	14	16	18	12
1643	14	16	15	23	11
1644	16	14	18	14	11
1645	12	17	16	17	11
1646	13	13	18	14	12
1647	14	13	12	15	12
1648	12	17	16	9	9
1649	13	11	14	16	9
1650	14	16	14	11	11
1651	12	16	16	15	7
1652	13	11	16	16	10
1653	15	16	14	13	11
1654	13	17	16	13	10
1655	13	14	18	16	9
1656	18	15	15	18	9
1657	14	18	15	12	12
1658	18	17	18	16	12
1659	14	17	19	16	10
1700	14	14	16	16	13
1701	17	17	15	12	11
1702	21	20	15	15	11
1703	15	24	18	15	9
1704	13	25	17	16	9
1705	18	24	18	15	10
1706	16	23	19	17	10
1707	20	22	20	18	11
1708	15	21	20	19	12
1709	20	19	20	20	14
1710	18	21	19	18	11
1711	18	21	20	18	10
1712	15	19	21	20	14
1713	19	22	17	18	12
1714	18	25	22	17	13
1715	16	27	19	17	13
1716	15	24	19	19	14
1717	11	18	19	16	13
1718	17	16	16	15	10
1719	15	20	16	16	11
1720	13	17	19	15	9

Table 6. Occupancy data for incident-free data set 74090462, Santa Monica eastbound.

Entries are for one-minute occupancies.

Direction of Travel →

Time \ Stations	15	16	17	18	19	20
710	15	14	12	24	19	16
711	17	13	27	28	17	19
712	16	14	25	26	15	16
713	16	17	28	28	16	15
714	17	28	31	28	16	16
715	17	31	48	25	16	18
716	21	25	31	24	17	14
717	24	32	30	26	17	16
718	22	35	26	30	17	19
719	38	29	30	25	22	17
720	28	23	27	26	16	20
721	23	35	26	26	18	19
722	21	30	29	25	19	19
723	34	28	32	24	19	18
724	28	28	41	27	19	15
725	24	27	28	27	18	19
726	27	46	26	25	19	22
727	35	37	27	26	17	19
728	34	26	30	25	19	20
729	25	21	35	25	18	22
730	21	23	50	23	19	40
731	21	23	31	24	18	31
732	21	30	35	22	25	26
733	20	31	31	23	34	23
734	28	26	33	24	30	22
735	24	39	33	27	33	21
736	21	37	29	30	37	24
737	23	27	30	32	39	19
738	24	26	24	34	38	18
739	30	33	37	33	38	20
740	25	28	44	31	37	21
741	28	37	33	32	33	20
742	30	40	34	29	36	18
743	28	34	44	29	35	16
744	30	32	46	29	40	19
745	29	36	39	32	32	28
746	24	42	28	27	27	27
747	44	34	24	33	23	18
748	43	28	33	29	24	17
749	24	29	36	28	21	20
750	22	38	43	29	22	20

Section 6. However, the problem of bottleneck patterns still remains in the algorithms we have developed.

Incidents in light traffic are not generally detected by the algorithms we have developed. Tignor[1] has investigated the application of single-exponential smoothing to detection in this regime. Another potentially effective means for detecting such incidents involves the use of traffic correlation and is discussed in Section 3 and Appendix A.

---

[1] S. C. Tignor, "Operational Analysis and Improvements for Freeway Moving-Merge Systems," Ph.D. dissertation, University of Michigan, Department of Civil Engineering, 1974.

3. STRUCTURES FOR INCIDENT DETECTION ALGORITHMS

In the simplest possible form, an incident detection algorithm consists of a comparison of the value of some function of the traffic data (a feature) to a threshold, with an incident being indicated if the value is larger than the threshold, for example. Previous incident detection algorithm developments were almost entirely of this sort.[1,2,3,4] In developing such algorithms, a variety of complex functions of the traffic data based upon time-series analysis techniques have been used. The first portion of this section is devoted to a discussion of features, including those based upon (double) exponential smoothing and traffic correlation.

We have found, however, that no algorithm which is based upon any single feature thus far identified gives satisfactory performance. Rather, performance in the range necessary for operational use has come with the development of algorithms that use several features. The particular structure we have adopted for combining several features is the binary decision with a state, which we describe in Section 3.2.

3.1 FEATURES

Features which we have used in defining incident detection algorithms can be categorized as simple features and time-series features.

3.1.1 Simple Features

The variables, occupancy and volume, upon which all the features are based are defined as follows:

OCC(i,0,t) — the one-minute occupancy, expressed as a percent, at station i, averaged across all lanes.

---

[1] A.R. Cook, "The Detection of Capacity Reducing Incidents on an Urban Freeway using Traffic Stream Measurements," Ph.D. dissertation, University of Michigan, Department of Civil Engineering, 1972.

[2] A.R. Cook and D.E. Cleveland, "The Detection of Freeway Capacity-Reducing Incidents by Traffic-Stream Measurements," Transportation Research Board, Record 495 (1974), 1-11.

[3] K.G. Courage and M. Levin, "A Freeway Corridor Surveillance Information and Control System," Texas Transportation Institute, Research Report 488-8, December 1968.

[4] H.J. Payne, D.N. Goodwin, and M.D. Teener, "Evaluation of Existing Incident Detection Algorithms," Report No. FHWA-RD-75-39, February 1975, prepared for the Federal Highway Administration (PB No. 241-883/AS).

Preceding page blank

OCC(i,j,t)	the one-minute occupancy, expressed as a percent, at station i, lane j, for $j \geq 1$.
VOL(i,0,t)	the one-minute count, expressed as vehicles per lane per hour, at station i, and averaged across all lanes.
VOL(i,j,t)	the one-minute count, expressed as vehicles per lane per hour, at station i, lane j, $j \geq 1$.

For example, using Figure 5 to illustrate, OCC(1,2,t) is the occupancy in lane 2 of station 1; OCC(2,0,t) is occupancy averaged across all lanes at station 2. Our convention will be that station i is the upstream station and station i+1 is the downstream station. The number of lanes at station i is denoted by N(i).

In the evaluation of algorithms available at the initiation of this study reported in our first interim report,[1] eighteen simple features were identified. Based upon the results of that evaluation, we have limited our attention to the occupancy and volume variables and those defined in Table 7. Only those simple features which are based upon occupancy and/or volume averaged over all lanes at a station were used in incident detection algorithms. Lane specific features are used in algorithms for detecting malfunctioning sensors and for locating the lane of an incident. Note the convention that an initial 'D' in a feature name indicates that downstream data are involved, e.g., DOCC(i,t) is the occupancy at the station downstream of station i.

The feature DOCCTD appears in the California Algorithm. The time lag used in this feature, here two minutes, was 20 seconds in the original California Algorithm. Experience in Los Angeles led to the change to the two minute lag.

3.1.2 Time-Series Features

Of the simple features defined above, only DOCCTD and SPDTDF (defined in Table 7) involve values of the traffic variables at more than one instant. The remaining simple features thus provide measures of the traffic pattern at one instant of time (actually, averaged over one minute). One characteristic of incident-generated traffic patterns is the typically abrupt development of a discontinuity in the traffic stream, particularly, e.g., as quantified by occupancy. Time-series techniques provide a basis for detecting such temporal discontinuities in occupancy, volume, in fact, in any of the simple features we have defined. The general idea is that the time series of the values of a feature can be used to forecast a

[1] H.J. Payne et al., Ibid.

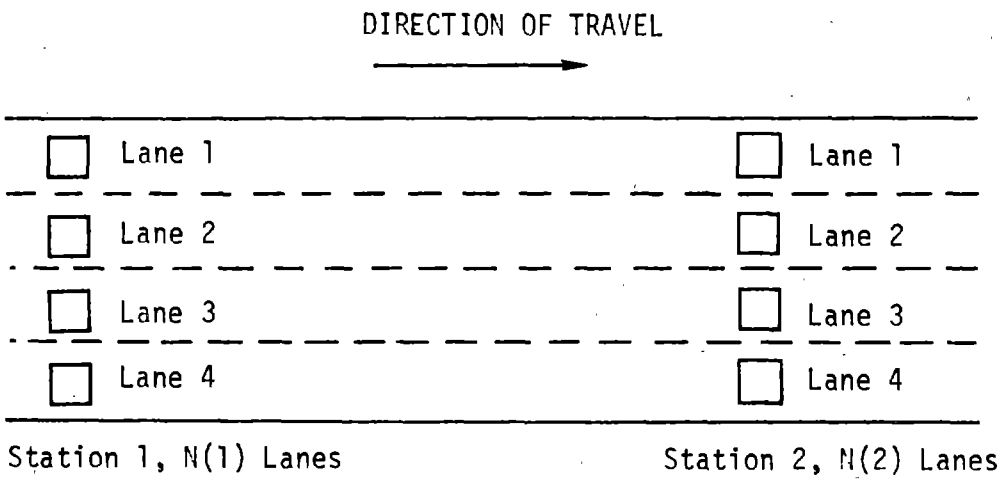

Figure 5. Lane sensor notation.

Table 7. Definitions of simple features.

Feature	Description	Definition
DOCC(i,t)[1]	Downstream occupancy	OCC(i+1,0,t)
OCCDF(i,t)	Spatial difference in occupancies	OCC(i,0,t) - OCC(i+1,0,t)
OCCRDF(i,t)	Relative spatial difference in occupancies	OCCDF(i,t)/OCC(i,0,t)
DOCCTD(i,t)	Relative temporal difference in downstream occupancy	[OCC(i+1,0,t-2)-OCC(i+1,0,t)]/ OCC(i+1,0,t-2)
SPD(i,t)[2]	Speed	VOL(i,0,t)/[OCC(i,0,t)xG]
SPDTDF(i,t)	Relative temporal difference in speed	[SPD(i,t-2)-SPD(i,t)]/ SPD(i,t-2)
OCCL5(i,j,t)	Five-minute average lane-specific occupancy	$1/5 \sum_{k=0}^{4} OCC(i,j,t-k)$
VOLL5(i,j,t)	Five-minute average lane-specific volume	$1/5 \sum_{k=0}^{4} VOL(i,j,t-k)$
SPDL5(i,j,t)[2]	Five-minute average lane-specific speed	VOLL5(i,j,t)/[OCCL5(i,j,t)xG]
OCC5(i,t)	Five-minute average occupancy	$1/5 \sum_{k=0}^{4} OCC(i,0,t-k)$

[1] In the first interim report, this designation was used for the standard-normal-deviate feature.

[2] The G-factor appearing in this definition is empirically determined so that SPD (and SPDL5) are estimates of speed in miles per hour. The factor used in this report is 2.86 and was determined from Los Angeles surveillance system data. See Appendix D.

future value (e.g., the value at the time of the next algorithm execution) and that an incident will cause a significant discrepancy between the actual and forecasted value. Here, we will delineate two time-series approaches which lead to two classes of features.

3.1.2.1 Double Exponential Smoothing

For any time series, say $\{f(t_0+k\Delta),\ k=0,1,\ldots,K\}$, where Δ is the time interval between samples, the technique of double exponential smoothing can be applied.[1] The procedure is defined as

$$s_1(t) = a\ f(t) + (1-a)s_1(t-1) \qquad (1)$$

$$s_2(t) = a\ s_1(t) + (1-a)s_2(t-1) \qquad (2)$$

The parameter a is termed a smoothing constant. The time series $s_1(t)$ and $s_2(t)$ are the exponentially and double exponentially smoothed series.

A linear prediction, $\hat{f}(t)$, for the coming minute ($\tau=1$) is developed from these smoothed series by means of the following equations. They are the means by which the model corrects for a trend.

Let

$$\hat{f}(t) = A(t) + \tau B(t) \quad , \qquad (3)$$

where

$$A(t) = 2\ s_1(t) - s_2(t) \qquad (4)$$

and

$$B(t) = \frac{a}{(1-a)}\ (s_1(t) - s_2(t)) \quad . \qquad (5)$$

The forecasting error is then

$$e(t) = \hat{f}(t) - f(t) \quad . \qquad (6)$$

The indication of an incident is based on the tracking signal, defined in terms of the error series as follows:

$$y(t) = y(t-1) + e(t) \qquad (7)$$

$$z(t) = y(t)/m(t-1) \quad . \qquad (8)$$

[1] R.G. Brown, Smoothing, Forecasting and Prediction of Discrete Time Series, Englewood Cliffs, N.J., Prentice-Hall, 1963.

The series $z(t)$ is the tracking signal; $m(t)$ is an exponentially smoothed, mean absolute deviation defined parametrically in terms of a smoothing constant α by

$$m(t) = \alpha|e(t)| + (1-\alpha)m(t-1) \quad . \tag{9}$$

The use of $m(t)$ in equation (8) is intended to normalize the tracking signal on the basis of a current estimate of variability.

Computations based on equations (1), (2), (7), and (9) require initial values for $s_1(t)$, $s_2(t)$, $y(t)$ and $m(t)$, which have been chosen as follows:

$$s_1(t_0) = f(t_0) \quad , \tag{10}$$

$$s_2(t_0) = f(t_0) \quad , \tag{11}$$

$$y(t_0) = 0 \quad , \tag{12}$$

and

$$m(t_1) = \sigma\sqrt{\frac{4}{\pi(2-\alpha)}} \tag{13}$$

where σ is the standard deviation of the error[1] computed from the first six values. Reflecting this, t_1 is taken to be $t_0+5\Delta$, and the computation of the tracking signal from equation (8) begins at $t_1+\Delta$.

Based upon results reported in the first interim report, our attention in the use of double-exponential smoothing has been restricted to the feature SOCCDF, defined by equation (8) when $f(t)$ is taken to be OCCDF as defined in Table 7. The parameters a and α were those found to be most effective in a previous study,[2,3] i.e., a = .3 and α = .1.

3.1.2.2 Traffic Stream Correlation

When viewed from above, the arrangement of vehicles on a roadway forms a pattern. In light traffic, this pattern tends to be stable with time and moves along with the vehicles, changing slowly as it does. At higher traffic levels, this pattern changes more rapidly due to the increase in inter-vehicle conflicts. When traffic is very congested and vehicles undergo marked acceleration-deceleration cycles, a different kind of stable traffic pattern develops in the form of waves (or regions with closely spaced vehicles) which move in the upstream direction.

These stable traffic patterns are reflected in the traffic data recorded from sensor stations in the form of a statistical correlation of

---

[1] R.G. Brown, Ibid.

[2] A.R. Cook, Ibid.

[3] A.R. Cook and D.E. Cleveland, Ibid.

fluctuations between adjacent stations. In this section, we discuss the theoretical basis for such correlation and develop analytical relationships for identifying such correlation in traffic data.

The theory of Lighthill and Whitham[1] suggests that irregularities or small disturbances in a traffic stream are propagated at a characteristic wave speed defined as the slope of the tangent to the volume-density curve at the point defining the traffic conditions (see Figure 6). Under

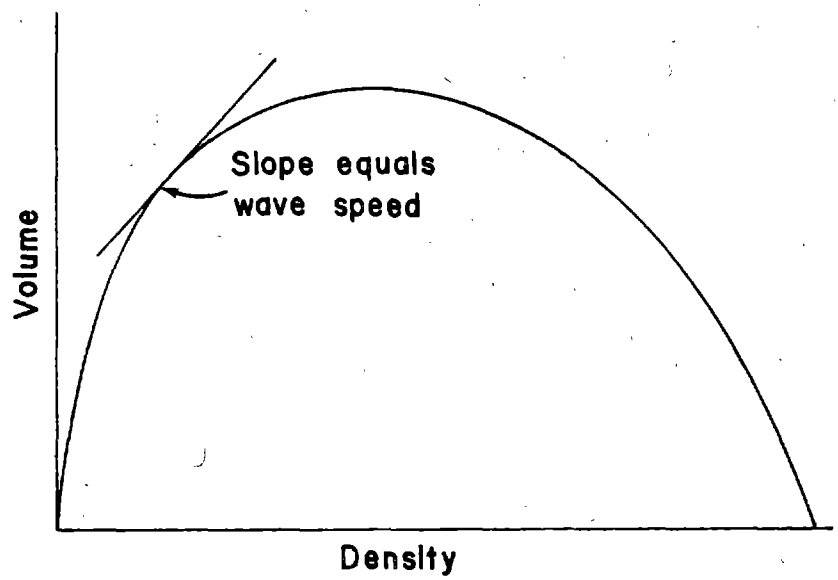

Figure 6. The wave speed in a traffic stream.

free-flow conditions, the wave speed is very nearly the mean traffic stream speed; as the traffic density increases, the wave speed decreases, reaching zero at capacity. At even higher densities, this theory predicts a negative wave speed.

The implication of this theory is that in uncongested conditions, i.e., at lighter densities with corresponding volumes below capacity, traffic fluctuations observed at an upstream station should be observable at a downstream station with a time lag defined by the ratio of the separation distance to the wave speed. Near capacity, the wave speed is near zero, leading to large time lags. This, combined with the redistribution of the traffic pattern which occurs over a period of time, largely eliminates the correlation of traffic fluctuations suggested.

---

[1]M.J. Lighthill and G.A. Whitham, "On Kinematic Waves II. A Theory of Traffic Flow on Long Crowded Roads," Proc. Royal Society of London, Series A, Vol. 229, (1955), 317-345.

The theory also suggests that, in congested conditions, fluctuations at a downstream station will propagate upstream. This has been previously observed,[1] as seen in table 2, and is a frequent cause of false alarms in incident detection algorithms.

The upstream-to-downstream correlation of traffic fluctuations suggested by this theory and observed in traffic data in the lighter density regime has served as the basis for previous attempts to detect incidents by looking for disruptions in the traffic correlation.[2,3,4] (An alternative approach to the detection of incidents in this lighter density regime is described by Tignor.[5])

The approach taken here is to take advantage of traffic correlation, both upstream to downstream--as observed in light to moderate traffic--and downstream to upstream--as observed in congested traffic, to improve the forecast of traffic variables. Thus, for example, a fluctuation in incident-free traffic which gives the instantaneous picture of a discontinuity would be accounted for and, therefore, would not give rise to an unusual forecast error. On the other hand, a fluctuation due to an incident would not be reflected in the traffic correlation and, therefore, would result in unusually large forecast errors.

The detailed developments of the traffic correlation feature are contained in Appendix A as are some preliminary results obtained with its use for incident detection. Examination of these developments reveals a close connection to the Box-Jenkins technique.[6] That is, the form of the

---

[1] T. Lam and R. Rothery, "The Spectral Analysis of Speed Fluctuations on a Freeway," Transportation Science, Vol. 4, (August 1970), 293-312.

[2] J.L. Barker, "Determination of Discontinuities in Traffic Flow as a Factor in Freeway Operation Control," Traffic Engineering, Nov. 1961, 11-17,50.

[3] M. Sakasita and A.D. May, "Development and Evaluation of Incident Detection Algorithms for Electronic Detector Systems on Freeways," Special Report, Institute of Transportation and Traffic Engineering, University of California, Berkeley, Calif., 1974.

[4] C.L. Dudek et al., "Detecting Freeway Incidents under Low Volume Conditions," presented at the 1975 Annual Meeting of the Transportation Research Board, Washington, D.C., 13-17 January, 1975.

[5] S. C. Tignor, "Operational Analysis and Improvements for Freeway Moving-Merge Systems," Ph.D. dissertation, University of Michigan, Department of Civil Engineering, 1974.

[6] George E. P. Box and Gwilynn M. Jenkins, Time Series Analysis Forecasting and Control, Holden-Day, 1970.

forecast which is used is one included in the Box-Jenkins approach, but we used means other than that technique to identify the form of the forecast and the forecast model coefficients. In general, we found traffic to be too irregular for application of the Box-Jenkins technique. In fact, our procedure involves on-line identification of forecast model coefficients.

Based upon our preliminary examination, it appears that this approach, on its own, is not sufficiently distinctive of incidents to provide the basis for operational incident-detection algorithms. As we have noted, as the traffic condition approaches capacity flow, station-to-station traffic correlation tends to disappear.

The traffic correlation feature may yet prove to be useful for detecting incidents in light traffic. This conjecture derives from a limited number of tests in light traffic where we found correlation to be a consistent phenomenon. On the other hand, the downstream-to-upstream correlation associated with very heavy traffic, while observed, was found, even with an on-line procedure for computing forecast model coefficients, to lack sufficient regularity to be useful for incident detection. Fortunately, other means were eventually identified (see Section 5.4) to successfully suppress false alarms due to compression waves.

3.2 BINARY DECISION TREES

To develop and test incident detection algorithms which use several features, we have adopted the general structure of the binary decision tree. In this discussion, we are concerned, first, with those without states. We shall describe and illustrate the coding of trees so that one can use the function NTREE to represent an incident detection algorithm. We shall also specify the rules for coding which must be followed. A subroutine CTREE has been developed that examines a tree coding to check for errors. Application of this function will be illustrated.

Next, we shall take up a discussion of binary decision trees with states. We shall see that coding is carried out in the same manner as for decision trees without states since the state can be handled as an additional feature. Hence NTREE and CTREE are also applicable to trees with states.

Documentation pertaining to the function NTREE and the subroutine CTREE is provided in Volume 4 of this report.

3.2.1 Binary Decision Trees Without States

A binary decision tree consists of a set of nodes connected by links to form a tree-like structure. A node is either a decision node or a terminal node. A decision node consists of a comparison of a feature to a threshold and a specification of two successor nodes--one which is next

to be examined if the comparison is true, and the second, if the comparison is false. The elementary building block of a binary decision tree is illustrated in Figure 7. Each successor node may be a decision node or a terminal node. The root node is the first decision node.

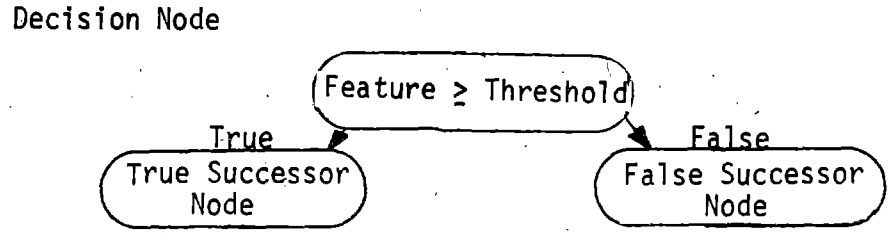

Figure 7. Elementary Building Block of a Binary Decision Tree

A terminal node consists of an assignment of a state value. For purposes of coding an incident detection algorithm, state values are chosen to represent incident-free or incident conditions. Later we shall see how we can make use of the state value to represent a more complex variety of traffic conditions.

The California algorithm has the structure of a simple binary decision tree. In Figure 8, this algorithm is again illustrated along with the nomenclature we have introduced above.

To define a binary decision tree representing an incident detection algorithm, one must

(1) label decision nodes
(2) assign terminal state values
(3) specify the feature associated with each decision node, and
(4) specify the threshold associated with each decision node.

Labeling Decision Nodes

Decision nodes are labeled by integers, 1,..., N, where N is the total number of decision nodes. The first decision node, also known as the root node, must be labeled '1'. The remaining decision nodes must be numbered so that a successor node number is larger than the corresponding decision node.

Terminal State Values

A terminal state value is assigned to each terminal node. Each such value must be a nonnegative integer. The user must associate his own meaning with each terminal state value.

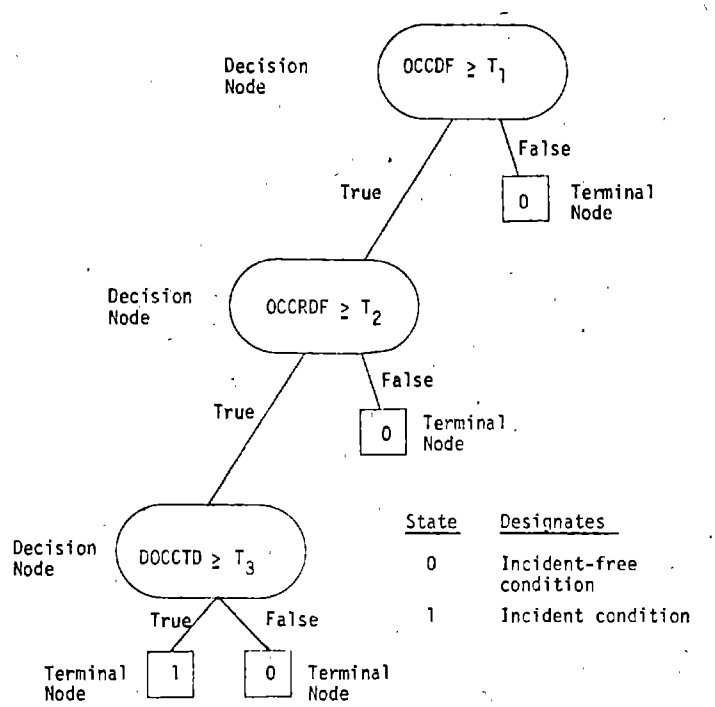

Figure 8. The California algorithm considered as a binary decision tree.

Feature Specification

It is assumed that feature values will be provided to the function NTREE in the form of a vector FEATS. For each decision node one must identify the correponding location in the FEATS vector for the appropriate feature value.

Threshold Specification

It is assumed that the thresholds will be provided to the function NTREE in the form of a vector PARMS. This vector is of length N, equal to the number of the decision nodes. PARMS(J) is the threshold used at the decision node whose number is J.

An array NTR is used to code the structure of the decision tree. It contains information pertaining to each of the decision nodes. NTR is organized as a sequence of N 3-tuples, one 3-tuple for each decision node. The first element in the 3-tuple is the identifying number of

the feature whose value is to be tested at that node. The second element is either a decision node number or a terminal state designation which will be selected if the value of the feature is greater than or equal to the value of the threshold associated with this node (true successor node). The third element is the decision node number or terminal state designation to be selected otherwise, i.e., if the feature is less than the threshold (false node). In order to distinguish between the two possible meanings for the second and third elements, i.e., as a decision node number or as a terminal state designation, we use the convention that terminal state values are coded as their negative. Thus, if the second or third element is greater than or equal to one, it will be interpreted as a decision node number; otherwise the negative of the number will be taken to be the terminal state value.

Exercise of the function NTREE is made in the form

I = NTREE(NTR, PARMS, FEATS)

The variable I is set equal to the value of the terminal state reached after successive comparisons of feature values to thresholds.

Example. Consider the California algorithm illustrated in Figure 8. Node labeling and feature designation is illustrated in Figure 9. Note that terminal state values are indicated by nonnegative integers within boxes which represent terminal nodes. This is the value which NTREE would return if comparisons of the feature values to corresponding thresholds lead to this terminal node.

For this example, there are three decision nodes (N=3). The array NTR would be chosen as follows:

		Value	Meaning
Decision Node 1	NTR(1)	1	Feature 1 is used at decision node 1
	NTR(2)	2	If feature 1 $\geq$ threshold 1, go to decision node 2
	NTR(3)	0	If feature 1 < threshold 1, the terminal state is 0
Decision Node 2	NTR(4)	3	Feature 3 is used at decision node 2
	NTR(5)	3	If feature 3 $\geq$ threshold 2, go to decision node 3
	NTR(6)	0	If feature 3 < threshold 2, the terminal state is 0
Decision Node 3	NTR(7)	2	Feature 2 is used at decision node 3
	NTR(8)	-1	If feature 2 $\geq$ threshold 3, terminal state is 1
	NTR(9)	0	If feature 2 < threshold 3, terminal state is 0

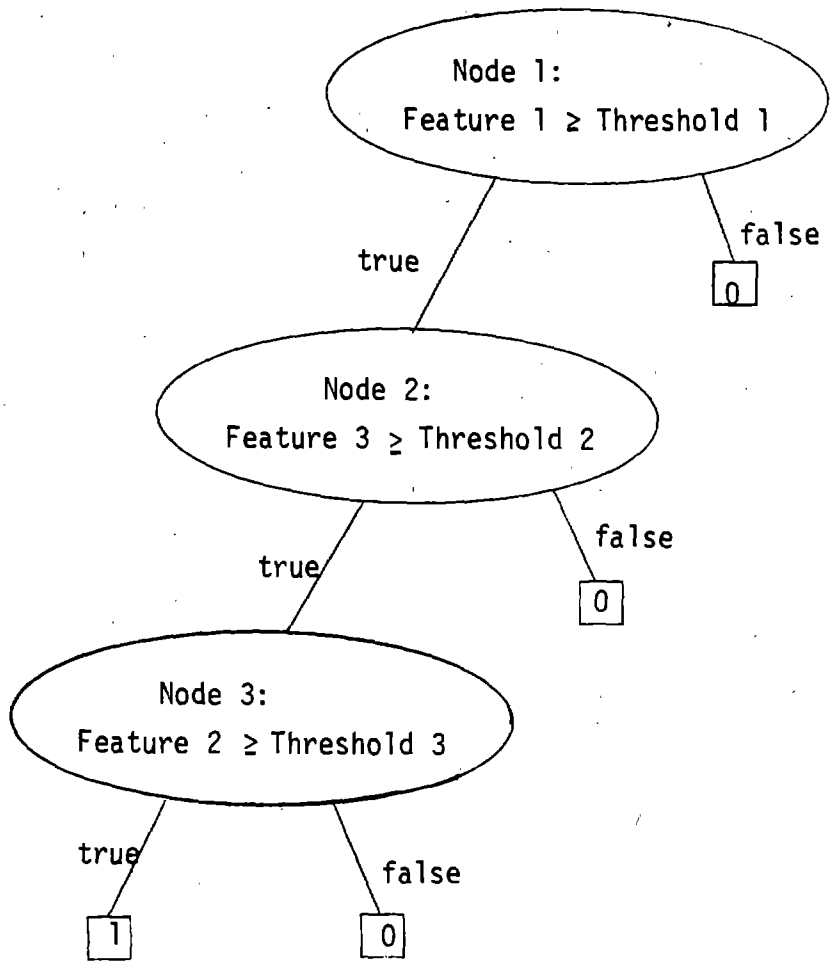

Feature No.	Name
1	OCCDF
2	DOCCTD
3	OCCRDF

State	Designates
0	Incident-free
1	Incident

Figure 9. Coding the California algorithm as a binary decision tree.

Note that terminal state values are distinguished from decision node numbers by the fact that terminal state values are coded as their negative.

After some experience with coding, it is found to be convenient to write NTR in the form

NTR(1), NTR(2), NTR(3)
NTR(4), NTR(5), NTR(6)

.
.
.

so that in this example we have

1, 2, 0
3, 3, 0
2, -1, 0

Note that the labeling of the decision node for which the 3-tuple is pertinent is implicit in the order of NTR.

Continuing with this example, if we now specify the N-tuples PARMS and FEATS, we can call the function NTREE and get back a terminal state value. For example, if we set PARMS = (8, 15, .15) and compute feature values from Table 1, station 25, we obtain the following sequence of terminal state values:

Time	State
715	0
716	0
717	0
718	1
719	1
720	0

3.2.2 Binary Decision Trees with States

You may think that we have already been discussing states in connection with binary decision trees, and, if so, you are right. The new concept that we introduce here is that the state value determined from a call to NTREE can be saved and used as a feature in a subsequent call to NTREE. Assuming that you have mastered the coding procedure described above, you will be pleased to know that coding of binary trees with

states is done in precisely the same way. Hence we can proceed immediately to an example.

Example. Consider the version of the California algorithm presented in Figure 2. First, we draw up a binary tree representation with nodes and features numbered, as indicated in Figure 10. You should be able to easily verify the following NTR table:

4, 2, 3
3, -2, 0
1, 4, 0
3, 5, 0
2, -1, 0

With PARMS = (1, .5, 8, .5, .15), one gets the sequence of states previously identified in connection with this algorithm in the introduction.

3.2.3 Validity Checks for Coding Algorithms

The coding of an incident detection algorithm must satisfy certain requirements in order that NTREE functions properly. After the NTR array and the PARMS vector are defined by the user, they should be checked, using sub-routine CTREE, to determine if NTR defines a legal tree. When the subroutine is called (using CALL CTREE (NNODES, NTR, PARMS), where NNODES is the number of nonterminal nodes, NTR is a vector 3×NNODES long, and PARMS is a vector NNODES long), the tree definition is printed (on the default printer unit, using PRINT statements), unless an error is found in the NTR definition. The types of errors that are detected by CTREE are:

1. NNODES is not in the range of 1-100
2. Illegal branches, i.e., a branch leads to its own parent node or to a node whose number is larger than NNODES
3. More than one branch leads to the same node
4. More than one node has no parent node
5. No root node
6. Root node is not the first node (number 1)
7. Node appears before its parent node

If any of these errors are found, a message is printed and the program is halted. Otherwise, a tree description is printed. For example, to represent the algorithm of Figure 10, the following statements are used:

```
DIMENSION NTR(15), PARMS(5)
DATA NTR/4,2,3,3,-2,0,1,4,0,3,5,0,2,-1,0/
```

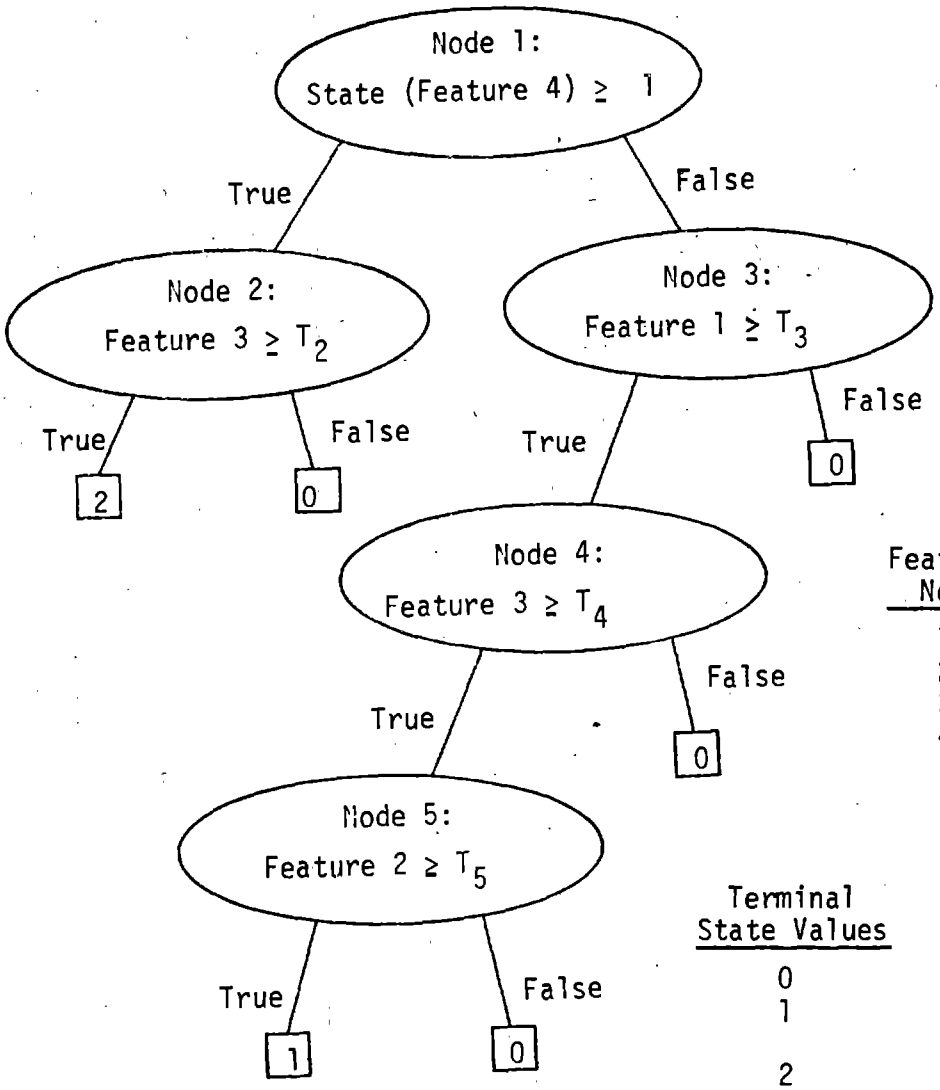

Feature No.	Name
1	OCCDF
2	DOCCTD
3	OCCRDF
4	State

Terminal State Values	Meaning
0	Incident-free
1	Incident occurred
2	Incident continuing

Figure 10. Coding of a version of the California algorithm as a binary decision tree with a state.

To specify threshold values, one might use

```
DATA PARMS/1.,.5,.8,.5,.15/
```

The following call: CALL CTREE(5, NTR, PARMS) will produce this output.

```
TREE STRUCTURE SCAN  ************

NODE 1.  IF FEATURE 4 IS GREATER THAN OR EQUAL TO 1.00E+00, GO TO
         NODE NUMBER 2.  ELSE, GO TO NODE NUMBER 3.

NODE 2.  IF FEATURE 3 IS GREATER THAN OR EQUAL TO 5.000E-01, TERMINAL
         VALUE = 2.  ELSE, TERMINAL VALUE = 0.

NODE 3.  IF FEATURE 1 IS GREATER THAN OR EQUAL TO 8.00E+00, GO TO
         NODE NUMBER 4, ELSE, TERMINAL VALUE = 0.

NODE 4.  IF FEATURE 3 IS GREATER THAN OR EQUAL TO 5.000E-01, GO TO
         NODE NUMBER 5, ELSE, TERMINAL VALUE = 0.

NODE 5.  IF FEATURE 2 IS GREATER THAN OR EQUAL TO 1.500E-01, TERMINAL
         VALUE = 1.  ELSE, TERMINAL VALUE = 0.
```

4. EVALUATION CRITERIA AND CALIBRATION METHODOLOGY

The performance of an incident detection algorithm can be measured in terms of the fraction of incidents detected, i.e., the detection rate, and the instances in which a test of incident-free data yields an incident signal. The rate of such false signals is the false alarm rate. These criteria are formalized and discussed in Section 4.1.

In choosing a set of thresholds for any incident-detection algorithm, it is seen that a tradeoff between the detection rate and the false alarm rate is involved. Improvement of the detection rate is generally had at the cost of an increased number of false alarms. Threshold selection or calibration involves adjustment of thresholds to achieve points on a tradeoff curve defining "noninferior" performance, a concept discussed in Section 4.2. For multiple-feature algorithms, calibration involves solution of a set of optimization problems in which the false alarm rate is minimized, subject to a minimum detection rate.

The evaluation and calibration methodologies have been embodied in a computer program, CALB, described briefly in Section 4.3. and documented in Volume 4 of this report. A discussion of data requirements for exercising this program is also contained in Section 4.3.

4.1 EVALUATION CRITERIA

Simplifying things somewhat, four possibilities arise when an incident detection algorithm is executed, as indicated below.

		Actual Condition	
		Incident-free	Incident
Condition indicated by algorithm	Incident-free		Missed Detection
	Incident	False Alarm (Rate: α)	Detection (Rate: β)

In this section, the concepts of detection and false alarm rates are formalized and the fundamental need to trade off detection capability against the false alarm rate is brought out.

As we have seen, the result of one execution of an incident-detection algorithm structured as a binary decision tree with a state is the assignment of a value to the state variable. The possible values of the state variable are chosen to represent, at a minimum, incident-free or incident conditions. It is useful, both operationally and for developing performance measures, to use distinct state values to distinguish between the first incident signal and the continuation of the same incident.

For convenience in our discussion here, we will assume the following values of the state are possible:

Preceding page blank

State	Designates
0	Incident-free conditions
1	Incident occurred
2	Incident continuing

Algorithms may have more possible state values or may use different state values with the same meanings, but these values are sufficient to define the performance measures.

The results of the application of an incident-detection algorithm to data pertaining to a section of freeway over a specified interval of time can be conveniently displayed in tabular form, e.g., as in Tables 8 and 9.

In the instance of the incident-free data (Table 8), one can easily count the number of incident signals or false alarms, equal to the number of 1's in the table. Note that a '2' indicates continuation of the incident and is not counted as a false alarm. Accumulating the results over a number of incident-free data sets and defining

N_F Total number of tests performed by the algorithm

N_{FA} Total number of false alarm signals generated by the algorithm,

the false alarm rate can then be computed as

$$\alpha = \text{false alarm rate (percent)} \equiv 100 \cdot \frac{N_{FA}}{N_F} .$$

Assessment of results pertaining to incident data sets is carried out somewhat differently. For each such data set, we want to know if the incident was detected. However, for a signal to be useful, it is necessary that (1) it be generated within a reasonable interval following the occurrence of the incident and (2) it be associated with a station or a section near the location of the incident. Specifically, we have required that, to be counted as a detection, a signal be generated in a time-space set such as that enclosed within a box in Table 9. For purposes of computing performance measures, we have adopted the requirement that the signal be generated

(1) At a station either immediately upstream or immediately downstream of the incident site, and

(2) Within a time interval extending from five minutes before to twenty minutes after the (estimated) time of occurrence of the incident.

Table 8. State values produced by the California algorithm* for the incident-free data set 74090454.

*$T_2 = .5$, $T_3 = 8$, $T_4 = .5$, $T_5 = .15$.

Direction of Travel →

Time \ Stations	32	31	30	29	28	27	26	25	24	23	22	21	20	19
830	0	0	0	0	0	0	0	0	0	0	0	0	0	0
831	0	0	0	0	0	0	0	0	0	0	0	0	0	0
832	0	0	0	0	0	0	0	0	0	0	0	0	0	0
833	0	0	0	0	0	0	0	0	0	0	0	0	0	0
834	0	0	0	0	0	0	0	0	0	0	0	0	0	0
835	0	0	0	0	0	0	0	0	0	0	0	0	0	0
836	0	0	0	0	0	0	0	0	0	0	0	0	0	0
837	0	0	0	0	0	0	0	0	0	0	0	0	0	0
838	0	0	0	0	0	0	0	0	0	0	0	0	0	0
839	0	0	0	0	0	0	0	0	0	0	0	0	0	0
840	0	0	0	0	0	0	0	0	0	0	0	0	0	0
841	0	0	0	0	0	0	0	0	0	0	0	0	0	0
842	0	0	0	0	0	0	0	0	0	0	0	0	0	0
843	0	0	0	0	1	0	0	0	0	0	0	0	0	0
844	0	0	0	0	2	0	0	0	0	0	0	0	0	0
845	0	0	0	0	0	0	0	0	0	0	0	0	0	0
846	0	0	0	0	1	0	0	0	0	0	0	0	0	0
847	0	0	0	0	2	0	0	0	0	0	0	0	0	0
848	0	0	0	0	2	0	0	0	0	0	0	0	0	0
849	0	0	0	0	2	0	0	0	0	0	0	0	0	0
850	0	0	0	0	2	0	0	0	0	0	0	0	0	0
851	0	0	0	0	0	0	0	0	0	0	0	0	0	0
852	0	0	0	0	0	0	0	0	0	0	0	0	0	0
853	0	0	0	0	0	0	0	0	0	0	0	0	0	0
854	0	0	0	0	0	0	0	0	0	0	0	0	0	0
855	0	0	0	0	0	0	0	0	0	0	0	0	0	0
856	0	0	0	0	0	0	0	0	0	0	0	0	0	0
857	0	0	0	0	0	0	0	0	0	0	0	0	0	0
858	0	0	0	0	0	0	0	0	0	0	0	0	0	0
859	0	0	0	0	0	0	0	0	0	0	0	0	0	0
900	0	0	0	0	0	0	0	0	0	0	0	0	0	0

Table 9. State values produced by the California algorithm* for the incident data set 74051501, Santa Monica eastbound.

Incident occurred at 7:15:40 between stations 25 (upstream) and 26 (downstream).

$^{*}T_2 = .5,\ T_3 = .8,\ T_4 = .5,\ T_5 = .15.$

Direction of Travel →

Time \ Stations	18	19	20	21	22	23	24	25	26
700	0	0	0	0	0	0	0	0	0
701	0	0	0	0	0	0	0	0	0
702	0	0	0	0	0	0	0	0	0
703	0	0	0	0	0	0	0	0	0
704	0	0	0	0	0	0	0	0	0
705	0	0	0	0	0	0	0	0	0
706	0	0	0	0	0	0	0	0	0
707	0	0	0	0	0	0	0	0	0
708	0	0	0	0	0	0	0	0	0
709	0	0	0	0	0	0	0	0	0
710	0	0	0	0	0	0	0	0	0
711	0	0	0	0	0	0	0	0	0
712	0	0	0	0	0	0	0	0	0
713	0	0	0	0	0	0	0	0	0
714	0	0	0	0	0	0	0	0	0
715	0	0	0	0	0	0	0	0	0
716	0	0	0	0	0	0	0	0	0
717	0	0	0	0	0	0	0	0	0
718	0	0	0	0	0	0	0	1	0
719	0	0	0	0	0	0	0	2	0
720	0	0	0	0	0	0	0	2	0
721	0	0	0	0	0	0	0	2	0
722	0	0	0	0	0	0	0	2	0
723	0	0	0	0	0	0	0	2	0
724	0	0	0	0	0	0	0	2	0
725	0	0	0	0	0	0	0	2	0
726	0	0	0	0	0	0	0	2	0
727	0	0	0	0	0	0	0	2	0
728	0	0	0	0	0	0	0	2	0
729	0	0	0	0	0	0	0	0	0
730	0	0	1	0	0	0	0	0	0
731	0	0	0	0	0	0	0	0	0
732	0	0	0	0	0	0	0	1	0
733	0	1	0	0	0	0	0	0	0
734	0	0	0	0	0	0	0	0	0
735	1	0	0	0	0	0	0	0	0

Space-time set used for computing detection rate.

The reason for using a time interval that extends earlier than the time of detection is that the time of occurrence of the incident is an estimate extracted from data. We did not want to exclude a valid detection because of an erroneous estimate of the time of occurrence of the incident. Two stations were used for similar reasons--the location assigned to the incident cannot in all cases be assumed to be correct. We emphasize that detection performance depends upon the time-space sets chosen.

Having adopted a convention for counting detections, we then define

N_I Number of incident data sets

N_D Number of incidents detected

and then

$$\beta = \text{detection rate} \equiv 100 \cdot \frac{N_D}{N_I}$$
(percent)

A second aspect of detection performance which is of importance is the speed of detection, or delay time from occurrence of an incident to its detection. For each of the N_D incidents which are detected, we can compute

τ_i, $i = 1, \ldots, N_D$ Interval from estimated time of occurrence to time of detection.

These results can be displayed in several ways. For our purposes, we have chosen to compute the mean time to detect (among incidents detected),

$$M_D = \frac{1}{N_D} \sum_{i=1}^{N_D} \tau_i ,$$

and to generate a cumulative distribution from

$N_D(t)$ Number of incidents detected in time less than or equal to t

Specifically, we have generated plots of $N_D(t)/N_I$ versus t, e.g., as displayed in Figure 11 for the California algorithm (T_2=.5, T_3=8, T_4=.5, T_5=.15). Note that with our convention for counting incidents, the detection rate, β, is equal to 100 $N_D(20)/N_I$.

4.2 THRESHOLD CALIBRATION METHODOLOGY

An algorithm is defined by a binary tree structure and a set of thresholds, $T = \{(T_j, j=1,\ldots,n)\}$. For each value of T, one can derive the false alarm rate $\alpha(T)$ and the detection rate $\beta(T)$. This pair, $[\alpha(T)$,

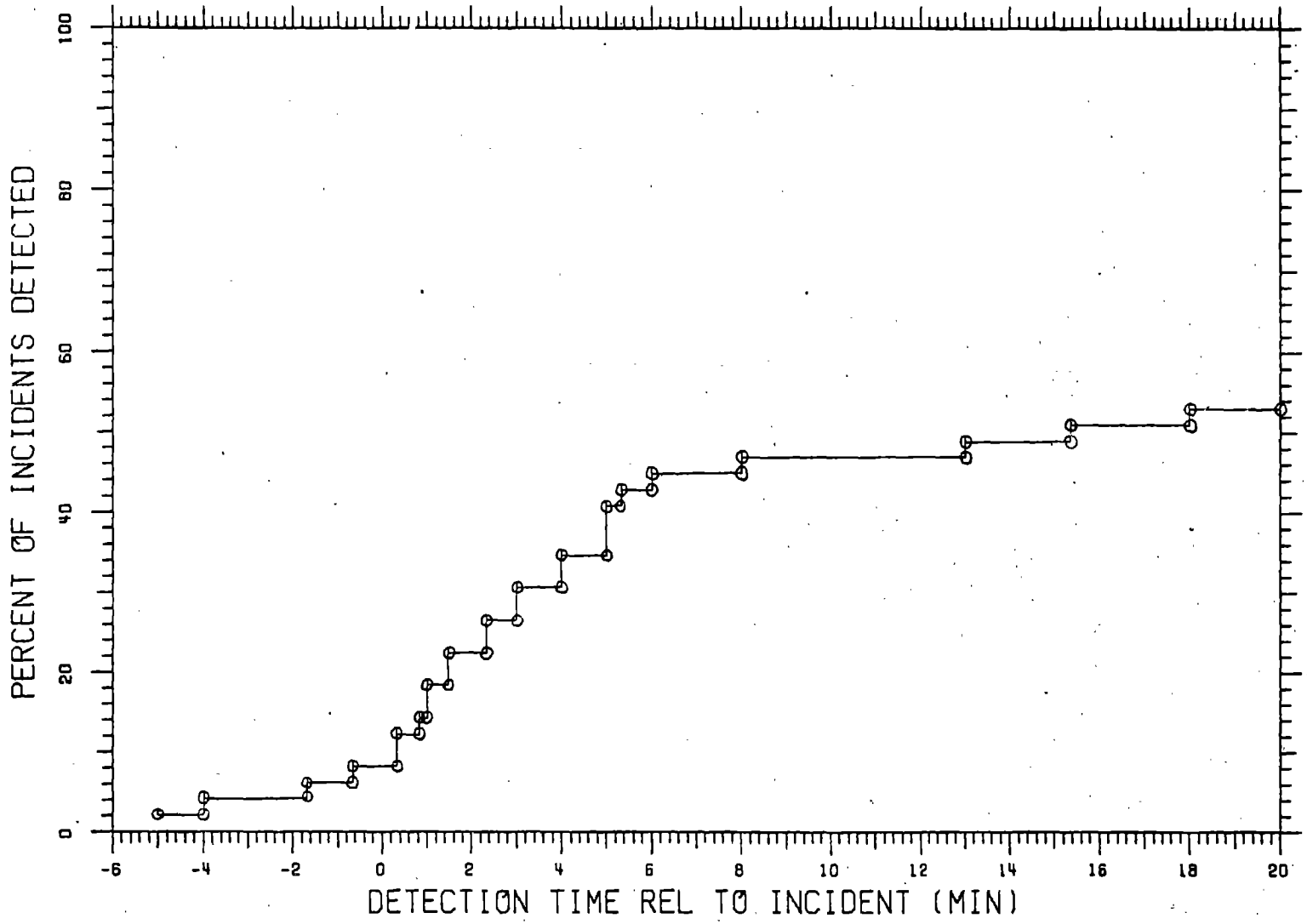

*T_2=.5, T_3=8, T_4=.5, T_5=.15

Figure 11. Cumulative distribution of detection rate versus time to detect for the California algorithm* (figure 8).

$\beta(T)]$, can be displayed as a point in a plane, Figure 12. For convenience, the pair $[\alpha(T^k), \beta(T^k)]$ is labeled 'k'.

Associated with any point 'k', (for example, '1'), there is a region (for '1', the shaded region) which is dominated by that point; that is, performance pairs in the region have false alarm rates at least $\alpha(T^k)$ and detection rates not greater than $\beta(T^k)$. Points in this region (e.g., points '2' and '3') are inferior since better performance is achieved by the use of T^k. A point which is not inferior to any other point is non-inferior. The set of noninferior points defines the tradeoff curve for that algorithm. Points '1', '4', '5', and '6' of Figure 12 are non-inferior.

In Figure 13, performance pairs are plotted for Algorithm 7, illustrated in Figure 14. Inferior points are identified by open circles. The solid circles denote points that are noninferior among points represented by circles. The points represented by circles were generated by evaluating this algorithm for the 540 threshold sets obtained by all possible combinations for which individual thresholds were chosen as follows:

$$T_1 = 8, 10, 12, 14, 16, 18, 20, 22, 24, 26$$

$$T_2 = .30, .32, .34, .36, .38, .40$$

$$T_3 = 12, 13, 14, 15, 16, 17, 18, 19, 20$$

Thus, one could identify the tradeoff curve for a particular algorithm by selection from performance results obtained for a large collection of specified threshold sets.

However, we note that a noninferior point can be characterized as the solution to an optimization problem:[1]

Problem P(y):

$$\min_T \left[\alpha(T) \,\middle|\, \left\{\beta(T) > y\right\}\right] = \alpha(T^*)$$

That is, the algorithm is noninferior with the threshold set T* if the false alarm rate $\alpha(T^*)$ is least for all choices of threshold sets which produce a detection rate not less than $\beta(T^*)$. Calibration of an algorithm consists of solving a collection of such problems, each with y taken to be a specified detection rate.

---

[1] H. J. Payne, E. Polak, D. C. Collins, and W.S. Meisel, "An Algorithm for Bicriteria Optimization Based on the Sensitivity Function," IEEE Trans. Auto. Cont., Vol 20, No. 4 (August 1975), pp 546-548.

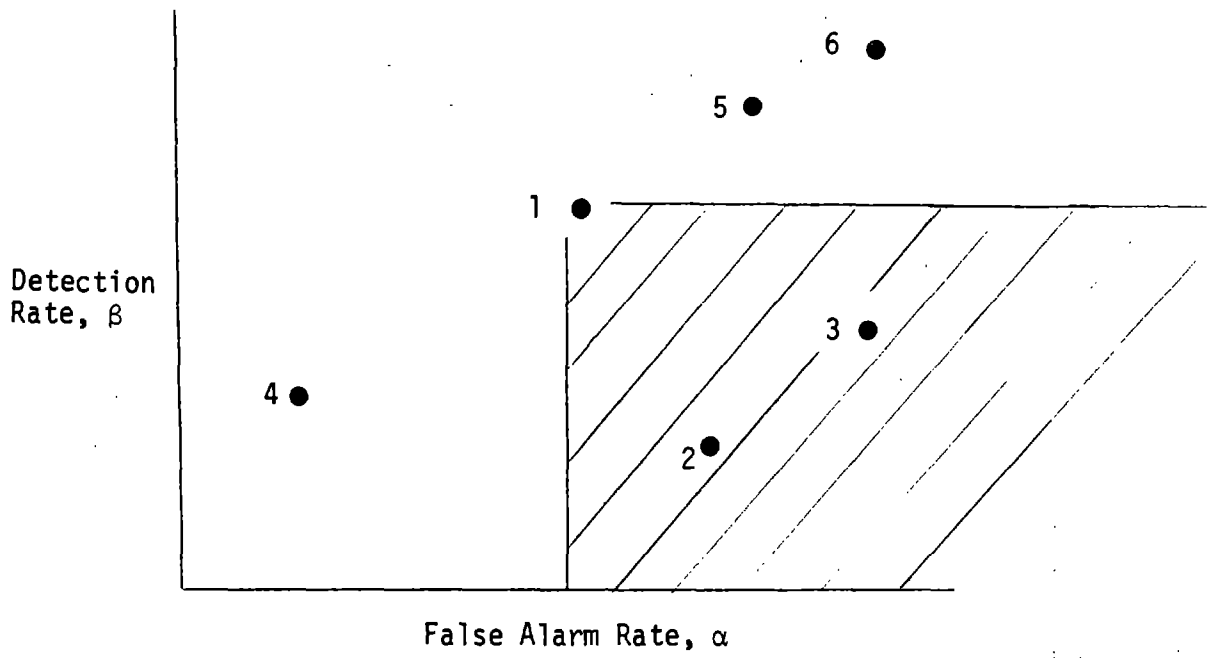

Figure 12. Detection rate and false alarm rate pairs for an incident detection algorithm.

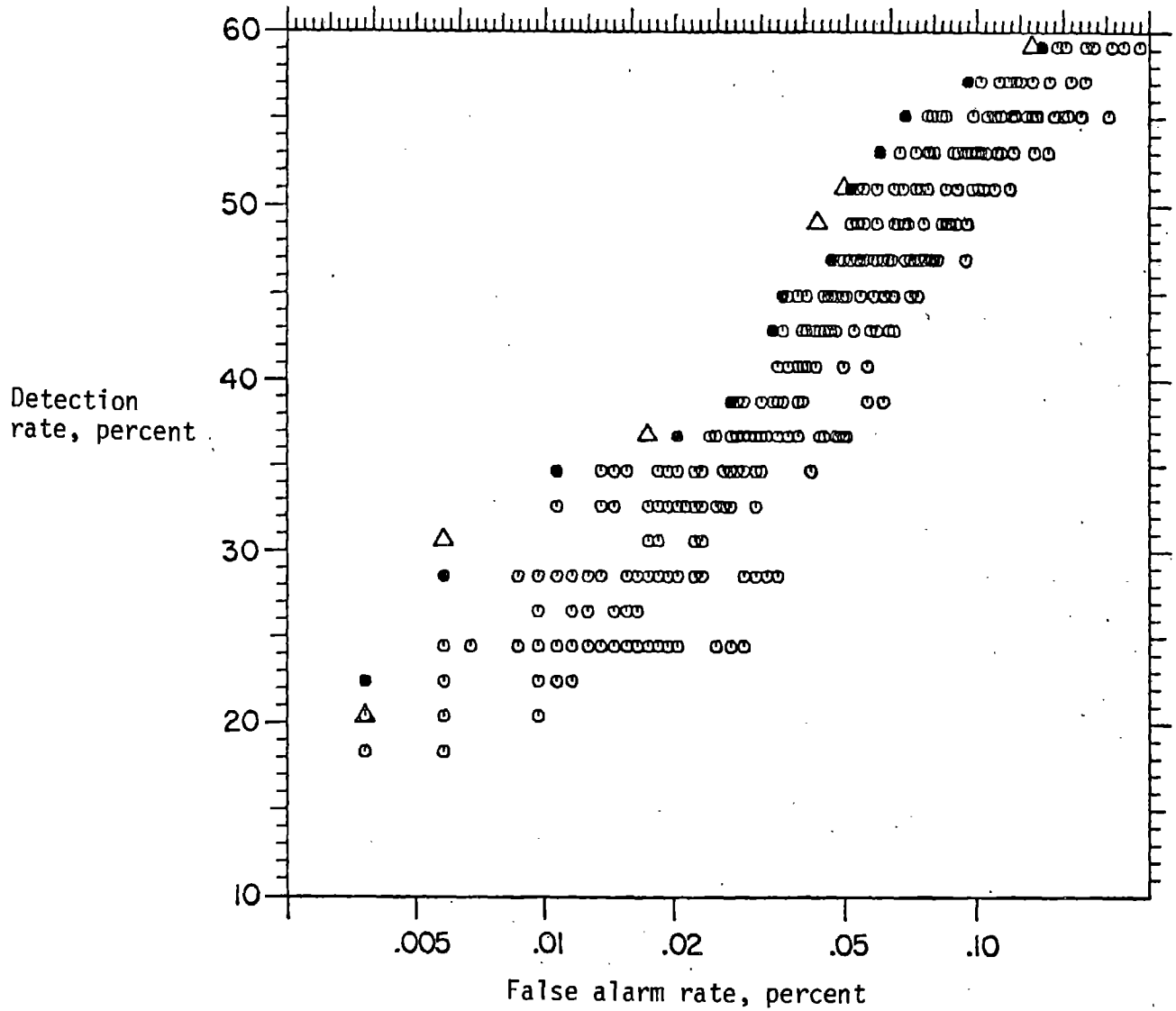

Figure 13. Performance pairs for Algorithm 7.

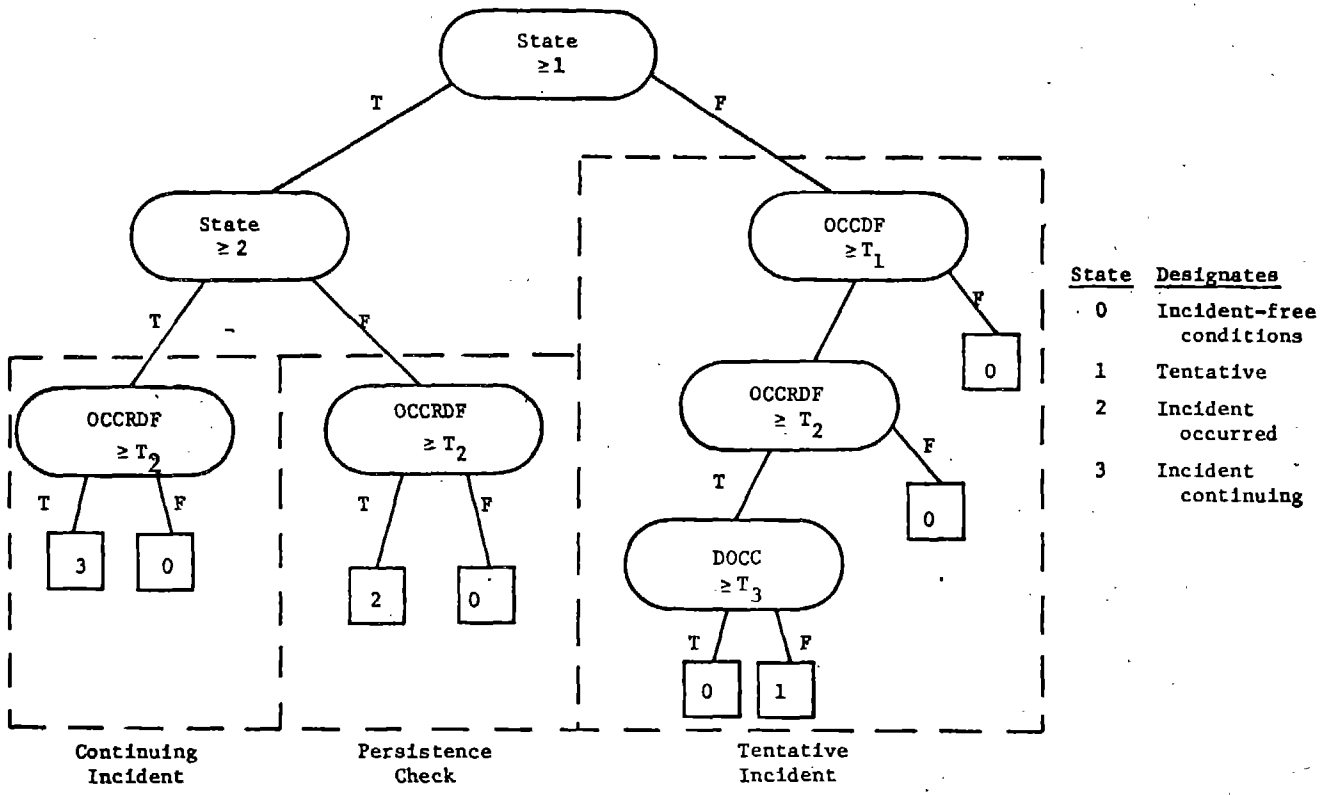

Figure 14. Decision tree for Algorithm 7.

In Figure 13 triangles are points which were generated by software which we developed to exploit the characterization of a noninferior point as the solution of the above optimization problem. In the next section, the use of this software is described.

4.3 EVALUATION AND CALIBRATION SOFTWARE AND RELATED DATA REQUIREMENTS

Software was developed to evaluate a multiple-feature algorithm and to calibrate thresholds by means of the optimization technique identified in the previous section. The capabilities of this software and required data are described here.

4.3.1 Evaluation and Calibration Software

The calibration methodology identified in the previous section has been embodied in a computer program CALB whose structure is illustrated in Figure 15. This program has two major options--evaluation and calibration.

When the evaluation option is selected, the detection and false alarm rates for an algorithm with specified thresholds are computed. In addition, cases in which the algorithm produced a detection signal are printed. For incidents, the case printed is the first case which produced the detection signal. The printed list of false alarms and detections is an important diagnostic tool in assessing the performance of an algorithm.

When the calibration option is exercised, several sets of thresholds are determined, each set being the solution of the optimization problem. The resultant detection and false alarm rates define the tradeoff curve for that algorithm. The optimization procedure we have used is a structured random search, described in more detail in Volume 4 of this report.

Use of this software requires that the user prepare a data base, define certain parameters, and write several subroutines to provide program access to the data and parameters. These requirements are discussed in detail in Volume 4 of this report.

4.3.2 Data Requirements

The calibration software identifies noninferior threshold values by exercising an optimization routine which involves repeated evaluations of an algorithm. The quality of the calibration depends very much on the size of the data base.

To identify required sizes of the incident-free and incident data bases, we will first determine confidence limits on the detection and

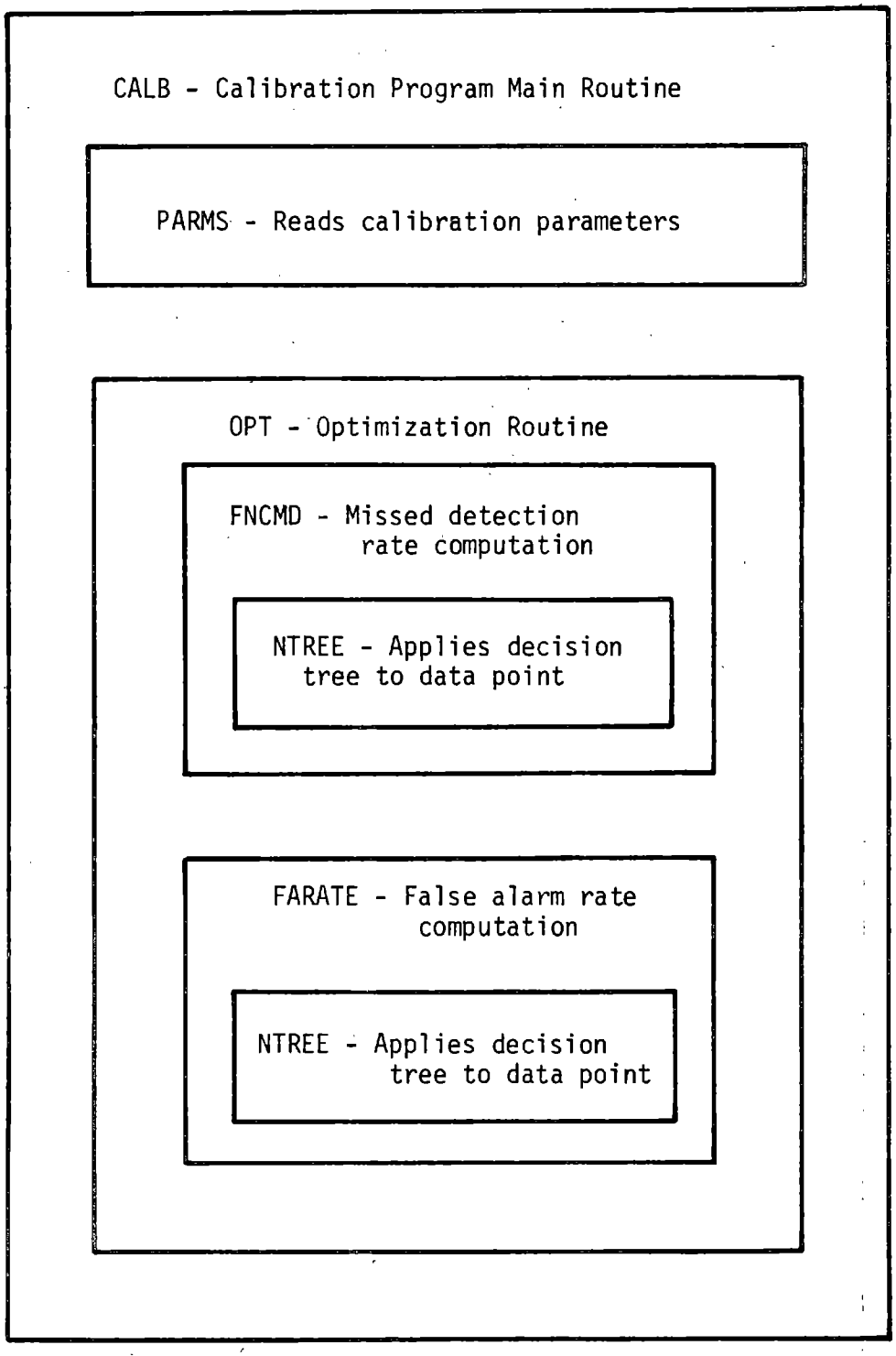

Figure 15. Structure of calibration program.

false alarm rates for data bases of specified size. Suppose there are N_F incident-free cases and N_I incident data sets and that the computed rates are α(false alarm) and β(detection).

If α_0 is the underlying probability of false alarm, the number of false alarms determined from a data base is described by a binomial distribution. When a large number of independent cases is used to compute the false alarm rate, α, it is very nearly normally distributed. It can be shown[1] that the probability that α_0 is in the range

$$\frac{1}{1+k^2/N_F}\left(\alpha + \frac{k^2}{2N_F} \pm k\sqrt{\frac{\alpha(1-\alpha)}{N_F} + \frac{k^2}{4N_F^2}}\right) \qquad (1)$$

is $\gamma(k)$, with $(k,\gamma(k))$ determined by the normal distribution.[2] Some useful values are given in Table 10.

Table 10. Parameters for confidence limits

k	$\gamma(k)$
2.57	.99
2.00	.9545
1.96	.95
1.64	.90

Identical relations apply to the detection rate with $\beta(\beta_0)$ replacing $\alpha(\alpha_0)$ and N_I replacing N_F.

As the successive incident-free cases are somewhat dependent, the effective number of cases is less than the number of cases in the data base. Hence, the true confidence intervals are somewhat larger than those given by (1).

Values of confidence limits for selected values of false alarm rates and missed detection rates are given in Tables 11 and 12, respectively. These tables indicate a very considerable computational requirement for calibration. Fortunately, it is possible to reduce this requirement by at

[1] B. W. Lindgren and G. W. McElrath, Introduction to Probability and Statistics, New York, The Macmillan Company, 1959.

[2] $\gamma(k)$ = probability $\{-k<X<k\}$ where X has the normal distribution N(0,1).

Table 11. 95% confidence limits (γ=.95) for false alarm rates.

	α = .05%		α = .25%	
N_F	Lower Limit (%)	Upper Limit (%)	Lower Limit (%)	Upper Limit (%)
100	.0006	3.7951	.0144	4.1665
1000	.0052	.4771	.0775	.8033
2000	.0088	.2827	.1068	.5839
5000	.0155	.1612	.1447	.4317
10000	.0214	.1170	.1694	.3688
20000	.0272	.0920	.1897	.3294
100000	.0379	.0659	.2209	.2829

Table 12. 95% confidence limits (γ=.95) for detection rates.

	β = 50%		β = 80%	
N_I	Lower Limit (%)	Upper Limit (%)	Lower Limit (%)	Upper Limit (%)
10	23.66	76.34	49.02	94.33
20	29.93	70.07	58.40	91.93
50	36.64	63.36	66.96	88.76
100	40.38	59.62	71.11	86.66
200	43.14	56.86	73.91	84.95
500	45.63	54.37	76.27	83.27
1000	46.91	53.09	77.41	82.36

least an order of magnitude without any loss in the quality of the calibration by culling from the data base only those cases where a change in the threshold in the specified ranges can make a difference in whether the algorithm produces an incident signal.

Consider calibration of the California algorithm where we consider thresholds in the ranges $T_2 \geq .3$, $T_3 \geq 5$, $T_4 \geq .3$, and $T_5 \geq 0$. (See page 38.) From the structure of the algorithm, it is evident that, for any particular case, the algorithm will not produce a nonzero state value for thresholds in these ranges if the algorithm with the thresholds $T_2=.3$, $T_3=5$, $T_4=.3$, and $T_5=0$ does not. Hence, we need not repeatedly evaluate these cases. The reduced data base is therefore defined by cases for which the algorithm produces a nonzero state value with the (minimum) thresholds identified.

Starting with N_F, N_I of adequate size to obtain satisfactory confidence limits on the false alarm and detection rates, the culling process will yield data bases of sizes $\overline{N}_F$ and $\overline{N}_I$. Careful culling will produce an incident-free data base such that $\overline{N}_F$ is considerabily smaller than N_F while $\overline{N}_I$ is still nearly N_I. The program CALB accepts as parameters the number of incident-free cases and the number of incident data sets which are eliminated by this culling process.

It is the responsibility of the user to cull his data and to determine the number of cases skipped. To aid the user in this effort, the program CULDTA has been developed and is documented in Volume 4 of this report. Examples of culling are given in analyses of Section 5.

4.4 PAIRWISE COMPARISON OF ALGORITHMS

The following question arises: Given tradeoff curves for two algorithms, how do we know if the differences are statistically significant? Here we present a simple means for resolving this question which is based upon a comparison of the two false alarm rates for the two algorithms corresponding to the <u>same</u> detection rates. The basis for this is detailed in Appendix C. The idea of the test for statistical significance is whether the difference observed could be attributed to two outcomes of an experiment involving two algorithms with identical false alarm rates.

Figures 16 and 17 provide the needed information for judging whether the differences are statistically significant at levels of .10, .05 and .01. For example, a difference is statistically significant at the .10 level if the probability that this (or a larger) difference would be observed from two outcomes pertaining to two algorithms with the same false alarm rate is .10. To illustrate use of Figure 17, consider the comparison of two algorithms which both provide a detection rate of 51%, while the false alarm rates are .222% and .070%, respectively. This pair of false alarm rates is identified on the figure as point A and lies <u>above</u> the curve pertaining to the .01 level of significance, hence the difference

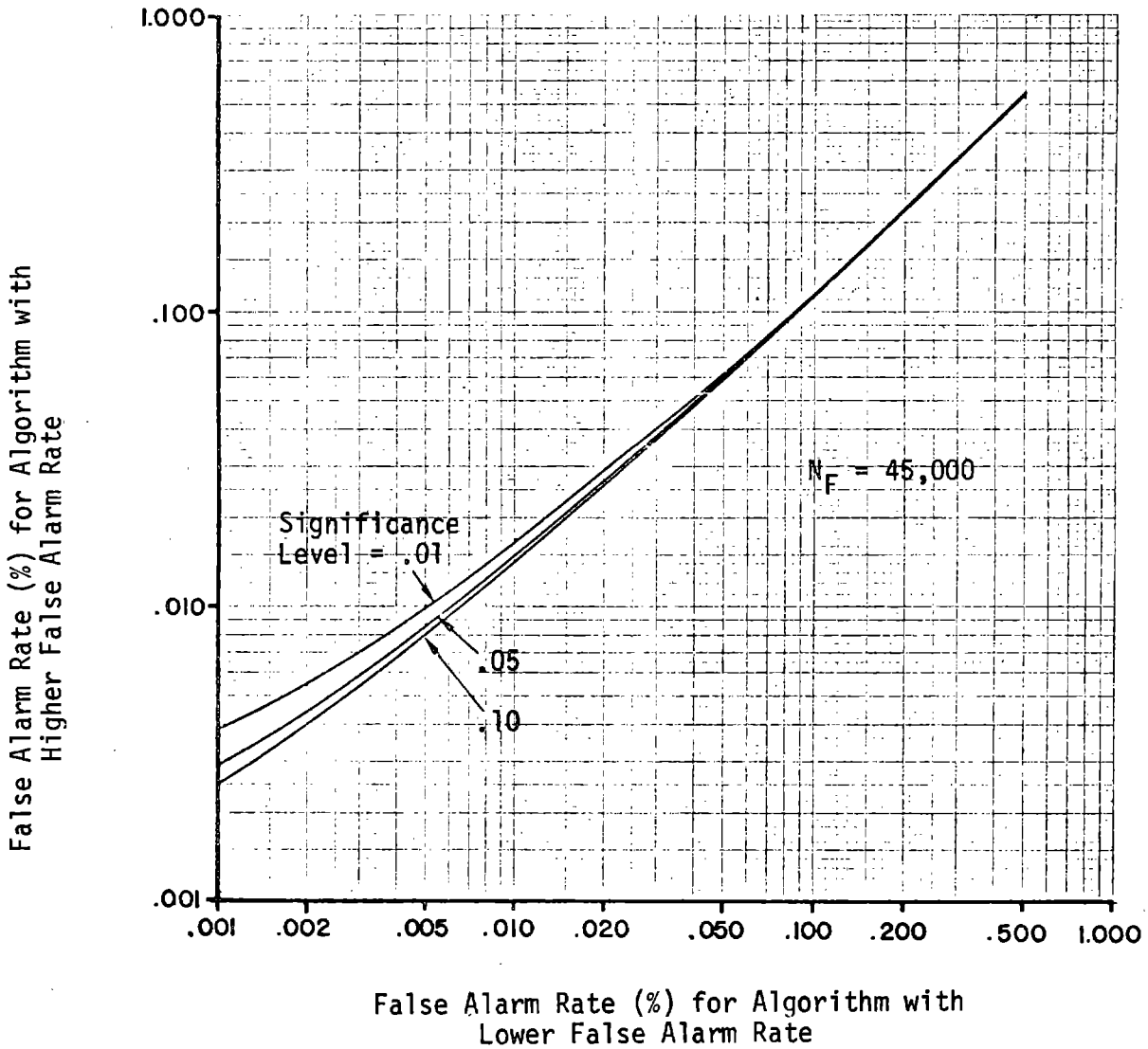

Figure 16. Comparison of false alarm rates for two algorithms, N_F = 45,000.

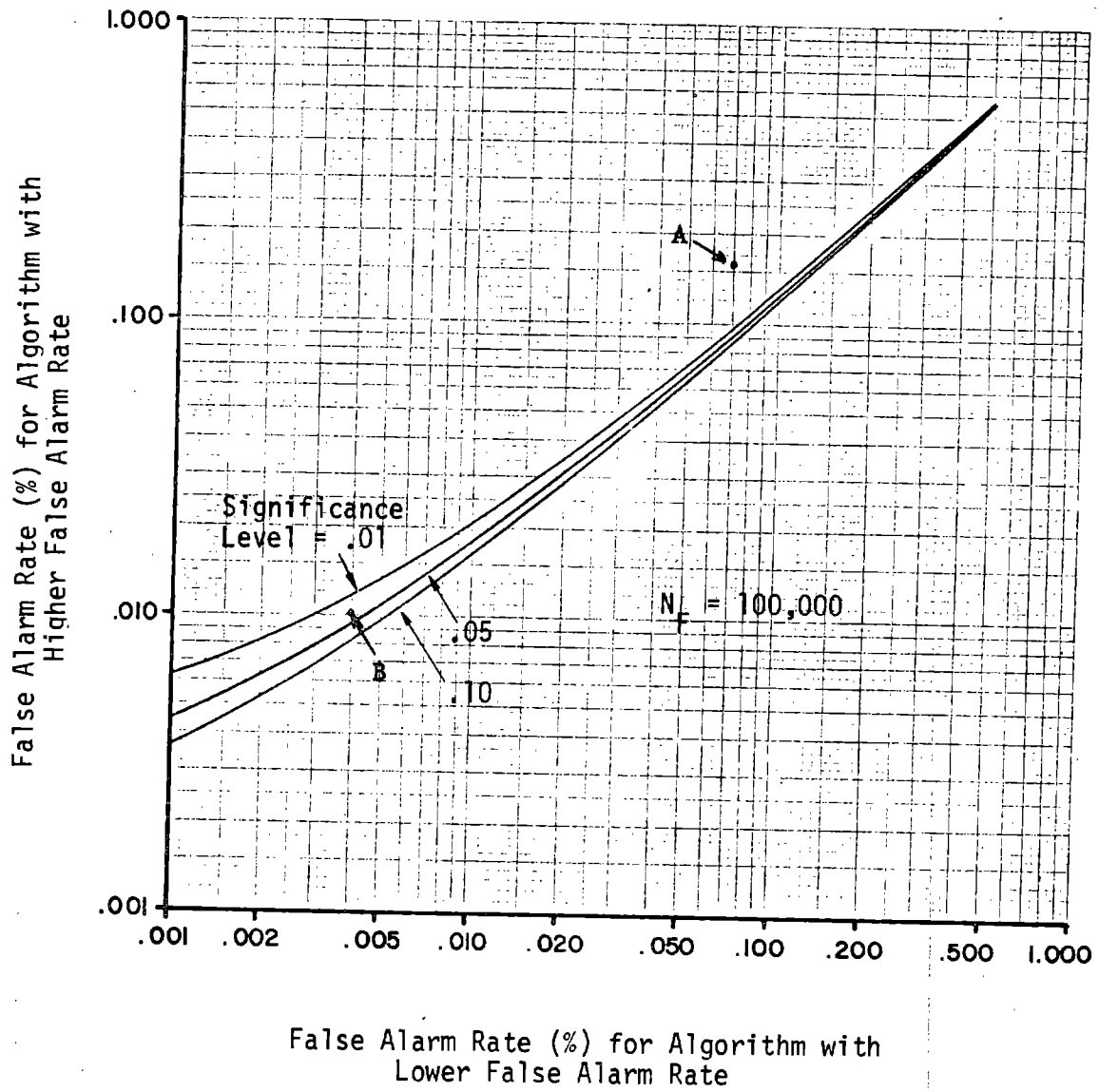

Figure 17. Comparison of false alarm rates for two algorithms, N_F = 100,000.

is statistically significant at a level less than .01. Point B corresponds to false alarm rates of .004% and .010% and lies between the curves for significance levels .01 and .05. Hence this difference is significant at a level less than .05 but more than .01.

In examining comparative tradeoff curves in the remainder of this volume, Figures 16 and 17 can be similarly used to judge statistical significance of the differences observed. Note that one should compare false alarm rates pertaining to the same detection rate.

4.5 DEPENDENCE OF PERFORMANCE MEASURES ON THE DATA BASE

It should be evident that the measures of performance which are produced by the software we have described depend upon the data base used. As a result, one should take care in making application of the resultant measures to assess potential performance in an operational environment. If the environment in which an algorithm is to be used is not accurately represented by the data base we have used to obtain performance measures, differences in these measures from those we have computed can be expected.

It will be seen in the analyses in the next three sections that there are significant differences in the performance measures for the same algorithm with fixed thresholds due to the differences in the data bases. Specifically, results obtained for the Los Angeles and Minneapolis data bases are significantly different. Part of these differences derives from the fact that the Los Angeles data base includes a substantial number of incident data sets pertaining to incidents with only a slight impact on traffic data. By examining a range of incident types, including some with only a relatively slight impact, we were better able to define the limits of performance of the algorithms considered. As a result, however, our results lead to detection rates substantially lower than those reported in previous studies.[1,2] These differences are reconciled, however, by use of a common data base.[3]

When a common data base is used to evaluate several algorithms, relative performance of the algorithms is of most importance. That is if one algorithm yields better performance than a second with respect to a common data base, one expects this ordering to hold as well in an operational environment even though the absolute measures of performance may not be the same. Our algorithm development is based on this idea and was tested in part by comparing algorithm performance measures for two data bases, one from Los Angeles, the second from Minneapolis.

---

[1] A.R. Cook and D. E. Cleveland, Ibid.

[2] K.G. Courage and M. Levin, Ibid.

[3] H.J. Payne, D.N. Goodwin, and M.D. Teener, Ibid.

5. BASIC ALGORITHM DEVELOPMENT WITH THE LOS ANGELES DATA BASE

Using the binary decision tree structure as a basis and a portion of the Los Angeles data base, a sequence of ten algorithms were defined, calibrated, and evaluated. This development was guided by careful examinations of algorithm performance so that sources of false alarms, in particular, could be identified. With an understanding of the sources of false alarms, new algorithms were defined, calibrated, and evaluated.

As a result of this development, we have been able to identify several algorithms with markedly improved performance relative to that for algorithms previously considered. These new algorithms are entirely based upon features which are simple functions of occupancy.

For ease of reference, definitions of algorithms and calibration and evaluation results have been assembled in Appendix B.

5.1 GENERAL ANALYSIS PROCEDURE

Each algorithm we considered was analyzed using a common procedure, in steps we now describe.

5.1.1 The Los Angeles Data Base

The Los Angeles data base includes a total of 118 incident and 25 incident-free data sets, taken from the portion of the Los Angeles freeway system illustrated in Figure 18. The incident data sets used in this evaluation are described in Table 13 by probably time of incident occurrence, location, classification number, traffic level, and incident type. Location is specified by the station immediately upstream of the site of the incident and lane of occurrence (M denotes median; RS, right shoulder; numbers denote lanes) where such information was available. Definitions of the last three items are given in Table 14. The incident-free data sets used in this evaluation are described in Table 15 by location, time period, and data excluded.

In general, each data set was derived from one-minute averages of occupancy and volume, updated every minute and averaged over all lanes. Data pertaining to each incident cover a time span of twenty-six minutes from five minutes prior to the incident to twenty minutes after the incident for the upstream and downstream stations surrounding the incident length and covers all stations for the section of the freeway identified. In certain instances, however, data pertaining to some time periods and stations were removed from a data set because it appeared that an incident had occurred or equipment had malfunctioned.

Various subsets of the collections of incident and incident-free data sets were used in different stages of our study. Thus, in Tables 13 and 15 we distinguish four subsets of these collections. The first

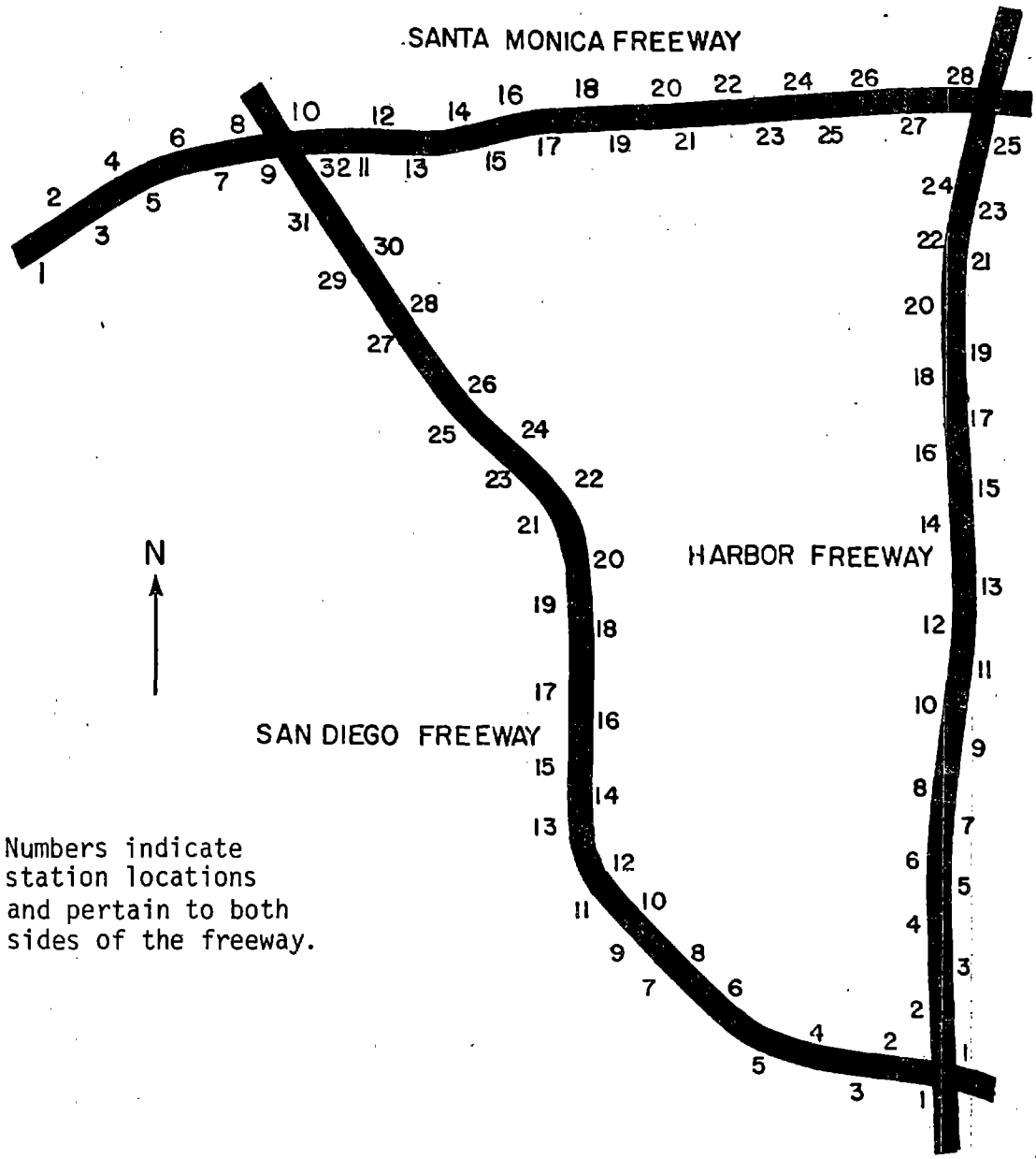

Figure 18. Los Angeles data collection site.

Table 13. Incident data sets in the Los Angeles data base.

Data Set I.D.	Fwy No.	Estimated Time of Occurrence	Location Upstream Station	Lane	Class	Traffic Level	Type	Included in Los Angeles Data Base	Full Los Angeles Data Base	Sensor Configuration Study	Lane Identification Study
74031201	5	163340	20		2	2	DISL		X		
74031301	1	154900	22	5	2	2	TCOL	X	X		X
74031302	5	134900	25	1	2	3	DISL		X		X
74031303	5	170600	13		2	2	TCOL		X		
74032102	6	183600	24	2	1	1	DISL		X		X
74032201	6	130640	14	4	1	3	TCOL		X		X
74032202	2	174800	21	4	1	3	TCOL	X	X		X
74032203	1	181600	23		1	1	GAWK	X	X		
74032502	6	151500	21		1	1	DISL		X		
74032603	5	160430	23		3	1	GAWK		X		
74032901	2	172700	27		2	1	TCOL	X	X		
74032902	4	173940	14		2	1	TCOL	X	X		
74040101	5	155300	18		3	2	GAWK		X		
74040102	5	144240	20		1	2	TCOL				
74040103	2	174930	20	1	1	2	DISL	X	X		X
74040301	6	143500	12		1	3	TCOL		X		
74040302	6	153000	24	2	1	2	DISL		X		X
74040401	2	144740	13	M	2	2	TCOL		X		X
74041603	1	102000	22	3	2	1	DISL		X		X
74041901	5	155020	09	1	1	3	TCOL		X		X
74042201	1	091500	21	5	1	1	DISL	X	X		X
74042401	1	064000	21		2	2	DISL	X	X		
74042402	1	070100	21		2	2	TCOL	X	X		
74042403	1	071540	17		2	1	TCOL	X	X		
74042601	2	070940	23	M	2	3	TCOL	X	X		X
74042602	1	074800	22	4	2	1	DISL		X		X
74042605	6	143400	20		1	2	TCOL		X		
74042606	4	160700	16	1	1	1	TCOL		X		X
74051501	1	071540	25	RS	1	2	DISL	X	X		X

Table 13. Incident data sets in the Los Angeles data base (continued).

Data Set I.D.	Fwy. No.	Estimated Time of Occurrence	Location Upstream Station	Lane	Class	Traffic Level	Type	Included in Los Angeles Data Base	Full Los Angeles Data Base	Sensor Configuration Study	Lane Identification Study
74051502	3	074520	09	1	1	2	DISL		X		X
74051503	1	082620	19		1	1	DISL		X		
74052101	1	085300	18		2	1	TCOL		X		
74052102	5	090400	19		2	2	TCOL		X		
74052201	5	083240	10		1	2	TCOL		X		
74052202	2	140230	22		1	3	DISL	X	X		
74052203	2	160840	26	3	1	2	TCOL		X		X
74052204	5	162000	20	3	1	2	TCOL		X		X
74052301	2	160800	04		1	4	TCOL	X	X		
74052302	2	162600	27		1	3	TCOL	X	X		
74052303	2	163710	13		1	2	TCOL	X	X		
74052304	2	164500	12		1	3	DISL		X		
74052305	2	170100	14		1	1	TCOL		X		
74052306	2	174000	27		1	1	DISL		X		
74052403	3	144000	31		1	2	TCOL	X	X		
74052404	2	161440	23		3	1	NOTH	X	X		
74052802	1	073900	13	2	2	1	DISL		X		X
74052804	4	090400	28		1	1	TCOL	X	X	X	
74052902	2	075400	27		1	3	DISL		X		
74053001	1	063640	14	1	1	3	TCOL	X	X		X
74053003	3	074200	29		1	1	TCOL		X	X	
74053004	5	074730	18		1	1	DISL		X		
74060301	2	075900	07		2	3	TCOL	X	X		
74060501	5	080200	16	1	1	1	TCOL		X		X
74060603	2	155640	27		1	1	DISL				
74060701	1	075800	21		1	1	TCOL	X	X		
74061301	4	161100	16		1	1	DISL				
74061302	4	151640	30		1	2	TCOL	X	X		
74061701	1	082520	13		1	1	TCOL		X		
74061901	2	170300	22	2	1	2	TCOL		X		X
74062401	1	090300	25		1	1	DISL	X	X		
74062402	5	084620	20	3	1	1	SPIL		X		X
74062501	1	075140	21		1	1	DISL	X	X		

Table 13. Incident data sets in the Los Angeles data base (continued).

Data Set I.D.	Fwy No.	Estimated Time of Occurrence	Location Upstream Station	Location Lane	Class	Traffic Level	Type	Included in Los Angeles Data Base	Included in Full Los Angeles Data Base	Included in Sensor Configuration Study	Included in Lane Identification Study
74070302	2	084900	03		1	4	TCOL		X		
74071201	2	062500	05		4	4	GAWK		X		
74072501	4	075640	28		1	1	TCOL		X	X	
74073001	4	061000	27	4	1	3	DISL		X	X	X
74083001	3	144200	29		4	4	DISL		X	X	
74100201	3	110700	30		1	3	TCOL	X	X	X	
74100701	3	074200	28		2	1	GAWK	X	X	X	
74100702	3	075800	31		4	1	TCOL	X	X	X	
74100703	3	153800	30		1	2	DISL	X	X	X	
74100704	4	154100	29		1	2	DISL	X	X	X	
74100706	4	163600	29	1	1	2	DISL		X	X	X
74100707	4	163240	26		1	3	DISL	X	X	X	
74100708	3	070330	25		1	2	DISL				
74100710	4	162900	25		4	3	DISL		X	X	
74100711	1	070200	03		4	3	DISL		X		
74100712	1	070200	06		4	3	GAWK		X		
74100714	2	073400	07		4	4	GAWK		X		
74100715	1	080220	11		1	1	DISL		X		
74100716	2	080900	10		1	3	DISL		X		
74100717	1	082600	10		1	1	DISL		X		
74100801	3	082700	31		4	2	DISL	X	X	X	
74100802	4	092200	30		4	3	DISL	X	X	X	
74100803	3	092200	26		4	3	GAWK	X	X	X	
74100804	4	094000	32		3	3	GAWK	X	X	X	
74100805	3	171120	29		2	2	DISL	X	X	X	
74100806	4	180320	32		2	3	SPIL	X	X	X	
74100901	3	075400	29		4	1	DISL	X	X	X	
74100902	3	075900	27		4	1	DISL	X	X	X	
74100903	4	082100	32		1	1	TCOL	X	X	X	

Table 13. Incident data sets in the Los Angeles data base (concluded).

Data Set I.D.	Fwy No.	Estimated Time of Occurrence	Location Upstream Station	Location Lane	Class	Traffic Level	Type	Included in Los Angeles Data Base	Included in Full Los Angeles Data Base	Included in Sensor Configuration Study	Included in Lane Identification Study
74100904	2	164400	26	1	1	1	TCOL		X		X
74100906	3	171820	30		1	2	GAWK		X	X	
74101002	4	085600	32		4	3	DISL	X	X	X	
74101003	3	160640	30		1	1	DISL		X	X	
74101004	4	161100	30		4	2	DISL	X	X	X	
74101005	3	160620	25		1	2	DISL	X	X	X	
74101006	3	162900	26		4	3	TCOL	X	X	X	
74101007	3	173200	31		1	1	DISL	X	X	X	
74101008	4	175000	32		4	3	DISL	X	X	X	
74101101	4	071000	27		1	2	GAWK	X	X	X	
74101102	3	074600	27		1	3	DISL	X	X	X	
74101104	4	075500	26		4	2	DISL	X	X	X	
74101106	4	082100	27		4	2	DISL		X	X	
74101107	3	171400	28		3	1	GAWK		X	X	
74111402	5	074700	18		3	1	GAWK		X		
74120502	2	065700	23		4	3	DISL		X		
74120503	1	072640	26		1	2	DISL		X		
74120505	1	075600	25		4	1	DISL		X		
74120507	1	075720	25		3	1	TCOL		X		
74120508	1	083000	16		1	1	DISL		X		
75012301	2	164500	20		1	2	DISL		X		
75012302	1	070300	23		4	2	DISL				
75012303	2	122420	25		1	1	GAWK				
75012305	2	175300	23	3	1	1	DISL		X		X
75022701	1	081000	13	2	1	1	DISL		X		X
75022801	5	132740	24		1	3	DISL				

Table 14. Incident data set characteristics definitions.

CLASS

Class 1 - good data set; incident has definite impact on traffic conditions.

Class 2 - inadequate location; good data set but incident location is vague; usually only a station number is indicated.

Class 3 - unusual data set; good data set but unusual incident such as animal on roadway, malfunctioning detectors, etc.

Class 4 - marginal data set; incident has little or no apparent impact on traffic conditions.

TRAFFIC LEVEL

Traffic levels 1 and 5 - occupancy greater than 24%.

Traffic levels 2 and 6 - occupancy less than 24%, volume 1400 vehicles per lane per hour, or greater.

Traffic levels 3 and 7 - occupancy less than 24%, volume between 700 and 1400 vehicles per lane per hour.

Traffic levels 4 and 8 - occupancy less than 24%, volume less than 700 vehicles per lane per hour.

FREEWAY NUMBER

Freeway no. 1 - SME, Santa Monica Eastbound

Freeway no. 2 - SMW, Santa Monica Westbound

Freeway no. 3 - SDN, San Diego Northbound

Freeway no. 4 - SDS, San Diego Southbound

Freeway no. 5 - HAN, Harbor Northbound

Freeway no. 6 - HAS, Harbor Southbound

INCIDENT TYPE

TCOL - traffic collision

DISL - disabled vehicle

GAWK - gawking

NOTH - nothing; false alarm

SPIL - spilled load

Table 15. Incident-free data sets in the Los Angeles data base.

Data Set No.	Freeway	From	To	Excluded Data	Reason for Exclusion	Included in Los Angeles Data Base	Included in Full Los Angeles Data Base	Sensor Configuration Study
74042350	HAN	0640	0925			X	X	
74042353	SME	0640	0815	Time ≥ 0815	Incident	X	X	
74042354	SMW	0640	0925	Stations 6,7,8	Malfunction	X	X	
74042358	SMW	1110	1355	1) Stations 26,27 2) Stations 6,7,8	Bad data Malfunction	X	X	
74042359	SMW	1610	1855	1) Stations 6,7,8 2) Stations 23-27; Time 1709-1730	Malfunction Incident	X	X	
74042360	SMW	2110	2355	Stations 6,7,8	Malfunction	X	X	
74042363	SDS	2110	2355			X	X	X
74042364	HAN	1109	1345	Time ≥ 1345	Incident	X	X	
74042067	SDN	1110	1355	Stations 25-27; Time ≥ 1331	Malfunction	X	X	X
74042368	SDN	1610	1840	Stations 22-24 Time ≥ 1839	Malfunction	X	X	X
74042369	SDN	2110	2300			X	X	X
74061053	SMW	0630	0925			X	X	
84061054	SMW	1110	1400			X	X	
74090450	SDN	0640	0925	Stations 22-24	Malfunction	X	X	X
74090451	SDN	1110	1354:40	1) Stations 22-24 2) Stations 28-32; Time 1230	Malfunction Incident	X	X	X
74090452	SDN	1610	1855	Stations 22-24	Malfunction	X	X	X
74090453	SDN	2110	2355	Stations 22-24	Malfunction	X	X	X
74090454	SDS	0640	0925	Stations 1-16; Time 0639-0850	Malfunction	X	X	X
74090455	SDS	1110	1354:40	Station 32; Time 1110-1214:40 Station 31; Time 1125:40-1214:40	Bad data Bad data	X	X	X
74090458	HAN	0640	0925			X	X	
74090459	HAN	2100	2355			X	X	
74090462	SME	0640	0925			X	X	
74090463	SME	2110	2355			X	X	
74090464	SMW	1619	1855	Stations 23-28; Time 1705-1810	Incident	X	X	
74090465	SMW	2110	2355				X	

of these is termed simply the "Los Angeles data base" since it is the one most used. This data base coincides with the data base used in the first interim report. Unless otherwise noted in Section 5 analysis was done with this data base. The second pair of subsets is termed the "full Los Angeles data base." It includes all the data in the "Los Angeles data base" and an additional 60 incident data sets. This data base was used to evaluate results obtained in working with the Los Angeles data base. The remaining subsets of data were used in the sensor configuration and lane identification studies, respectively, as reported in Section 6.

5.1.2 Coding the Algorithm

The first step in the general procedure specific to an algorithm is defining it and coding it as a binary tree with a state. To illustrate this and succeeding aspects of our general analysis procedure, we will indicate details for the version of the California algorithm illustrated in Figure 8. This algorithm was considered earlier as an example in Section 3.2.1. Coding the structure of the algorithm involves specification of the array NTR as was done there.

5.1.3 Culling the Data

The incident-free data contained in excess of 100,000 valid cases for our tests. As noted in Section 4.3.2, computational effort is greatly reduced by culling from this, and from the incident data, only those cases which might generate an incident signal for the range of thresholds considered.

The algorithm of Figure 8 involves the use of three features: OCCDF, OCCRDF, and DOCCTD. Experience with these features indicates that useful ranges for the first two features are OCCDF ≥ 5 and OCCRDF $\geq .3$. The way this algorithm is constructed, one would associate incidents with positive values of DOCCTD. However, we also planned to investigate modifications to this algorithm which did not use DOCCTD so that for purposes of generating a culled data base, no restriction was placed on DOCCTD. Therefore, to obtain a culled data base suitable for the algorithm of Figure 8 and several others, we selected cases for which a nonzero state was generated by the algorithm displayed in Figure 19.[1] This was accomplished through the use of the program CULDTA. Details of the use of this program in this instance are given in Volume 4 of this report.

[1]Actually, a more complex tree was used (to remove cases involving missing data).

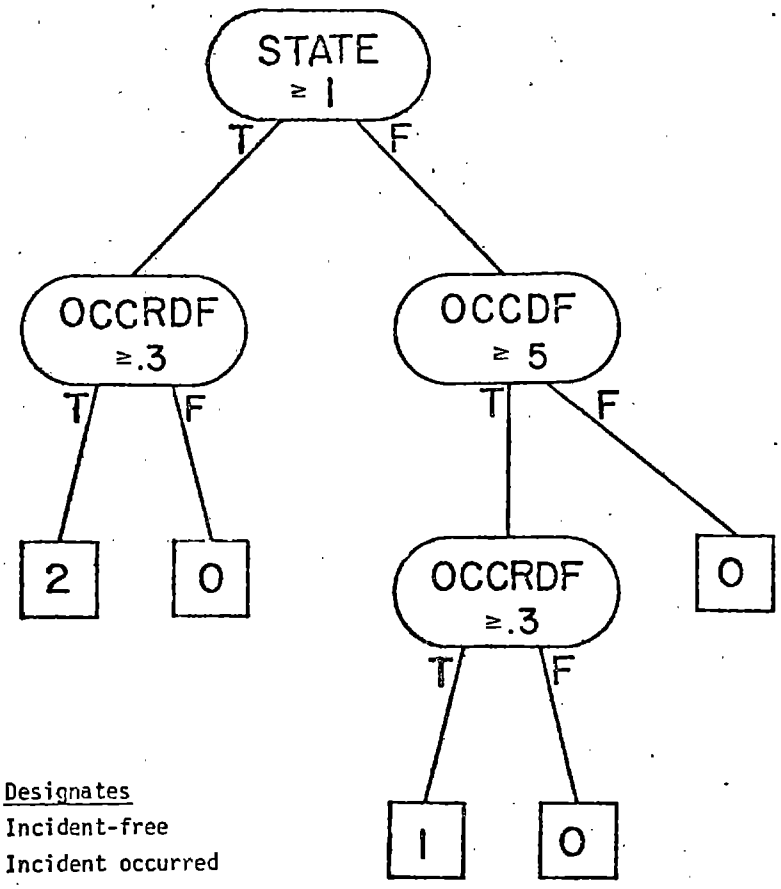

State	Designates
0	Incident-free
1	Incident occurred
2	Incident continuing

Figure 19. Decision tree used to cull data for calibration.

Application of CULDTA to our data base yielded

N_F = 104,217 [Total number of valid incident-free cases]

$\overline{N}_F$ = 3,495 [Total number of incident-free cases in the culled data base]

N_I = 49 [Total number of incident data sets]

$\overline{N}_I$ = 40 [Total number of incident data sets in culled data base]

The number of skipped incident-free cases ($\overline{N}_F$-N_F=100,722) and the number of skipped incident data sets (N_I-$\overline{N}_I$=9) are needed in the evaluation/calibration program CALB. Note that CALB will use only 3.35% of the valid incident-free cases and that the maximum detection rate that can be achieved is ($100\overline{N}_I/N_I$)=82%.

5.1.4 Calibration

The next step in the general procedure is the application of the calibration option for the program CALB. This requires the construction of several user-supplied subprograms, also described in Volume 4.

Having these subprograms, the use of CALB is governed by specification of the input data indicated in Table 16. Specific values are those used to calibrate the example algorithm. A portion of the computer-generated output for this example is presented in Table 17.

5.1.5 Evaluation

The evaluation option can be used to print out the labels for those cases which produce the incident alarm state. Our labels provide identification of the data set number, the sensor station (freeway segment number and station number), and the time. For the example algorithm and the set of thresholds, T_2=.498, T_3=7.66, T_4=.498, T_5=.049, CALB produced the output given in Table 18. This information can be used directly to identify the nature of the incident-free cases which produce false alarms and to determine which incidents were detected and the times of detection. The label information has been used extensively to guide development of algorithms as will be discussed in detail in following sections.

5.1.6 Time-to-Detect Statistics

The last general step in our procedure was to produce time-to-detect statistics (mean times to detect) and the plot of detection rate versus time to detect as defined in Section 4.1. Figure 11 presented there is the plot for the example algorithm we have been discussing.

Table 16. Input data for the program CALB.

THRESHOLD CALIBRATION

7 DETECTION PROBABILITIES

.80
.70
.60
.50
.40
.30
.20

NUMBER OF NON-INCLUDED INCIDENTS = 9

NUMBER OF NON-INCLUDED NON-INCIDENT POINTS = 100,722

3 THRESHOLDS, 4 PARAMETERS

	INITIAL POINT	LOWER BOUND	UPPER BOUND	INITIAL STEPSIZE
1 -	5.00	5.00	30.00	5.00
2 -	0.00	-3.00	1.00	.10
3 -	0.30	0.30	1.00	.25
4 -	1.00			

STATE STORED AS FEATURE 4

ALARM STATE IS 1

STEP SIZE REDUCTION FACTOR - 2.000

10 MAXIMUM CONSECUTIVE FAILURES AT GIVEN STEPSIZE

100 MAXIMUM ITERATIONS

Table 17. Sample calibration output from the program CALB.

```
PASS NO.  2

DESIRED PROBABILITY OF DETECTION = .7000

OPTIMAL FALSE ALARM RATE = .008828

CORRESPONDING DETECTION PROBABILITY = .7143

OPTIMAL THRESHOLDS = 6.8036  .0562  .3069

FINAL STEPSIZE = .00781250
```

Table 18. Sample case labels produced by the program CALB.

Label Number	Data Set No.	Time	Freeway	Station
492	74042201	923	1	22
493	74042201	930	1	21
494	74042201	933	1	22
495	74051501	718	1	25
496	74051501	732	1	25
497	74053001	652	1	14
498	74032203	1818	1	23
499	74032203	1822	1	23
500	74032203	1824	1	23
501	74032203	1829	1	23
502	74060701	804	1	21
503	74060701	809	1	21
504	74060701	811	1	22
505	74062401	908	1	25
506	74062501	754	1	21
507	74031301	1550	1	23
508	74042403	728	1	17
509	74042403	731	1	17
510	74042601	710	2	22
511	74032901	1731	2	27
512	74040103	1751	2	20
513	74040103	1809	2	20
514	74052404	1615	2	22
515	74052303	1638	2	13
516	74052202	1404	2	22
517	74032202	1743	2	21
518	74032202	1802	2	21
519	74032202	1804	2	21
520	74100201	1110	3	30
521	74100201	1114	3	31
522	74100201	1123	3	31
523	74100701	749	3	29
524	74100703	1536	3	31
525	74100805	1719	3	29
526	74100901	759	3	30
527	74101902	754	3	27
528	74101007	1740	3	31
529	74052804	900	4	28
530	74052804	902	4	27
531	74052804	908	4	28
532	74100704	1546	4	29
533	74100804	944	4	32
534	74100804	945	4	31
535	74100806	1820	4	32
536	74100903	822	4	32
537	74100903	839	4	32
538	74061302	1522	4	30
539	74061302	1530	4	30
540	74061302	1536	4	30
541	74032902	1736	4	13
542	74032902	1738	4	14
543	74032902	1742	4	14
544	74042350	643	5	24
545	74042350	654	5	17
546	74042350	658	5	22

5.2 THE CALIFORNIA ALGORITHM AND SIMPLE VARIANTS

The California algorithm as originally developed involves the use of three features: OCCDF, OCCRDF, and DOCCTD. In this section, we will analyze the performance of this algorithm and several simple variants.

First, consider the California algorithm with no distinction between the "incident occurred" and "incident continuing" conditions, illustrated in Figure 20. Coding is given in Table 75. With this form of the algorithm, each assignment of the state value '1' in incident-free data is taken as a false alarm. Calibration results for this algorithm denoted as Algorithm 1, are given in Table 76 along with the computed mean times to detect. The plot of distribution of times-to-detect is presented in Figure 55.

The principal purpose in presenting results for Algorithm 1 is to illustrate the effect on the false alarm rate which is obtained by the more realistic device of distinguishing state values for "incident occurred" and "incident continuing". Algorithm 2, illustrated in Figure 21, embodies this distinction. To see the effect of the use of the "continuing incident" state value, algorithm 2 was evaluated using the threshold values previously determined for algorithm 1; results are given in Table 78. As expected, detection performance is not affected but false alarm rates are generally lower. This is not to say that use of the "continuing incident" state value improves performance--it does not--but it more accurately reflects the operational impact of false alarms.

Next, algorithm 2 was calibrated and evaluated with results given in Table 79 and Figure 57. It will be noted that these results represent some improvement over those displayed in Table 78. The more striking fact, however, is the behavior of the threshold associated with DOCCTD. For threshold sets 4 through 7, the thresholds obtained are such that this feature is effectively not used, a fact which gives rise to some question concerning the utility of DOCCTD as a feature.

To explore this, two variants of the California algorithm were considered. The first of these, Algorithm 3 (see Figure 22 and Table 83), uses only two features: OCCDF and OCCRDF. Calibration and evaluation results are given in Table 84 and Figure 60. Performance of algorithm 3 is seen to be poorer than that of the California algorithm (i.e., No. 2) so that DOCCTD apparently has some value.

The second variant involves replacement of DOCCTD by DOCC, the occupancy at the downstream station leading to Algorithm 4 displayed in Figure 23. This choice was motivated by the observations that (1) the most prevalent cause of false alarms in Algorithms 2 and 3 is a compression wave which moves in a direction counter to the flow of the traffic, (2) in heavy traffic with compression waves the downstream

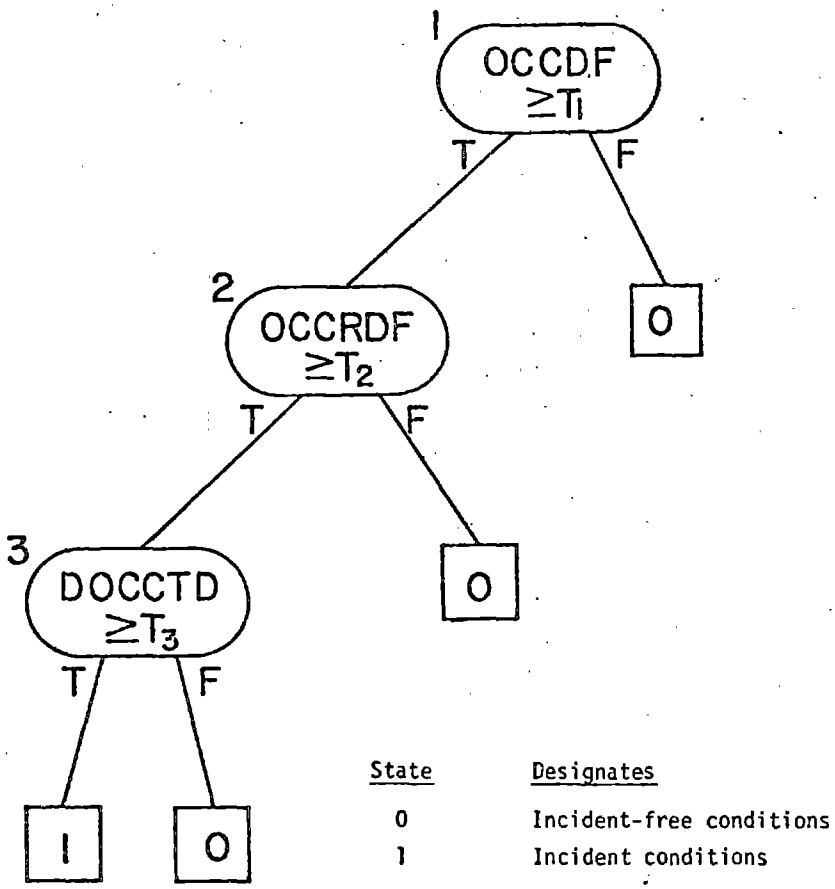

Figure 20. Decision tree for Algorithm 1.

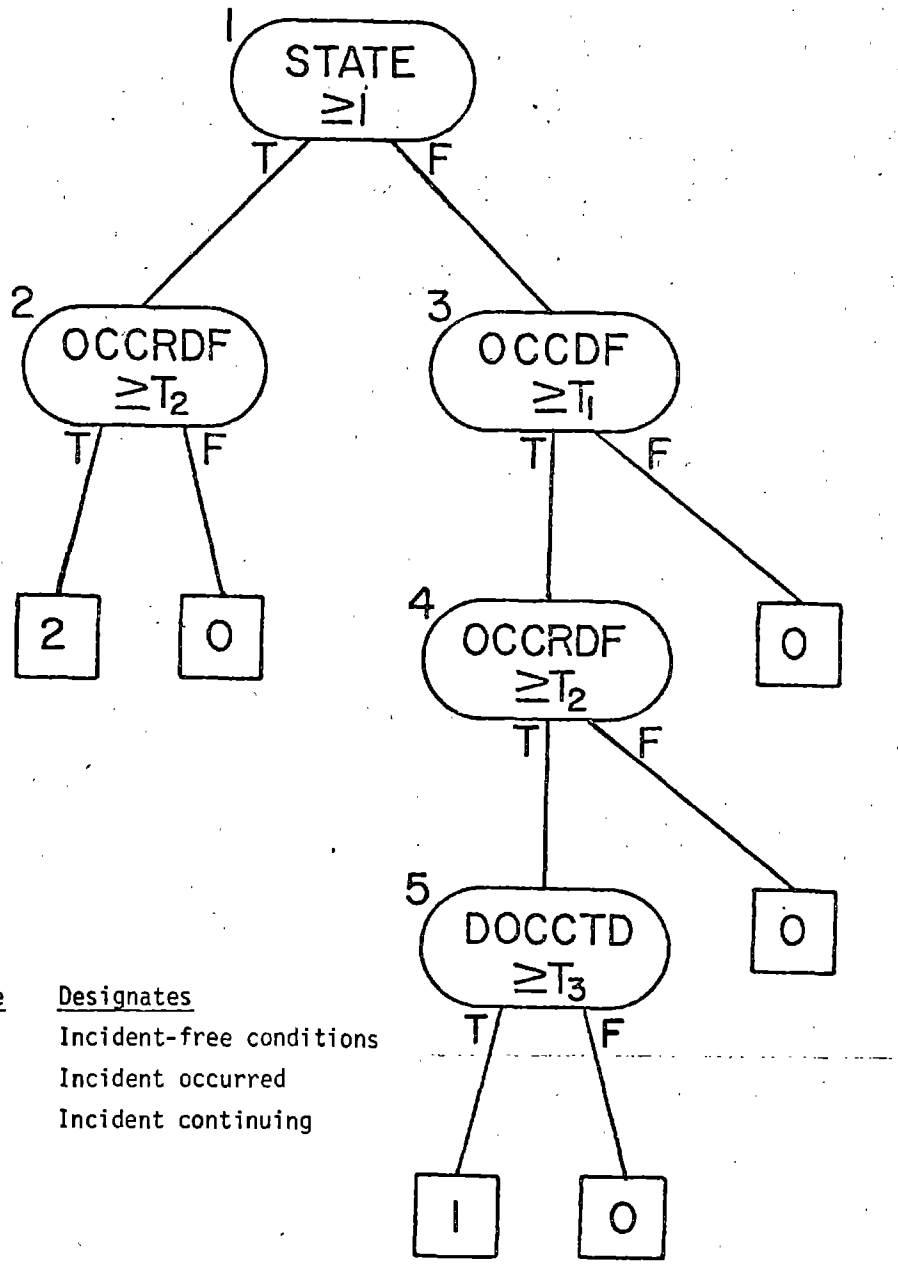

State	Designates
0	Incident-free conditions
1	Incident occurred
2	Incident continuing

Figure 21. Decision tree for Algorithm 2.

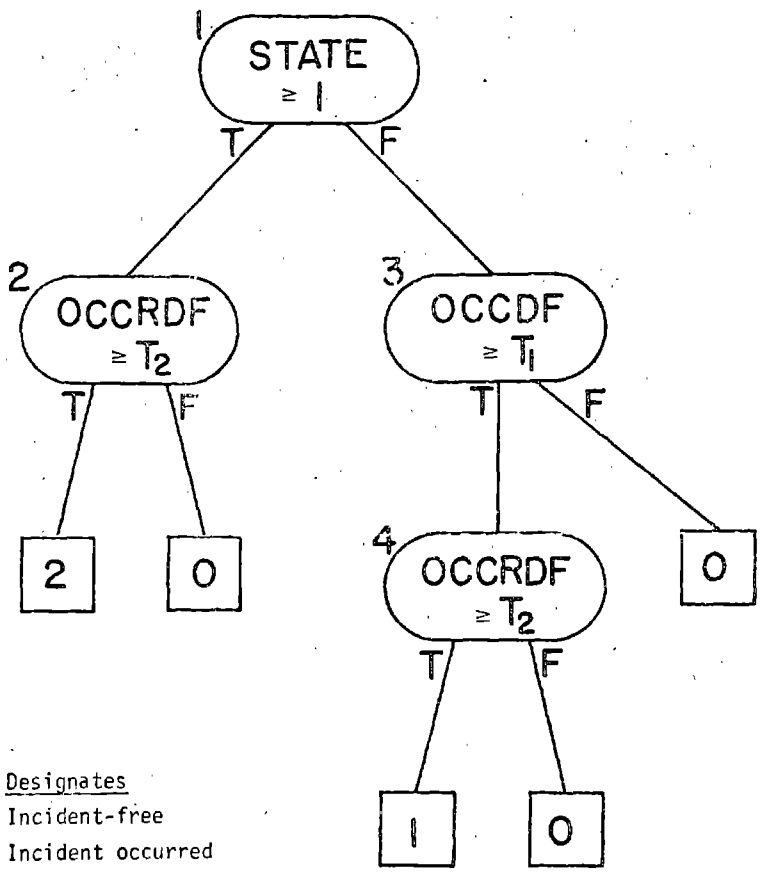

State	Designates
0	Incident-free
1	Incident occurred
2	Incident continuing

Figure 22. Decision tree for Algorithm 3.

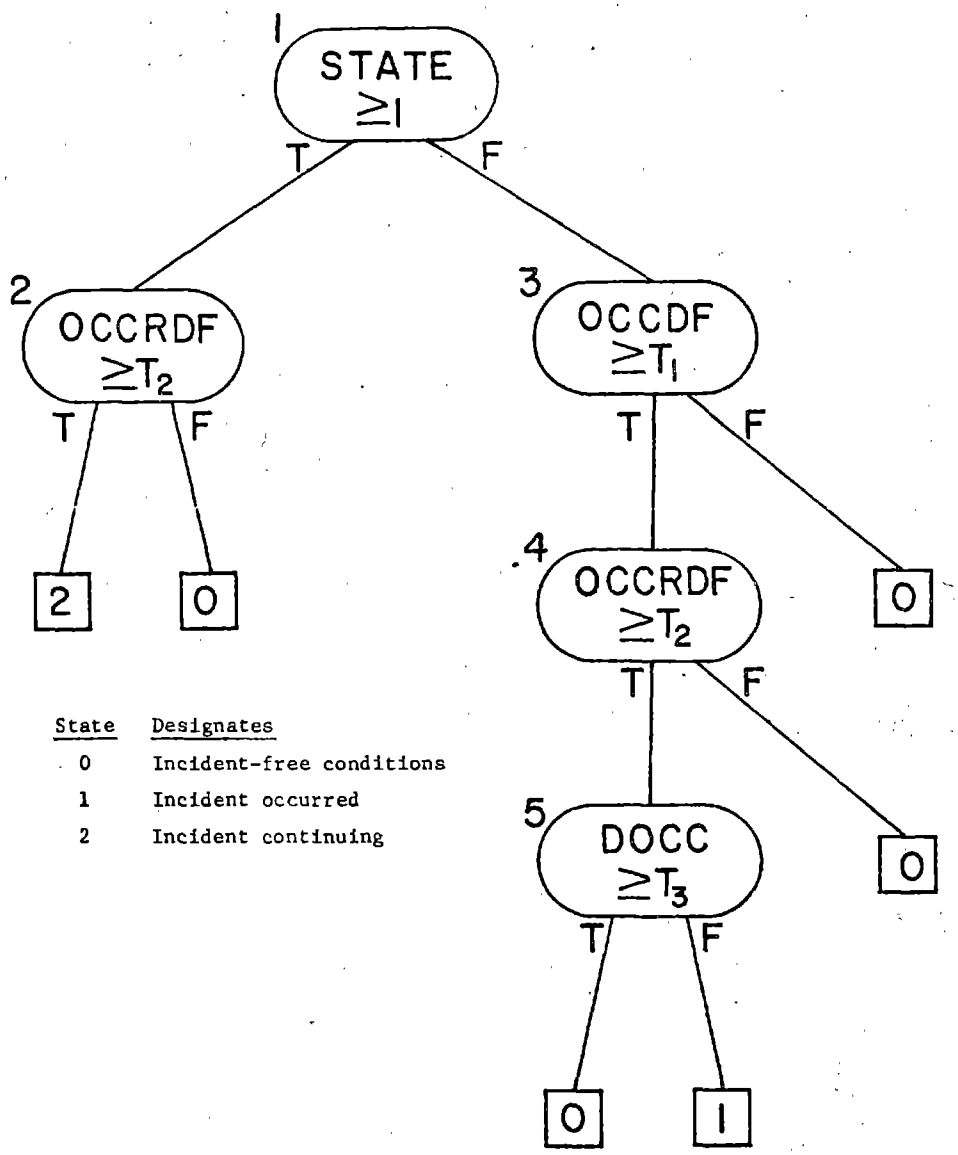

State	Designates
0	Incident-free conditions
1	Incident occurred
2	Incident continuing

Figure 23. Decision tree for Algorithm 4.

occupancy rarely drops below 20% (in the Los Angeles data), and (3) incidents generally produce downstream occupancies substantially less than 20%.

Evidence for these three statements are derived from the label printouts and examination of the corresponding one-minute occupancy maps. A partial label printout for Algorithm 2 is provided in Table 19, with false alarms for incident-free data set No. 74090454 being given. The one-minute occupancy map for this data set was previously given as Table 2 in the introduction where the presence of compression waves was noted. Correspondence of false alarm labels to the passage of compression waves is easily seen. On the other hand, examination of Table 1 supports the observation of low downstream occupancy under incident conditions.

Calibration and evaluation results for Algorithm 4 are given in Table 86 and Figure 62. To aid in comparing the algorithms thus far discussed, detection vs. false alarm rates are presented in Figure 24. Substantial improvements relative to Algorithm 2 are evident. (The methodology and results presented in Section 4.4, particularly Figures 16 and 17 on pages 56 and 57, can be used to judge the statistical significance of observed differences in false alarm rates, at a given detection rate. From these results, one sees that the differences in false alarm rates for Algorithm 4 and those for Algorithms 2 and 3, at detection rates of 62% or less, are significant at the .01 level. Other pairwise differences are generally significant at levels greater than .10.)

Examination of false alarms associated with Algorithm 4 indicates that compression waves still contribute significantly and that most of the remaining false alarms appear to be due to bottlenecks, specifically, at the head of queues.

5.3 ALGORITHMS WITH A PERSISTENCE REQUIREMENT

Many--but not all--disturbances in incident-free traffic are short-lived and, while they may produce an incident signal, the associated "incident-continuing" state value does not last long if it is produced at all. This is in contrast to the majority of incidents which produce a discontinuity in the traffic stream which generally lasts at least several minutes. Thus, it has been suggested that improved performance might be obtained by requiring that the discontinuity persist for a period of time.

The state feature of the binary tree structure we have adopted provides a convenient means of accommodating a persistence requirement. In its simplest form, one sets the state value equal to 1 (say) when a discontinuity is first detected and then signals an incident (state value equal to 2, say) if the next test (for that station or section) indicates the discontinuity has persisted. A concrete realization of this is Algorithm 5, the California algorithm with a persistence requirement, illustrated in Figure 25. Results of the calibration and evaluation are given in Table 89 and Figure 65.

Table 19. Partial label printout of Algorithm 2, $T_1 = 4.99$, $T_2 = .563$, $T_3 = .013$

Label No.	Data Set No.	Time	Location Freeway	Location Station
414	74090454	645	4	2
415	74090454	719	4	26
416	74090454	720	4	30
417	74090454	723	4	28
418	74090454	725	4	29
419	74090454	730	4	31
420	74090454	734	4	32
421	74090454	744	4	32
422	74090454	749	4	31
423	74090454	753	4	32
424	74090454	757	4	28
425	74090454	759	4	30
426	74090454	803	4	32
427	74090454	805	4	32
428	74090454	811	4	32
429	74090454	814	4	30
430	74090454	815	4	26
431	74090454	820	4	32
432	74090454	831	4	32
433	74090454	843	4	28
434	74090454	849	4	28
435	74090454	904	4	28

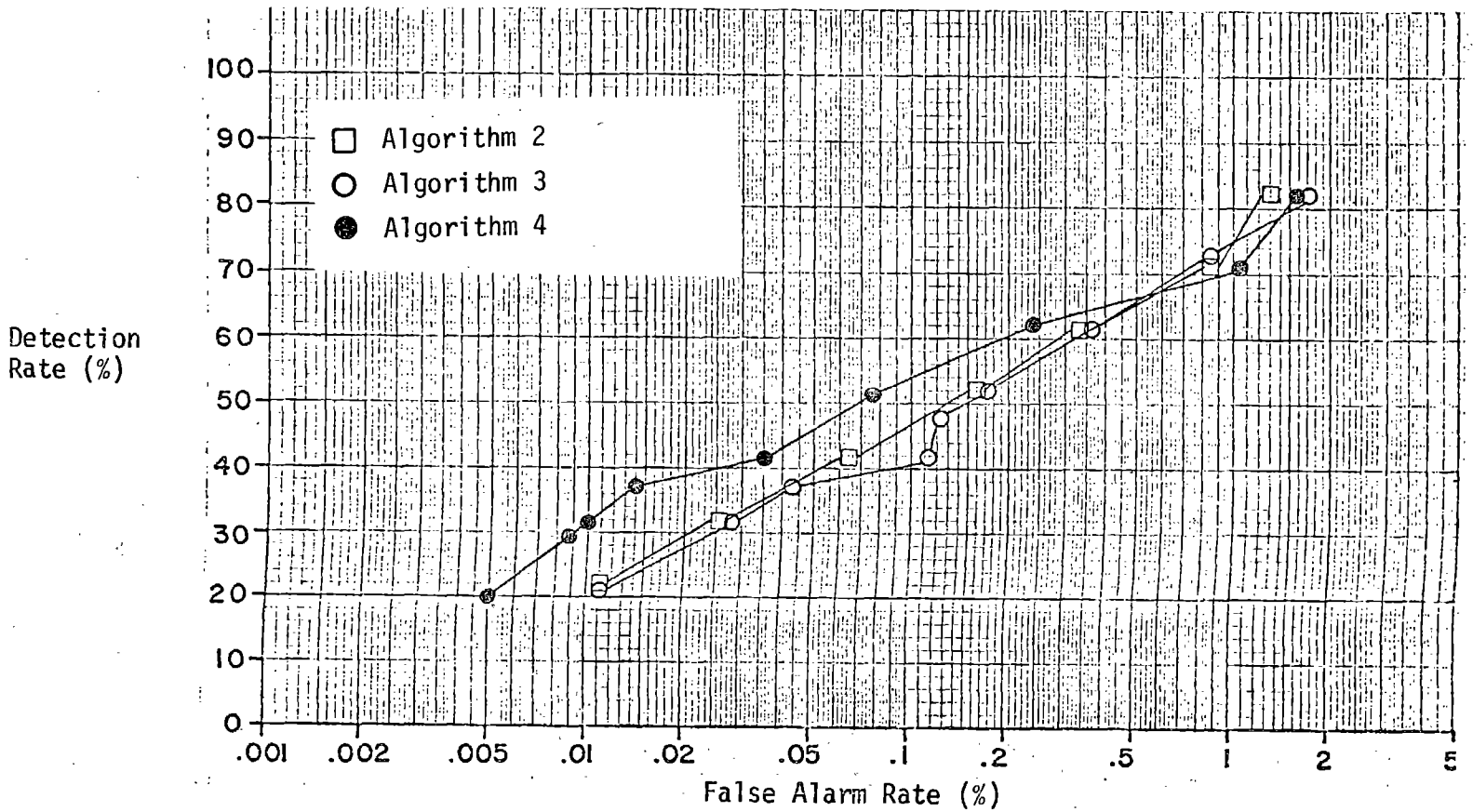

Figure 24. Comparison of performance of Algorithms 2, 3, and 4.

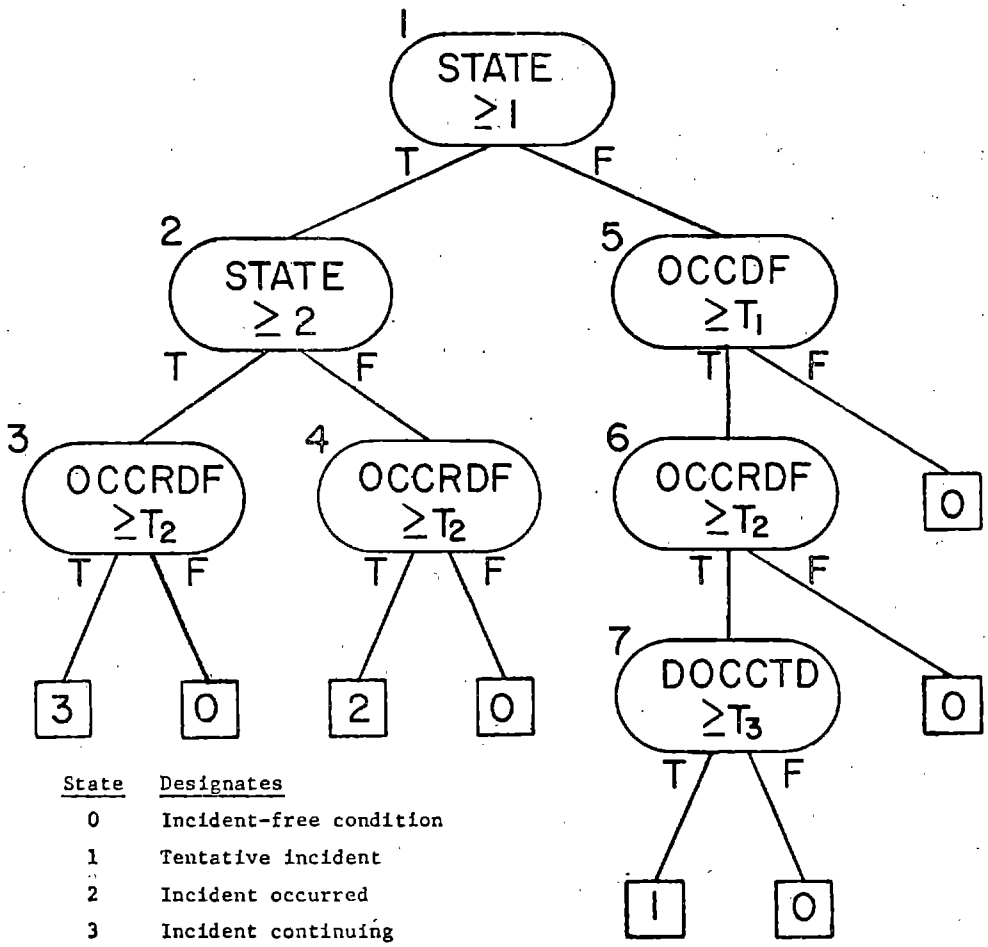

State	Designates
0	Incident-free condition
1	Tentative incident
2	Incident occurred
3	Incident continuing

Figure 25. Decision tree for Algorithm 5.

Algorithms 6 and 7 are the two variants of the California algorithm discussed in the previous section, but with a persistence requirement added. Definition and results for Algorithm 6 are given in Figures 26 and 67 and Table 91. Those for Algorithm 7 are given in Figures 27 and 70 and Table 94.

It will be noted in each of these algorithms that persistence is checked by the use of the feature OCCRDF using the same threshold as that used in the "tentative incident signal" portion of the algorithm. This is, of course, only one of many possible mechanizations of the persistence requirement. Use of the same threshold at both points in the algorithm was dictated by a desire to reduce the burden on the calibration program. (Generally, it is more difficult to get good results with the same computing time when more distinct thresholds are involved.)

Performance of these three new algorithms is displayed in Figure 28. Algorithm 7 is clearly superior in terms of the tradeoff between detection and false alarm rates. (Differences in false alarm rates for Algorithm 7 and those for Algorithms 5 and 6, at detection rates of between 31% and 51%, are significant at the .01 level.)

5.4 AN ALGORITHM THAT SUPPRESSES COMPRESSION WAVES

We noted earlier that compression waves in heavy traffic are a principal source of false alarms and some success in eliminating such false alarms has been obtained with the algorithms described in the previous two sections. Further effort was undertaken to improve performance in heavy traffic by attempting to account for a certain regularity in the pattern of traffic associated with compression waves.

Consider the data displayed in Table 2 for incident-free data set 74090454. As we have noted, compression waves are manifested by sudden large increases in occupancy which move through the traffic stream in a direction counter to the direction of travel. In Table 2, a single series of such large occupancy values is isolated by boxes. Attempts were made to account for this pattern through the use of correlation analysis but it was found that the patterns were not sufficiently regular for this technique to be successful.

Therefore, we considered grosser means to account for the observed patterns. It will be noted in Table 2 that the large increase at one station is typically followed some two to five minutes later by a large increase at the next upstream station. The typical station spacing in Los Angeles is one-half mile corresponding to a shock wave speed of six to fifteen miles per hour. The fact that a compression wave has passed over a station can be captured by the simple test displayed in Figure 29, where $T_5 = 30$ and $T_2 = -.250$ have been found to be effective.[1]

---

[1] The use of negative values for thesholds, here $T_2 = -.250$, has no special significance in itself, but only reflects the fact the corresponding feature, here DOCCTD, is expected to have a negative value when the condition for which the corresponding comparison is being made occurs. The arrival of a shock wave produces a sharp rise in downstream occupancy and therefore produces negative values of DOCCTD.

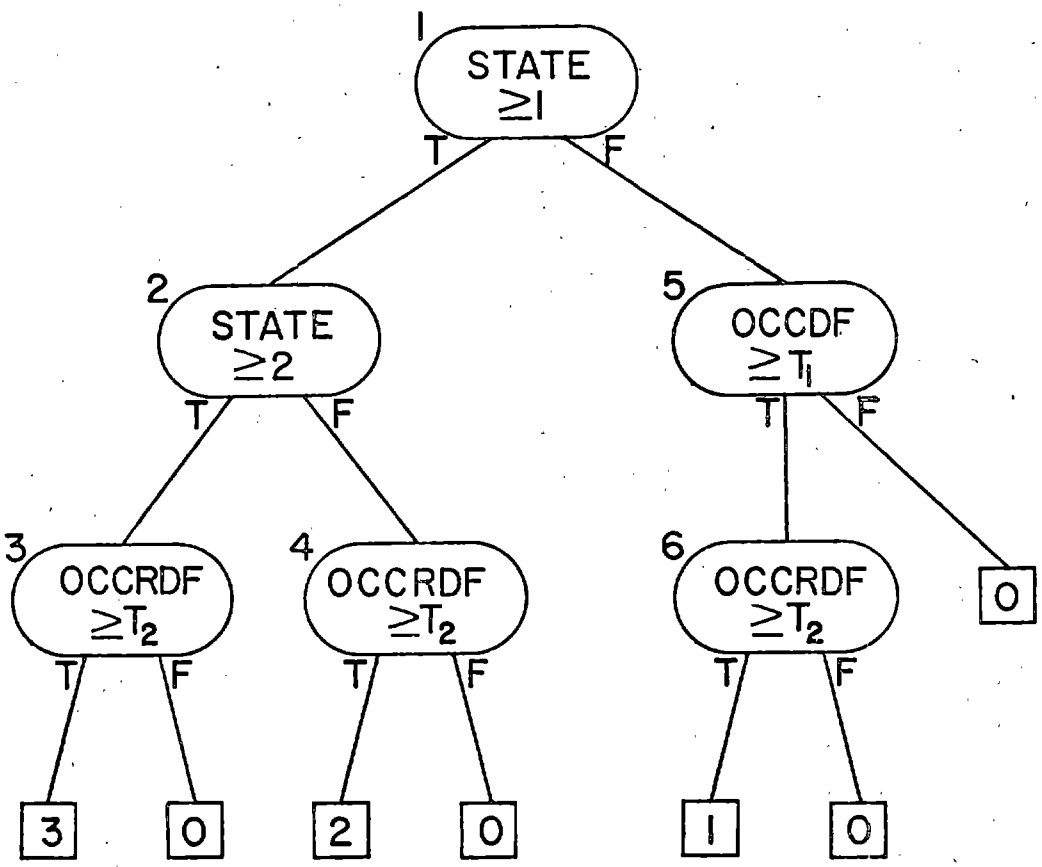

State	Designates
0	Incident-free conditions
1	Tentative incident
2	Incident occurred
3	Incident continuing

Figure 26. Decision tree for Algorithm 6.

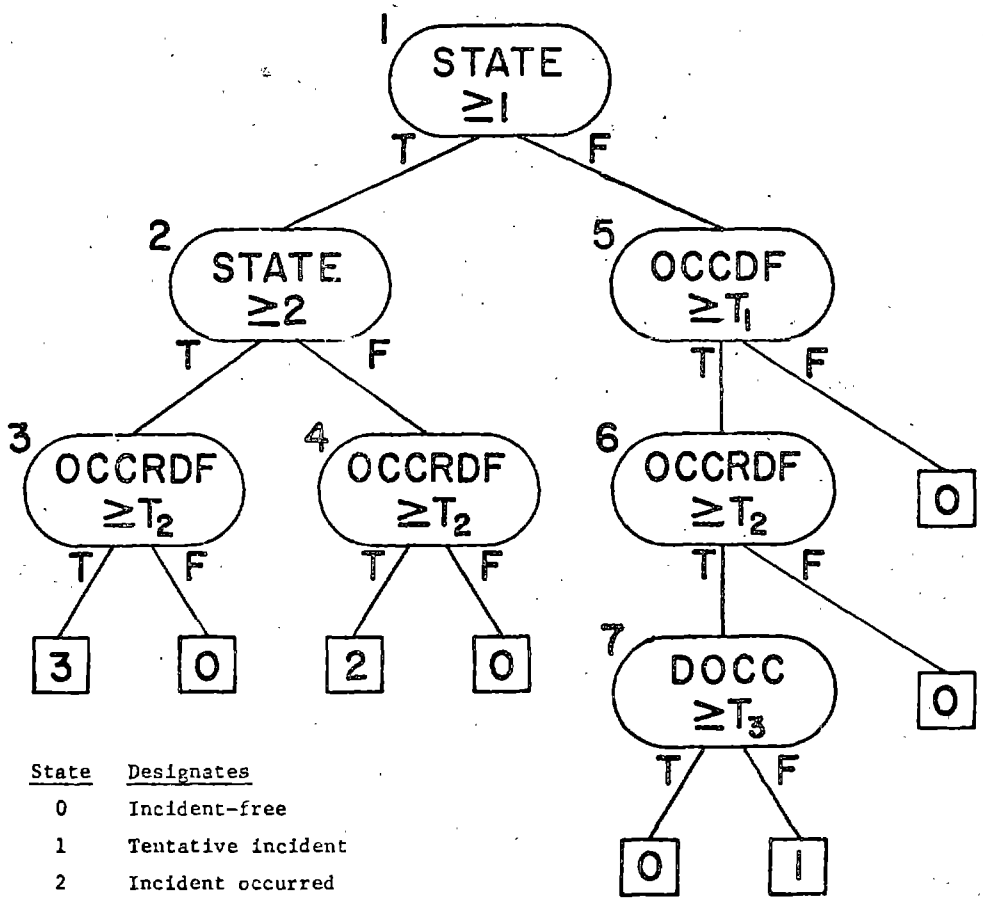

State	Designates
0	Incident-free
1	Tentative incident
2	Incident occurred
3	Incident continuing

Figure 27. Decision tree for Algorithm 7.

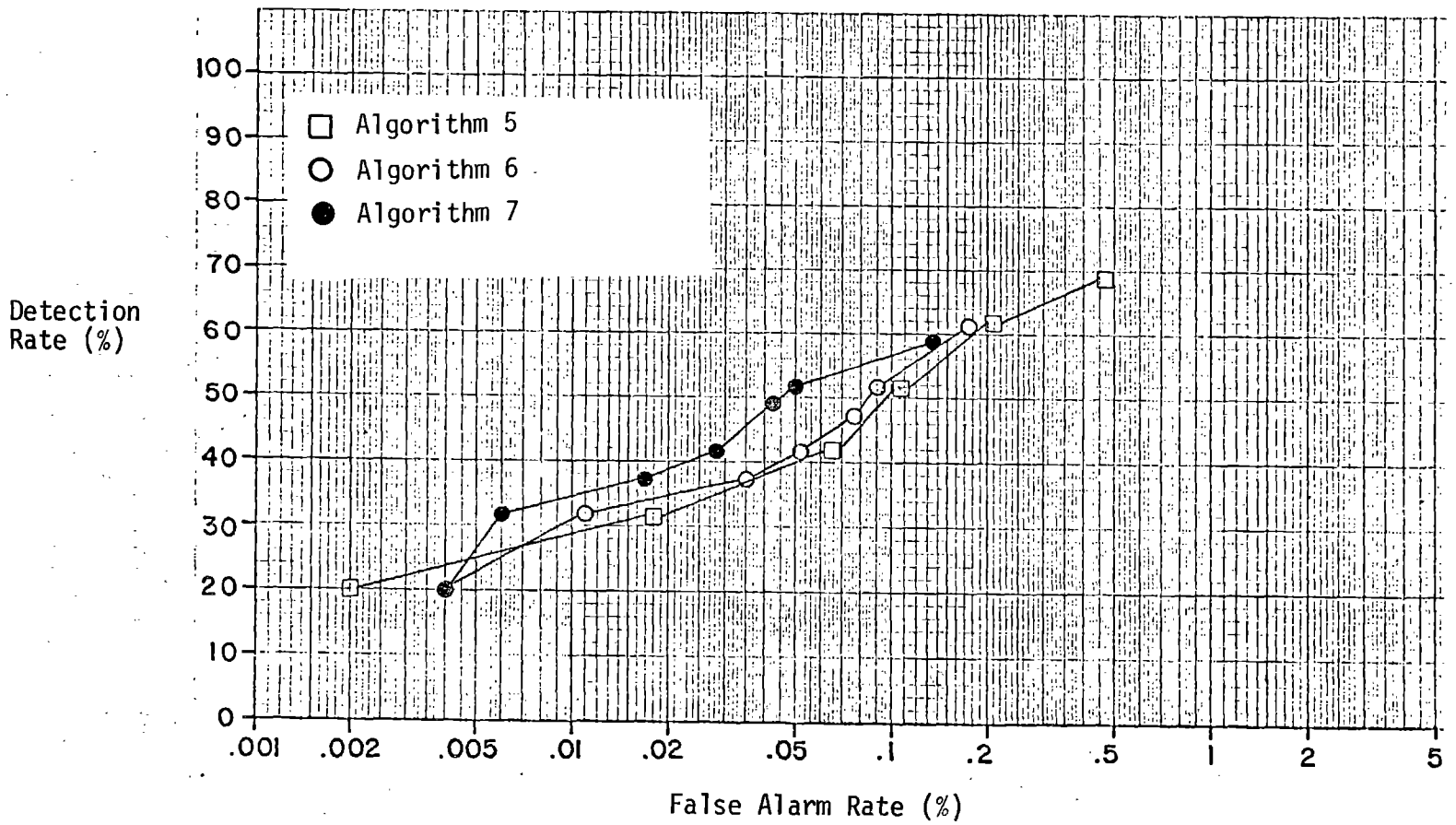

Figure 28. Comparison of performance of Algorithms 5, 6, and 7.

Of course, incidents also produce patterns which would yield a positive result for this test. In heavy traffic with compression waves, one would expect that a positive result for this test would be followed, typically within five minutes, by a positive result at the next upstream station. Thus incidents are distinguished by the fact that there was no compression wave identified at the downstream station in the previous five minutes.

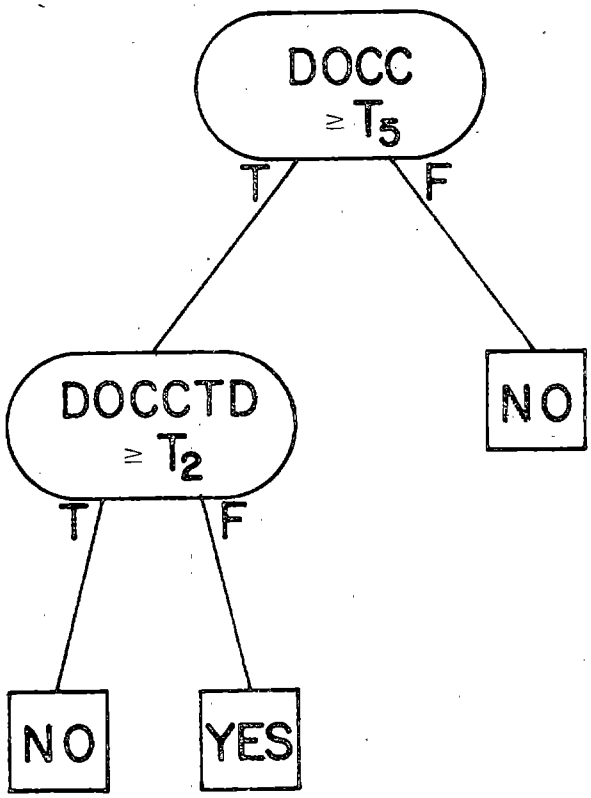

Figure 29. Test for Presence of a Compression Wave.

Introduced here, is Algorithm 8 which uses the state feature in an unusual way--essentially to suppress incident detection at any station for a period of five minutes following detection of a compression wave at the downstream station. This algorithm, complete with a persistence requirement and a continuing incident state, may appear to be complex as it does involve thirty decision nodes, but its componets have straightforward interpretations. The algorithm is displayed in Figure 30.

In this figure, one can discern a repeated use of the simple test for presence of a compression wave. The test is phrased in terms of downstream features, DOCC and DOCCTD. Remaining elements of the algorithm are essentially those of Algorithm 7. In Figure 30, that portion indicated as "tentative incident check," when compared to Algorithm 7 (Figure 27, p. 84),

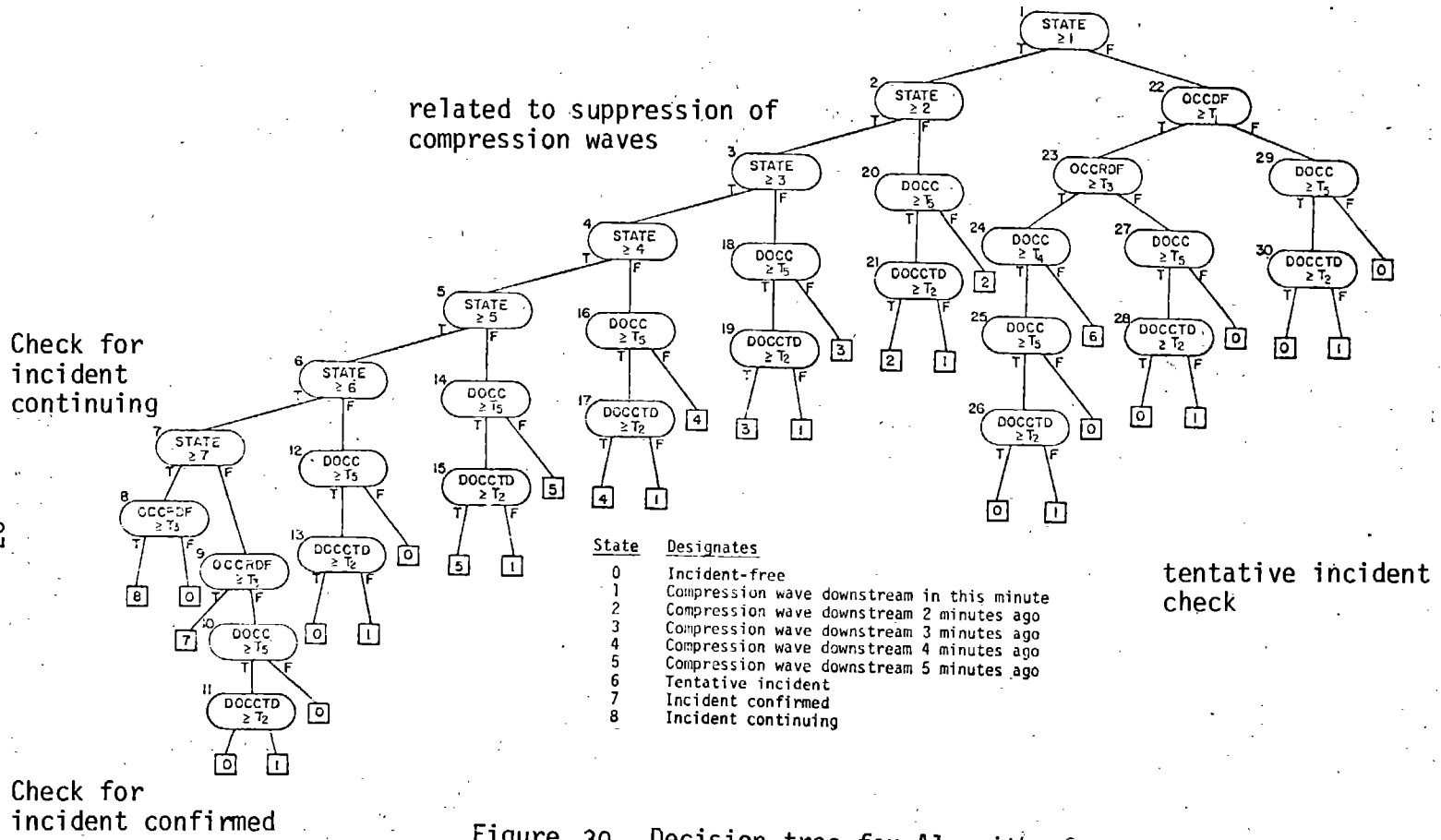

Figure 30. Decision tree for Algorithm 8.

can be seen to be derived from the "tentative incident check" portion of Algorithm 7 by replacing the terminal nodes with zero state value by the subtree of Figure 29. At this point in the algorithm, 'NO' is coded as '0' and 'YES', as '1'. That is, when the prior state is incident-free, here coded by the state value zero, and the check for incident is negative, in Algorithm 8 a further test is made for passage of a shock wave at the downstream station. Similarly, in that portion of the algorithm in which the "check for incident confirmed" is made, a negative result leads, in Algorithm 8, to the test for passage of a shock wave at the downstream station.

The portion of Algorithm 8 which is "related to suppression of compression waves" serves as a counter once a shock wave is found at the downstream station. Note that a prior state value of one through five indicates a recent passage of a shock wave at the downstream station. Suppose the prior state value were three. Exercise of the decision tree would start at decision node 1, proceed to decision nodes 2, 3, 4, and then to 16. At this point, one again checks for a passage of a shock wave in the last minute. If this check is positive, the state is reset to one. Otherwise, the state value is set to four, i.e., the count in minutes since passage of the most recent shock wave is advanced from three to four. If the prior state value were five, and a new shock wave were not found, the state value would be set to zero, freeing the algorithm to test for incident conditions again.

Due to the complexity of this algorithm, the question arose whether a simpler tree might produce the same results. A tree optimization procedure[1] was applied and yielded an equivalent tree which is given in Figure 79. This new tree has the minimum number of decision nodes, 21.

To minimize the burden on the calibration program, the number of distinct thresholds has been limited to four by taking T_5 = 30%. Calibration and evaluation results are given in Table 106 and Figure 80. Noting the relatively slight variation in the threshold corresponding to DOCCTD, a second calibration was executed with T_2 = -.300. Results are presented in Table 108 and Figure 81.

We also calibrated the version of the algorithm without the persistence requirement, Algorithm 9. Results for this algorithm are presented in Table 113 and Figure 85. A comparison of performance results for Algorithms 8 and 9 is shown in Figure 31. None of the differences in false alarm rates are significant at the .01 level. Significance of any particular pair can be ascertained by reference to Figure 17, page 57. For example, the difference pertaining to Algorithms 8 and 9 at a detection rate of 51%, i.e., false alarm rates of .038% and .070%, respectively, is seen to be significant at the .05 level.

---

[1] H. J. Payne and W. S. Meisel, "An Algorithm for Constructing Optimal Binary Decision Trees," submitted for publication.

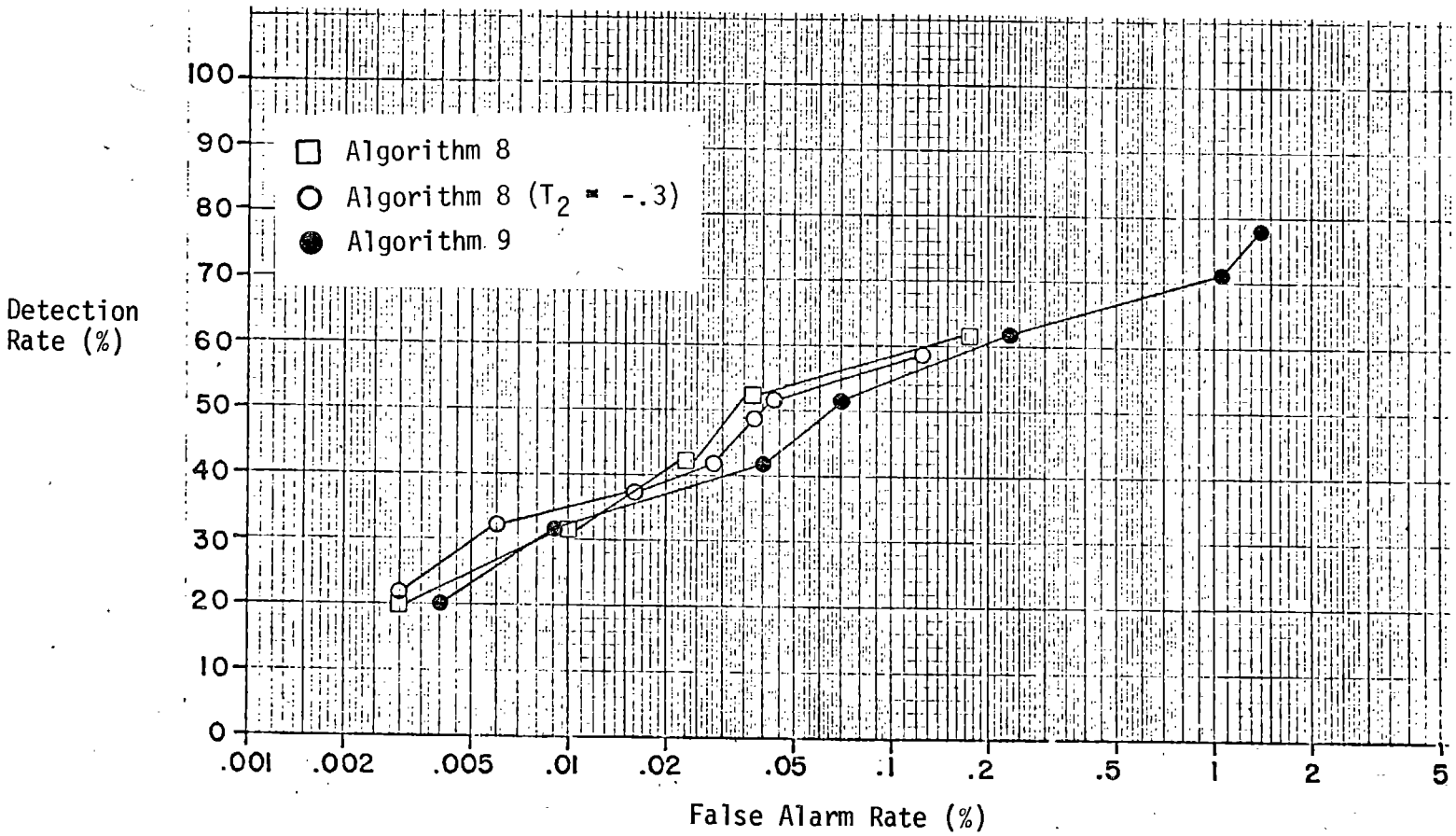

Figure 31. Comparison of performance for Algorithms 8 and 9.

Best results were obtained for Algorithm 8 with T_2 determined by the calibration program. Further, by comparing these results to those presented in Figure 28, it can be seen that Algorithm 8 achieves the best detection-versus-false-alarm-rates tradeoff of all nine algorithms considered. However, examination indicates that this superiority of performance is had at the expense of some increase in the mean time-to-detect.

Examination of false alarms produced by Algorithm 8 indicates that those due to compression waves are relatively few in number. Thus, the device, introduced in this algorithm, of suppressing incident detection when compression waves are present is very successful. The remaining false alarms appear to be related to bottlenecks, specifically at the head of a queue.

5.5 AN ALGORITHM BASED ON A SPEED FEATURE

Incidents that occur in light-to-moderate traffic often do not produce capacities at their sites less than the volume of oncoming traffic and therefore do not produce marked discontinuities as measured by occupancy. The algorithms considered above often fail to detect such incidents. To address this class of incidents, we considered a tenth algorithm, illustrated in Figure 32. This algorithm involves the speed feature, SPDTDF (see Table 7). The rationale for the structure of this algorithm was to use two different subtrees for two regimes of traffic level. For occupancies less than T_2 (taken to be 25%), a test involving the temporal change in speed was used. For occupancies greater than T_2, the test was that used in Algorithms 4 and 7, i.e., involved DOCC. Other structures for distinguishing between traffic levels might be considered, but time limited our attention to this algorithm. Results of calibration and evaluation are given in Table 116 and Figure 88. They were not as good as those for Algorithms 7 and 8. Detection of incidents in the light-to-moderate traffic regime thus remains a problem.

5.6 COMPARISONS OF THE ALGORITHMS

Three measures of performance have been used in our analysis of algorithms: detection rate, false alarm rate, and mean time to detect. The first two were jointly used to calibrate thresholds. Considering all three together, we can identify noninferior algorithms by the property that no other algorithm has simultaneously a greater detection rate, a lower false alarm rate, and a lower mean time-to-detect. These algorithms are defined by the algorithm number and the threshold set number.

All the calibration and evaluation results for the ten algorithms were considered together to identify the noninferior algorithms listed in Table 20. While no one algorithm emerges as clearly superior, Algorithms 4, 7, 8, and 9 dominate the list. Recall that Algorithm 7 is

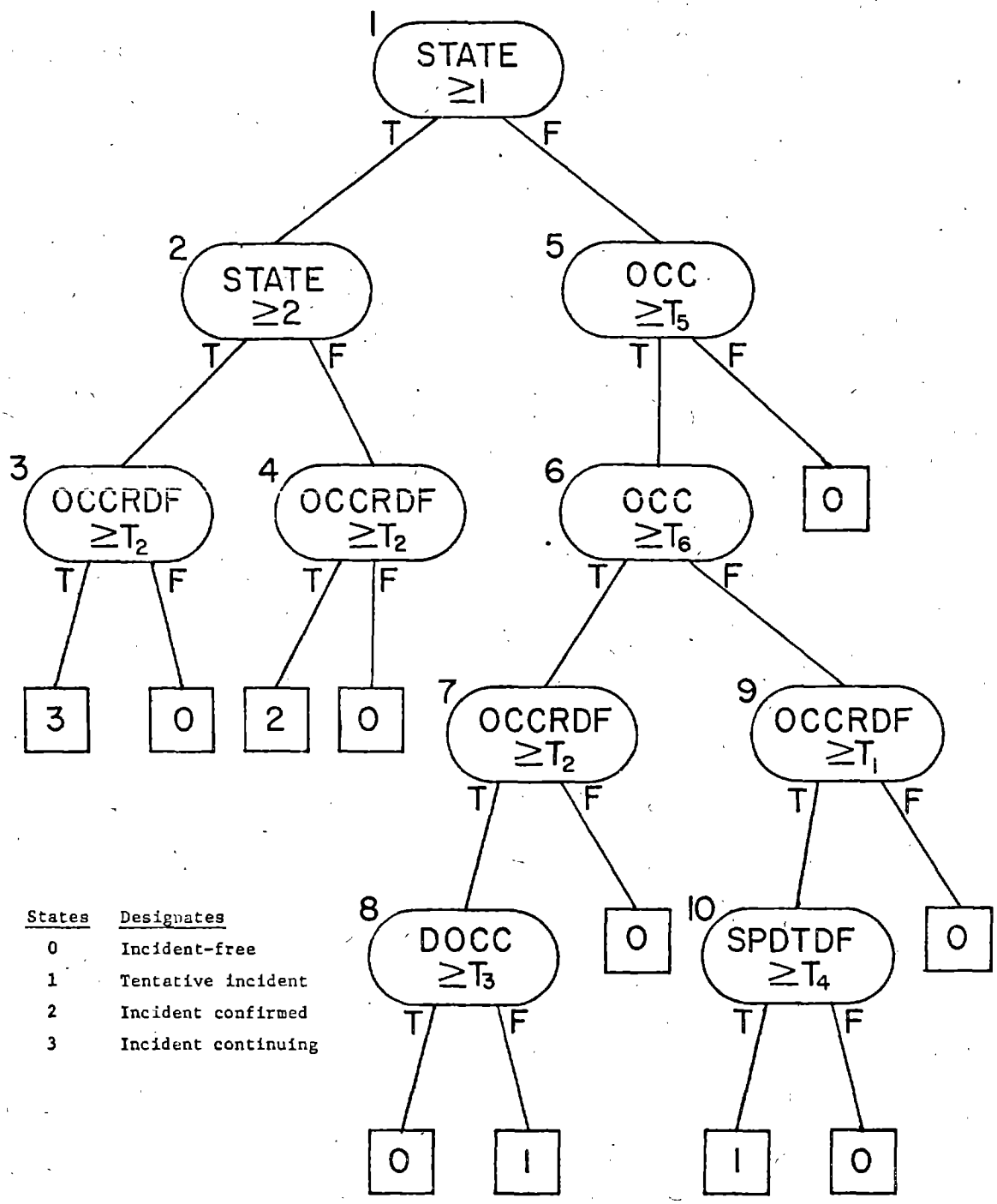

Figure 32. Decision tree for Algorithm 10.

Table 20. Noninferior algorithms.

Algorithm Number	Threshold Set No.	Detection Rate (%)	False Alarm Rate (%)	Mean Time-to-Detect (Minutes)
2	1	82	1.341	.77
4	1	82	1.577	.64
3	1	82	1.693	.24
9	1	78	1.408	.83
2	2	71	.883	.01
9	2	69	1.190	.47
6	1	61	.158	3.84
9	3	61	.230	2.08
7	1	59	.134	3.25
8	2	51	.038	4.79
7	2	51	.050	4.31
10	2	51	.065	3.59
4	4	51	.074	3.43
10	3	47	.057	3.73
8	3	41	.024	5.63
7	4	41	.029	4.85
4	5	41	.035	4.40
9	5	41	.040	4.12
4	6	37	.014	5.20
7	6	31	.006	5.84
9	6	31	.009	4.98
8	4	31	.010	4.93
2	6	31	.026	4.64
5	6	20	.002	7.43
6	7	20	.004	6.93

Algorithm 4 with a persistence requirement added and that Algorithm 8 is Algorithm 9 with a persistence requirement added. Of particular note is the fact that Algorithm 9 appears in the list at both high and low detection rates.

Two final comparisons were given here--one, presented in Figure 33, is of Algorithms 2 and 9 and a third algorithm we denote as Algorithm 11. This algorithm uses the feature SOCCDF (see first interim report), a doubly exponentially smoothed version (see Section 3.1.2) of the feature OCCDF; the decision tree in this case consists of a single node with a single threshold. Values of SOCCDF less than the threshold produce an incident alarm. Calibration of Algorithm 11 produced the results in Table 21. Algorithm 2 represents the best algorithm presently in use; Algorithm 9 is one of the best algorithms we have produced. The conclusion to be drawn is that the simplest of the multiple-feature algorithms we considered--essentially, the California algorithm--is clearly superior to the best algorithm based on double-exponential smoothing, and the algorithms we developed demonstrate a clear superiority with respect to the California algorithm. (Differences in false alarm rates, for detection rates of 62% or less, are all significant at the .01 level, except for the difference between Algorithms 2 and 11 at the detection rate 62%.)

The second comparison, displayed in Figure 34, is between the performance of Algorithms 2, 7, and 8 obtained by evaluations on the full Los Angeles data base. It can be seen that the relative ordering of performance for these three algorithms found in the course of our developments is maintained on the full Los Angeles data base.

To summarize our developments, characteristics of the ten new incident detection algorithms are given in Table 22. The structure of these algorithms can be distinguished according to: (1) whether the feature DOCCTD or DOCC is used to examine the downstream impact on the traffic pattern - Algorithms 1, 2, and 5 use DOCCTD, Algorithms 3 and 6 do not employ any such check, and Algorithms 4, 7, 8, 9, and 10 use DOCC; (2) whether a persistence check is employed - Algorithms 1, 2, 3, 4, and 9 do not require persistence, while Algorithms 5, 6, 7, 8, and 10 do involve a persistence check; and (3) whether the algorithm checks for presence of compression waves - only Algorithms 8 and 9 use such a check. Algorithm 10 is unique in that distinct tests for presence of an incident are used in two traffic regimes (light and moderate).

In terms of overall performance, the best simple algorithm is apparently Algorithm 7. Algorithms 4 and 10 are reasonable, alternative simple algorithms. The best performance is associated with the two most complex algorithms, Algorithms 8 and 9. The relative advantage of these latter two algorithms is directly due to their ability to avoid false alarms in the presence of shock waves. In environments lacking shock wave, this relative advantage would not be present.

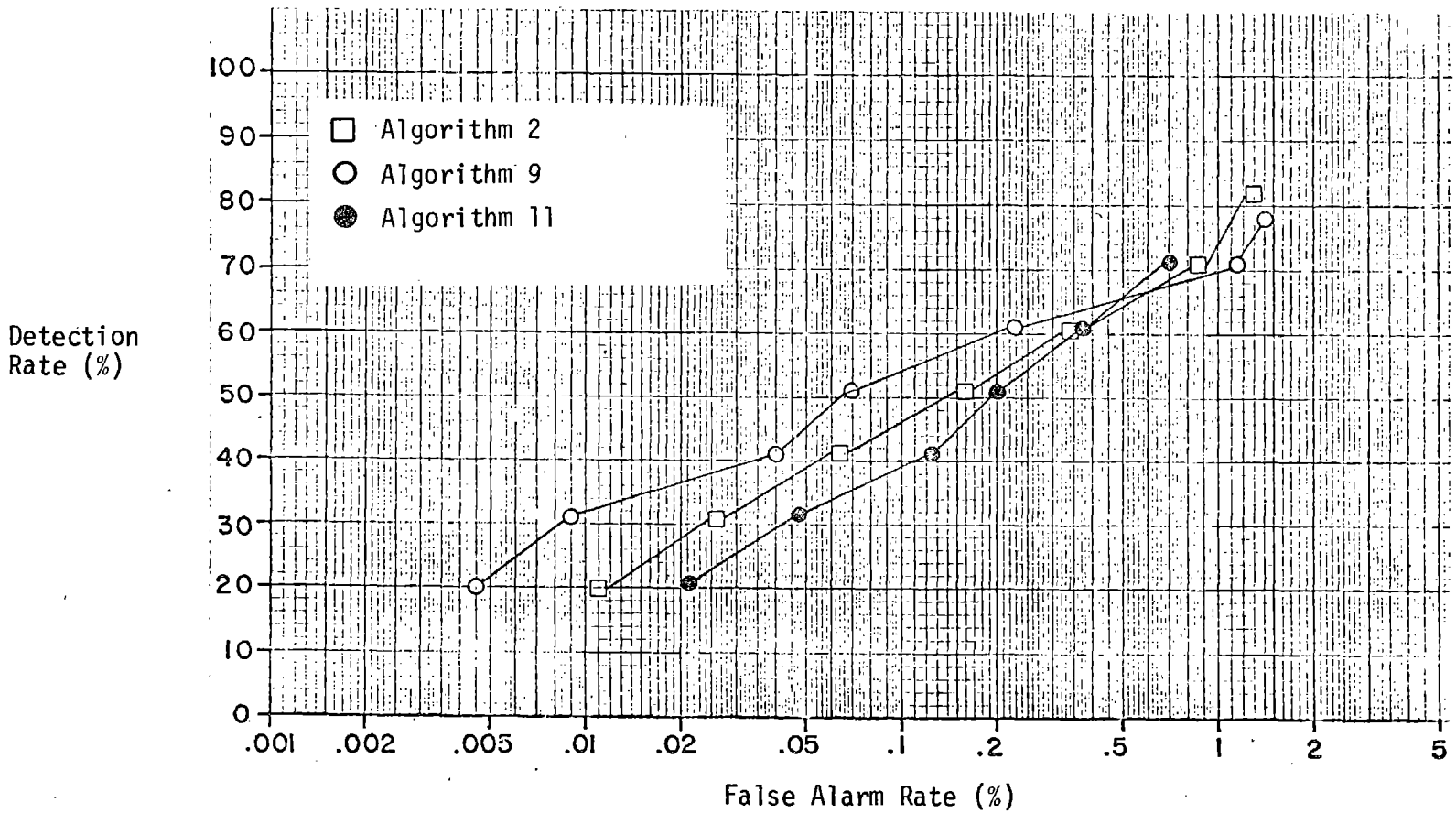

Figure 33. Comparison of performance of Algorithms 2, 9, and 11.

Table 21. Calibration results for Algorithm 11.

Threshold Number	Detected (%) Rate	False Alarm Rate (%)	Threshold
1	71.4	.7053	-3.29
2	61.2	.3730	-3.88
3	51.0	.2000	-4.52
4	40.8	.1256	-5.06
5	30.6	.0483	-6.14
6	20.4	.0213	-7.52

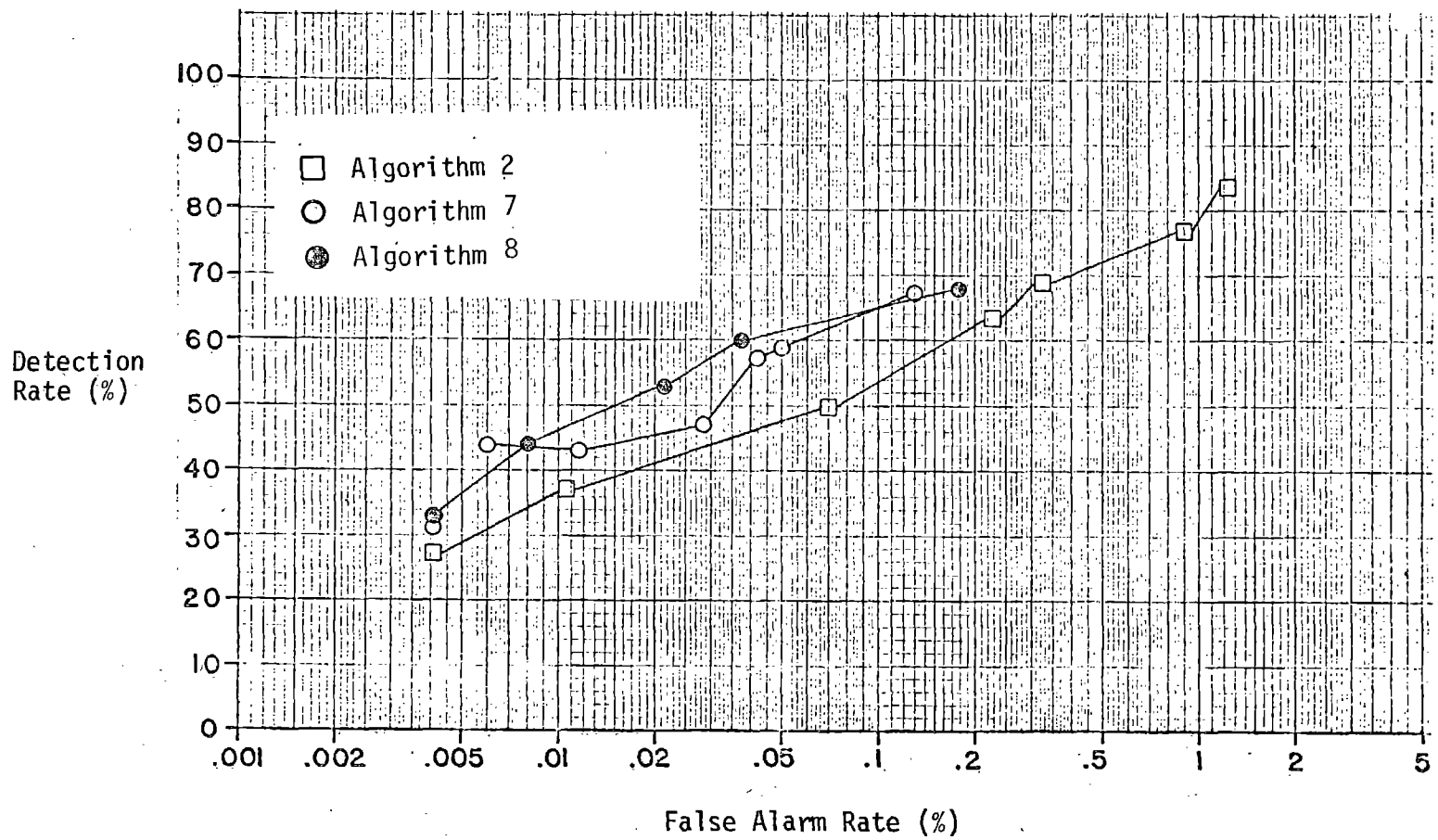

Figure 34. Comparison of performance of Algorithms 2, 7, and 8, (based on full Los Angeles data).

Table 22. Characteristics of the ten new incident detection algorithms.

Algorithm No.	Features Used	Comments
1	OCCDF, OCCRDF, DOCCTD	Essentially the California algorithm
2	OCCDF, OCCRDF, DOCCTD	Essentially the California algoritm with an incident continuing state
3	OCCDF, OCCRDF	Same as Algorithm 2, but without DOCCTD check
4	OCCDF, OCCRDF, DOCC	Same as Algorithm 2, but use of DOCC replaces use of DOCCTD
5	OCCDF, OCCRDF, DOCCTD	Essentially the California algorithm with a check for persistence
6	OCCDF, OCCRDF	Algorithm 3 with a check for persistence
7	OCCDF, OCCRDF, DOCC	Algorithm 4 with a check for persistence, best simple algorithm
8	OCCDF, OCCRDF, DOCC, DOCCTD	Has form of Algorithm 4 plus check for compression wave and persistence, especially effective in "stop-and-go" traffic
9	OCCDF, OCCRDF, DOCC, DOCCTD	Algorithm 8 without a persistence check, especially effective in "stop-and-go" traffic
10	OCC, OCCTDF, DOCC, SPDTDF	Distinguishes two traffic regimes (light and moderate) for purposes of detecting incidents

6. FURTHER ALGORITHM DEVELOPMENT AND EVALUATION WITH THE LOS ANGELES DATA BASE

In this section, we present results of several additional investigations (executed on the Los Angeles data base). These investigations have (1) led to a technique for adjusting algorithms (actually, features) to reduce the adverse impact of geometric anomalies on algorithm performance, (2) provided insight into the effect that the configuration of sensors has on algorithm performance, (3) provided means for implementing algorithms with updates at other than one-minute intervals, (4) led to simple algorithms for detecting malfunctioning detectors, and (5) led to a simple and effective algorithm for identifying the lane of occurrence of an incident.

6.1 EFFECTS OF GEOMETRICS

Nonuniform traffic results not only from the presence of incidents but also from the presence of certain combinations of traffic demand and geometric conditions. If the nonuniformity is severe enough in the latter instance, false alarms will result. In addressing this issue, we have taken the point of view that the effects of geometrics are significant only when they have a significant impact on the performance of incident detection algorithms. Thus, for example, a lane drop is not deemed to be significant if the usual traffic demand at that location produces traffic patterns which do not generate false alarms. Consequently, we have not developed a treatment which is based on a physical description of the geometric situation. Rather, we have sought to identify significant geometric anomalies by examining false alarms and by identifying consistently nonuniform patterns in traffic data.

Adjustments to incident detection algorithms to reduce false alarms associated with geometric conditions can take the form of adjustments to thresholds, as is done in the Los Angeles system. However, this implies station-specific calibration, and it is very difficult to acquire a sufficient number of incident data sets for one section of freeway to provide a sound basis for this approach. Consequently, we investigated a second approach which involves the normalization of features used in the algorithm.

6.1.1 Geometric Anomalies in the Los Angeles System

Our approach is illustrated by our treatment of the Los Angeles system. Specifically, consider the incident alarm cases obtained for Algorithm 7 by exercising the CALB program. A partial listing of these cases is given in Table 23. A significantly anomalous geometric condition is identified by repeated occurrences of false alarms corresponding to a certain location and reference to freeway design plans. This listing of false alarms is typical of the complete listing of false alarms in that repeated occurrences are associated with the San Diego freeway northbound (freeway segment 3), Station 31. This station is located just upstream of the

Preceding page blank

Table 23. A partial listing of false alarms for Algorithm 7, T_1=8.1,T_2=.313,T_3=16.81.

Case Label No.	Data Set No.	Time	Location Freeway	Location Station
83	74090450	642	3	2
84	74090450	646	3	31
85	74090450	652	3	31
86	74090450	706	3	1
87	74090450	714	3	9
88	74090450	717	3	31
89	74090450	719	3	10
90	74090450	722	3	8
91	74090450	729	3	2
92	74090450	730	3	31
93	74090450	731	3	10
94	74090450	737	3	2
95	74090450	737	3	25
96	74090450	740	3	31
97	74090450	741	3	10
98	74090450	744	3	31
99	74090450	750	3	31
100	74090450	806	3	29
101	74090450	807	3	25
102	74090450	808	3	10
103	74090450	810	3	31
104	74090450	815	3	10
105	74090450	817	3	31
106	74090450	854	3	31
107	74090450	919	3	31

connector to the Santa Monica freeway. The geometrics are schematically depicted in Figure 4. Many of the locations for which there are frequent false alarms are near freeway-to-freeway interchanges.

Certain combinations of traffic demand and geometrics give rise to consistent differences in the occupancies at adjacent stations. Inasmuch as the algorithms which have proved most effective are all based on differences in occupancies at adjacent stations, these differences degrade the performance of incident detection algorithms. The pattern in which the upstream occupancy is larger than the downstream occupancy can lead to a false alarm if the discrepancy is large enough. On the other hand, if the typical pattern at some location is for the upstream occupancy to be less than the downstream occupancy, the detection of incidents will be hindered.

To verify such consistent differences, occupancy data was analyzed by pairs of stations. A typical case is that for stations 31 and 32, San Diego freeway northbound. Figure 35 is a scattergram of station 31 occupancy versus station 32 occupancy. For this it is evident that station 31 occupancy is generally higher than station 32 occupancy, particularly when station 32 occupancy is less than 20%. In this area, there are four lanes of traffic at station 31 which splits into three mainline lanes at station 32 and two connector lanes. As the volume of traffic on the connector is substantial, four lanes of traffic have the use of five lanes in the vicinity of station 32.

The traffic pattern prone to producing the most false alarms is the one in which the downstream occupancy values are in the range which occurs when there is an incident, say, less than 20%. Using only cases in which the downstream occupancy is less than 20%, a least squares fit through the origin was computed yielding a line with slope 1.481. Thus, when DOCC<20%, one expects OCC=1.481xDOCC. In Table 24, the computed slopes are given for each station in the Los Angeles system. By referring to this table and to Figure 18, it will be observed that consistent discontinuities (k differing from 1) are commonly found in the vicinty of freeway-to-freeway interchanges.

6.1.2 Adjusting Features for Geometric Anomalies

Denoting a computed slope by k, the regression results are used to make the following adjustments to features:

$$\overline{OCCDF}=OCC-k\ DOCC$$

$$\overline{OCCRDF}=\overline{OCCDF}/OCC$$

Thus, the adjusted value of OCCDF (i.e., $\overline{OCCDF}$) represents the deviation from the typical difference in occupancy values.

These adjustments were made for those stations with k>1.20 or k<.80 to produce the "geometrically adjusted Los Angeles data base," reflecting the

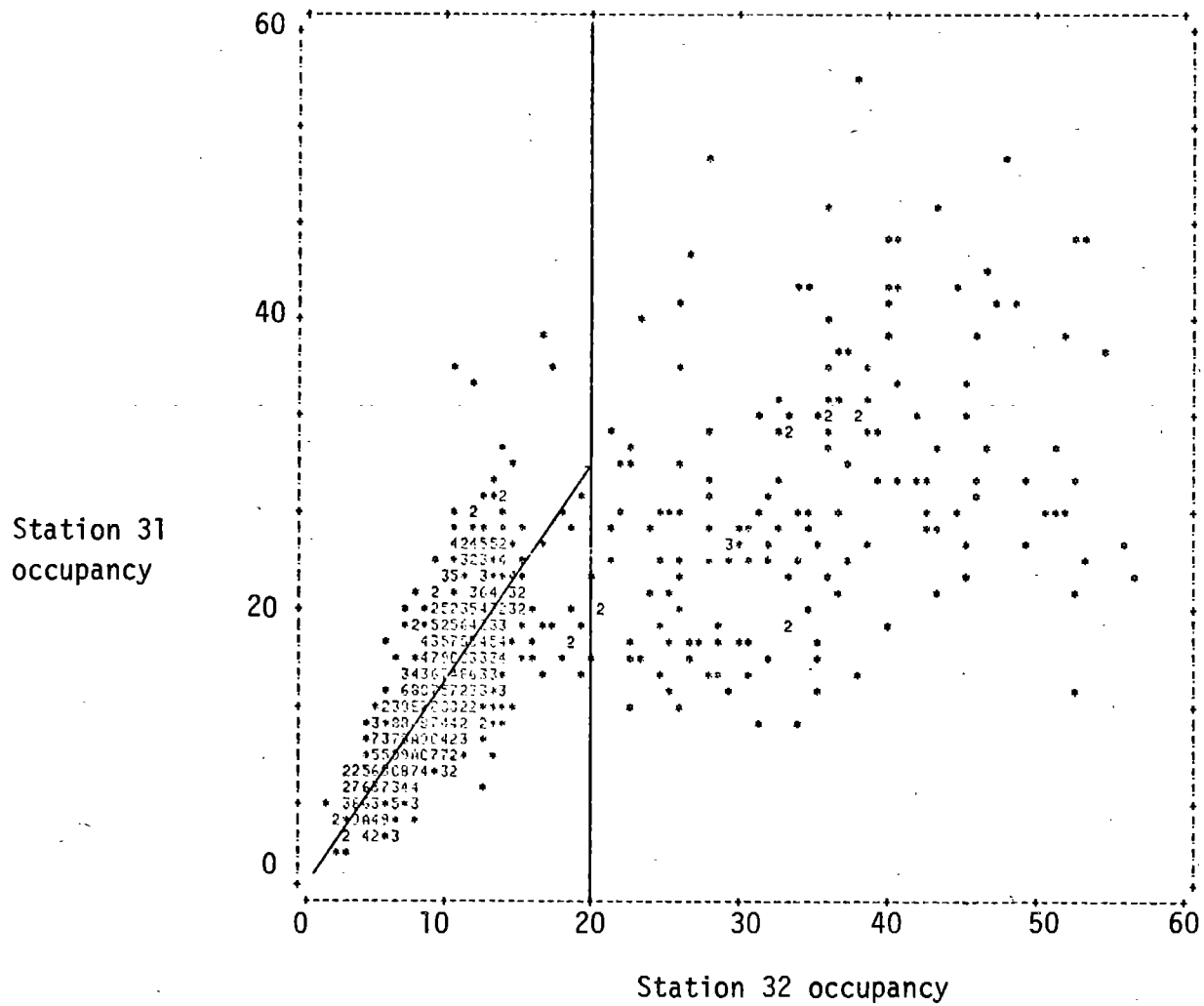

Figure 35. Scattergram of station 31 occupancy versus station 32 occupancy, San Diego freeway northbound, Los Angeles data base.

Table 24. Slopes obtained from regressing upstream occupancy against downstream occupancy.

Station	Santa Monica Freeway Eastbound	Santa Monica Freeway Westbound	San Diego Freeway Northbound	San Diego Freeway Southbound	Harbor Freeway Northbound
1	1.502		.892		.943
2	.653	.589	1.100	1.213	.982
3	.879	1.220	.998	.938	1.014
4	1.097	.987	1.034	.892	.959
5	1.081	.952	1.049	1.031	1.029
6	1.025	1.252	1.000	.956	.870
7	.987	.736	.993	.908	1.199
8	.979	1.290	.955	.990	.865
9	.739	.953	.892	.961	.981
10	.742	1.165	1.269	1.023	.912
11	.785	.998	.810	.912	1.168
12	.981	1.443	1.018	.925	.816
13	1.287	1.030	1.034	1.222	1.163
14	.988	.978	1.067	.948	1.104
15	1.176	1.098	.996	.944	1.063
16	.903	.938	.911	.912	1.016
17	1.163	.909	1.059	1.056	1.079
18	1.050	1.057	.890	.865	1.086
19	1.290	1.016	1.189	1.117	1.213
20	1.154	1.070	.767	.836	.902
21	1.163	1.015	1.064	1.039	1.321
22	1.092	.940	.857	1.035	1.137
23	1.109	1.080	1.036	1.080	1.071
24	1.039	.892	.934	1.146	1.379
25	1.086	1.133	1.157	1.060	
26	1.011	.887	1.026	1.165	
27		.758	.765	1.109	
28		1.216	.927	1.294	
29			1.054	.945	
30			.973	1.126	
31			1.481	1.079	
32				.797	

fact that, in practice, one would limit ones attention to a few stations where a significant problem exists.

Exercising Algorithm 7 with the normalized (geometrically adjusted) features and with the same thresholds as used to produce the results in Table 2, we did obtain a reduction in the number of false alarms associated with geometric anomalies. Table 25, a partial listing of false alarms is typical of the results obtained and illustrates the reduction in false alarms. The number of false alarms at station 31, San Diego northbound, in the data set 74090450 is reduced from eleven to three, for example. The false alarm rate measured over all the incident-free data sets is reduced from .135% to .092%.

However, detection performance apparently is adversely affected. Of the twenty-eight incidents detected without normalization of features, three incidents are missed with normalization. All three of these incidents occurred in the section immediately downstream of station 31, San Diego northbound. An examination of these three incidents (74052403, 74100703, and 74100801) reveals that none produced a large change in the traffic pattern. In fact, one might regard their detection (with unnormalized features) as coincidental as the patterns involved do not differ from the typical pattern at this location. Further, reference to Table 13 reveals that lane blockage information is lacking for these incidents suggesting that all disabled vehicles may have been located in the median or right shoulder.

We next proceeded to recalibrate Algorithms 4, 7, 8, and 9 on the geometrically adjusted data base, i.e., using normalized features. These results are given in Table 88 and Figure 68 for Algorithm 4; in Table 97 and Figure 76 for Algorithm 7; in Table 110 and Figure 87 for Algorithm 8; and in Table 115 and Figure 91 for Algorithm 9. The comparative performance for Algorithm 7, illustrated in Figure 36, is typical of these results, and reflects the observations made above. (The differences observed are generally not significant at the .10 level.)

Despite the unconvincing nature of these quantitative results, it is our opinion that the normalization procedure developed here is as good a procedure for improving performance in geometrically anomalous sections as is available.

6.2 EFFECTS OF SENSOR CONFIGURATION

Sensors in the form of presence detectors are the source of data for incident detection. The configuration of sensors, therefore, can be expected to have a significant effect upon the performance of incident detection algorithms. One objective of this study is to quantify this effect and to develop recommendations for effective configurations.

Table 25. A partial listing of false alarms for algorithm 7, T_1=8.1, T_2=.313, T_3=16.8, using normalized features.

Case Label No.	Data Set No.	Time	Location Freeway	Location Station
55	74090450	642	3	2
56	74090450	706	3	1
57	74090450	714	3	9
58	74090450	722	3	8
59	74090450	729	3	2
60	74090450	737	3	2
61	74090450	737	3	25
62	74090450	744	3	18
63	74090450	752	3	31
64	74090450	801	3	31
65	74090450	804	3	10
66	74090450	806	3	29
67	74090450	807	3	25
68	74090450	808	3	10
69	74090450	826	3	31
70	74090450	1147	3	17

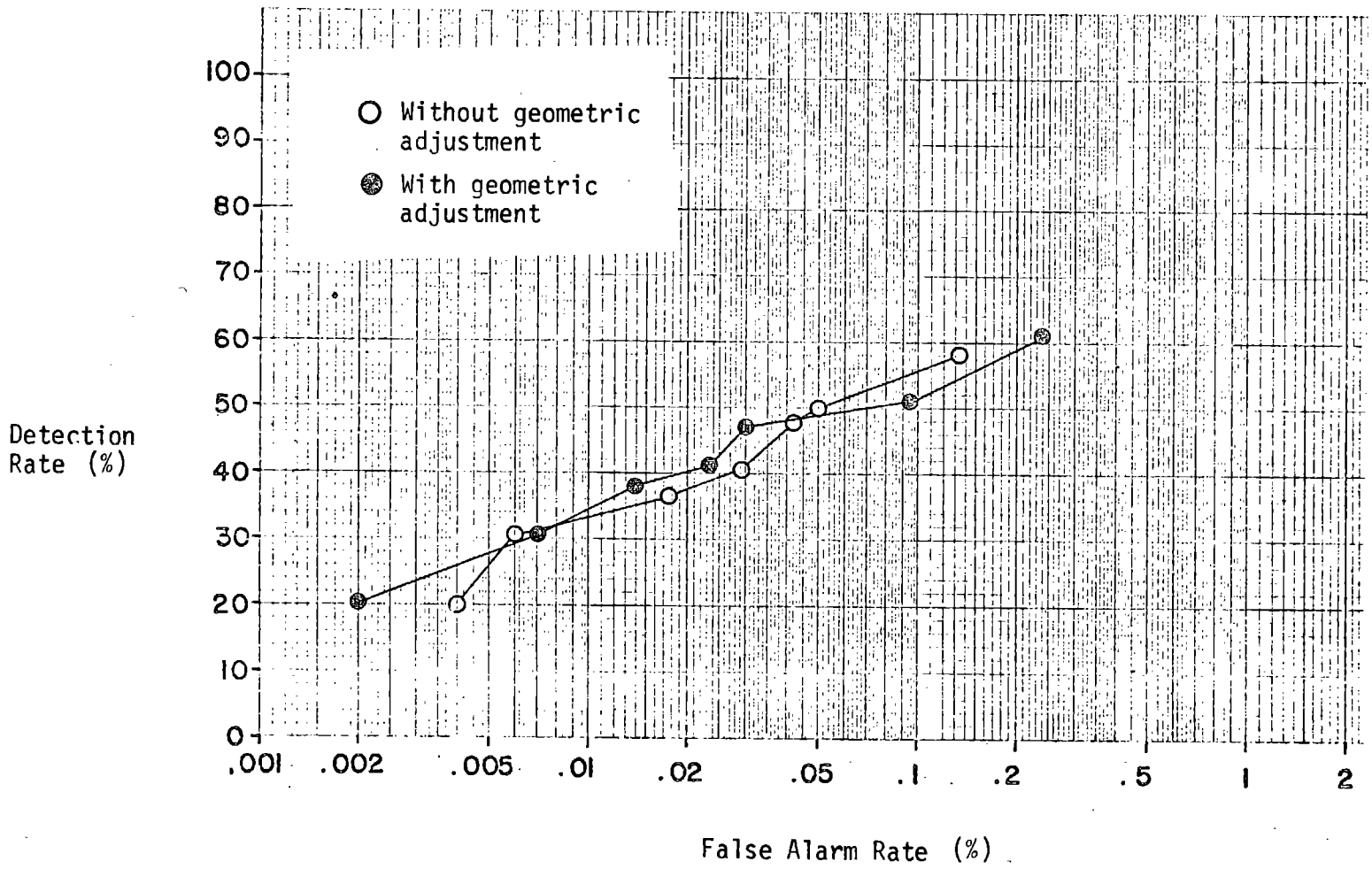

Figure 36. Comparison of performance for Algorithm 7, with and without geometric adjustments.

In all other work on this study, algorithm performance is based upon the use of all available sensor data. The approach taken to elicit the dependence of algorithm performance upon sensor configuration is to develop the same quantitative measures of performance for specified subsets of the full set of sensors.

6.2.1 Sensor Configurations

Two aspects of the sensor configuration are of interest to us: (1) the instrumented lanes at a station and (2) the separation between stations. It should be recognized at the outset that our treatment of sensor configuration is limited by the existing configuration. That is, we can only consider sensor configurations which are subsets of the Los Angeles and Minneapolis configurations. All of our attention will, in fact, be focused on a segment of the San Diego freeway in Los Angeles within which nearly all lanes are instrumented. This segment includes stations 24 through 32 in both directions. The full sensor configuration, denoted Configuration A, is shown in Figure 37. In this and succeeding figures, the symbol ■ denotes a loop for which data were collected and used in analyses; the symbol □ denotes a loop for which data were not available, or were not used for the particular configuration considered.

Two alternative configurations are defined as subsets of Configuration A. Configuration B, Figure 38, has sensors in lane 2 and all stations are employed, i.e., stations are at the minimum available spacings.

Configuration C, Figure 39, has sensors in all (available) lanes, but only every other station is used, i.e., stations 24, 26, 28, 30 and 32.

The remaining segments of the Los Angeles and Minneapolis systems do not permit consideration of variations of sensor instrumentation within a station. In the remainder of the Los Angeles system, except for another segment of the San Diego freeway for which very little incident data are available, partial station instrumentation is most common. There are full-count stations, but these do not occur frequently enough to allow their use in the manner described above. Data from the Minneapolis system are primarily available in the form of averages across all lanes, preventing any examination of partial station configurations.

6.2.2 Data Bases

For the alternative sensor configurations illustrated in Figures 37 to 39, the incident and incident-free data sets used are those indicated in Tables 13 and 15, respectively, as noted by entries in the column headed by "Sensor Configuration Study."

6.2.3 Algorithm Performance

Algorithms 2, 7, and 8 were examined. For each algorithm and each sensor configuration, thresholds previously determined by calibration on the Los Angeles data base were used to obtain performance evaluations in the usual form of detection and false alarm rates and means of times-to-detect. For Algorithm 2, these results are given in Tables 81; for Algorithm 7, in

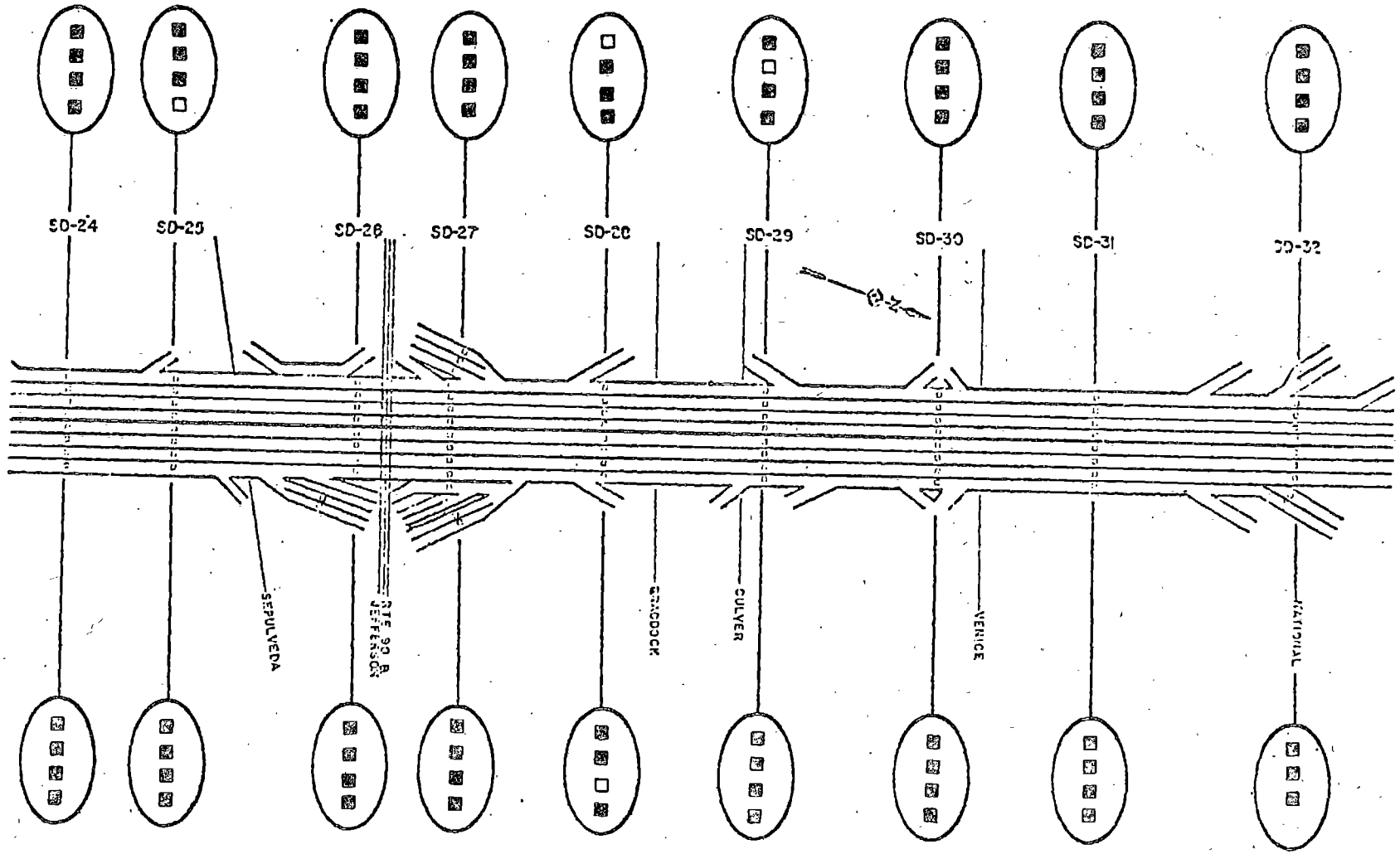

Figure 37. Sensor configuration A.

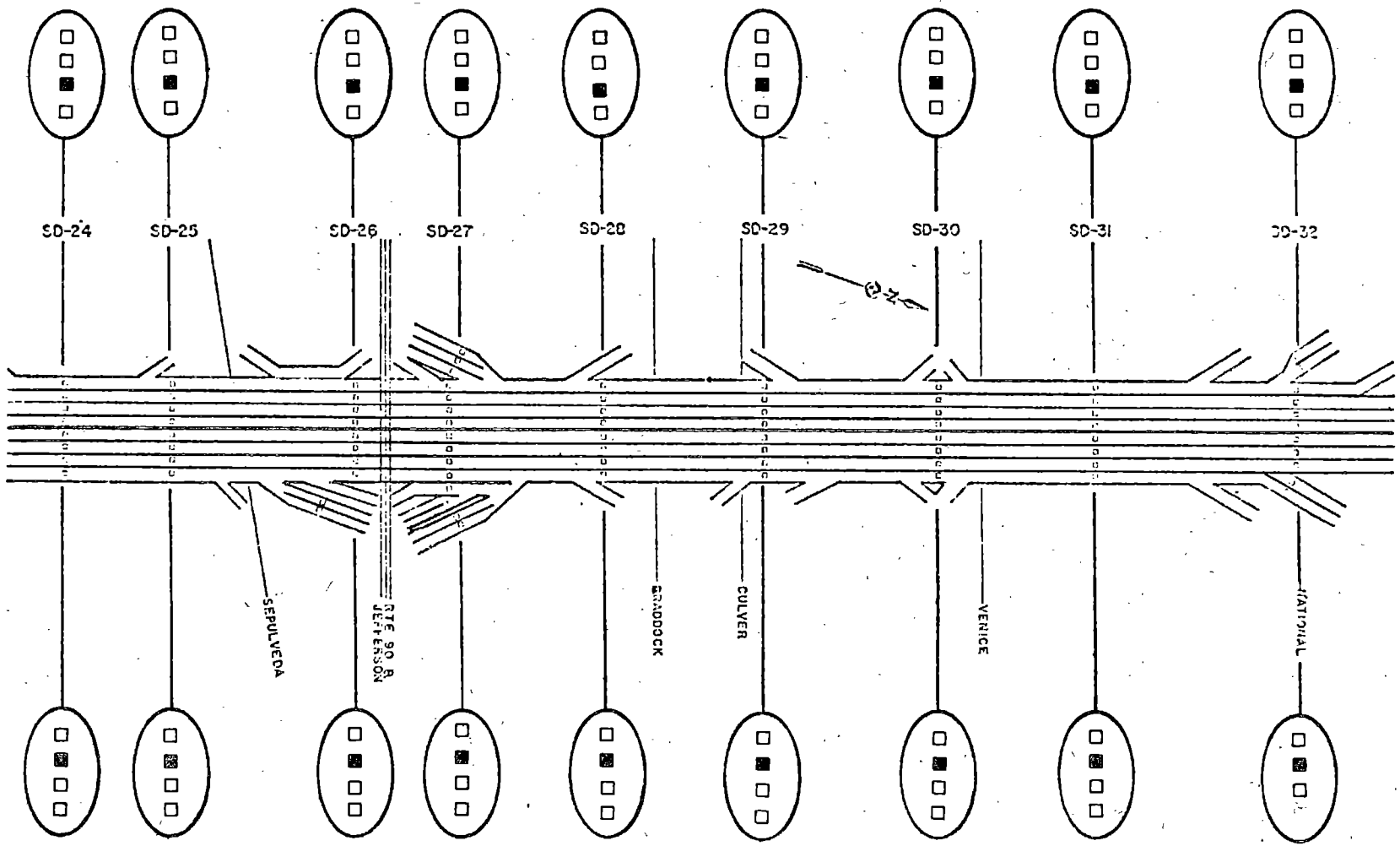

Figure 38. Sensor configuration B.

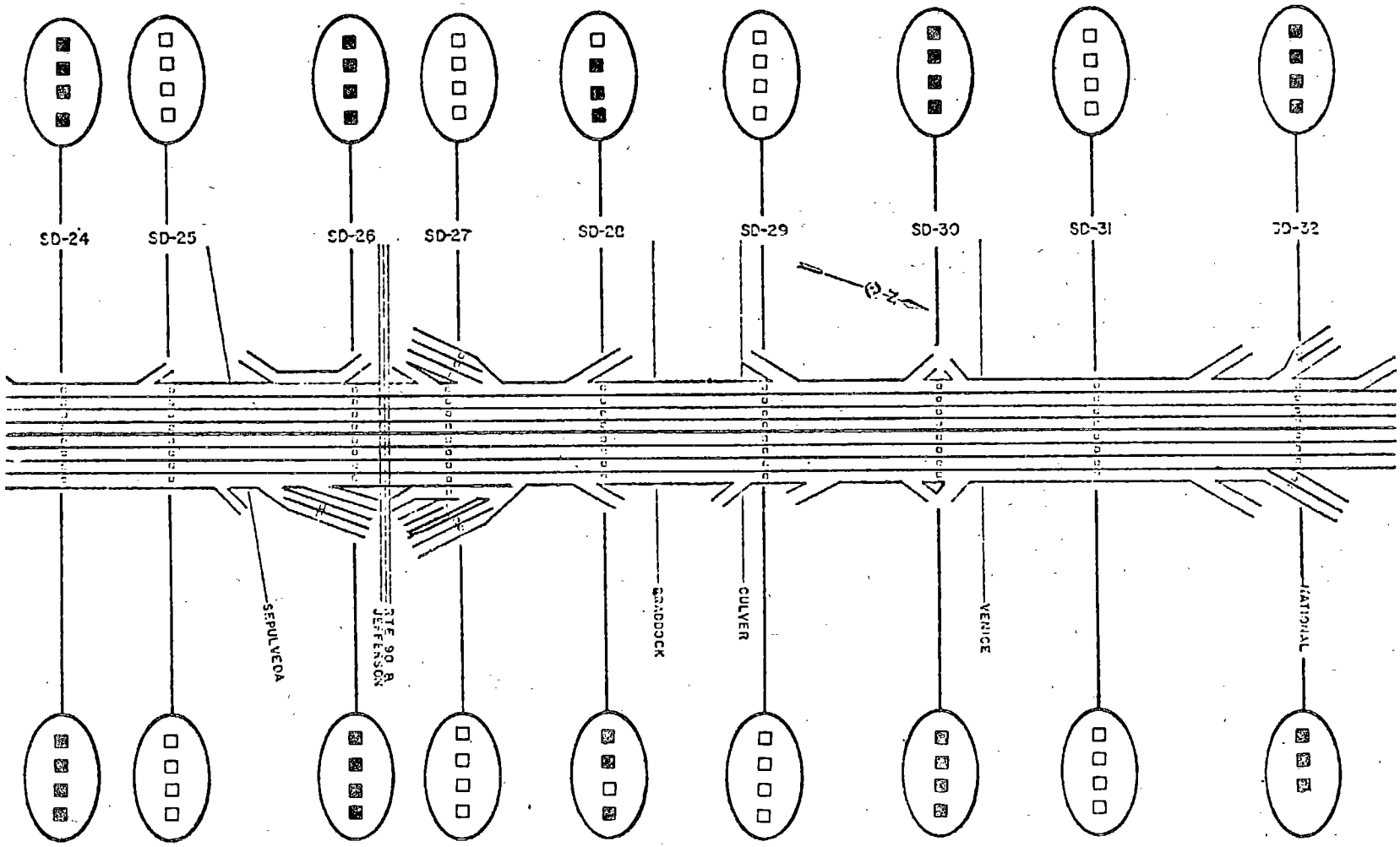

Figure 39. Sensor configuration C.

Table 96; and for Algorithm 8, in Table 108. Comparative performance results are displayed separately for these three Algorithms in Figures 45, 46, and 47, respectively. On the whole, performance on this data base is poorer than on the larger Los Angeles data base, primarily because a relatively large fraction of the incidents are of the difficult-to-detect variety. Due to the small number of samples (13,357 tests, 8,267 tests and 6,576 incident-free tests, for configurations A, B, and C, respectively), differences in false alarm rates are found not to be significant at the .10 level.

Algorithm 7 was recalibrated for each sensor configuration, with results for sensor Configuration A being given in Table 98 and Figure 77; those for sensor Configuration B, in Table 99 and Figure 78; and those for sensor Configuration C, in Table 100 and Figure 79. Comparative performance results are given in Figure 48.

Collectively, these results indicate

- At a given detection rate, false alarm rates for Configurations B and C are, generally, about twice those for Configuration A, with Configuration C having slightly better performance than Configuration B. Thus, the use of more detectors up to the point represented by Configuration A yields improved performance.

- Surprisingly, times-to-detect showed no consistent pattern. One would expect Configuration C to experience significantly longer times-to-detect since detections are generally related to the back-up of the queue from the site of the incident over the upstream detector station. Two previous studies[1,2] of station spacing have identified an effect of station spacings on times-to-detect, though neither of these was based on actual traffic data.

The lack of very clear differences in the times-to-detect for the three configurations may be due to the fact that the detection-related performance measures were based on very few cases. While 35 incidents were involved in the analyses, only about one-third of these were readily detected so that relatively few incidents entered in the computation of the times-to-detect.

---

[1] C. L. Dudek and H. Whitson, "Toward Automatic Incident Detection on the North Central Expressway," Dallas Freeway Corridor Study Report RF953-7, prepared for the Federal Highway Administration, Office of Research, Traffic Systems Division under Contract No. DOT-FH-11-7964, August 1973.

[2] H. J. Payne, "Analysis and Evaluation of the California Logic for Incident Detection," Final Report, Part III, USCEE Report 464, University of Southern California, Department of Electrical Engineering, December 1973.

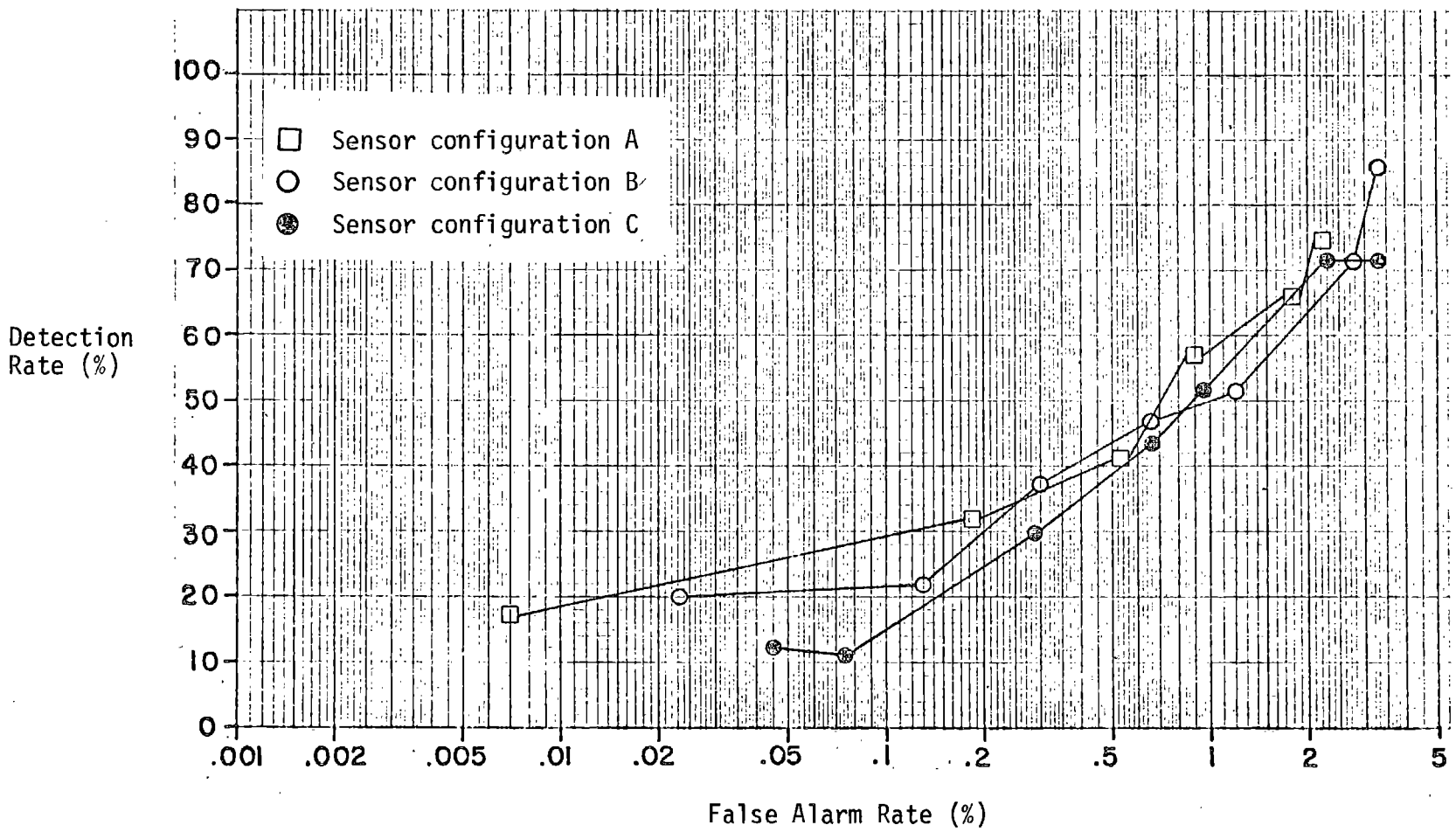

Figure 40. Comparison of performance of Algorithm 2 for three sensor configurations.

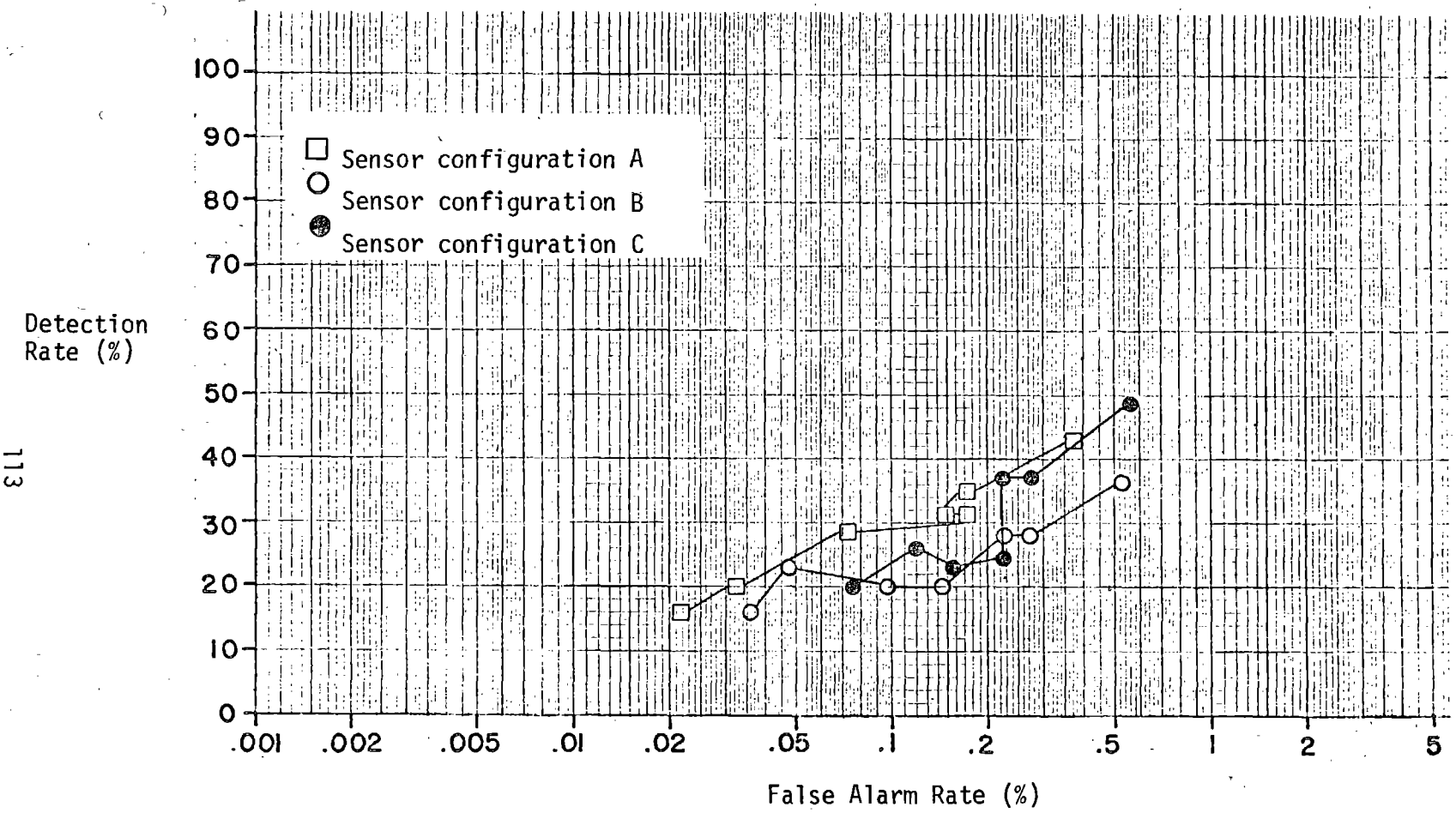

Figure 41. Comparison of performance of Algorithm 7 for three sensor configurations.

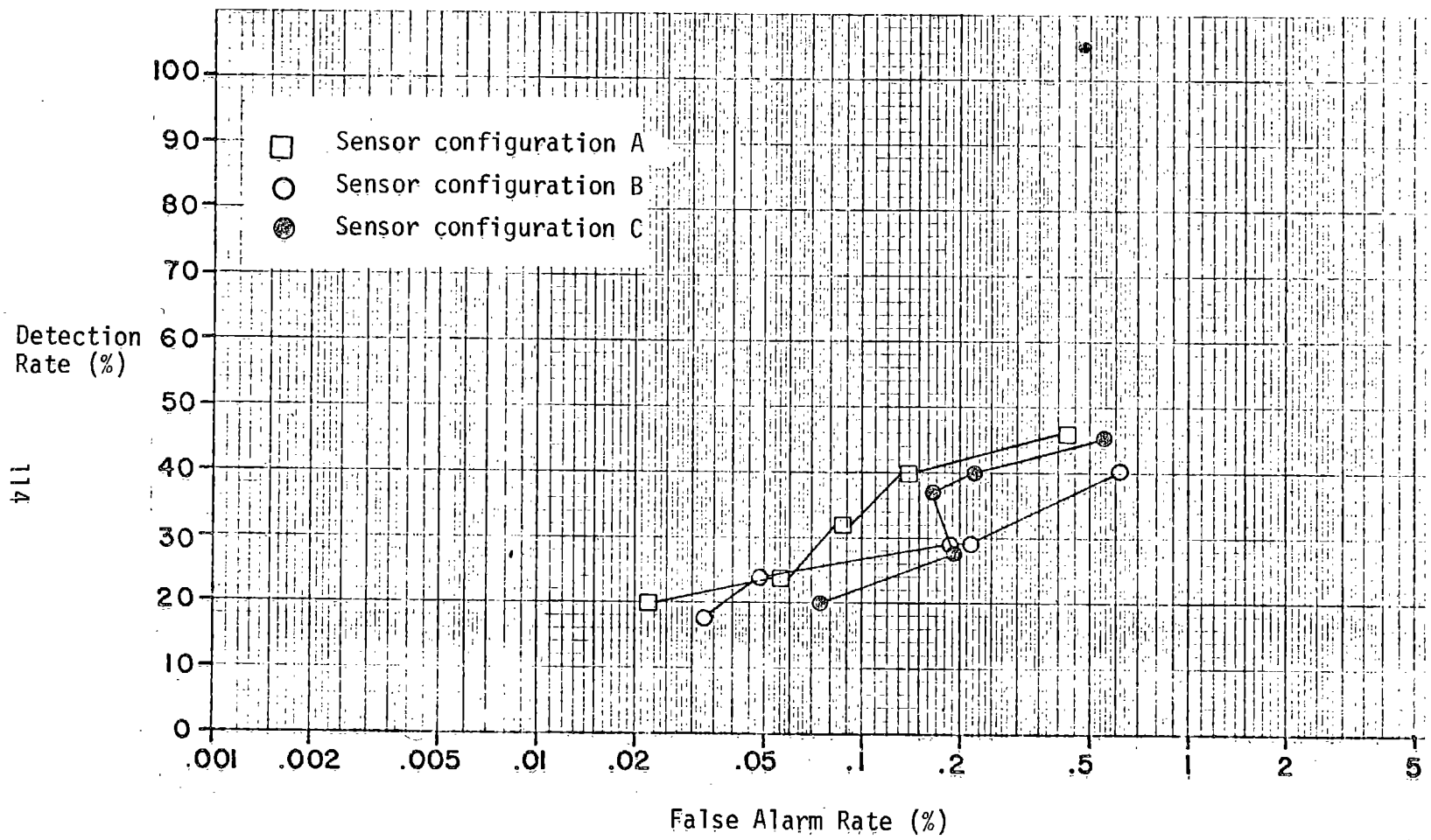

Figure 42. Comparison of performance of Algorithm 8 for three sensor configurations.

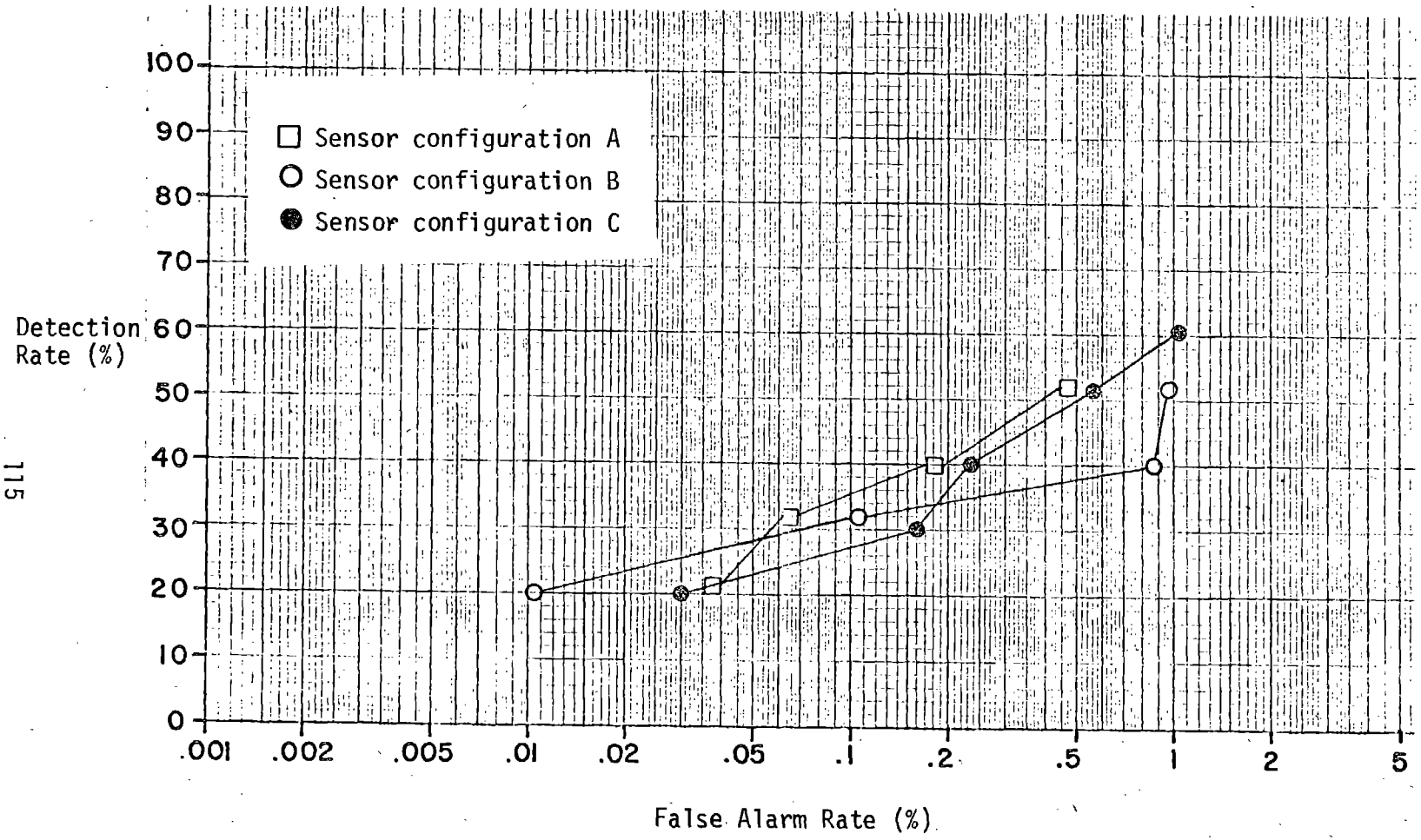

Figure 43. Comparison of performance of Algorithm 7 recalibrated for three sensor configurations.

Comparing the performance of the three algorithms for each of the sensor configurations, one sees that Algorithm 8 is, generally, the best and Algorithm 7 the next best, a conclusion consistent with that found in the original development of these algorithms with the Los Angeles data base.

Finally, we note that recalibrating thresholds for Algorithm 7 did not produce marked changes except for Configuration B. It would appear that the thresholds are not very sensitive to sensor spacing in the range of one-half to one mile, but are sensitive to the instrumentation within a station. These conclusions must be regarded with some caution, however, since they are deduced from examination of a single algorithm on a limited data base and with only three sensor configurations.

6.3 FREQUENCY OF ALGORITHM EXECUTION

In all of the developments we have undertaken, algorithms were executed at one-minute intervals. In contrast, at present in Chicago, Los Angeles. and Minneapolis algorithms are executed at either 20- or 30-second intervals. The choice of the one-minute interval for this study was largely dictated by a desire to limit computational expenses associated with the testing of candidate algorithms.

Operational use of the more frequent algorithm executions will have the following effects:

- Computational burden will be increased
- Modifications to the algorithms presented here will be required
- Detection times will be reduced
- The number of false alarms will be increased

That the computational burden will be increased is evident. Tests executed at 20-second intervals will require three times the computation required for tests at one-minute intervals.

To follow through the remaining consequences, we will consider a specific algorithm, Algorithm 7, previously discussed. We will consider making tests at 20-second intervals. This algorithm uses the occupancy-based features OCCDF, OCCRDF, and DOCC. These are based on one-minute average occupancies so that it is necessary to generate one-minute average occupancies updated every twenty seconds.

To modify Algorithm 7 to provide for more frequent updating requires revision to that portion of the algorithm which checks for persistence. Specifically, it is necessary to introduce two more state values that cause the algorithm to wait for a minute after a tentative incident condition is detected. The modified algorithm is presented in Figure 44 (and the relevant coding in Table 94).

State Value	Designates
0	Incident-free
1	Tentative incident
2	Tentative incident
3	Tentative incident
4	Incident confirmed
5	Incident continuing

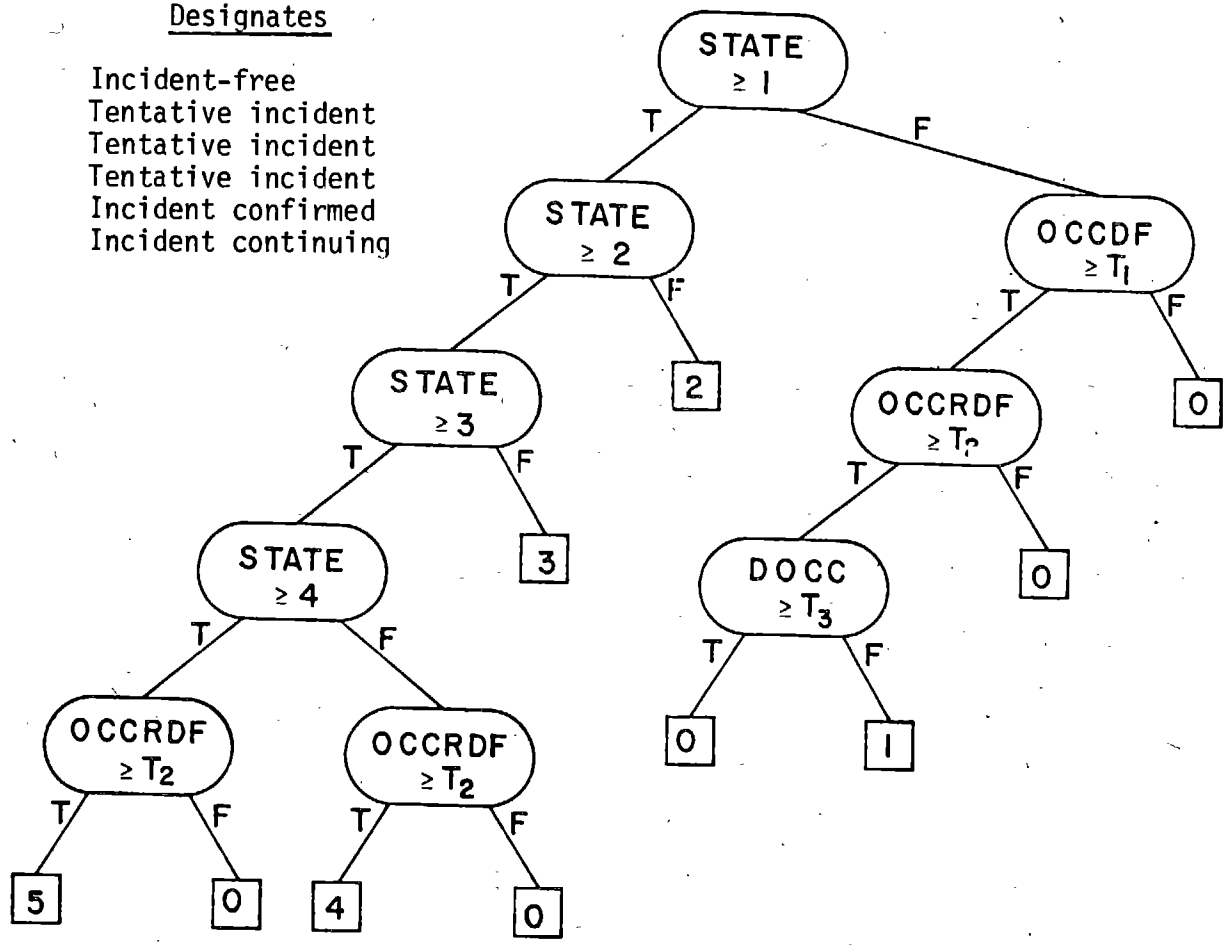

Figure 44. Algorithm 7 modified for testing at 20-second intervals.

This modified form of the algorithm was evaluated with the choice of thresholds T_1=12.9, T_2=.360, and T_3=16.6, obtained previously by calibration on the Los Angeles data base, Table 95. In this table one finds the mean-time-to-detect using one-minute intervals to be 4.31 minutes. With 20-second updates, four incidents are detected 20 seconds sooner, six are detected 40 seconds sooner, and one, 80 seconds sooner. For the 25 incidents detected by each form of the algorithm, this gives a mean reduction of 16 seconds.

This result agrees closely with the prediction based on the following simple argument. Assume that the instant at which the traffic pattern is such as to trigger a detection is random with respect to the algorithm execution times and that the pattern presists after this time. Then if S seconds remain before the next 20-second update, S, S+20, or S+40 seconds remain before the next minute update, with each possibility equally likely. Thus, the difference in times to detect is

$$\frac{1}{3}[S+(S+20) + (S+40)]-S = 20 \text{ seconds} ,$$

very nearly that observed in the data.

This argument generalizes in the following way. As compared to the times-to-detect for one-minute updates, the expected difference in times-to-detect for update every t seconds is (60-t)/2 seconds. Thus, for example, using updates at 30-second intervals, saves, on the average, 15 seconds in the time to detect.

Examination of false alarms for the 20-second update form of Algorithm 7 indicates that the false alarm rate actually decreases but the number of false alarms in a given period increases substantially. (Limited quantitative results indicate a 50% increase.)

Taken together, these conclusions suggest that the slight improvement in mean time-to-detect obtained by testing more frequently than once per minute is not justified in view of the increase in the number of false alarms and the increased computational burden.

6.4 ALGORITHMS FOR LANE CLASSIFICATION OF FREEWAY INCIDENTS

Successful identification of the lane locations of freeway incidents potentially serves two functions: (1) to direct emergency response vehicles and (2) to provide advance warning on message signs to freeway motorists.

Three methods exist for this purpose: (1) visual surveillance, (2) incident detection algorithms employing individual lane data, and (3) lane classification algorithms initiated by incident detection algorithms. This report concerns the third type only.

Characteristic differences in traffic stream data from lanes blocked by incidents are expected:

1. High OCC (occupancy) in the involved lane at the upstream station.
2. Low OCC " " " " " " downstream " .
3. Low SPD (speed) " " " " " " upstream " .
4. High SPD " " " " " " " downstream " .
5. Low VOL (volume) " " " " " " upstream " .

Use of these features, or combinations of them, provide a basis for lane-classification algorithms.

The characteristic differences between involved and noninvolved lanes are expected to be present at upstream or downstream stations during various time periods following the occurrence of an incident. Practicality must be considered in choosing the time period to be inspected by an algorithm. For example, identification of involved lanes based on data accumulated over a ten-minute period following an incident may be most effective, in terms of accuracy, but would defeat the purpose of making lane information available to assistance vehicles. On the other hand, algorithms employing data accumulated prior to a detection alarm would be ideal.

An evaluation of algorithms employing OCC, VOL, and SPD data during various time intervals is presented here.

6.4.1 The evaluation data base

To estimate the performance of potential algorithms, a data base was required. Accurate lane documentation was a criterion for inclusion in the data base. Of the forty-six incident data sets identified as having lane documentation, seventeen were eliminated for the following reasons:

8 incidents were not detected by the detection algorithm[1],
4 incidents occurred on collectors or on/off ramps,
3 data sets lacked sensor data,
2 data sets contained data read errors.

Twenty-nine data sets were thus available for use in a manual evaluation (see Table 13). Twenty-second OCC, VOL, and SPD maps were generated for these data sets.

The breakdown of the incident locations was as follows:

[1]The detection algorithm employed was Algorithm 7 calibrated to a detection rate of 60% and a false alarm rate of .34%.

7% - median
31% - lane 1
17% - lane 2
17% - lane 3
14% - lane 4
10% - lane 5
3% - right shoulder

6.4.2 Algorithms employing upstream station data

Twenty-second OCC, VOL, and SPD data from upstream stations were examined over one-, two-, and five-minute intervals immediately following detection. A dominance method was employed to identify the lanes with (1) the maximum values of OCC, (2) the minimum values of VOL, and (3) the minimum values of SPD (VOL/OCC)(see Tables 26-28). For each feature, the number of times each lane had an appropriate maximum or minimum value was totaled over each interval being examined. The lane with the majority of appropriate maximum or minimum values was identified as the likely incident lane. If no one lane dominated the others, a "no-decision" state was reached (see Table 29). These predictions were matched against the actual blocked lanes. The percentage of cases in which the predicted lane matched or was adjacent to the actual lane was used as a measure of performance. (A few data sets had data for adjacent lanes only). It was felt that an algorithm identifying an adjacent lane would still be effective as an aid to emergency vehicles. The results of these evaluations are shown in Tables 30 through 35. The test involving VOL was eliminated due to the highly fluctuating nature of twenty-second lane volume data. Most of these cases led to "no-decision" states.

The classification performance of these algorithms was not substantially high.

6.4.3 Algorithms Employing Downstream Station Data

Downstream OCC data were also examined. Blocked lanes downstream of an incident would be expected to exhibit lower OCC values than non-involved lanes. An examination of eighteen data sets showed promising results. The two-minute interval immediately following each alarm was inspected for dominance by a particular lane. Four minimum OCC values out of the six twenty-second intervals in the two-minute period were a requirement for dominance. Data sets for incidents occurring in lane 2 and having downstream data for lanes 1 and 3 only were not considered, as such cases would yield adjacent lane identifications by default.

The results of this test are shown in Table 36. This algorithm reduced the number of lane 1 incidents classified in lane 3. The 77% performance level of this test may not be spectacular, but it does approach acceptable performance. It implies that downstream data should be considered an integral part of a lane classification algorithm.

Table 26. Occupancy dominance, lane 3.

740624-02

OCCUPANCY

FWY	5	5	5	5
STA	20	20	20	20
LANE NO	1	3	1	3
TIME				
848++	29	35	25	29
+	42	64	17	27
+	34	26	21	16
849++	28	30	28	20
+	23	33	26	16
+	32	40	23	10
850++	30	45	14	15
+	39	67	18	9
+	46	59	15	9
851++	41	52	7	8
+	27	45	11	6
+	29	52	6	8 — Detection
852++	26	47	12	11
+	27	35	14	11
+	25	42	10	9
853++	25	46	14	8
+	25	38	15	12
+	24	34	17	12
854++	28	40	11	21
+	41	50	13	15
+	34	48	15	13
855++	26	43	17	12
+	22	28	16	6
+	31	42	15	16
856++	28	44	10	11
+	33	31	9	11
+	24	0	13	4
857++	27	43	8	7

Lane numbering begins in left lane and goes toward the right shoulder.

Lane is shown for lanes 1 and 3 only since these are the only instrumented lanes.

Maximum OCC at each 20-sec circled

Note consistent dominance of upstream lane 3 over lane 1

Table 27. Volume dominance, lane 1.

740426-01

VOLUME

FWY	2	2	2	
STA	22	22	22	
LANE NO.	1	3	4	
TIME				
708++	1800	1440	2160	
+	1800	1260	900	
+	1440	1980	1080	
709++	1800	1980	1260	— Incident Occurs in Median
+	1080	1260	1440	
+	720	1260	1260	— Drop in Upstream Volume Lane 1
710++	360	1260	1440	
+	180	1800	1440	
+	900	900	1080	
711++	360	900	1440	— Detection Occurs
+	0	720	720	One Minute
+	180	540	1080	
712++	360	1080	720	
+	0	900	1080	Two Minute
+	0	540	1260	
713++	360	1260	1080	
+	720	1260	1440	
+	360	1800	1080	
714++	360	900	1260	
+	540	1440	1080	
+	540	900	1260	Five Minute
715++	720	900	900	
+	360	2160	900	
+	180	540	1080	
716++	0	1620	1260	
+	540	1620	900	
+	360	900	1440	
717++	540	1260	900	

Lowest Vol. at Each 20-Sec Circled

Note consistent dominance of lane 1

Table 28. Speed dominance, lane 4.

740403-02

SPEED

FWY	6	6	6	6
STA	24	24	24	24
LANE NO.	1	2	3	4
TIME				
1530++	37	35	34	33
+	40	37	32	36
+	35	31	32	36
1531++	24	18	9	29
+	17	16	5	14
+	15	15	17	16
1532++	13	10	14	19
+	17	11	16	22
+	16	13	13	12
1533++	16	12	11	9
+	19	22	14	13
+	25	18	12	14
1534++	24	20	16	19
+	27	21	23	15
+	25	29	28	19
1535++	26	29	27	24
+	30	32	30	24
+	32	32	31	24
1536++	32	30	25	27
+	29	31	31	28
+	27	31	27	26
1537++	28	32	34	28
+	28	33	33	32
+	28	28	28	29
1538++	27	27	30	29
+	27	25	28	30
+	30	27	30	31
1539++	30	30	27	30

— Detection

Lowest SPD at each 20-sec circled

Note consistent dominance of lane 4

Table 29. No volume dominance.

740422-01

VOLUME

FWY	1	1	1	1	1
STA	21	21	21	21	21
LANE NO	1	2	3	4	5
TIME					
914++	1620	1440	1620	1260	1800
+	1620	1440	1800	1620	1620
+	1800	1800	1800	1980	1440
915++	1980	2160	1080	1800	2160
+	1980	1620	1980	1080	2340
+	1980	1800	2160	1620	1620
916++	1800	1800	1980	1620	1980
+	1440	1800	1440	1620	1800
+	1800	1620	1800	1980	2160
917++	1800	1620	1980	1800	2520
+	1800	2160	1800	1980	1440
+	1620	1800	1620	1440	1440
918++	1800	1980	1800	1620	1800
+	2160	1620	1620	1980	1980
+	1440	2160	1620	1980	2160
919++	1800	1440	1800	900	1620
+	1260	1260	1080	900	1800
+	1620	1800	1800	1800	1260
920++	1620	1800	1260	1440	1980
+	1440	1260	1620	1260	1800
+	1800	1620	1620	1260	2160
921++	1440	1800	2160	1440	1800
+	2160	1620	1620	1440	2160
+	1800	1800	1260	1080	1800
922++	1620	1620	1260	1620	1800
+	1260	1440	1440	1440	1260
+	1440	1620	1620	1800	2160
923++	1620	1620	1080	720	1800

Incident Occurs Lane 5

Detection

One Minute

Two Minute

Five Minute

No One Lane Exhibits Dominance

Table 30. OCC at upstream station, one-minute interval following alarm.

FEATURE - OCC AT UPSTREAM STATION

TIME - 1 MIN. FOLLOWING ALARM

NO. CASES - 22

ACTUAL OR ADJACENT LANE PREDICTED -

13 (59%)

PREDICTED LANE	ACTUAL LANE M	1	2	3	4	5	RS
1		1	3	2			
2							
3	1-	5		2	2		
4	1			1	3		
5						1	

Table 31. OCC at upstream station, two-minute interval following alarm.

TIME - 2 MIN. FOLLOWING ALARM

NO. CASES - 23

ACTUAL OR ADJACENT LANE PREDICTED -

12 (52%)

PREDICTED LANE	ACTUAL LANE M	1	2	3	4	5	RS
1	1	1	2	2	1		
2							
3		5		3	2		
4	1		2		2		
5						1	

Table 32. OCC at upstream station, five-minute interval following alarm.

TIME - 5 MIN. FOLLOWING ALARM

NO. CASES - 23

ACTUAL OR ADJACENT LANE PREDICTED -

14 (60%)

PREDICTED LANE	ACTUAL LANE M	1	2	3	4	5	RS
1	1	2	2	1	1	1	
2							
3	1	4		4	2		
4	1		2		2		
5						1	

Table 33. SPD at upstream station, one-minute interval following alarm.

FEATURE - SPD AT UPSTREAM STATION

TIME - 1 MIN. FOLLOWING ALARM

NO. CASES - 22

ACTUAL OR ADJACENT LANE PREDICTED -

13 (59%)

PREDICTED LANE \ ACTUAL LANE	M	1	2	3	4	5	RS
1	1		2				
2							
3	1	6	1	3	2	1	
4			1	1	3		
5							

Table 34. SPD at upstream station, two-minute interval following alarm.

TIME - 2 MIN. FOLLOWING ALARM

NO. CASES - 22

ACTUAL OR ADJACENT LANE PREDICTED -

13 (59%)

PREDICTED LANE \ ACTUAL LANE	M	1	2	3	4	5	RS
1	2		2	1			
2							
3		6	1	4	2	1	
4			1		2		
5							

Table 35. SPD at upstream station, five-minute interval following alarm.

TIME - 5 MIN. FOLLOWING ALARM

NO. CASES - 22

ACTUAL OR ADJACENT LANE PREDICTED -

14 (63%)

PREDICTED LANE \ ACTUAL LANE	M	1	2	3	4	5	RS
1	1	1	2		1		
2							
3		4	1	5	1	1	
4			1		2		
5					1		

Table 36. OCC at downstream station, two-minute interval following alarm.

FEATURE - OCC AT DOWNSTREAM STATION

TIME- 2 MIN. FOLLOWING ALARM

NO. CASES (TOTAL) - 25

NO. INVALID CASES - 7

NO. CASES USED - 18

ACTUAL OR ADJACENT PREDICTED - 14 (77%)

PREDICTED LANE	ACTUAL LANE M	1	2	3	4	5	RS
1	2	4	1	1	1		
2							
3		2		3	2		
4					1	1	
5							

Downstream SPD was also examined, but showed no promising results.

6.4.4 An Algorithm Employing Both Upstream and Downstream Data

The results reported in the previous two sections imply that in some cases upstream tests lead to accurate lane identification while in others, downstream tests are most effective. This appears to be reasonable if some characteristics of an incident are considered. First, if an incident occurred much closer to the downstream station, the effects of the incident on the blocked lane should be most apparent at that station, while traffic at the upstream station may still be equally distributed over the lanes. The same logic should apply to incidents located much closer to the upstream station. Nevertheless, an incident occurring in a particular lane should cause a sudden drop in occupancy to propagate downstream at a speed approximating traffic speed due to the sudden absence of vehicles in the blocked lane. This low occupancy should continue until the blocked lane is cleared, unless the incident is located far enough upstream for a redistribution of the traffic pattern to occur. However, the effect of the incident on upstream lane data should not be quite as marked and should not occur quite so fast. This length of time depends on the size and speed of the queue forming behind the incident. In addition, vehicles merging into adjacent lanes to avoid the incident should cause fluctuations in upstream data masking the incident's effect on a particular lane. Thus it appears that downstream lane data should be more effective in permitting lane identification, unless, as previously noted, the incident occurs considerably closer to the upstream station. A method for determining when upstream versus downstream data should be used seems required.

Many data sets examined exhibited sudden drops in occupancy in blocked lanes at the downstream station. These drops were apparent approximately twenty seconds to one minute after the occurrence of the incident and often persisted (see Tables 37 and 38). Upstream OCC increases occurred approximately one minute thereafter in the blocked lanes and subsequently spread to all upstream lanes as expected. Thus accurate prediction should be most effective at the downstream station during the initial few minutes following the incident. Incidents occurring just below the upstream station should affect the upstream lane data also during this interval, as the queue would reach this station rather rapidly (Table 39).

The incident detection algorithm, however, generally detected the incidents a few minutes after the incident occurred. Thus the one or two minutes immediately preceding the detection alarm should be examined by the classification algorithm.

Table 37. Sudden drop in downstream lane occupancy.

740515-01

OCCUPANCY

FWY	1	1	1	1	
STA	25	25	25	25	
LANE NO.	1	3	1	3	
TIME					
714++	17	26	18	15	
+	19	22	21	25	
+	13	16	19	20	
715++	16	16	19	17	
+	20	16	16	17	
+	16	17	13	14	Disabled Vehicle Right Shoulder
716++	20	23	16	14	
+	21	19	24	15	
+	22	13	13	7	Downstream Drop Lane 3
717++	34	20	16	9	
+	40	36	14	8	
+	46	65	13	8	Upstream Rise Lane 3
718++	30	38	13	6	
+	25	44	11	4	
+	27	36	13	9	
719++	29	37	13	12	Detection
+	36	34	14	9	
+	34	28	9	10	
720++	34	24	11	5	
+	24	25	12	11	
+	21	26	10	7	
721++	41	34	8	9	
+	42	30	9	9	
+	34	28	17	13	
722++	50	36	11	11	
+	34	35	9	10	
+	37	22	11	8	
723++	34	28	10	12	

Table 38. Sudden drop to zero of downstream lane occupancy.

740605-01

OCCUPANCY

FWY	5	5	5	5	
STA	16	16	17	17	
LANE NO.	1	3	1	3	
TIME					
800++	19	19	16	19	
+	19	19	15	19	
+	17	27	16	16	
801++	20	19	11	19	
+	19	18	16	21	
+	22 U	25	10 D	18	
802++	16	23	21	27	Incident (Lane 1)
+	17	18	22	35	
+	19	16	38	36	
803++	19	20	0	16	Downstream Drop
+	17	20	0	13	
+	24	19	0	24	
804++	47	27	0	18	Upstream Rise Lane 1
+	99	53	0	22	Upstream Rise Lane 3
+	99	89	0	24	
805++	99	68	0	21	
+	99	38	0	24	
+	44	61	0	17	Detection Occurs
806++	57	83	0	24	
+	53	99	0	24	
+	55	65	0	22	
807++	51	89	0	22	Note Persistance of Downstream Low OCC in Lane 1
+	56	36	0	25	
+	94	33	0	23	
808++	99	38	0	25	
+	99	99	0	19	
+	57	63	0	22	
809++	59	51	0	26	

Table 39. Sudden rise in upstream lane occupancy.

740522-03

OCCUPANCY

FWY	2	2	2	2	
STA	26	26	25	25	
LANE NO.	1	3	1	3	
TIME					
1606++	14	13	22	18	
+	17	24	22	23	
+	13	20	33	23	
1607++	12	23	25	25	
+	12	14	21	23	
+	13	20	17	23	
1608++	9	19	20	20	
+	11	11	16	21	
+	10	12	18	28	Collision Lane 4
1609++	12	12	13	24	
+	14	17	13	15	
+	9	13	14	15	
1610++	11	16	12	13	
+	28	29	15	10	Upstream Rise Lane 3
+	37	47	11	12	
1611++	28	38	12	12	
+	25	25	16	15	
+	21	31	12	10	Detection
1612++	25	25	14	18	
+	38	45	12	19	
+	40	30	7	19	
1613++	43	38	12	13	
+	39	23	8	16	
+	44	35	11	9	
1614++	37	30	14	15	
+	28	22	8	14	
+	25	20	14	15	
1615++	41	29	8	16	
+	39	24	11	13	
+	43	24	16	15	
1616++	27	26	9	10	

U D

Downstream Station Shows no Lane Dominance

Upstream Lane 3 Dominance Apparent One Minute Before Detection

The theory presented above may be incorporated in the following algorithm. (See Figure 45.)

(1) OCC data is averaged for each lane at the downstream station over the one-minute period prior to the detection alarm.

(2) The lane with the lowest OCC average is identified as a candidate for the incident lane.

(3) To measure the intensity of the candidate lane's difference from the other lanes, a percent mean deviation test is performed on the downstream lane data, as follows:

   a) The one-minute lane averages are now averaged over all lanes to give the mean station occupancy.

   b) The candidate lane's individual OCC average is subtracted from the station average.

   c) The ratio of this deviation to the station average is then computed. This computation yields a feature with values between 0 and 1. A feature value of 0 represents no difference between downstream lanes while a value close to 1 implies a considerable deviation between the predicted lane and the others.

(4) If the deviation feature is small it is probable that the incident's effect will be more apparent at the upstream station. Thus the feature is compared to a threshold, T1. If the feature value is greater or equal to the chosen threshold, the lane identified in step 2 is considered to be the involved lane. Otherwise:

(5) The OCC's for each upstream station lane are averaged over the one-minute interval prior to the detection alarm.

(6) The lane with the highest OCC average is considered to be the involved incident lane.

6.4.5 Testing the Algorithm

The algorithm from Section 6.4.4 was manually tested on the evaluation data base for five values of the deviation threshold, T1: 0.0, .10, .15, .20, 1.00. The test with T1=0 employed downstream data only, and the test with T1=1 employed upstream data only (see Tables 40 through 52).

Each test performed was evaluated in four categories: (1) those cases in which no data were available for the blocked lane (at the station determined by the deviation feature) but data existed for adjacent lanes and

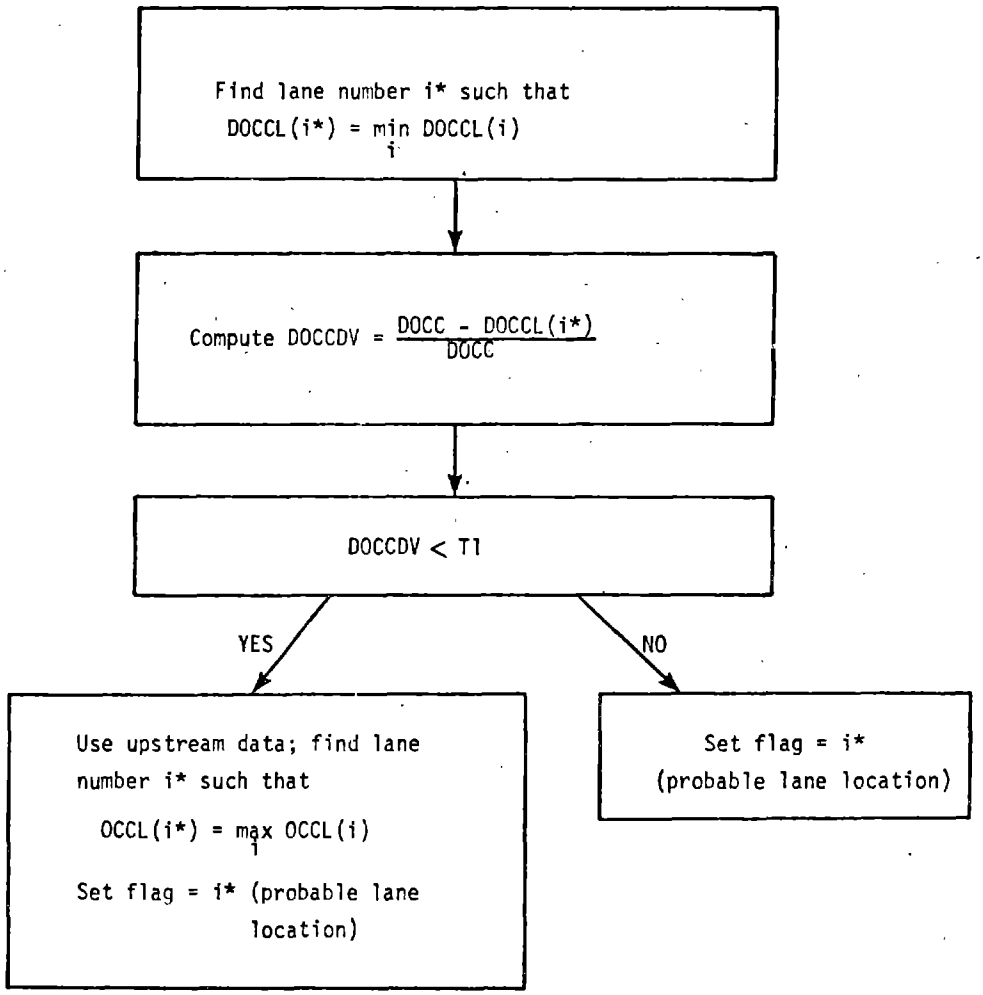

DOCC = one-minute OCC average for downstream station

DOCCL(i) = one-minute OCC average for downstream lane i

OCCL(i) = one-minute OCC average for upstream lane i

Figure 45. An algorithm employing upstream and downstream occupancy data for lane identification of an incident.

Table 40. OCC at downstream station (threshold = 0.0), one-minute interval before alarm--overall performance.

FEATURE - OCC AT DOWNSTREAM STATION

(THRESHOLD = 0.0)

TIME - 1 MIN. PRIOR TO ALARM

*OVERALL PERFORMANCE

NO. CASES - 24

ACTUAL OR ADJACENT PREDICTED -

21 (87.5%)

PREDICTED LANE \ ACTUAL LANE	M	1	2	3	4	5	RS
1	2	4			1		
2		2	1	1			
3		1	1	3	1		1
4		1			2	3	
5							

Table 41. OCC at downstream station (threshold = 0.0), one-minute interval before alarm--cases where data existed for actual lane.

*CASES IN WHICH DATA EXISTED FOR ACTUAL LANE

NO. CASES - 15

ACTUAL LANE PREDICTED -

12 (80%)

ACTUAL OR ADJACENT PREDICTED -

13 (87%)

PREDICTED LANE \ ACTUAL LANE	M	1	2	3	4	5	RS
1	2	4					
2		1	1				
3		1		3			
4		1			2		
5							

Table 42. OCC at downstream station (threshold = 0.0), one-minute interval before alarm--cases with no data for actual lane.

*CASES WITH NO DATA FOR ACTUAL LANE

NO. CASES - 9

ADJACENT LANE PREDICTED -

8 (89%)

PREDICTED LANE \ ACTUAL LANE	M	1	2	3	4	5	RS
1					1		
2		1		1			
3			1		1		1
4						3	
5							

Table 43. OCC at upstream or downstream station determined by deviation feature (threshold = .10), one minute interval before alarm--overall performance.

OCC AT UPSTREAM OR DOWNSTREAM STATION DETERMINED BY DEVIATION FEATURE WITH THRESHOLD = .10

TIME - 1 MIN. PRIOR TO ALARM

*OVERALL PERFORMANCE

NO. CASES - 29

ACTUAL OR ADJACENT PREDICTED - 26 (90%)

PREDICTED LANE \ ACTUAL LANE	M	1	2	3	4	5	RS
1	2	4					
2		2	4	1			
3		2	1	4	1		1
4		1			3	3	
5							

Table 44. OCC at upstream or downstream station determined by deviation feature (threshold = .10), one-minute interval before alarm--cases where data existed for actual lane.

*CASES IN WHICH DATA EXISTED FOR ACTUAL LANE

NO. CASES - 22

ACTUAL LANE PREDICTED - 16 (73%)

ACTUAL OR ADJACENT PREDICTED - 19 (86%)

PREDICTED LANE \ ACTUAL LANE	M	1	2	3	4	5	RS
1	2	3					
2		2	4				
3		2	1	4			
4		1			3		
5							

Table 45. OCC at upstream or downstream station determined by deviation feature (threshold = .10), one-minute interval before alarm--overall performance.

*CASES IN WHICH NO DATA EXISTED FOR ACTUAL LANE

NO. CASES - 7

ADJACENT PREDICTED - 7 (100%)

PREDICTED LANE \ ACTUAL LANE	M	1	2	3	4	5	RS
1							
2		1		1			
3					1		1
4						3	
5							

Table 46. OCC at upstream and downstream station determined by deviation feature (threshold = .15), one-minute interval before alarm--overall performance.

OCC AT UPSTREAM OR DOWNSTREAM

STATION DETERMINED BY DEVIATION

FEATURE WITH THRESHOLD = .15

*OVERALL PERFORMANCE

NO. CASES - 29

ACTUAL OR ADJACENT

26 (90%)

PREDICTED LANE \ ACTUAL LANE	M	1	2	3	4	5	RS
1	2	3					
2		3	4				
3		2	1	5	1		1
4		1			3	3	
5							

Table 47. OCC at upstream and downstream station determined by deviation feature (threshold = .15), one-minute interval before alarm--cases where data existed for actual lane.

*CASES IN WHICH DATA EXISTED FOR ACTUAL LANE

NO. CASES - 23

ACTUAL LANE PREDICTED -

17 (74%)

ACTUAL OR ADJACENT LANE PREDICTED -

21 (91%)

PREDICTED LANE \ ACTUAL LANE	M	1	2	3	4	5	RS
1	2	3					
2		2	4				
3		2	1	5			
4		1			3		
5							

Table 48. OCC at upstream and downstream station determined by deviation feature (threshold = .15), one-minute interval before alarm--cases with no data for actual lane.

*CASES IN WHICH NO DATA EXISTED FOR ACTUAL LANE

NO CASES - 6

ADJACENT PREDICTED -

6 (100%)

PREDICTED LANE \ ACTUAL LANE	M	1	2	3	4	5	RS
1							
2		1					
3					1		1
4						3	
5							

Table 49. OCC at upstream and downstream station determined by deviation feature (threshold = .20), one-minute interval before alarm--overall performance.

OCC AT UPSTREAM OR DOWNSTREAM

STATION DETERMINED BY DEVIATION

FEATURE WITH THRESHOLD = .20

*OVERALL PERFORMANCE

NO. CASES - 29

ACTUAL OR ADJACENT

25 (86%)

PREDICTED LANE \ ACTUAL LANE	M	1	2	3	4	5	RS
1	2	3					
2		3	4			1	
3		2	1	5	1		1
4		1			3	2	
5							

Table 50. OCC at upstream and downstream station determined by deviation feature (threshold = .20), one-minute interval before alarm--cases where data existed for actual lane.

*DATA EXISTED FOR ACTUAL LANE

NO. CASES - 24

ACTUAL LANE PREDICTED

17 (71%)

ACTUAL OR ADJACENT LANE PREDICTED -

21 (87.5%)

PREDICTED LANE \ ACTUAL LANE	M	1	2	3	4	5	RS
1	2	3					
2		2	4			1	
3		2	1	5			
4		1			3		
5							

Table 51. OCC at upstream and downstream station determined by deviation feature (threshold = .20), one-minute interval before alarm--cases with no data for actual lane.

*NO DATA EXISTED FOR ACTUAL LANE -

NO. CASES - 5

ADJACENT PREDICTED -

5 (100%)

PREDICTED LANE \ ACTUAL LANE	M	1	2	3	4	5	RS
1							
2		1					
3					1		1
4						2	
5							

Table 52. OCC at upstream station (threshold = 1.00), one-minute interval before alarm--overall performance.

OCC AT UPSTREAM STATION DETERMINED
BY DEVIATION
FEATURE WITH THRESHOLD = 1.00
TIME - 1 MIN. PRIOR TO ALARM
*OVERALL PERFORMANCE
NO. CASES - 28
ACTUAL LANE PREDICTED -
13 (46%)
ACTUAL OR ADJACENT LANE PREDICTED -
18 (64%)

PREDICTED LANE	ACTUAL LANE: M	1	2	3	4	5	RS
1		3				2	
2		1	3			1	
3	1	4	2	5	2		1
4	1				2		
5							

an adjacent lane was chosen; (2) those cases in which data existed for the actual lane and the actual lane was chosen, (3) those in which data were available for the actual lane and either the actual or an adjacent lane was chosen, and (4) the number of times either the actual or adjacent lane was chosen out of all cases considered.

The number of cases used for each test varies because some cases had to be eliminated when the feature test pointed to a station for which sensor data was unavailable causing an adjacent lane to be chosen by default.

For purposes of evaluation median incidents were considered lane 1 incidents and right shoulder incidents were considered lane 4 incidents. The one case in which a right shoulder incident occurred and was predicted, a lane 3 incident is counted as a correct adjacent lane prediction since data existed for lanes 1 and 3 only. This case corresponds to the 1 in row 3 of the RS column in many of the tables.

The best results were obtained when the threshold values of .10 or .15 were employed (Tables 43 through 48). The actual lane was predicted approximately 70% of the time when data was available for that lane. Overall, either the actual or an adjacent lane was chosen 90% of the time.

6.4.6 Interpretation and Accuracy of the Performance Evaluation

The success of the lane classification algorithm must be viewed in connection with the incident detection algorithm employed. The results imply that lane classification of incidents is approximately 90% effective for incidents detected by the detection algorithm.

The actual performance of the algorithm tested may be slightly better, or worse, due to possible inaccuracies in the documentation of the incidents used in the evaluations.

6.4.7 Practical Evaluation and Recommendations

The algorithm presented is recommended for use in conjunction with an incident detection algorithm for the following reasons:

(1) High performance

(2) Relatively simplistic nature - minimal computational burden.

(3) Employs lane OCC data only.

(4) Use of downstream percent deviation threshold permits further calibration on-line and may be adjusted for systems with different senser configurations.

(5) Use of data prior to detection alarm permits instantaneous lane predictions.

(6) Exhibits reasonable performance at stations where data is collected for less than all lanes.

It is recommended that a downstream deviation threshold of .15 be used, although the algorithm does not exhibit major sensitivity to small changes in this value.

6.5 SENSOR MALFUNCTION DETECTION ALGORITHMS

One of the more serious problems plaguing freeway surveillance and incident detection systems is that of sensor malfunctions. These malfunctions not only result in loss of surveillance but often trigger false alarms. Algorithms employing aggregated lane sensor data may be used to detect such malfunctions.

6.5.1 Types of Malfunctions

Many types of sensor hardware malfunctions can occur. Most of these equipment problems, however, appear in one of the following five ways:

1. Sensors stuck on or off
2. Chattering
3. Pulse Breakup (Pulsing)
4. Hanging
5. Intermittent malfunctioning

In normal, incident-free traffic, if a sensor is stuck in the on or off position, the malfunction is easily discernible. In the off position, occupancy, volume, and speed "zero out"; in the on position, the sensor usually gives occupancy values of 99% coupled with zero volume and speed. Complete lane blockages in the vicinity of detectors, however, may cause similar appearing data (see Tables 53 and 54). In addition, light night traffic may often exhibit periods in which OCC, VOL, and SPD are zero.

Chattering occurs when a sensor provides random presence indications. These pulses are usually of short duration (i.e. less than 2/15 second) and often appear to occur with no relation to actual traffic.

When chattering occurs, OCC and VOL are both either abnormally low or abnormally high, depending on the rate of chattering. However, because of the short duration of the pulses, speed values would be unreasonably high, regardless of the chattering rate (see Tables 55 through 58).

Table 53. Zero occupancies due to an incident at 6:12, sta 27, lane 4.

FWY	4	4	4	4
STA	27	27	27	27
LANE NO.	1	2	3	4
TIME				
608++	5	8	14	4
609++	7	7	12	4
610++	5	5	8	4
611++	5	8	16	1
612++	9	12	29	0
613++	15	19	29	1
614++	9	16	31	0
615++	13	18	34	0
616++	17	22	34	0
617++	16	21	20	0
618++	7	12	18	0
619++	21	24	28	0
620++	24	23	27	0
621++	20	26	30	0
622++	26	27	26	0
623++	25	24	26	0
624++	23	27	29	0
625++	27	29	31	0
626++	32	34	35	0
627++	25	42	39	77
628++	34	32	36	0
629++	30	33	37	0
630++	29	38	36	0
631++	32	37	40	1
632++	25	28	29	0
633++	33	29	35	2
634++	28	26	29	0

Table 54. Ninety-nine percent occupancies due to an incident at 8:36, sta 19, lane 1.

740515-03

OCCUPANCY

FWY	1	1
STA	19	19
LANE NO.	1	3
TIME		
830++	53	32
831++	27	23
832++	20	24
833++	23	21
834++	21	25
835++	36	23
836++	99	24
837++	99	29
838++	99	31
839++	99	29
840++	99	28
841++	99	27
842++	99	32
843++	82	23
844++	29	26
845++	18	31
846++	16	26
847++	17	21
848++	15	20
849++	18	23
850++	21	26

Table 55. Scan data from a chattering sensor, lane 4.

740725-01

FWY	4	4
STA	18	18
LANE NO.	3 Normal Data	4 Chattering
TIME		
735 0	0111000000000000	0000000000000000
735 1	0000000000000000	0000000000000000
735 2	0000000000000000	0000000001000000
735 3	0011110000000000	0000000001000000
735 4	0000000000000000	0000000000000000
735 5	0000001111000000	0100000000000000
735 6	0000000000000000	0000000000000000
735 7	0111100000000000	0000000000000000
735 8	0000000000000000	0000000000000000
735 9	0001110000000000	0000000000000000
73510	0011110000000001	0000000000000000
73511	1110000000000000	0000000000000000
73512	0000000000000000	0000000000000000
73513	0000111100000000	0000000000000000
73514	0000000000000001	0010000000000000
73515	1110000011110000	0000000000000000
73516	0000000001111110	0000000000000010
73517	0000000000000000	0000000000000000
73518	0000000000000000	0000000000000000
73519	0000000000000000	0000000000000000
73520	0000000000000000	0000000000000000
73521	0000000001111000	0000000000000000
73522	0000000000000000	0000000000000000
73523	0000000000001111	0000000000000000
73524	1000000000000000	0000000000000000
73525	0000000000000000	0000000000010000
73526	1111000000000000	0000000000000000
73527	0000000000000000	0000000000000000
73528	0000000011110000	0000000000010000
73529	0000000000000000	0000000000000000
73530	0111100000000000	0000000000000000
73531	0000000000001110	0000000000000000
73532	0000000000000000	0000000000010000
73533	0000000000000000	0000000000000000
73534	0000000000000000	0000000000000000
73535	0000001111100000	0000000010000000
73536	0000000000000000	0000000000000000
73537	0000000001111100	0000000000000000
73538	0000000000000000	0000000000000000
73539	0000000000001110	0000000001100000
73540	0000000000000000	0000000000000000
73541	0000001111000000	0000000000000000

Table 56. Five-minute OCC map of chattering sensor (sta 18, lane 4) and intermittent hanging on (sta 14, lane 1).

740725-01

OCCUPANCY

FWY	4	4	4	4	4	4	4	4	4
STA	18	18	18	18	15	15	14	14	14
LANE NO.	1	2	3	4	1	3	1	2	4
TIME									
---	---	---	---	---	---	---	---	---	---
730++	13	12	11	0	13	10	17	10	11
735++	14	13	12	0	13	10	24	11	13
740++	12	12	11	0	12	10	22	12	12
745++	15	15	12	0	14	11	18	12	14
750++	12	13	11	0	14	11	28	13	14
755++	12	12	11	0	12	10	25	10	12
800++	13	13	11	0	11	9	15	9	12
805++	9	10	10	0	11	10	27	10	14
810++	9	10	9	1	9	10	35	9	10
815++	11	11	10	1	9	10	45	11	11
820++	12	12	10	1	11	10	23	11	13
825++	12	13	9	0	12	9	28	11	12
830++	12	12	10	1	12	10	17	10	10
835++	11	12	8	1	11	9	16	10	11
840++	10	10	10	0	10	9	10	9	10
845++	10	10	8	0	9	10	10	10	11
850++	8	9	8	0	8	8	9	8	8
855++	9	10	9	0	9	9	11	9	9
900++	8	9	6	0	9	8	16	9	11
905++	7	7	5	0	7	7	17	8	7
910++	6	7	6	0	7	7	9	7	7
915++	8	8	6	0	7	7	11	7	8
920++	7	9	7	0	7	7	15	8	9
925++	8	9	7	0	8	8	12	9	9
930++	7	8	7	0	8	7	10	9	10

Table 57. Five-minute VOL map of chattering sensor (sta 18, lane 4) and hanging on (sta 14, lane 1).

740725-01

VOLUME

FWY	4	4	4	4	4	4	4
STA	18	18	18	18	14	14	14
LANE NO.	1	2	3	4	1	2	4
TIME							
730++	2184	1812	1656	408	1956	1548	1608
735++	2160	1860	1836	396	1956	1632	1608
740++	1980	1764	1824	420	1836	1776	1572
745++	2412	2052	1848	540	1980	1764	1788
750++	1980	1944	1728	432	2004	1932	1848
755++	2004	1644	1680	456	1704	1572	1608
800++	2040	1824	1692	432	1740	1440	1620
805++	1512	1512	1536	336	1680	1536	1860
810++	1536	1500	1416	624	1356	1416	1392
815++	1884	1632	1620	576	1212	1620	1476
820++	1908	1764	1596	588	1728	1668	1704
825++	2028	1812	1452	552	1644	1644	1632
830++	1872	1752	1488	612	1836	1548	1308
835++	1716	1668	1344	564	1620	1608	1416
840++	1716	1548	1464	504	1524	1380	1440
845++	1596	1500	1344	480	1632	1488	1404
850++	1452	1308	1212	348	1404	1308	1128
855++	1584	1512	1416	552	1404	1320	1188
900++	1320	1356	996	444	1320	1404	1284
905++	1224	1140	900	396	1344	1212	984
910++	1092	1080	1008	396	1044	1128	984
915++	1356	1188	996	456	1140	1092	1068
920++	1200	1272	1200	276	1140	1260	1224
925++	1272	1332	1164	360	1356	1344	1248
930++	1224	1164	1092	324	1140	1308	1272

Table 58. Five-minute SPD map of chattering sensor (sta 18, lane 4) and hanging on (sta 14, lane 1).

740725-01

SPEED

FWY	4	4	4	4	4	4	4
STA	18	18	18	18	14	14	14
LANE NO.	1	2	3	4	1	2	4
TIME							
---	---	---	---	---	---	---	---
730++	55	49	52	191	44	52	48
735++	54	49	52	174	38	52	42
740++	55	51	54	160	39	51	45
745++	55	48	51	191	42	51	45
750++	54	49	54	191	33	50	45
755++	56	48	52	170	37	52	46
800++	54	47	51	175	43	52	45
805++	57	49	53	159	30	53	45
810++	56	49	54	183	21	51	46
815++	55	50	54	181	16	50	44
820++	55	49	53	189	37	52	46
825++	55	49	54	179	29	49	45
830++	54	48	52	186	40	51	43
835++	55	49	54	187	44	52	45
840++	57	50	52	179	52	50	47
845++	55	49	54	176	52	50	42
850++	57	48	53	150	50	52	44
855++	56	49	53	188	46	50	44
900++	55	51	53	187	36	50	42
905++	57	50	55	163	39	52	46
910++	53	51	55	166	44	50	45
915++	57	50	53	188	44	53	45
920++	59	49	53	153	40	51	46
925++	54	49	55	162	42	47	47
930++	59	50	55	150	47	49	42

On the microscopic level, chattering is apparent by presence indications of short duration, although such pulses can be caused by vehicles changing lanes directly over sensors.

Pulse breakup occurs when actual presence indications become divided into more than one pulse. Volumes are higher since each vehicle causes multiple counts. Occupancies are lower and hence SPD values are unreasonably high. Pulse breakup is characterized in scan data by extremely short headways (periods between pulses).

A hanging detector is one that remains in either the on or off state longer than usual. When hanging on, occupancies are increased, volume is often normal, but speed is decreased (see Tables 56 through 59). A hanging off sensor causes low-occupancies, reasonable volume, and high speeds.

It is conceivable that many freeway lane sensors may be characterized by little or no traffic during the night or early morning hours. Algorithms employing low-end checks on VOL or OCC would falsely classify these sensors as malfunctioning. Short aggregate times (e.g. 20 seconds) would be more subject to such misclassifications than longer aggregate periods (e.g. 5 or 10 minutes). Also, during extremely heavy traffic, vehicles may often remain standing above sensors for relatively long periods, (e.g. 20 or 30 seconds) causing 99% or 100% occupancies and zero SPDs and VOLs. Such extreme values are unlikely, however, for long aggregate periods.

Although employing long averaging periods appears to be the solution, early malfunction detection is sacrificed. Such delays may permit the first invalid data values to trigger the incident detection algorithm, causing false alarms.

A solution to this problem would be to employ a preliminary data screening routine. This routine would immediately detect stuck on or off sensors based on twenty-second data and consider such sensors "tentatively" malfunctioning pending a five-minute average OCC check. A description of a potential routine is presented below (See Figure 46):

(1) Data on the smallest aggregate level available (e.g. twenty or thirty seconds) is checked for 0 or 99% OCC values. A "preliminary malfunction" flag is set for sensors with these values. The number of times this flag is set could be recorded on a disk file for occasional examination by operation personnel or by more advanced malfunction logic.

(2) Data from sensors with the preliminary malfunction flag set is not used by the feature generator or incident detection routines.

Table 59. Scan data from sensor hanging on (lane 1).

740725-01

FWY	4	4
STA	14	14
LANE NO.	1	1
TIME	----	----
81136	0000000000000000	0000000000000000
81137	0000000000111111	0000000000000000
81138	1111111111111111	0000000000000000
81139	1111111111111111	0000000000000111
81140	1111111111111111	1100000000000111
81141	1111111111111111	1000000000000000
81142	1111111111110000	0000000000000000
81143	0000011111111111	0000000000000000
81144	1111111111111111	0000000001111100
81145	1111111110000000	0001111100000000
81146	0000111111111111	0000000000000000
81147	1111111111111111	0000000000000111
81148	1111100000000000	1000000000000000
81149	0000000000000000	0000000000000000
81150	0000000000000000	0000000000000000
81151	0000000000000000	0000000000000000
81152	0000000000011111	0000111110000000
81153	1111111111110000	0000000000000000
81154	0000000000000000	0000000000011110
81155	0000011111111111	0000000000000000
81156	1111111111111111	0000000000000000
81157	1111111100000000	0000000000001111
81158	0000000000000000	1000000000000000
81159	0000000000000000	0000000000000000
812 0	0000000001111111	0000000000000000
812 1	1111111111111111	0000011110000000
812 2	1111000000000000	0000000000000000
812 3	0000000000011111	0001110000000000
812 4	1000000000111110	0000000000000000
812 5	0000000000000000	0000011110000000
812 6	0000111100111100	0000001111000000
812 7	0000000001111100	0000000000000111
812 8	0000000000000000	1000000111000000
812 9	0000000000000000	0000000000000000
81210	0000000000000111	0000000000000000
81211	1000000000000000	0000000000000011
81212	0000000001111000	1000000000000000
81213	0000000000000000	0000000000000000
81214	0000000000000000	0000000000000000
81215	0000000000000000	0000000000000000
81216	0111000000000000	0111000000000000
81217	0000000000000000	0000000000000000
81218	0000000000000000	0011110000000000

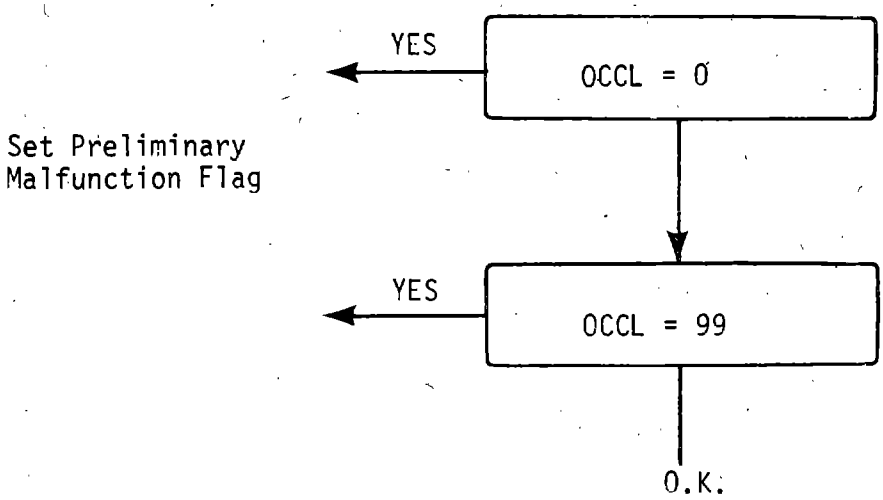

OCCL = 20-second lane-specific OCC

Figure 46. Preliminary data screening routine to detect stuck on or off sensors without affecting indcident detection.

(3) The preliminary malfunction flag is reset at the beginning of each minute interval.

(4) Five-minute data tests could then be employed. (These will be discussed in the next section.) If the five-minute data averages exhibited extreme values, a malfunction flag is set for that sensor. This flag could then be; (1) used to suppress use of the corresponding traffic data for the next five-minute interval, (2) used to alert an operator, or (3) stored for later retrieval for maintenance purposes. This flag could be reset if an incident occurred during the five-minute interval.

Such a routine would:

(1) Prevent incident false alarms based on data from stuck on/off or intermittently operating sensors.

(2) Prevent sensors from becoming classified as malfunctioning due to brief periods of 0 or 99% OCC values caused by light or heavy traffic. Preliminarily removing sensors with 0 or 99% OCC values caused by the occurrence of an actual incident should not greatly affect incident detection. An incident leading to such extreme values will most likely be so severe so that the remaining sensors will easily reflect the incident condition.

A sensor intermittently malfunctioning may, on occasion, exhibit any of the previous problems, while operating normally the rest of the time. On the aggregate data level, this type of problem is difficult to detect as sudden fluctuations in data tend to become "smoothed out." The erratic data produced often resembles extremely heavy traffic patterns in which compression waves cause high or low OCC fluctuations. Intermittent malfunctions are easiest to detect on the raw scan level by comparison to neighboring sensors (see Table 60).

The effects of the various malfunction on aggregate data may be summarized as follows:

Condition	Malfunction
0% OCC	Stuck off
99% OCC	Stuck on
0 VOL or SPD	Stuck on or off
Low OCC and VOL	Chattering - low rate
High OCC and VOL	Chattering - high rate
High SPD	Chattering
High VOL, low OCC	Pulse breakup
High SPD	Pulse breakup

Table 60. Scan data of intermittent hanging on (lane 1).

740725-01

FWY	4	4
STA	14	14
LANE NO.	1	2
TIME		
---	---	---
73245	1000000000000000	0000000000000000
73246	0000011110000000	0000000000000111
73247	0111100000000011	1000000000000000
73248	1100000000000000	0000000011111000
73249	0001111000000000	0000000000000000
73250	0000000011100000	0000011111000000
73251	0000000000000000	0001111000000000
73252	0001111000000000	0000000000000000
73253	0000011100000000	0000000000011110
73254	0000000000000000	0000000000000000
73255	0000000000000000	0000000001111000
73256	0000000000000000	0000000000000000
73257	0000000000000000	1111000000000000
73258	0000111111111111	0000000000011111
73259	1111111100000000	1000000000111110
733 0	0000000000001111	0000000000000000
733 1	1111111111111111	0000000000000000
733 2	1111111111111111	0000000000000000
733 3	1111111111111111	0111000000000000
733 4	1111111111111111	0000000000000000
733 5	1111111111111111	0000000000000111
733 6	1111111111111111	1000000111110000
733 7	1111111111111111	0000000111110000
733 8	1111111111111111	0000000000000000
733 9	1111111111111111	0000111100000000
73310	1111111111111111	0000001110000000
73311	1111111111111111	0000001111000000
73312	1111110000000000	0000000000000111
73313	0000000000000000	1000000000000000
73314	0001111111111111	0000000000000000
73315	1111111111111111	0000000000000000
73316	1111111111111111	0000000000000000
73317	1111111111111111	0000000000000000
73318	1111111111111111	0000000011110000
73319	1111111111111111	0000000000000000
73320	1111111111110000	0000000001111000
73321	1111000000000000	0000000001111000
73322	0000000000000111	0000000000000000
73323	1000000000000000	0000000000000000
73324	1111000000000000	0000000000000000
73325	0000011110000000	0000000000000000

Condition	Malfunction
High OCC, low SPD	Hanging on
Low OCC, high SPD	Hanging off
Erratic OCC	Intermittent operation

6.5.2 Types of Malfunction Detection Algorithms

Two types of malfunction detection algorithms are considered: (1) those based on individual sensor tests and (2) those employing comparison checks between neighboring sensors. These algorithms will be discussed in relation to the common types of malfunctions identified.

6.5.2.1 Single-sensor algorithms

Single-sensor algorithms have the simpler form. They involve simple checks of aggregate data from individual sensors against predetermined bounds. Sensors with data out of bounds are considered to be malfunctioning.

The period over which sensor data should be accumulated before being tested is one question raised by such algorithms. The time period used must be considered with respect to light and heavy traffic and incident detection.

At the present time, both Los Angeles (CALTRANS) and Chicago freeway systems employ single sensor malfunction algorithms. These algorithms will be evaluated in terms of the types of malfunctions previously discussed.

CALTRANS Malfunction Routine. CALTRANS' malfunction logic presently employs three data validity tests (see Figure 47). Checks are made against five-minute averages updated every five minutes. The first test checks for OCC values greater than 95%. If a sensor's OCC value is above this limit, the sensor's malfunction flag is set. Such a test would be effective in catching sensors stuck in the on position. However, problems would occur with incidents involving complete lane blockages in the vicinity of the sensor (e.g. see incident Nos. 74073001 and 74051503 in Tables 53 and 54).

The second data test checks for a volume less than two vehicles during the five-minute period. This corresponds to an average volume less than twenty-four vehicles per lane per hour. Although this test would detect sensors stuck either in the on or off state, again problems would occur with incidents in the detector vicinity. In addition, some lanes may exhibit such low volumes during early morning hours, although whether this is indeed the case is not known, as no night data was available.

Checks are made against five-minute averages updated every five minutes

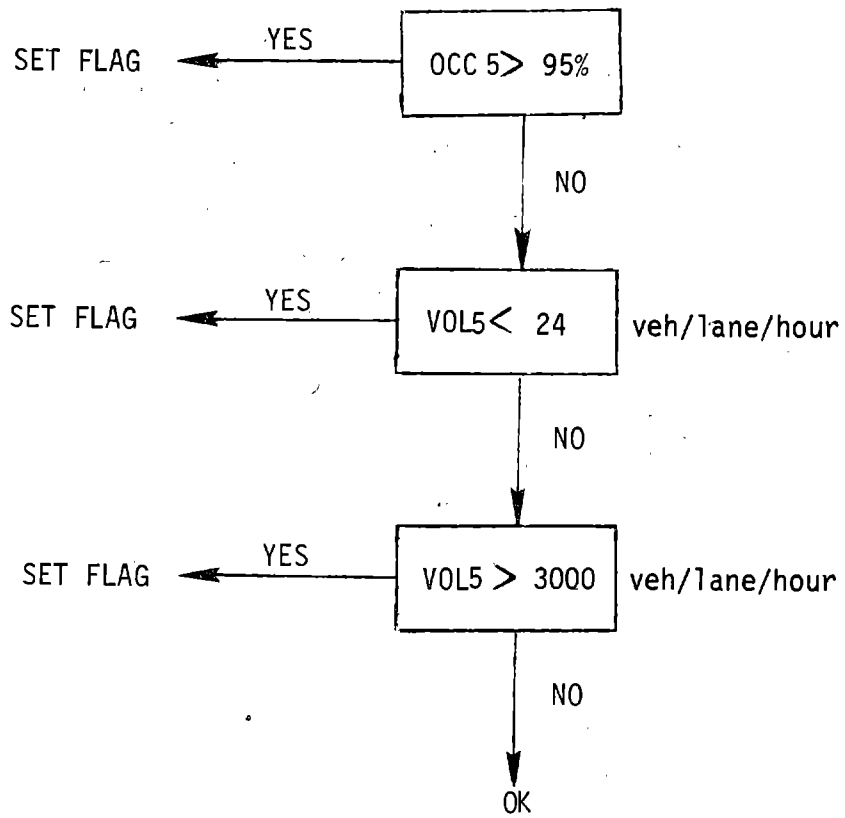

Figure 47. Caltrans malfunction routine.

The third test checks for a volume greater than 250 vehicles, i.e. 3000 veh/lane/hr. Such a test would detect a sensor exhibiting pulse breakup or chattering at a high rate. Characteristics of this algorithm may be summarized as follows:

(1) It will detect

- sensors stuck on or off
- pulse breakup
- chattering at a high rate

(2) It will not detect

- chattering at low or medium rates
- pulse breakup in very light traffic
- hanging on or off
- intermittent operation

(3) Its five-minute aggregation interval will permit brief traffic fluctuations caused by extremely light or heavy traffic.

(4) Its five-minute aggregation interval will not prevent incident false alarms caused by sensors becoming stuck on or off.

(5) Extreme values caused by an incident will trigger a malfunction.

Chicago Malfunction Routine. Chicago's malfunction algorithm employs two data validity checks (see Figure 48). These checks are based on one-minute averages updated every minute.

The first test checks for a volume greater than 35 vehicles, i.e. 2100 veh/lane/hour. Experience, however, indicates that this figure is probably too low; 42-43 vehicles (2520-2580) would be a better threshold. This test will detect pulsing problems and high rate chattering.

The second test checks for speed (VOL/OCC) values greater than 68 miles per hour. Such a test would detect most chattering problems, pulse breakup, and hanging off.

The malfunction routine also lists sensors with zero occupancies but does not remove these sensors from use since the detection logic employed checks for zero values of OCC at the downstream station.

The Chicago algorithm may be summarized as follows:

Checks are made against
one-minute data updated
every one minute

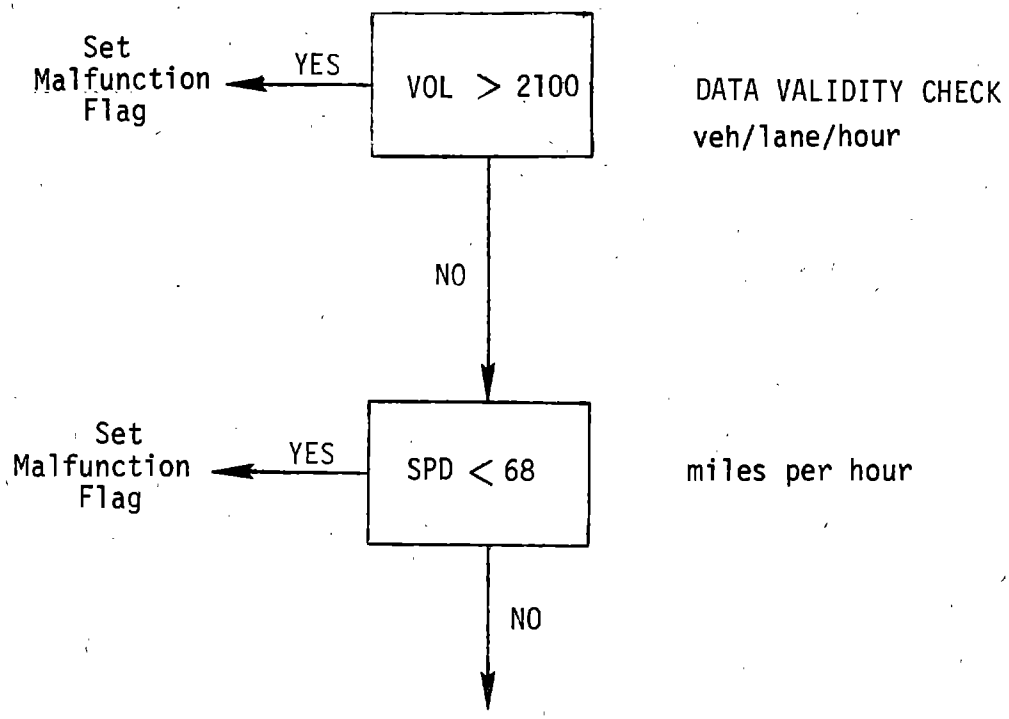

Figure 48. Chicago malfunction routine.

(1) It will detect

- chattering
- pulse breakup
- hanging off
- sensors stuck off (although these sensors must be manually removed from use)

(2) It will not detect

- stuck on sensors
- hanging on
- intermittent operation

(3) The one-minute averaging interval may prevent some malfunction-caused incident false alarms

It is recommended that the preliminary data processor, previously discussed, coupled with a five-minute OCC, SPD and VOL test be evaluated for potential use. Such a malfunction routine would employ the better features from both the Los Angeles and Chicago algorithms and theoretically would detect most malfunctions, the exceptions being hanging on and intermittent operation (see Figures 49 and 50).

6.5.2.2 Neighbor comparison malfunction algorithms

Although single-sensor algorithms may be effective in detecting extreme cases of malfunctioning detectors, such algorithms have difficulty detecting sporadic malfunctions. Data from such intermittent malfunctions often appear reasonable on their own, often resembling the pattern produced by very heavy or light traffic. For example, data from a sensor intermittently hanging on might resemble compression waves moving through heavy traffic; a sensor intermittently stuck off would appear as light traffic. Although fluctuations from these sensors are apparent on the microscopic level or over short aggregation intervals (see Table 61), they would disappear over long averaging periods (see Table 56). This kind of problem is a major cause of incident false alarms since detection logic usually employs short averaging intervals. A sudden OCC increase is interpreted as an upstream rise, and an OCC decrease as a downstream drop due to an incident. Only when accumulated data from these sensors are compared to data from adjacent lane sensors do these data appear unreasonable.

It has not been resolved whether malfunction logic employing twenty- or thirty-second data capable of detecting intermittent malfunctions before they cause false alarms can be devised. Such algorithms would have a difficult time distinguishing between data from malfunctions and those from actual incidents in heavy or light traffic. Neighbor comparisons

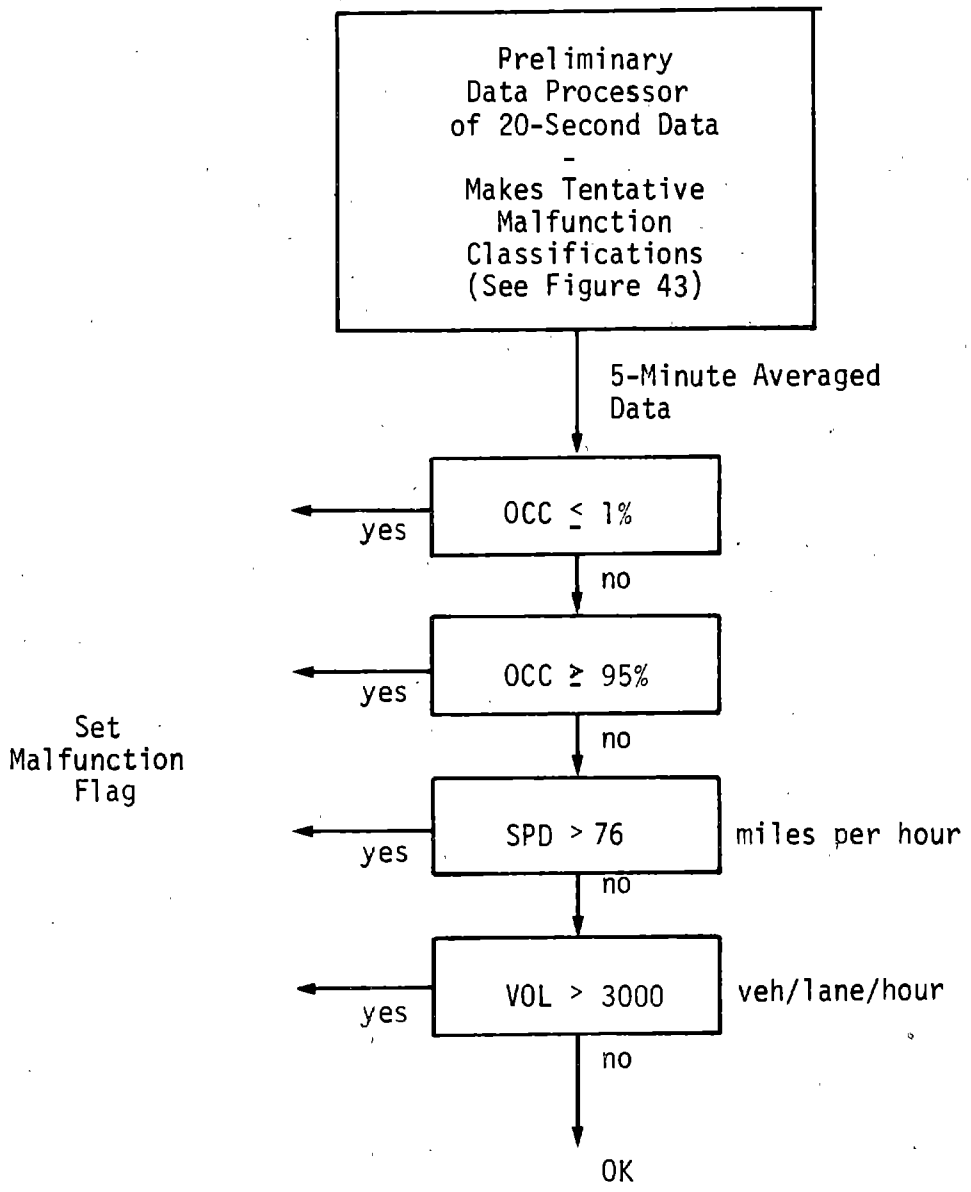

Figure 49. Single-sensor malfunction algorithm.

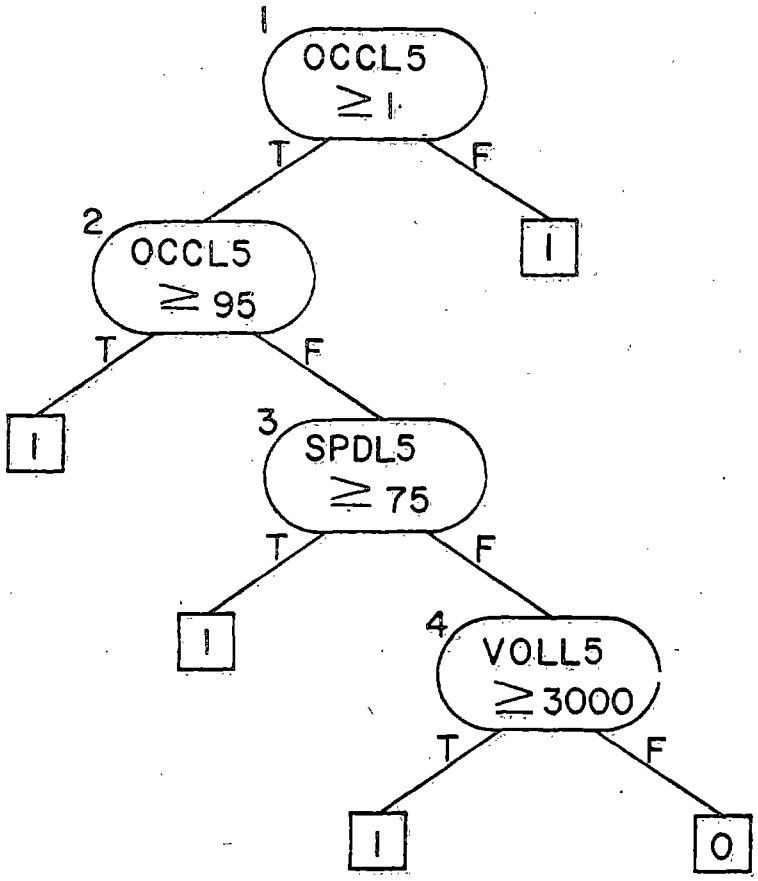

State	Designates
0	No malfunction
1	Sensor Malfunction

Feature No.	Name
1	OCCL5 (five-minute average lane-specific occupancy)
2	SPDL5 (five-minute average lane-specific volume)
3	VOLL5 (five-minute average lane-specific speed)

Decision Node	NTR	Threshold
1	1,2,-1	2
2	1,-1,3	95
3	2,-1,4	75
4	3,-1,0	3000

Figure 50. Decision tree and coding for single-sensor malfunction algorithm.

Table 61. Erratic 20-second OCC's from intermittent hanging on (lane 1).

740725-01

OCCUPANCY

FWY	4	4	4
STA	14	14	14
LANE NO.	1	2	4
TIME			
810++	58	10	15
+	88	12	8
+	60	12	7
811++	19	12	6
+	48	13	15
+	62	5	7
812++	51	10	5
+	19	9	19
+	66	12	14
813++	37	8	17
+	6	5	8
+	18	11	13
814++	59	12	15
+	85	15	14
+	39	12	11
815++	22	14	15
+	22	7	8
+	36	12	8
816++	11	10	16
+	12	11	7
+	46	17	13
817++	14	10	13
+	7	7	9
+	12	15	23
818++	9	8	15
+	61	10	17
+	52	10	7
819++	21	13	14
+	13	10	11
+	13	9	18
820++	16	16	11

would not be valid over such short averaging periods since large differences between lanes are often found in these intervals. Nevertheless, if the percentage of invalid data coming from an intermittently malfunctioning detector was large enough, a consistent deviation between the malfunctioning sensor and its station neighbors should exist. This consistent deviation could easily be detected by an algorithm employing data aggregated over a long period, e.g., five minutes. Such an algorithm may not initially prevent an incident false alarm, but additional false alarms could be communicated to the malfunction routine to prevent the detector from being misclassified as malfunctioning.

A neighbor comparison algorithm was developed for purposes of illustration only since time did not permit an actual evaluation and threshold calibration. This algorithm was designed to identify intermittent hanging on only during low-density traffic (since hanging on resembles slow moving traffic under high occupancy conditions) and sporadic operation (i.e., intermittently stuck off) during medium or high-density traffic. Sporadic operation is difficult to detect during light traffic periods.

The potential algorithm employs five traffic data features:

F1 OCC5 - Mean station OCC - five minute average (average occupancy across all lanes at a given detector station)

F2 The ratio of the OCC average from the lane with the maximum five minute OCC to the mean station OCC.

F3 The maximum twenty or thirty-second OCC value from the previous five minutes from the lane with the maximum five-minute OCC.

F4 The ratio of the OCC average from the lane with the minimum five-minute OCC to the mean station OCC.

F5 The minimum twenty- or thirty-second OCC value from the previous five minutes from the lane with the minimum five-minute OCC.

Examples of these features can be seen in Table 62.

Table 62. Feature computation

740725-01
5-Minute Occupancy (810-815)

FWY	4	4	4	4
STA	14	14	14	14
LANE NO.	1	2	3	4
TIME				
815	45	11	12	11

Feature values

$F_1 = (45 + 11 + 12 + 11)/4 = 19$

$F_2 = 45/19 = 2.36$

$F_3 = 88$ (From Table 61)

$F_4 = 11/19 = .57$

$F_5 = 5$ (From Table 61)

The algorithm would identify lane 1 as a probable malfunction

The mean station OCC is tested for medium- or low-density traffic conditions (e.g., < 20%). If such a condition exists, a check is made for a sensor with an OCC average twice as large as the mean station OCC. If such a sensor is found, the previous five minutes of twenty- or thirty-second data is checked for average values greater than, for example, fifty percent. Such high values are unlikely for a normal detector under light traffic conditions.

A mean station OCC value greater than ten percent is usually associated with traffic which is distributed evenly over all lanes. Unusually low OCC values in one lane may be caused by an intermittently stuck off sensor. Thus the algorithm test for traffic conditions greater than ten percent OCC. If this is the case, a check is made for a lane with an OCC one-half as large or less than the mean station OCC. If such a lane exists, the twenty- or thirty-second data is checked for unreasonably low values (two or three percent). Figure 51 illustrates the binary decision tree representing this algorithm. (This tree will not pass the CTREE tests since node 4 can be reached from nodes 1, 2, or 3. However, this tree can still be executed using NTREE).

The number of lanes used in the mean station OCC computation should be at least four. Otherwise, data from a malfunctioning detector may cause the mean OCC to fail the tests at nodes 1 or 4 when actually the average OCC is within these bounds. Two ways to prevent such problems would be (1) to compare each lane individually to the mean of the others and compute the ratios from these values or (2) to include all lanes from the surrounding upstream and downstream detector stations in the mean traffic average to produce a more accurate value.

Although the algorithm presented was not fully evaluated, it is included to be considered for actual testing and to illustrate how data from neighboring sensors may be used in aiding detection of intermittent malfunctions. Similar algorithms could be employed in conjunction with single-sensor algorithms to provide a comprehensive sensor malfunction system.

F1 = OCC5, 5-min station OCC average

$F2 = \frac{OCCL5(i^*)}{OCC5}$, OCCL5(i*) is the 5-min OCC average from the lane with the maximum 5-min OCC average at a given station.

F3 = OCC(i*), the maximum 20 or 30-second OCC value from the previous 5 minutes from lane i*.

$F4 = \frac{OCCL5(j^*)}{OCC5}$, OCCL5(j*) is the 5-min OCC average from the lane with the minimum 5-min OCC average at a given station.

F5 = OCC(j*), the minimum 20 or 30-second OCC value from the previous 5 minutes from lane j*

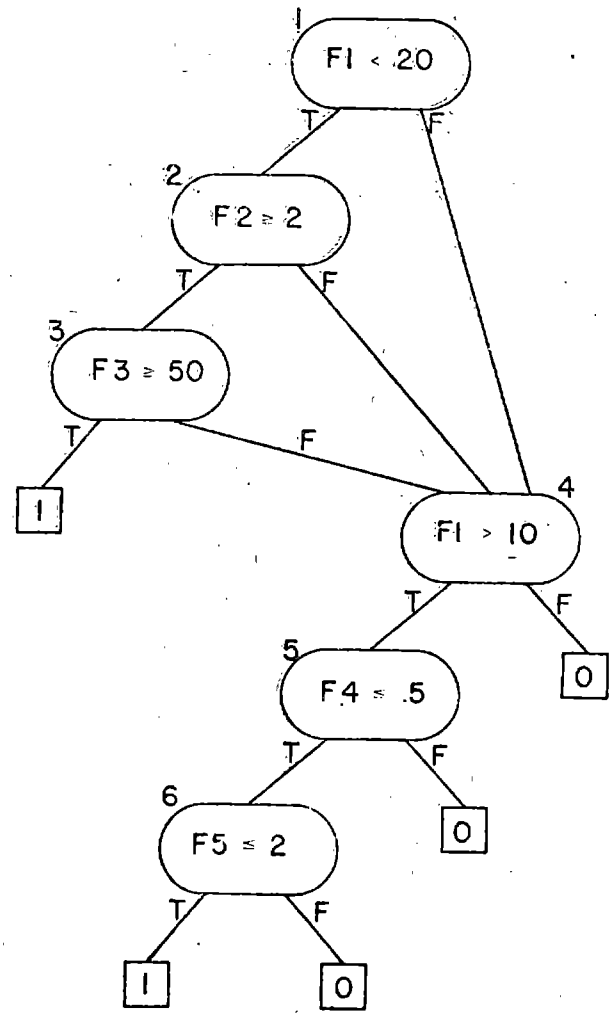

State	Designates	Decision Node	NTR	Threshold
0	No Malfunction	1	1,4,2	20.0
1	Probably Malfunction	2	2,3,4	2.0
		3	3,-1,4	50.0
		4	1,5,0	10.0
		5	4,0,6	0.5
		6	5,0,-1	2.0

Figure 51. A mean comparison malfunction algorithm using occupancy for detection of intermittent operation and hanging on.

7. EVALUATION WITH THE MINNEAPOLIS DATA BASE

Data collected over a portion of a Minneapolis freeway for the Minnesota Highway Department were used to provide independent evaluations of results obtained from the development of algorithms based only upon Los Angeles data. The Minneapolis data were collected under both clear and snowy conditions so that the effects of weather could also be examined.

7.1 THE MINNEAPOLIS DATA BASE

Data received from the Minnesota Highway Department consisted of thirty-second occupancies and volumes for all stations under surveillance in Minneapolis. A schematic of a portion of the surveillance system, that on Route I-35, is illustrated in Figure 52. Preparation and use of data were limited to this portion of the system. All data were received in a form which was aggregated over all lanes at a given station. The labeling scheme for sensor stations is given in Table 63. Distinct station numbers are used for opposite sides of the roadway. At the bend in the roadway, the relationship of sensor stations is somewhat complex. Table 64 lists, for each station, the stations immediately upstream and downstream, where they exist.

From the data received, 36 incident and 5 incident-free data sets were identified for use and were reformatted to conform to the condensed format developed for the Los Angeles data. This allowed us to use common software on both data bases. The identification numbers and characteristics of the data sets in the Minneapolis data base are given in Tables 65 (incident-free) and 66 (incident). Each data set contains data for the entire surveillance system. Two of the incident-free data sets and ten of the incident data sets pertain to snowy conditions.

7.2 ALGORITHM EVALUATIONS

To test the effectiveness of algorithms developed previously using only Los Angeles data, Algorithms 2, 7, and 8 were selected for examination. For each algorithm, we first evaluated performance with respect to the Minneapolis data base using thresholds previously found (i.e., "L.A. thresholds") and then performed a calibration on the Minneapolis data base.

For Algorithm 2, these results are presented in Tables 81 and 82 and Figure 63. For Algorithm 7, results are given in Tables 96 and 103 and Figure 81. For Algorithm 8, results are given in Tables 108 and 111 and Figure 88. To provide a direct comparison of these results and those using the Los Angeles data base, three sets of results, in the form of detection and false alarm rates, are plotted together for each algorithm in Figures 53, 54 and 55. In each figure

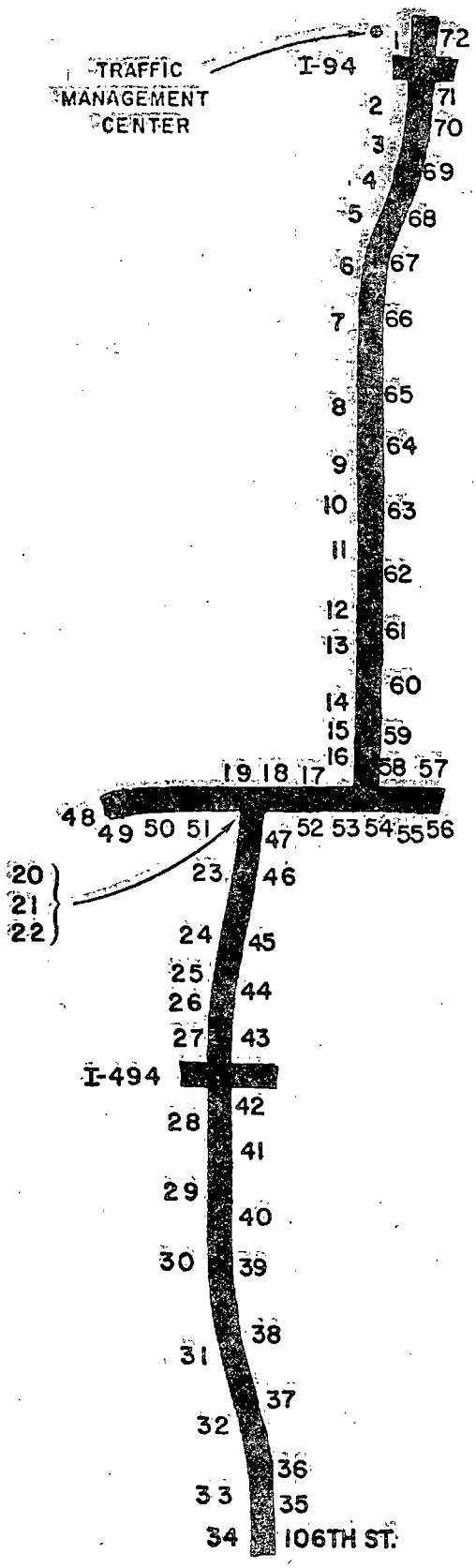

Figure 52. Minneapolis data collection site.

Table 63. Minneapolis station labeling.

Minneapolis Station		TSC Station No.			No. Lanes
No.	Name	Freeway	Station	Direction	
001	(012S)	35	01	S	2
002	(020S)	35	02	S	3
003	(020SM)	35	03	S	2
004	(026S)	35	04	S	4
005	(028S)	35	05	S	4
006	(031S)	35	06	S	4
007	(035S)	35	07	S	4
008	(038S)	35	08	S	4
009	(042S)	35	09	S	3
010	(046S)	35	10	S	3
011	(050S)	35	11	S	3
012	(051S)	35	12	S	3
013	(053S)	35	13	S	3
014	(055S)	35	14	S	3
015	(060S)	35	15	S	3
016	(061SX)	35	16	S	1
017	(061SM)	35	17	S	1
018	(061S)	35	18	S	2
019	(062S)	35	19	S	3
020	(063SX)	35	20	S	2
021	(063S)	35	21	S	2
022	(063SM)	35	22	S	2
023	(066S)	35	23	S	2
024	(070S)	35	24	S	2
025	(073S)	35	25	S	2
026	(076S)	35	26	S	2
027	(078S)	35	27	S	2
028	(082S)	35	28	S	2
029	(086S)	35	29	S	2
030	(090S)	35	30	S	2
031	(094S)	35	31	S	2
032	(098S)	35	32	S	2
033	(102S)	35	33	S	2
034	(106S)	35	34	S	2
035	(106N)	35	35	N	3
036	(102N)	35	36	N	2
037	(098N)	35	37	N	2
038	(094N)	35	38	N	2
039	(090N)	35	39	N	2
040	(086N)	35	40	N	2
041	(082N)	35	41	N	2
042	(078N)	35	42	N	2
043	(076N)	35	43	N	2
044	(073N)	35	44	N	2
045	(070N)	35	45	N	2
046	(066N)	35	46	N	2
047	(063NX)	35	47	N	2
048	(063E)	35	48	N	2
049	(622E)	35	49	N	2
050	(621E)	35	50	N	2
051	(063E)	35	51	N	2
052	(063N)	35	52	N	2
053	(062EM)	35	53	N	1
054	(062N)	35	54	N	3
055	(061NX)	35	55	N	1
056	(061N)	35	56	N	2
057	(620W)	35	57	N	2
058	(061NM)	35	58	N	1
059	(060N)	35	59	N	3
060	(055N)	35	60	N	3
061	(053N)	35	61	N	3
062	(050N)	35	62	N	3
063	(046N)	35	63	N	3
064	(042N)	35	64	N	4
065	(038N)	35	65	N	4
066	(035N)	35	66	N	4
067	(031N)	35	67	N	4
068	(028N)	35	68	N	4
069	(026N)	35	69	N	4
070	(020NX)	35	70	N	2
071	(020N)	35	71	N	3
072	(016N)	35	72	N	2

Table 64. Upstream-downstream pointers for Minneapolis stations.

TSC Station No.			Upstream Station			Downstream Station		
Freeway	Station	Direction	Freeway	Station	Direction	Freeway	Station	Direction
35	01	S	--	--	--	35	02	S
35	02	S	35	01	S	35	04	S
35	03	S	--	--	--	35	04	S
35	04	S	35	02	S	35	05	S
35	05	S	35	04	S	35	06	S
35	06	S	35	05	S	35	07	S
35	07	S	35	06	S	35	08	S
35	08	S	35	07	S	35	09	S
35	09	S	35	08	S	35	10	S
35	10	S	35	09	S	35	11	S
35	11	S	35	10	S	35	12	S
35	12	S	35	11	S	35	13	S
35	13	S	35	12	S	35	14	S
35	14	S	35	13	S	35	15	S
35	15	S	35	14	S	35	18	S
35	16	S	35	15	S	--	--	--
35	17	S	--	--	--	35	19	S
35	18	S	35	15	S	35	19	S
35	19	S	35	18	S	35	21	S
35	20	S	35	19	S	--	--	--
35	21	S	35	19	S	35	23	S
35	22	S	--	--	--	35	23	S
35	23	S	35	21	S	35	24	S
35	24	S	35	23	S	35	25	S
35	25	S	35	24	S	35	26	S
35	26	S	35	25	S	35	27	S
35	27	S	35	26	S	35	28	S
35	28	S	35	27	S	35	29	S
35	29	S	35	28	S	35	30	S
35	30	S	35	29	S	35	31	S
35	31	S	35	30	S	35	32	S
35	32	S	35	31	S	35	33	S
35	33	S	35	32	S	35	34	S
35	34	S	35	33	S	--	--	--
35	35	N	--	--	--	35	36	N
35	36	N	35	35	N	35	37	N
35	37	N	35	36	N	35	38	N
35	38	N	35	37	N	35	39	N
35	39	N	35	38	N	35	40	N
35	40	N	35	39	N	35	41	N
35	41	N	35	40	N	35	42	N
35	42	N	35	41	N	35	43	N
35	43	N	35	42	N	35	44	N
35	44	N	35	43	N	35	45	N
35	45	N	35	44	N	35	46	N
35	46	N	35	45	N	35	52	N
35	47	N	35	45	N	--	--	--
35	48	N	--	--	--	35	49	N
35	49	N	35	48	N	35	50	N
35	50	N	35	49	N	35	51	N
35	51	N	35	50	N	35	53	N
35	52	N	35	46	N	35	54	N
35	53	N	35	51	N	35	54	N
35	54	N	35	52	N	35	56	N
35	55	N	35	54	N	--	--	--
35	56	N	35	54	N	35	59	N
35	57	N	--	--	--	35	58	N
35	58	N	35	51	N	35	59	N
35	59	N	35	56	N	35	60	N
35	60	N	35	59	N	35	61	N
35	61	N	35	60	N	35	62	N
35	62	N	35	61	N	35	63	N
35	63	N	35	62	N	35	64	N
35	64	N	35	63	N	35	65	N
35	65	N	35	64	N	35	66	N
35	66	N	35	65	N	35	67	N
35	67	N	35	66	N	35	68	N
35	68	N	35	67	N	35	69	N
35	69	N	35	68	N	35	71	N
35	70	N	35	69	N	--	--	--
35	71	N	35	69	N	35	72	N
35	72	N	35	71	N	--	--	--

Table 65. Incident-free data sets in the Minneapolis data base.

Data Set No.	Time From	Time To	Weather
74100171	0630	0900	Clear
74102471	1530	1800	Clear
74102471	1530	1800	Clear
75010771	1530	1800	Snow
75010971	0630	900	Snow

Table 66. Incident data sets in the Minneapolis data base.

Data Set No.	Estimated Time of Occurrence (HHMMSS)	Location Upstream Station	Lane	Type	Weather
74100331	164400	9	2	DISL	Clear
74100731	084200	49	1,2	TCOL	Clear
24100732	163300	7	Five off freeway	GAWK	Clear
74100733	165200	4	1	TCOL	Clear
74100734	071200	23	1,2	TCOL	Clear
74101031	173230	5	3	SPIL	Clear
74101131	164400	61	RS	GAWK	Clear
7410431	172000	29		TCOL	Clear
74101631	075000	11	M	DISL	Clear
74101632	164500	42	1,2	TCOL	Clear
74102232	160100	60		TCOL	Clear
74102231	074300	42	2	TCOL	Clear
74102331	163000	7	2	DISL	Clear
74102531	073100	25		TCOL	Clear
74102532	160800	18	M,1	DISL	Clear
74103131	072000	54	RS	GAWK	Hazy
74112731	073600	27	RS	TCOL	Clear
74121231	160900	13	2	TCOL	Clear
74121331	074100	52	2	DISL	Clear
74123031	162200	13	2	TCOL	Clear
75010231	154800	10	2,3,RS	DISL	Snow
75010232	160530	10	4	DISL	Snow
75010631	080200	23	M	DISL	Snow
75010831	081300	42	RS	DISL	Snow
75010832	161500	8	1,2,M	TCOL	Snow
75010833	163600	5	M	TCOL	Snow
75010834	165300	1	M	TCOL	Snow
75011331	071000	60	2,3	DISL	Clear
75011332	164700	9	2,3	DISL	Clear
75011431	082900	52	M	DISL	Clear
75011432	071230	46	2	DISL	Clear
75011433	154630	8	2	DISL	Snow
75011434	160400	4	2	DISL	Snow
75011631	173230	4	3	DISL	Clear
75011632	154630	19	card-board on road	SPIL	Clear

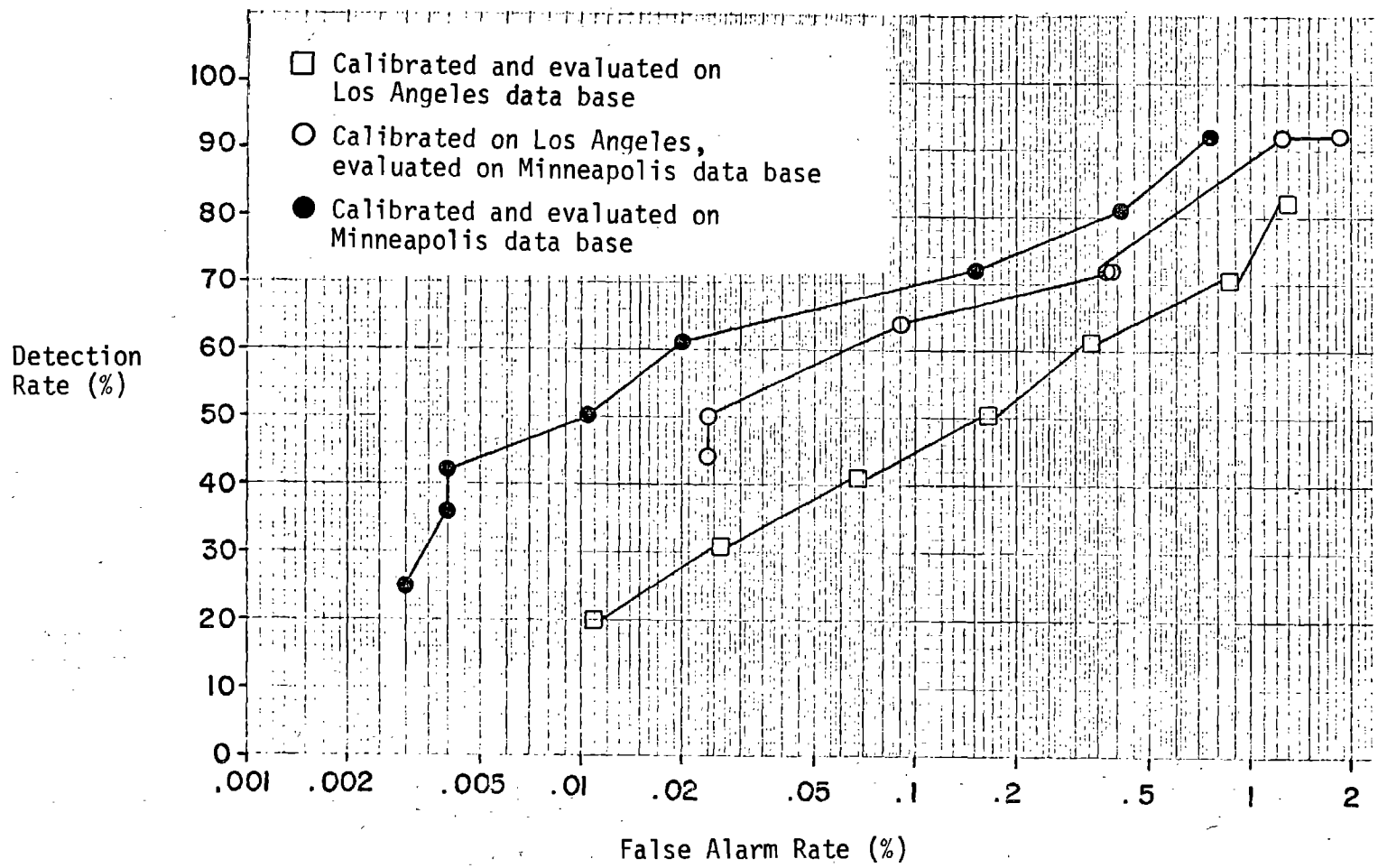

Figure 53. Comparison of performance of Algorithm 2 on Los Angeles and Minneapolis data bases.

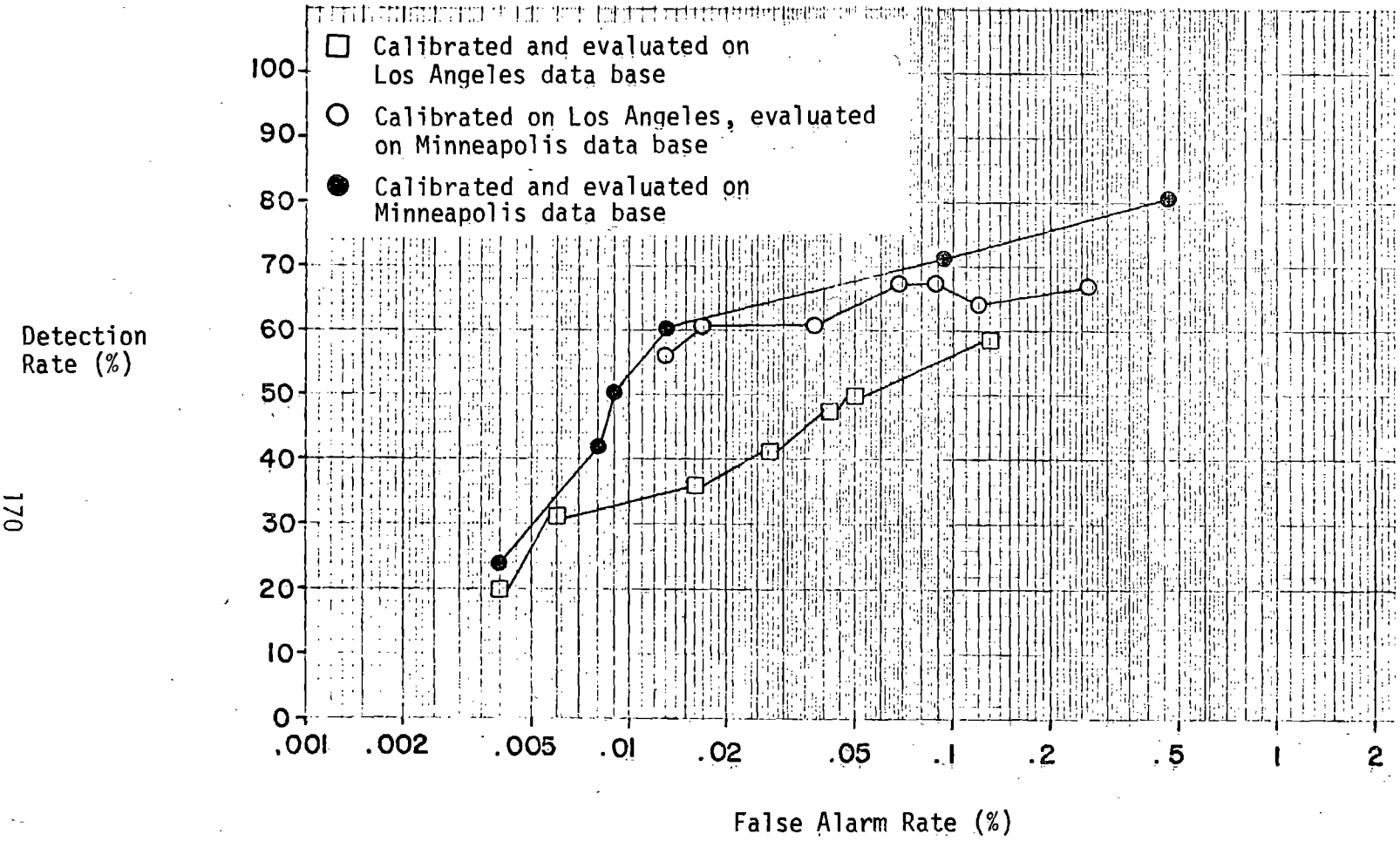

Figure 54. Comparison of performance of Algorithm 7 on Los Angeles and Minneapolis data bases.

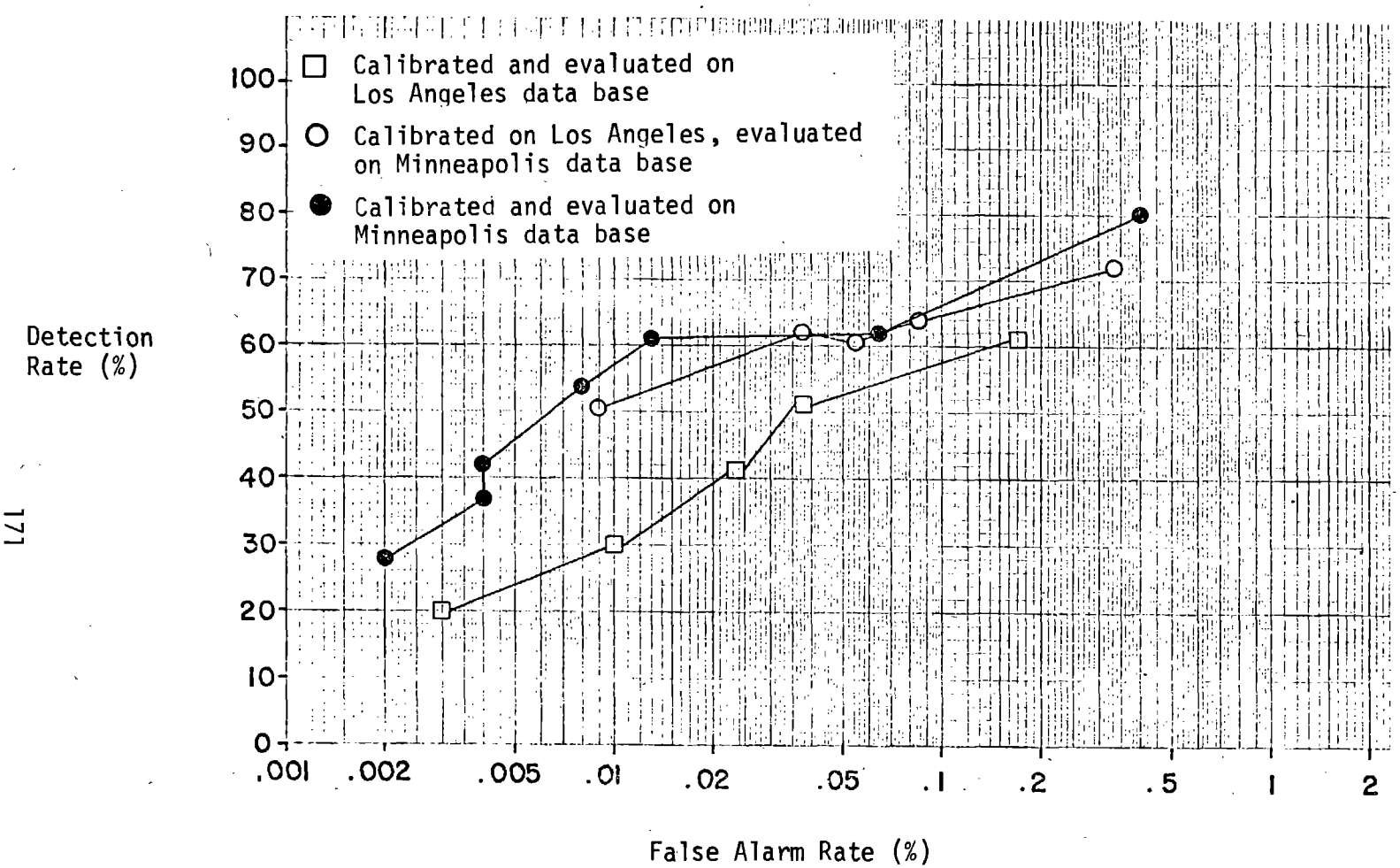

Figure 55. Comparison of performance of Algorithm 8 on Los Angeles and Minneapolis data bases.

we repeat results obtained by calibration and evaluation of the Los Angeles data base and give the two sets of results pertaining to the Minneapolis data base.

Performance is generally better on the Minneapolis data base and by calibration on that data base, performance is improved. These figures provide concrete illustrations of the point we made earlier--performance measures depend upon the data base. (Differences for Algorithm 2, Figure 53, are significant at the .01 level. For algorithms 7 and 8 differences between false alarms on the Los Angeles and Minneapolis data bases are significant at the .01 level, except for Algorithm 7 at detection rates less than 31%.)

Two important conclusions emerge from further examination of these results

- Satisfactory performance is obtained by using thresholds established by calibration on the Los Angeles data base.

- The relative performance of these three algorithms is the same on the Minneapolis and Los Angeles data bases.

Taken together, these conclusions indicate that the results we have obtained by developments on the Los Angeles data base--both in terms of good structures for algorithms and the specific thresholds-- are of general value. Implementing agencies other than the one responsible for the Los Angeles system can also expect good performance from the algorithms we have found. If yet better results are desired, calibration on a data base specific to the site can be carried out.

With regard to improvements in performance obtained by calibrating on the Minneapolis data base, evaluations were carried out on the same data base as used for calibration. To some extent, then, the improvements observed may not be real, but merely a reflection of fitting the thresholds to the specific data base.

7.3 EFFECTS OF WEATHER

One major reason for acquiring the Minneapolis data base was to investigate the effects of weather.

For this evaluation, Algorithms 2, 7, and 8 were again selected for examination. The Minneapolis data base was partitioned into a clear weather data base and a snowy-weather data base. Evaluation results for the three algorithms are given in Tables 83, 102, and 112, respectively, where thresholds previously found from calibration on the entire Minneapolis data base were used.

It will be noted that the false alarm rates, at a given detection rate, are generally lower for clear weather as compared to snowy weather data. However, it is not valid to draw the conclusion that algorithm performance, in practice, will be better under clear weather conditions. Our data were not derived from controlled experiments -- controlled in the sense that all relevant circumstances, e.g., traffic volume, were identical except for the weather condition. Hence other factors may account for the differences in performance observed.

The more relevant question is whether different sets of thresholds are justified for different weather conditions. To test this, Algorithm 7 was recalibrated on the separate weather condition data bases, yielding the results of Tables 103 and 104, and Figures 81 and 82. Comparing these results to those obtained by calibration of the entire Minneapolis data base, Figure 56 and 57 indicate that performance measures are very similar. There are differences to be found (but they are not significant at the .10 level), but the general conclusion is that there does not appear to be a need for (or benefit associated with) separate sets of thresholds dependent upon weather conditions. This conclusion is based, of course, on the specific conditions represented in the Minneapolis data base and cannot necessarily be extrapolated to conditions not represented there.

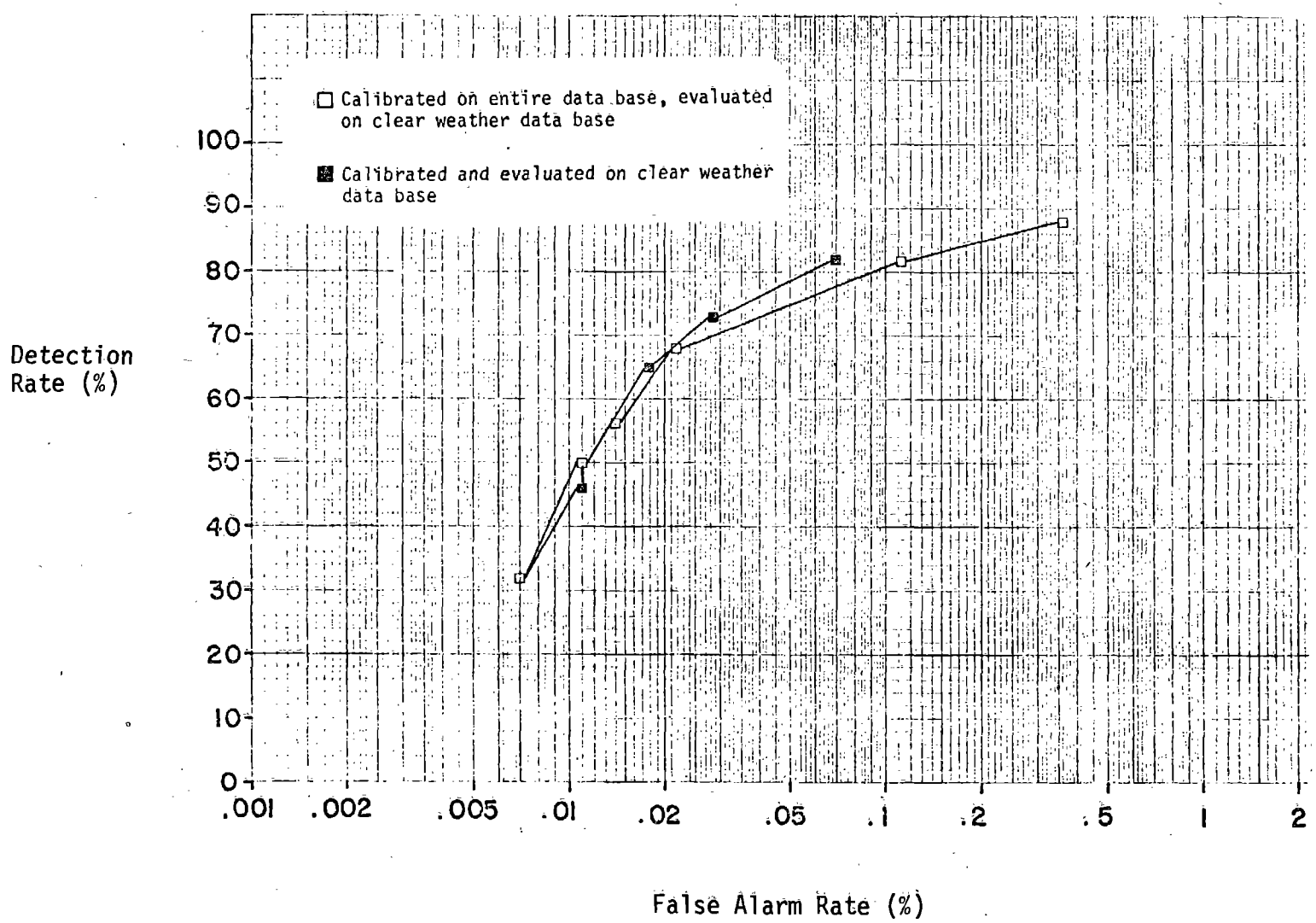

Figure 56. Comparison of performance of Algorithm 7 on Minneapolis clear weather data base.

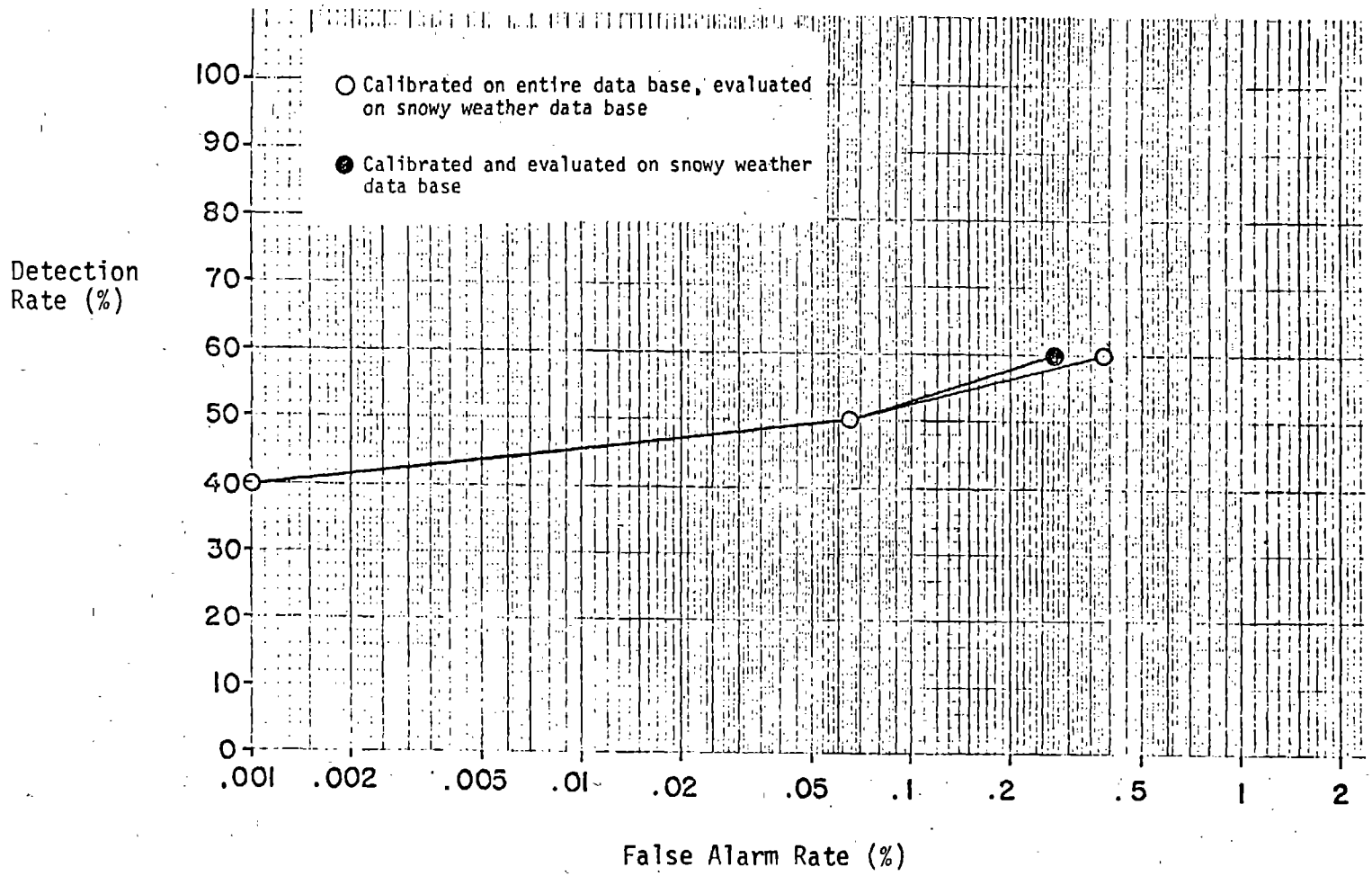

Figure 57. Comparison of performance of Algorithm 7 on Minneapolis snowy weather data base.

8. RECOMMENDATIONS FOR FURTHER RESEARCH

In the course of our investigations, we have identified alternative approaches to the construction of incident detection algorithms which we were not able to pursue fully or to pursue at all. One such approach is based upon traffic correlation analysis. A second is the use of individual lane occupany data. These approaches appear to have promise for improving the detection of incidents in light-to-moderate traffic, incidents that the algorithms we have developed have difficulty in detecting. In addition, as we have noted, false alarms due to bottleneck conditions also remain a problem. The second approach of using individual lane occupancy data may be of value in reducing such false alarms.

Details of a feature based upon the concept of traffic correlation are given in Appendix A, along with preliminary results obtained from its application to a few incidents. Two factors motivate our recommendation for further attention to algorithms based upon traffic correlation. First, traffic correlation is most consistent in the light-to-moderate regime with speeds near fifty miles per hour, and thus the corresponding feature is most sensitive in this regime to disruptions in the traffic stream. Second, it is precisely in this regime that incidents are found to be difficult to detect.

The success we had in constructing an algorithm for identifying the lane of occurrence of an incident suggests a refinement to the structures of the algorithms we have developed. This refinement involves the use of individual lane occupancy data downstream of the incident site, the same data found to be most useful in lane identification. And, since bottlenecks remain the most prevalent source of false alarms in our best performing algorithm (Number 8), this refinement is aimed at distinguishing between incidents and bottleneck conditions.

A candidate algorithm embodying this refinement is illustrated in Figure 58, it is a modification to Algorithm 7. The idea is that threshold T_2 associated with OCCRDF would be chosen as a relatively large value, say .6, so that the old test used in Algorithm 7 would be applied when large discontinuities are found. Bottlenecks do not typically produce such large discontinuities. In an intermediate range of values of OCCRDF associated with a choice of T_4 of, for example, .35, there is possible confusion between bottlenecks and incidents. Thus, in this range we would apply a more detailed test involving DOCC and a new feature, DOCCDV, defined as follows (refer to Section 3.1):

$$\mathrm{DOCCDV}(i,t) = \frac{\sum_{j=1}^{N(i+1)} \mathrm{OCC}(i+1,j,t) - N(i+1) \min_j \mathrm{OCC}(i+1,j,t)}{\sum_{j=1}^{N(i+1)} \mathrm{OCC}(i+1,j,t)}$$

Preceding page blank

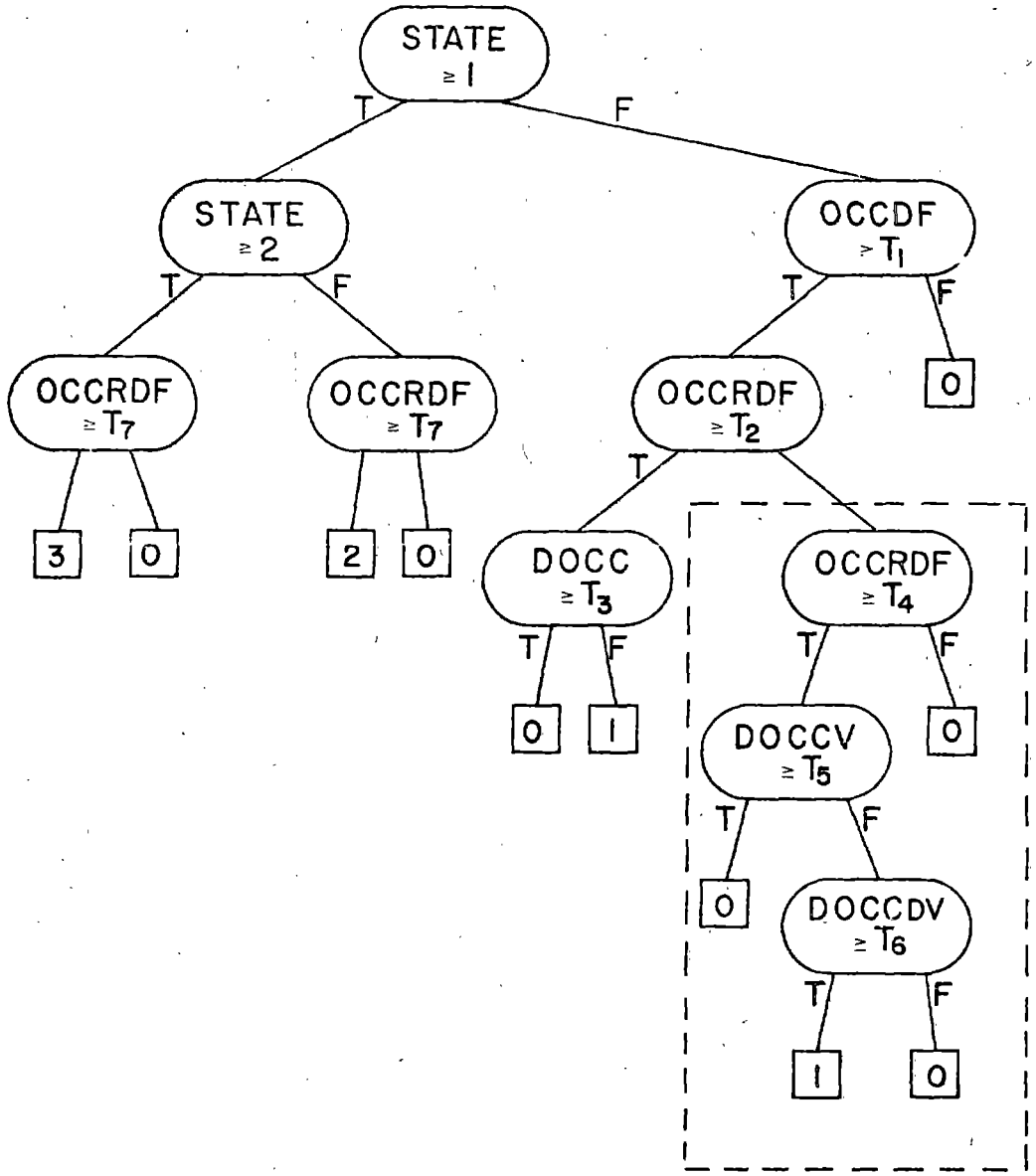

Figure 58. Suggested refinement to Algorithm 7.

(Note that this feature is defined in a similar manner to that for the feature ENRGSD which was examined in the first interim report.)

The sensor configuration study we undertook was limited by the fact that the data available to us involved sensor stations no closer (on the average) than one-half mile. Recently, a data base involving stations spaced at approximately 600-foot intervals (San Diego freeway in Los Angeles) has become available.

The procedures undertaken, as described in Section 6.2, can be applied to this data base as well. Various subsets of the data can be used to study, for example, sensor spacings ranging from 600 feet to a mile. The special value of this data base is that algorithm performance can be studied for this important range of sensor spacings for the same incidents, thus avoiding a possible confusion in results that might occur if different incidents for different sensor configurations were examined.

Our study of the effects of geometrics and means for reducing their adverse impacts on incident detection algorithm performance revealed the importance of this factor but was inconclusive with respect to the one technique examined for reducing adverse impacts. The approach we examined involved a normalization of features values (differences in occupancies) based upon typical traffic patterns. It is evident that further examination of this technique, and development and evaluation of others, is necessary to resolve this remaining problem.

Appendix A. TRAFFIC STREAM CORRELATION

CONTENTS

		Page
1.	TRAFFIC STREAM CORRELATION ANALYSIS	182
1.1	UPSTREAM-DOWNSTREAM CORRELATION ANALYSIS	182
1.2	COMPUTATION OF THE TREND	184
1.3	GENERALIZED CORRELATION ANALYSIS	184
2.	ALGORITHMS BASED UPON TRAFFIC STREAM CORRELATION	190
2.1	DEFINITION OF THE CORRELATION FEATURE	190
2.2	SAMPLE RESULTS	191
2.3	COMPUTER REQUIREMENTS	196
2.4	CANDIDATE ALGORITHMS	196

Preceding page blank

1. TRAFFIC STREAM CORRELATION ANALYSIS

Traffic stream correlation can be used to provide an improved forecast of a traffic variable. An example is the correlation observed in light to moderate traffic, between the present value of a traffic variable at one station and past values of the traffic variable at an upstream station. In this section, the basis for such forecasts is developed, first, in the context of using upstream-to-downstream correlation and, then, in the more general context of a dependent time series and one or more independent time series.

1.1 UPSTREAM-DOWNSTREAM CORRELATION ANALYSIS

We consider two time series, $x(k)$ and $y(k)$, corresponding to traffic data from upstream and downstream stations, respectively. As the theory suggests a correlation of fluctuations, it is appropriate to consider deviations of these traffic variables from the trends:

$$\tilde{x}(k) = x(k) - t_x(k) \tag{14}$$

and

$$\tilde{y}(k) = y(k) - t_y(k) \quad . \tag{15}$$

Determination of the trend values, $t_x(k)$ and $t_y(k)$, is deferred to the next section.

It is expected that values of $\tilde{y}(k)$ can be predicted from past values of $\tilde{x}(k)$. The problem we address at this point is the determination of those coefficients, $a(n|k)$, $n=n_0,\ldots,n_1$, which provide the best estimates

$$\hat{\tilde{y}}\,(k-m|k) = \sum_{n=n_0}^{n_1} a(n|k)\,\tilde{x}(k-m-n) \tag{16}$$

$$m=0,1,\ldots,$$

in the sense that the error

$$E(k) = \sum_{m=0}^{\infty} e^{-m\alpha}[\tilde{y}(k-m)-\hat{\tilde{y}}(k-m|k)]^2 \tag{17}$$

is least. This approach is chosen, in part, because of the computational convenience which results.

Straightforward computations yield the following equations for the coefficients:

$$\sum_{q=n_0}^{n_1} a(q|k)\,\sigma_{xx}\,(n,q|k) = \sigma_{xx}(n|k) \quad n=n_0,\ldots,n_1 \quad , \tag{18}$$

where $$\sigma_{xx}(n,q|k) = \sum_{m=0}^{\infty} e^{-m\alpha}\, \tilde{x}(k-m-n)\, \tilde{x}\,(k-m-q) \tag{19}$$

and $$\sigma_{yx}(n|k) = \sum_{m=0}^{\infty} e^{-m\alpha}\, \tilde{y}(k-m-q)\, \tilde{x}\,(k-m-n)\,. \tag{20}$$

Computational convenience derives from the fact that the required quantities can be computed recursively:

$$\sigma_{xx}(n,q|k+1) = e^{-\alpha}\sigma_{xx}(n,q|k) + \tilde{x}\,(k+1-n)\tilde{x}(k+1-q) \tag{21}$$

and

$$\sigma_{xx}(n|k+1) = e^{-\alpha}\sigma_{xx}(n|k)+\tilde{y}(k+1)\tilde{x}(k+1-n)\,. \tag{22}$$

Further, from (19) it can be seen that

$$\sigma_{xx}(n+1,q+1|k+1) = \sigma_{xx}(n,q|k) \tag{23}$$

Therefore, equation (23) can be employed for $n=n_0,\ldots,n_1-1$ and $q-n_0,\ldots,n_1-1$ to obtain most of the elements of $\sigma_{xx}(n,q|k+1)$. Finally, we note the symmetry of this array, i.e.

$$\sigma_{xx}(n,q|k) = \sigma_{xx}(q,n|k) \tag{24}$$

so that (21) need only be used to compute $\sigma_{xx}(n_0,q|k+1)$, $q=n_0,\ldots,n_1$. Symmetry can also be exploited to reduce storage requirements.

One can show that

$$E(k) = \sigma_{xx}(o,o|k)-\sum_{n=n_0}^{n_1} a(n|k) \sum_{q=q_0}^{n_1} a(q|k)\sigma_{xx}(n,q|k)\,, \tag{25}$$

where

$$\sigma_{yy}(n,q|k) = \sum_{m=o}^{n_1} e^{-m\alpha}\tilde{y}(k-m-n)\tilde{y}(k-m-q) \tag{26}$$

General derivations of equations 18 through 20 and 25 and 26 follow in subsection 1.3.

1.2 COMPUTATION OF THE TREND

We have found that σ_{xx}, etc., are determined by recursive, single exponential smoothing relations. To be consistent with this, the trend values are determined from exponential smoothing. Thus we compute

$$s_x^{(1)}(k+1) = e^{-\alpha} s_x^{(1)}(k) + (1-e^{-\alpha})\, x(k+1) \tag{27}$$

and compute the trend values as

$$t_x(k+1) = s_x^{(1)}(k) \tag{28}$$

with identical relations for the downstream variable obtained by replacing x with y.

When trends are present in the traffic data, it may be desirable to account for this by employing higher-order exponential smoothing.[1] For example, to account for a straight-line trend, one can employ double exponential smoothing as follows:

$$s_x^{(1)}(k+1) = e^{-\alpha} s_x^{(1)}(k) + (1-e^{-\alpha}) x(k+1) \tag{29}$$

and

$$s_x^{(2)}(k+1) = e^{-\alpha} s_x^{(2)}(k) + (1-e^{-\alpha})\, s_x^{(1)}(k+1) \tag{30}$$

The trend values are then taken as one-step forecasts:

$$t_x(k+1) = 2s_x^{(1)}(k) - s_x^{(1)}(k) + [e^{\alpha}-1][s_x^{(1)}(k)-s_x^{(2)}(k)] \; . \tag{31}$$

1.3 GENERALIZED CORRELATION ANALYSIS

The analyses in the two previous subsections apply more generally to y(k) considered to be a dependent time series and to x(k), an independent time series. For example, in congested traffic, fluctuations move in an upstream direction so that one could take y(k) to correspond to the upstream

[1] R. G. Brown, Smoothing, Forecasting and Prediction of Discrete Time Series, Englewood Cliffs, N.J., Prentice-Hall, Inc., 1962, p. 123ff.

station and x(k) to correspond to the downstream station. As a second example, in certain locations where on-ramp traffic is particularly heavy, one might wish to relate observed fluctuations in main-line occupancy (y) to fluctuations in the on-ramp volume (x).

In the situation of the latter example, an even better forecast might be obtained by using two independent time series, e.g., upstream occupancy and on-ramp volume. To handle this, a generalization of the development of subsection 1.1 is required and is taken up here.

As before, $\tilde{y}(k)$ is the time series of deviations from the trend of the dependent time series. Now we can consider a vector time series,

$$x(k) = \begin{bmatrix} x_1(k) \\ \vdots \\ x_p(k) \end{bmatrix} , \tag{32}$$

i.e., a collection of p independent time series. Trends for each component can be separately computed,

$$t_x(k) = \begin{bmatrix} t_{x_1}(k) \\ \vdots \\ t_{x_p}(k) \end{bmatrix} , \tag{33}$$

and then a vector of deviations, (34)

$$\tilde{x}(k) = \begin{bmatrix} x_1(k) - t_{x_1}(k) \\ \vdots \\ x_p(k) - t_{x_p}(k) \end{bmatrix} ,$$

can be identified.

The optimal forecast problem is then the determination of the array of coefficients

$$a(n|k) = \begin{bmatrix} a_1(n|k) \\ \vdots \\ a_p(n|k) \end{bmatrix} , n=n_0,\ldots,n_1 \tag{35}$$

which provide the best estimates

$$\hat{\tilde{y}}(k-m|k) = \sum_{n=n_0}^{n_1} \sum_{r=1}^{p} a_r(n|k)\tilde{x}_r(k-m-n), \tag{36}$$

in the sense that the error

$$E(k) = \sum_{m=o}^{\infty} e^{-m\alpha}\left[\tilde{y}(k-m) - \hat{\tilde{y}}(k-m|k)\right]^2 \tag{37}$$

is least.

To identify equations defining $a(n|k)$, we first define

$$\sigma_{yy}(n,q|k) = \sum_{m=o}^{\infty} e^{-m\alpha}\ \tilde{y}(k-m-n)\tilde{y}(k-m-q) \quad , \tag{38}$$

$$\sigma_{yx_j}(n|k) = \sum_{m=o}^{\infty} e^{-m\alpha}\ \tilde{y}(k-m)\ \tilde{x}_j(k-m-n) \quad , \tag{39}$$

and

$$\sigma_{x_i x_j}(n,q|k) = \sum_{m=o}^{\infty} e^{-m\alpha}\ \tilde{x}_i(k-m-n)\ \tilde{x}_j(k-m-q) \quad . \tag{40}$$

Now, inserting (36) into (37), we have

$$E(k) = \sum_{m=o}^{\infty} e^{-m\alpha}\left[\tilde{y}(k-m) \sum_{n=no}^{n_1} - \sum_{r=1}^{p} a_r(n|k)\ \tilde{x}_r(k-m-n)\right]^2$$

$$= \sum_{m=o}^{\infty} e^{-m\alpha}\left[y(k-m)\right]^2$$

$$-2 \sum_{n=n_o}^{n_1} \sum_{r=1}^{p} a_r(n|k) \sum_{m=o}^{\infty} e^{-m\alpha}\ \tilde{y}(k-m)\ \tilde{x}_r(k-m-n)$$

$$+ \sum_{n=n_o}^{n_1} \sum_{q=n_o}^{n_1} \sum_{r=1}^{p} \sum_{s=1}^{p} a_r(n|k)a_s(q|k) \sum_{m=o}^{\infty} e^{-m\alpha}\ \tilde{x}_r(k-m-n)\tilde{x}_s(k-m-q)$$

$$= \sigma_{xx}(o,o|k) - 2 \sum_{n=n_o}^{n_1} \sum_{r=1}^{p} a_r(n|k)\sigma_{yx_r}(n,q|k)$$

$$+ \sum_{n=n_o}^{n_1} \sum_{q=n_o}^{n_1} \sum_{r=1}^{p} \sum_{s=1}^{p} a_r(n|k)a_s(n|k)\sigma_{x_r x_s}(n,q|k)\ . \qquad (41)$$

Let

$$A = \begin{bmatrix} a_1(n_o|k) \\ \vdots \\ a_1(n_1|k) \\ \vdots \\ a_p(n_o|k) \\ \vdots \\ a_p(n_1|k) \end{bmatrix}, \qquad (42)$$

$$\sigma_{yx} = \begin{bmatrix} \sigma_{yx_1}(n_o) \\ \vdots \\ \sigma_{yx_1}(n_1) \\ \vdots \\ \sigma_{yx_p}(n_o) \\ \vdots \\ \sigma_{yx_p}(n_1) \end{bmatrix} , \tag{43}$$

$$\sigma_{x_i x_j} = \begin{bmatrix} \sigma_{x_i x_j}(n_o, n_o \ldots \sigma_{x_i x_j}(n_o, n_1) \\ \vdots \qquad\qquad \vdots \\ \sigma_{x_i \sigma_{x_j}}(n_1, n_o) \ldots \sigma_{x_i \sigma_{x_j}}(n_1, n_1) \end{bmatrix} , \tag{44}$$

and

$$\sigma_{xx} = \begin{bmatrix} \sigma_{x_1 x_1} & \cdots & \sigma_{x_1 x_p} \\ \sigma_{x_p x_1} & \cdots & \sigma_{x_p x_p} \end{bmatrix} . \tag{45}$$

Then, using vector-matrix notation,

$$E(k) = \sigma_{yy}(o,o|k) - 2A^t\sigma_{yx} + A^t\sigma_{xx}A \tag{46}$$

and

$$E(k) = \sigma_{xx}(o,o|k) - \sigma_{yx}{}^{t}\sigma_{xx}{}^{-1}\sigma_{yx} + \left[\sigma_{xx}A-\sigma_{xx}\right]^{t}\sigma_{xx}^{-1}\left[\sigma_{xx}A-\sigma_{yx}\right] . \tag{47}$$

As the last term is the only one involving A and is clearly nonnegative, the best choice of A is seen to be specified by

$$\sigma_{xx}A = \sigma_{yx} \quad , \tag{48}$$

and, for this choice,

$$E(k) = \sigma_{yy}(o,o|k) - \sigma_{yx}{}^{t}\sigma_{xx}{}^{-1}\sigma_{yx} \quad . \tag{49}$$

2. ALGORITHMS BASED UPON TRAFFIC STREAM CORRELATION

In this section, a traffic stream correlation feature is defined that is based upon a comparison of the forecast of a traffic variable to its actual value, using the past trend and the fluctuation forecast. This correlation feature may be used to define an incident-detection algorithm directly in the form:

traffic stream correlation feature > threshold,

or it may be incorporated in a multiple-feature algorithm. Attention here is given to the definition of the feature, some sample results, computational requirements, and recommendations for its use in incident-detection algorithms.

2.1 DEFINITION OF THE CORRELATION FEATURE

Using the notation of the previous section, the forecast of the dependent traffic variable is defined as the sum of a trend forecast and a fluctuation forecast:

$$\hat{y}(k+1) = t(k+1) + f(k+1) \tag{50}$$

where the trend forecast is defined by equation (28) if single exponential smoothing is used and by (31) if double exponential smoothing is used. The fluctuation forecast is given by

$$f(k+1) = \sum_{n=n_0}^{n_1} a(n|k)\, \tilde{x}(k+1-n) \;, \tag{51}$$

if a single independent time series is used and by equation (36) if more than one such series is used. An accumulated forecasting error is defined as

$$e(k+1) = \theta_1 e(k) + \theta_2[y(k+1) - \hat{y}(k+1)] \tag{52}$$

with $\theta_1 \geq 0$, $\theta_2 \geq 0$. To obtain a normalization of the accumulated forecasting error, we define the smoothed mean absolute deviation:

$$\mu(k+1) = (1-\gamma)\mu(k) + \gamma|y(k+1) - \hat{y}(k+1)| \tag{53}$$

and then the normalized forecast error:

$$\bar{e}(k+1) = e(k+1)/\mu(k) \quad . \tag{54}$$

This feature definition, resulting ultimately in $\bar{e}(k)$, is very similar to that for exponential smoothing features described in the first interim report.[1] It will be noted that when the correlation is weak, the contribution of the fluctuation forecast will be small so that the trend forecast will predominate, i.e., the feature will reduce to an exponential smoothing feature.

Software and related documentation of the correlation feature is given in Volume 4 of this report.

2.2 SAMPLE RESULTS

The software embodying the traffic correlation feature was exercised using both occupancy and volume data. As was previously found and reported[2] results were better with the occupancy data, and results reported here pertain only to occupancy data.

Results that illustrate the presence of traffic correlation and the reduction in the forecast error obtained by using the fluctuation forecast are presented in Tables 67 through 70. In all of these cases, parameters were as follows:

$$\alpha = 1/15$$

$$n_0 = 1$$

$$n_1 = 4$$

$$\theta_1 = \theta_2 = 1/2$$

$$\gamma = .1$$

First, upstream-to-downstream correlation was examined. That is, the fluctuations in upstream data were used to produce a forecast of downstream data. The traffic variables chosen were twenty-second occupancies in individual lanes. Tables 67 and 69 illustrate the use of single exponential smoothing while Tables 68 and 70 illustrate the use of double exponential smoothing. It can be seen from the values of the fluctuation coefficients ($a(1|k-1)$, etc.) that there is strong correlation of the fluctuations.

---

[1] H. J. Payne et al, Ibid, p. 49 ff.

[2] Ibid, p. 127.

Table 67. Single Exponential Smoothing, Data Set 74042354, Santa Monica Westbound, Station 9, Lane 2, Twenty-Second Occupancy

Time	$y(k)$	$s_y^{(1)}(k-1)$	$t_y(k)$	$e(k)$	Accumulated error $\mu(k-1)$	Mean absolute deviation $\bar{e}(k)$	Feature
74300.	8.0000	5.5575	5.5575	1.0682	1.7288	.6179	
74320.	6.0000	5.7151	5.7151	.6766	1.8002	.3758	
74340.	13.3300	5.7334	5.7334	4.1366	1.6487	2.5091	
74400.	8.6700	6.2234	6.2234	3.2916	2.2434	1.4672	

Table 68. Double Exponential Smoothing, Data Set 74042354, Santa Monica Westbound, Station 9, Lane 2, Twenty-Second Occupancy

Time	$y(k)$	$s_y^{(1)}(k-1)$	$s_y^{(2)}(k-1)$	$t_y(k)$	$e(k)$ (Accumulated error)	$\mu(k-1)$ (Mean absolute deviation)	$\bar{e}(k)$ (Feature)
74300.	8.0000	5.5575	5.2950	5.8381	.7442	1.7480	.4257
74320.	6.0000	5.7151	5.3221	6.1351	.3046	1.7894	.1702
74340.	13.3300	5.7334	5.3487	6.1447	3.7449	1.6240	2.3060
74400.	8.6700	6.2234	5.4051	7.0981	2.6584	2.1801	1.2194

Table 69. Upstream-to-Downstream Correlation with Single Exponential Smoothing, Data Set 74042354, Santa Monica Westbound, Station 10 (Upstream), Station 9 (Downstream), Lane 2 Twenty-Second Occupancy

Time	$y(k)$	$s_y^{(1)}(k-1)$	$t_y(k)$	$f(k)$	$\hat{y}(k)$	$e(k)$	$\mu(k-1)$	$\bar{e}(k)$
	$\tilde{y}(k)$	$\tilde{y}(k-1)$	$\tilde{y}(k-2)$	$\tilde{y}(k-3)$	$\tilde{y}(k-4)$			
	$\tilde{x}(k)$	$\tilde{x}(k-1)$	$\tilde{x}(k-2)$	$\tilde{x}(k-3)$	$\tilde{x}(k-4)$			
	$\sigma_{yx}(1\|k)$	$a(1\|k-1)$	$\sigma_{xx}(1,1\|k)$	$\sigma_{xx}(1,2\|k)$	$\sigma_{xx}(1,3\|k)$	$\sigma_{xx}(1,4\|k)$		
	$\sigma_{yx}(2\|k)$	$a(2\|k-1)$	$\sigma_{xx}(2,1\|k)$	$\sigma_{xx}(2,2\|k)$	$\sigma_{xx}(2,3\|k)$	$\sigma_{xx}(2,4\|k)$		
Time	$\sigma_{yx}(3\|k)$	$a(3\|k-1)$	$\sigma_{xx}(3,1\|k)$	$\sigma_{xx}(3,2\|k)$	$\sigma_{xx}(3,3\|k)$	$\sigma_{xx}(3,4\|k)$		
	$\sigma_{yx}(4\|k)$	$a(4\|k-1)$	$\sigma_{xx}(4,1\|k)$	$\sigma_{xx}(4,2\|k)$	$\sigma_{xx}(4,3\|k)$	$\sigma_{xx}(4,4\|k)$	Accumulated error	Mean absolute deviation	Feature
74300	3.0000	5.5675	5.5576	1.1729	6.7304	.1524	1.2829	.1188
	2.4425	-2.0811	2.0039	2.9438	-.7763			
	4.6707	2.8655	-.8492	1.9249	3.1372			
	50.2413	.5830	77.3402	3.4314	-5.5803	3.7709		
	19.3830	.2579	3.4314	73.8946	6.2692	-11.8611		
	-3.8507	-.1220	-5.5803	6.2692	78.2179	8.4488		
	.0753	-.0140	3.7709	-11.8611	8.4488	79.6495		
		fluctuation forecast coefficients						
74320								
	6.0000	5.7151	5.7151	3.7813	9.4964	-1.6720	1.2816	-1.3047
	.2849	2.4425	-2.3811	2.0939	2.9438			
	5.3795	4.6707	2.8655	-.8492	1.9249			
	43.3320	.6308	94.1680	16.5942	-9.1870	12.5184		
	18.9503	.2453	16.5942	77.3402	3.4314	-5.5803		
	-8.5219	-.0909	-9.1870	3.4314	73.8946	6.2692		
	1.4609	.0286	12.5184	-5.5803	6.2692	78.2179		
74340								
	13.3300	5.7334	5.7334	3.1566	8.8900	1.3840	1.5030	.9208
	7.5960	.2849	2.4425	-2.3811	2.0939			
	1.3626	5.3795	4.6707	2.8655	-.8492			
	86.0807	.4891	117.0338	40.6501	6.8206	7.1425		
	53.2096	.1394	40.6501	94.1680	16.5942	-9.1870		
	13.7959	-.0572	6.8206	16.5942	77.3402	3.4314		
	-5.0846	-.0451	7.1425	-9.1870	3.4314	73.8946		
74400								
	8.6700	6.2234	6.2234	2.3331	8.5564	.7488	1.7967	.4167
	2.4466	7.5966	.2849	2.4425	-2.3811			
	1.2747	1.3626	5.3795	4.6707	2.8655			
	83.8627	.6460	111.3425	45.3584	12.7449	10.5863		
	62.9397	.2641	45.3584	117.0338	40.6501	6.8206		
	24.3338	.0693	12.7449	40.6501	94.1680	16.5942		
	2.2542	-.1016	10.5863	6.8206	16.5942	77.3402		

Table 70. Upstream-to-Downstream Correlation with Double Exponential Smoothing, Data Set 74042354, Santa Monica Westbound, Station 10 (Upstream), Station 9 (Downstream), Lane 2, Twenty-Second Occupancy

Time	$y(k)$	$s_y^{(1)}(k-1)$	$t_y(k)$	$f(k)$	$\hat{y}(k)$	$e(k)$	$\mu(k-1)$	$\bar{e}(k)$
	$\tilde{y}(k)$	$\tilde{y}(k-1)$	$\tilde{y}(k-2)$	$\tilde{y}(k-3)$	$\tilde{y}(k-4)$			
	$\tilde{x}(k)$	$\tilde{x}(k-1)$	$\tilde{x}(k-2)$	$\tilde{x}(k-3)$	$\tilde{x}(k-4)$			
	$\sigma_{yx}(1\|k)$	$a(1\|k-1)$	$\sigma_{xx}(1,1\|k)$	$\sigma_{xx}(1,2\|k)$	$\sigma_{xx}(1,3\|k)$	$\sigma_{xx}(1,4\|k)$		
	$\sigma_{yx}(2\|k)$	$a(2\|k-1)$	$\sigma_{xx}(2,1\|k)$	$\sigma_{xx}(2,2\|k)$	$\sigma_{xx}(2,3\|k)$	$\sigma_{xx}(2,4\|k)$		
	$\sigma_{yx}(3\|k)$	$a(3\|k-1)$	$\sigma_{xx}(3,1\|k)$	$\sigma_{xx}(3,2\|k)$	$\sigma_{xx}(3,3\|k)$	$\sigma_{xx}(3,4\|k)$		
	$\sigma_{yx}(4\|k)$	$a(4\|k-1)$	$\sigma_{xx}(4,1\|k)$	$\sigma_{xx}(4,2\|k)$	$\sigma_{xx}(4,3\|k)$	$\sigma_{xx}(4,4\|k)$		
74300								
	8.0000	5.5575	5.8381	.9285	6.7667	.0430	1.3144	.0365
	2.1619	-2.8452	1.7422	2.7708	-1.0147			
	4.2151	2.5761	-1.2172	1.6643	3.0749			
	50.5334	.5796	79.2319	1.4824	-8.7433	2.0630		
	13.7053	.2545	1.4824	77.6003	4.9363	-13.9290		
	-12.0222	-.1247	-8.7433	4.9363	81.3664	7.4420		
	-.7716	-.0153	2.0630	-13.9290	7.4420	84.0148		
74320								
	6.0000	5.7151	6.1351	3.3975	9.5326	-1.7423	1.3063	-1.3337
	-.1351	2.1619	-2.8452	1.7422	2.7708			
	4.6521	4.2151	2.5761	-1.2172	1.6643			
	46.7050	.6219	91.8895	12.2454	-13.3100	8.9453		
	17.1509	.2397	12.2454	79.2319	1.4824	-8.7433		
	-11.0825	-.0977	-13.3100	1.4824	77.6003	4.9363		
	-.9466	.0239	8.9453	-8.7433	4.9363	81.3664		
74340								
	13.3300	5.7334	6.1447	2.7441	8.8888	1.3494	1.5290	.8826
	7.1855	-.1351	2.1619	-2.8452	1.7422			
	.3351	4.6521	4.2151	2.5761	-1.2172			
	77.1192	.4860	107.6050	31.0648	-.4675	2.7060		
	46.3318	.1373	31.0648	91.8895	12.2454	-13.3100		
	8.1422	-.0591	-.4675	12.2454	79.2319	1.4824		
	-9.6313	-.0467	2.7060	-13.3100	1.4824	77.6003		
74400								
	8.6700	6.2234	7.0981	1.4589	8.5570	.7312	1.8202	.4017
	1.5719	7.1253	-.1351	2.1619	-2.8452			
	.2256	.3351	4.6521	4.2151	2.5761			
	72.6723	.6437	100.7776	30.6203	.9752	3.3947		
	50.6565	.2626	30.6203	107.6050	31.0648	-.4675		
	14.2430	.0679	.9752	31.0648	91.8895	12.2454		
	-4.9607	-.1028	3.3947	-.4675	12.2454	79.2319		

Time

Accumulated error

Mean absolute deviation

Feature

fluctuation forecast coefficients

By examining values of the mean absolute deviation, $\mu(k-1)$, the reduction in forecast error provided by the fluctuation forecast can be seen. For example, from Table 67 which pertains to results without the fluctuation forecast, one finds $\mu(k-1)$ at 74300 to be 1.7288; results with the fluctuation forecasts, Table 69, indicate $\mu(k-1)$ at 74300 to be 1.2829. Similar improvements due to the fluctuation forecast can be seen by comparing results in Tables 68 and 70. A comparison of results for single- and double-exponential smoothing, Tables 69 and 70, shows little difference, with those for single-exponential smoothing slightly better.

Another set of results involves downstream-to-upstream correlations, i.e., the fluctuations in downstream data were used to produce a forecast of upstream data. The traffic variables chosen were one-minute occupancies averaged over all lanes. In Table 71 one-minute occupancy data are provided in the form of an occupancy map. Boxes isolate a sequence of large values of occupancy associated with the passage of a compression wave. In the absence of a fluctuation forecast, this wave produces very large forecast errors as can be seen in Table 72. In Table 73, substantial correlation is evident and the forecast error is seen to be substantially reduced.

2.3 COMPUTER REQUIREMENTS

Use of the correlation feature will involve substantially more computational effort than use of features previously identified for use in incident-detection algorithms. To address this issue, a count of the number of multiplications and divisions required for each element of the flow chart (Figure 4) was made and entered in Table 74. The parameter $\Delta n=n_1-n_0+1$ is the number of deviation-from-trend values used in the correlation analysis. In this count, single exponential smoothing was assumed. We note that single exponential smoothing requires seven multiplications.

From this table, it is seen that the growth in required operations is dominated by the term $(\Delta n)^3/3$. A total of 63 are required for each feature when $\Delta n=4$.

The correlation feature requires substantial memory in the form of stored values of several variables. Table 75 identifies storage requirements. It can be seen that growth in the storage requirements is dominated by the term $(\Delta n)^2/2$. When $n_0=1$, $n_1=4$, twenty-five words of memory are required for each feature.

2.4 CANDIDATE ALGORITHMS

Experience with the correlation feature has indicated that

- substantial upstream-to-downstream correlation is consistently present in light traffic but not in moderate-to-heavy traffic,
- substantial downstream-to-upstream correlation is present only when there are compression waves in heavy traffic.

Table 71. One-minute occupancy map, data set 74090454, San Diego southbound.

Direction of Travel →

Time \ Stations	32	31	30	29	28	27	26
710	15	20	20	18	22	26	22
711	13	21	19	18	22	28	26
712	16	19	20	19	21	32	26
713	13	18	16	18	30	25	25
714	14	22	17	18	25	23	24
715	14	20	20	26	44	29	26
716	14	18	18	25	34	26	24
717	13	21	19	36	26	21	25
718	14	24	21	48	29	25	21
719	16	26	32	28	31	26	25
720	21	24	47	19	26	39	23
721	14	26	32	27	26	21	22
722	14	52	32	22	29	19	23
723	14	27	23	20	50	18	24
724	13	26	21	21	30	22	26
725	24	21	22	62	23	26	24
726	39	20	23	38	23	28	23
727	23	21	65	29	22	30	23
728	26	24	43	28	23	23	25
729	31	26	26	29	22	30	23
730	30	60	22	35	22	24	23
731	31	41	21	30	17	26	24
732	37	29	27	26	23	18	26
733	50	26	35	22	37	22	24
734	53	22	31	21	29	26	26
735	48	21	32	21	25	22	23
736	29	28	33	39	21	24	23
737	37	33	28	26	22	30	27
738	38	29	44	21	20	23	24
739	40	25	38	21	21	20	27
740	53	23	43	19	30	23	24
741	37	47	44	22	36	26	23
742	41	30	42	23	38	28	26
743	38	26	38	21	31	22	25
744	56	24	29	33	29	23	22
745	64	25	24	38	27	27	24

Table 72. Single-Exponential Smoothing, Data Set 74090454, San Diego Northbound, Station 30, All Lanes, One-Minute Occupancy.

Time	$y(k)$	$s_y^{(1)}(k-1)$	$t_y(k)$	$e(k)$	$\mu(k-1)$	$\bar{e}(k)$
727	65.6000	22.3221	22.3221	22.5241	4.8959	4.6006
728	43.4400	25.1133	25.1133	20.4254	8.7341	2.3386
729	26.4399	26.2952	26.2952	10.2801	9.8933	1.0605
730	22.5100	26.3039	26.3039	3.2431	8.7375	.3712

Table 73. Downstream-to-Upstream Correlation with Single Exponential Smoothing, Data Set 74090454, San Diego Southbound, Station 30 (Upstream), Station 29 (Downstream), All Lanes, One-Minute Occupancy.

Time	$y(k)$	$s_y^{(1)}(k-1)$	$t_y(k)$	$f(k)$	$\hat{y}(k)$	$e(k)$	$\mu(k-1)$	$\bar{e}(k)$
	$\tilde{y}(k)$	$\tilde{y}(k-1)$	$\tilde{y}(k-2)$	$\tilde{y}(k-3)$	$\tilde{y}(k-4)$			
	$\tilde{x}(k)$	$\tilde{x}(k-1)$	$\tilde{x}(k-2)$	$\tilde{x}(k-3)$	$\tilde{x}(k-4)$			
	$\sigma_{yx}(1\|k)$	$a(1\|k-1)$	$\sigma_{xx}(1,1\|k)$	$\sigma_{xx}(1,2\|k)$	$\sigma_{xx}(1,3\|k)$	$\sigma_{xx}(1,4\|k)$		
	$\sigma_{yx}(2\|k)$	$a(2\|k-1)$	$\sigma_{xx}(2,1\|k)$	$\sigma_{xx}(2,2\|k)$	$\sigma_{xx}(2,3\|k)$	$\sigma_{xx}(2,4\|k)$		
Time	$\sigma_{yx}(3\|k)$	$a(3\|k-1)$	$\sigma_{xx}(3,1\|k)$	$\sigma_{xx}(3,2\|k)$	$\sigma_{xx}(3,3\|k)$	$\sigma_{xx}(3,4\|k)$	Accumulated error	Mean absolute deviation
	$\sigma_{yx}(4\|k)$	$a(4\|k-1)$	$\sigma_{xx}(4,1\|k)$	$\sigma_{xx}(4,2\|k)$	$\sigma_{xx}(4,3\|k)$	$\sigma_{xx}(4,4\|k)$		Feature
727								
	65.6000	22.3221	22.3221	23.8539	46.1760	10.8409	4.2099	2.5751
	43.2779	1.6653	.6790	-.8455	1.1165			
	4.1073	14.3637	40.3671	-.4628	-1.2109			
	1163.0542	.0244	2606.8115	1145.2710	295.9218	365.1981		
	2517.9258	.5917	1145.2710	2565.9854	604.4341	323.4282		
	698.8052	.1784	295.9218	604.4341	1001.0476	666.0732		
	559.5703	.2468	365.1981	323.4282	666.0732	1069.8301		
728			fluctuation forecast coefficients					
	43.4400	25.1133	25.1133	11.0692	36.1825	9.0492	5.7313	1.5789
	12.3267	43.2779	1.6653	.6790	-.8455			
	2.8824	4.1073	14.3637	40.3671	-.4628			
	1162.3188	-.0094	2455.5605	1130.4053	442.6368	339.7445		
	2613.7764	.9663	1130.4053	2606.8115	1145.2710	295.9218		
	1393.5337	-.0655	442.6368	1145.2710	2565.9854	604.4341		
	515.0002	.2749	339.7445	295.9218	604.4341	1001.0476		
729								
	26.4300	26.2952	26.2952	12.6190	38.9142	-1.7175	5.8840	-.2919
	.1343	18.3267	43.2779	1.6653	.6790			
	3.7165	2.8824	4.1073	14.3637	40.3671			
	1088.6816	-.0043	2305.5029	1069.3408	455.4918	434.1877		
	2450.4375	.9524	1069.3408	2455.5605	1130.4053	442.6368		
	1305.5967	.0741	455.4918	1130.4053	2606.8115	1145.2710		
	487.2277	.1897	434.1877	442.6368	1145.2710	2565.9854		
730								
	22.5100	26.3039	26.3039	2.9167	29.2206	-4.2140	6.5440	-.6440
	-3.7939	.1348	18.3267	43.2779	1.6653			
	3.7868	3.7165	2.8824	4.1073	14.3637			
	1004.3991	.0161	2170.6270	1011.0886	441.3807	459.5686		
	2281.4658	.0511	1011.0886	2305.5029	1069.3408	455.4918		
	1805.8125	.0939	441.3807	1069.3408	2455.5605	1130.4053		
	401.3107	-.0188	459.5686	455.4918	1130.4053	2606.8115		

Table 74. Operation Count for Elements of the Correlation Feature Computation.

Element	Number of Multiplications and Divisions: General	$\Delta n = 4$
Compute deviations from trend	0	0
Compute fluctuation forecast	Δn	4
Compute correlation feature; update mean absolute deviation	5	5
Update exponential smoothing of dependent variable	2	2
Update correlation arrays	$4\Delta n$	16
Compute new fluctuation[1] forecast coefficients	$\frac{(\Delta n)^3}{3} + (\Delta n)^2 - \frac{\Delta n}{3}$	36
TOTAL	$\frac{(\Delta n)^3}{3} + (\Delta n)^2 + \frac{14\Delta n}{3} + 7$	63

[1]Using Gaussian elimination; E. Isaacson, and H. B. Keller, Analysis of Numerical Methods, New York, John Wiley and Sons, Inc., 1966, p. 36.

Table 75. Storage Requirements for the Correlation Feature.

Variables	Storage Requirements per Feature	
	General	$n_0 = 1,\ n_1 = 4$
Smoothing variables	1	1
Deviations from trend	$n_1 + 2$	6
Correlation arrays	$\frac{\Delta n(\Delta n+1)}{2} + 1$	11
Fluctuation forecast coefficients	Δn	4
Error feature	3	3
Total	$\frac{\Delta n^2}{2} + \frac{3\Delta n}{2} + 7 + n_1$	25

A single-feature algorithm, based on upstream-to-downstream correlation using individual-lane, twenty-second occupancies, was briefly examined. Results were encouraging but we were unable to devote sufficient attention to this algorithm to draw any final conclusions.

There are presently no existing incident-detection algorithms which are known to be effective in light traffic. Of course, very severe incidents can be detected in light traffic by present algorithms, but present algorithms are most suitable for the moderate-to-heavy traffic regime. In view of this gap in coverage by incident-detection algorithms and the evidence of consistent correlation in light traffic, we regard algorithms based upon the traffic correlation feature as worthy of further attention.

In the earlier stages of our development of incident detection algorithms, as discussed in Section 5, compression waves produced a large fraction of the false alarms. A feature based upon downstream-to-upstream correlation was examined as a tool for substantially reducing such false alarms. However, we found that compression waves are not sufficiently regular for this feature to achieve this goal. As another technique (described in Section 5 and embodied in Algorithms 8 and 9) did prove to be successful, this approach was abandoned.

Appendix B

ALGORITHM DEFINITIONS, CALIBRATION AND EVALUATION RESULTS

Table of Contents

Page

Algorithm number 1

Decision tree, Figure 59 207
Coding, Table 76 208
Calibration and evaluation on Los Angeles data base, Table 77 . . . 209
Distribution of times-to-detect, Figure 60 210

Algorithm number 2

Decision tree, Figure 61 211
Coding, Table 78 212
Evaluation of Algorithm 1, Los Angeles thresholds, Table 79 213
Calibration and evaluation on Los Angeles data base, Table 80 . . . 214
Distribution of times-to-detect, Figure 62 215
Evaluation of Los Angeles thresholds, Table 81 216
Calibration and evaluation on Minneapolis data base, Table 82 . . . 217
Distribution of times-to-detect, Figure 63 220
Evaluation of Minneapolis thresholds, Table 83 221

Algorithm number 3

Decision tree, Figure 64 222
Coding, Table 84 223
California and evaluation on Los Angeles data base, Table 85 . . . 224
Distribution of times-to-detect, Figure 65 225

Algorithm number 4

Decision tree, Figure 66 226
Coding, Table 86 227
Calibration and evaluation on Los Angeles data base, Table 87 . . . 228
Distribution of times-to-detect, Figure 67 229
Calibration and evaluation on geometrically adjusted Los Angeles data base, Table 88 230
Distribution of times-to-detect, Figure 68 231

Algorithm number 5

Decision tree, Figure 69 232
Coding, Table 89 233
Calibration and evaluation on Los Angeles data base, Table 90 . . . 234
Distribution of times-to-detect, Figure 70 235

Algorithm number 6

Decision tree, Figure 71 236
Coding, Table 91 237
Calibration and evaluation on Los Angeles data base, Table 92 . . . 238
Distribution of times-to-detect, Figure 72 239

Table of Contents (continued)

Algorithm number 7

	Page
Decision tree, Figure 73	240
Coding, Table 93	241
Decision tree for twenty-second update version, Figure 74	242
Coding for twenty-second update version, Table 94	243
Calibration and evaluation on Los Angeles data base, Table 95	244
Distribution of times-to-detect, Figure 75	245
Evaluation of Los Angeles thresholds, Table 96	246
Calibration and evaluation on geometrically adjusted Los Angeles data base, Table 97	249
Distribution of times-to-detect, Figure 76	250
Calibration and evaluation on Los Angeles, sensor configuration A data base, Table 98	251
Distribution of times-to-detect, Figure 77	252
Calibration and evaluation on Los Angeles, sensor configuration B data base, Table 99	253
Distribution of times-to-detect, Figure 78	254
Calibration and evaluation on Los Angeles, sensor configuration C data base, Table 100	255
Distribution of times-to-detect, Figure 79	256
Calibration and evaluation on Minneapolis data base, Table 101	257
Distribution of times-to-detect, Figure 80	258
Evaluation of Minneapolis thresholds, Table 102	259
Calibration and evaluation on Minneapolis clear weather data base, Table 103	260
Distribution of times-to-detect, Figure 81	261
Calibration and evaluation on Minneapolis snowy weather data base, Table 104	262
Distribution of times-to-detect, Figure 82	263

Algorithm number 8

Decision tree, Figure 83	264
Coding, Table 105	265
Decision tree for an equivalent form, Figure 84	267
Coding for an equivalent form, Table 106	268
Calibration and evaluation on Los Angeles data base, Table 107	269
Distribution of times-to-detect, Figure 85	270
Evaluation of Los Angeles thresholds, Table 108	271
Calibration and evaluation on Los Angeles data base (T_2= -.300), Table 109	274
Distribution of times-to-detect, Figure 86	275
Calibration and evaluation on geometrically adjusted Los Angeles data base, Table 110	276

Table of Contents (continued)

Algorithm number 8 (cont.) Page

Distribution of times-to-detect, Figure 87 277
Calibration and evaluation on Minneapolis data base, Table 111 278

Distribution of times-to-detect, Figure 88 279
Evaluation of Minneapolis thresholds, Table 112 280

Algorithm number 9

Decision tree, Figure 89 281
Coding, Table 113 282
Calibration and evaluation on Los Angeles data base, Table 114 284
Distribution of times-to-detect, Figure 90 285
Calibration and evaluation on geometrically adjusted Los Angeles data base, Table 115 286
Distribution of times-to-detect, Figure 91 287

Algorithm number 10

Decision tree, Figure 92 288
Coding, Table 116 289
Calibration and evaluation on Los Angeles data base, Table 117 290
Distribution of times-to-detect, Figure 93 291

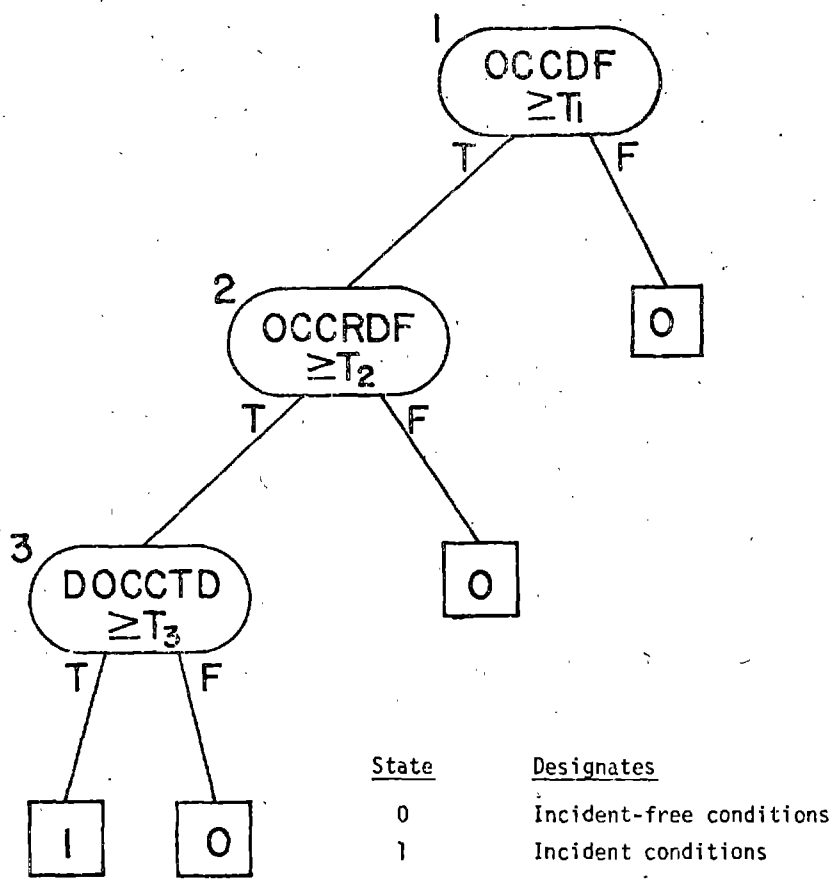

Figure 59. Decision tree for Algorithm 1.

Table 76. Coding for Algorithm 1.

Feature No.	Name
1	OCCDF
2	OCCRDF
3	DOCCTD

Decision Node	NTR	Threshold Vector
1	1,2,0	T_1
2	2,3,0	T_2
3	3,-1,0	T_3

Table 77. Calibration and evaluation of Algorithm 1 on Los Angeles data base.

$N_I = 49$ $\overline{N}_I = 41$

$N_F = 108{,}108$ $\overline{N}_F = 5002$

Threshold set	Detection rate (%)	False alarm rate (%)	Mean-time-to-detect (minutes)	Thresholds T_1	T_2	T_3
1	82	1.731	.85	5.3	.308	.061
2	71	1.140	1.99	5.8	.340	.112
3	61	.368	3.33	7.7	.498	.049
4	51	.244	5.09	5.0	.563	.013
5	41	.074	5.18	9.6	.617	.075
6	31	.015	6.00	15.3	.637	.245
7	20	.004	7.77	13.0	.710	.192

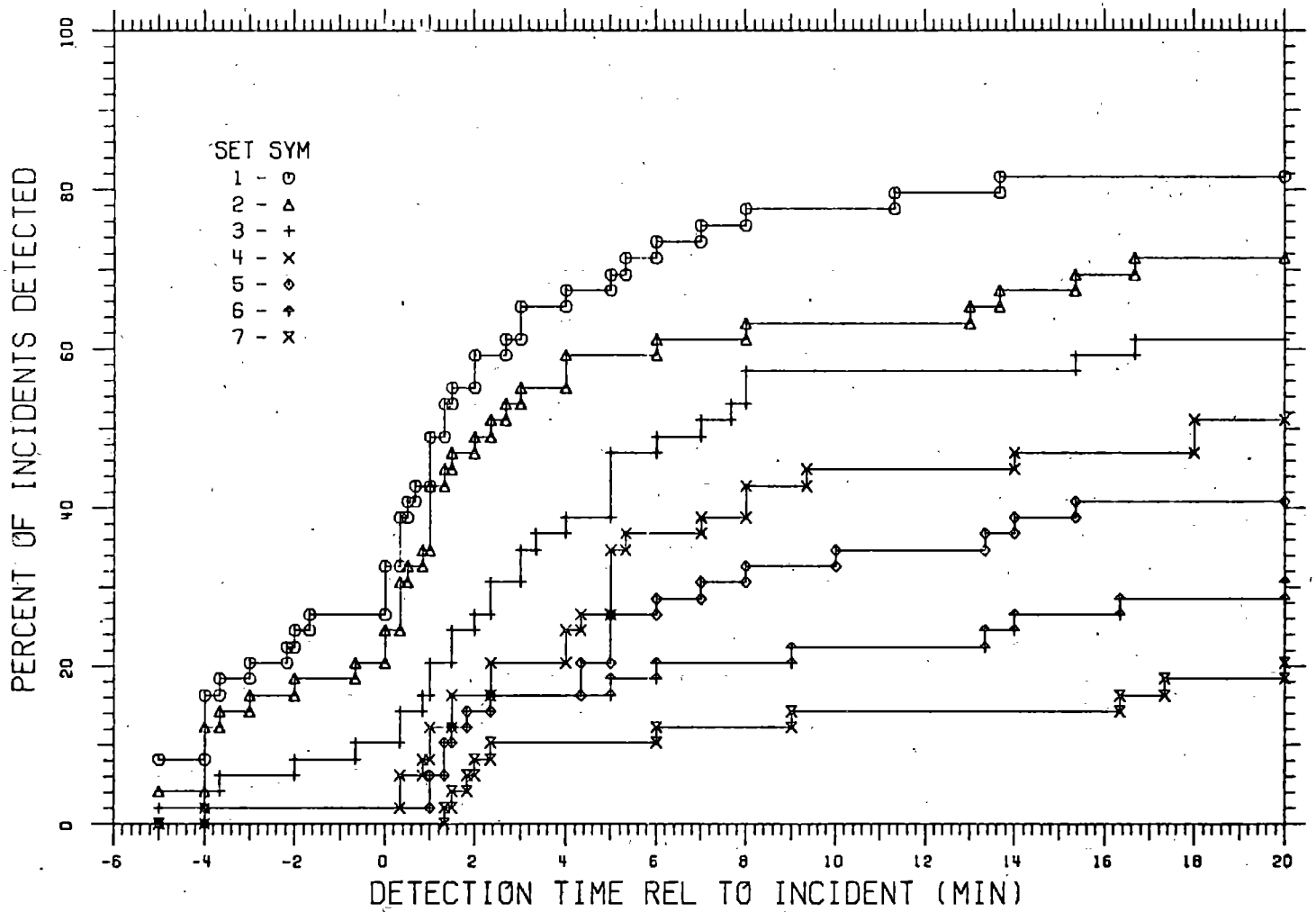

Figure 60. Distribution of times-to-detect for Algorithm 1, Los Angeles data base.

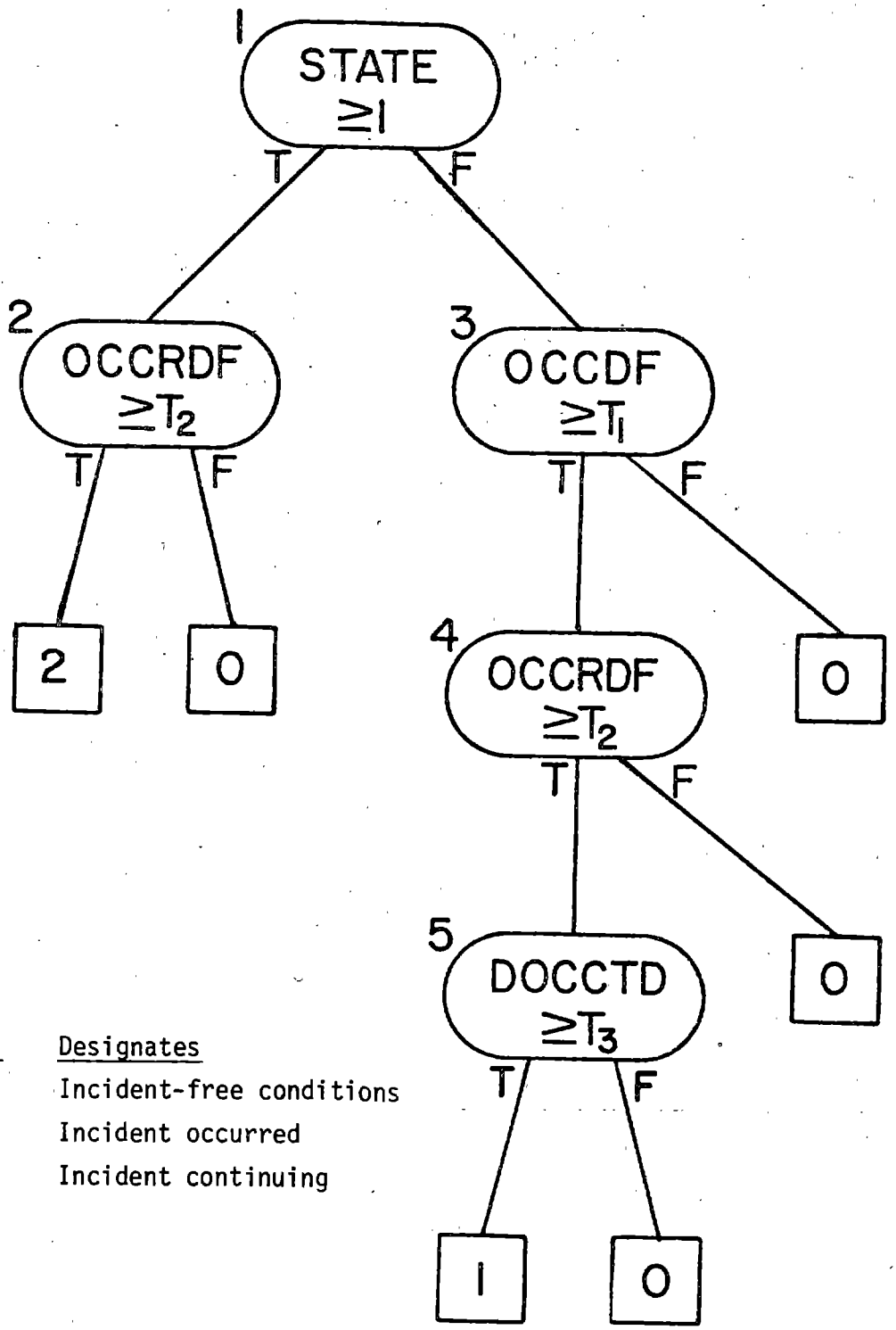

State	Designates
0	Incident-free conditions
1	Incident occurred
2	Incident continuing

Figure 61. Decision tree for Algorithm 2.

Table 78. Coding for Algorithm 2.

Feature No.	Name
1	OCCDF
2	OCCRDF
3	DOCCTD
4	State

Decision Node	NTR	Threshold Vector
1	4,2,3	1
2	2,-2,0	T_2
3	1,4,0	T_1
4	2,5,0	T_2
5	3,-1,0	T_3

Table 79. Evaluation of Algorithm 2 for thresholds determined for Algorithm 1 from Los Angeles data base (see Table 77).

Evaluation on Los Angeles data base, $N_I = 49$, $N_F = 104{,}217$

Threshold set	Detection rate (%)	False alarm rate (%)	Mean-time-to-detect (minutes)
1	82	1.294	.85
2	71	.901	1.99
3	61	.309	3.33
4	51	.222	5.09
5	41	.070	5.18
6	31	.015	6.00
7	20	.004	7.77

Table 80. Calibration and evaluation of Algorithm 2 on Los Angeles data base.

$N_I = 49$ $\overline{N}_I = 40$

$N_F = 104,217$ $\overline{N}_F = 3,495$

Threshold set	Detection rate (%)	False alarm rate (%)	Mean-time-to-detect (Minutes)	Thresholds T_1	T_2	T_3
1	82	1.341	.77	5.4	.325	.011
2	71	.883	.01	6.8	.307	.056
3	61	.346	3.34	15.0	.335	-.050
4	51	.169	4.87	9.9	.552	-1.112
5	41	.064	5.28	9.5	.629	-1.746
6	31	.026	4.64	21.3	.646	-2.080
7	20	.011	8.72	29.9	.685	-1.959

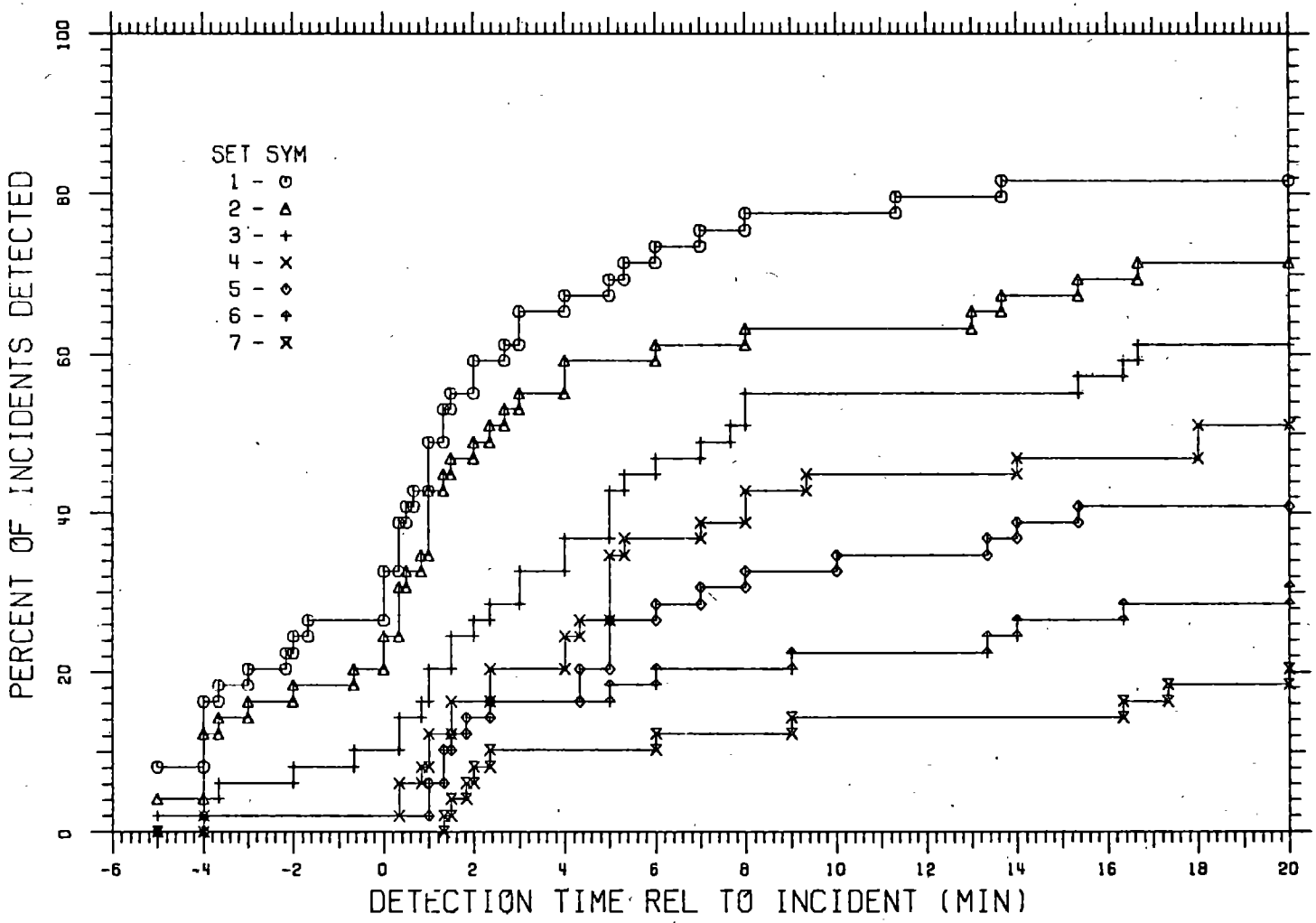

Figure 62. Distribution of times-to-detect for Algorithm 2, Los Angeles data base.

Table 81. Evaluation of Algorithm 2 for thresholds determined from Los Angeles data base (see Table 79).

Threshold set	Evaluation on full Los Angeles data base, N_I=111, N_F=104,217			Evaluation on Los Angeles, sensor configuration A data base, N_I= 35, N_F= 13,357		
	Detection rate (%)	False alarm rate (%)	Mean-time-to-detect (minutes)	Detection rate (%)	False alarm rate (%)	Mean-time-to-detect (minutes)
1	83	1.294	-.21	74	2.351	.60
2	77	.901	.35	66	1.834	1.78
3	69	.309	2.09	57	.906	2.77
4	63	.222	3.83	40	.524	3.10
5	50	.070	4.24	31	.187	3.88
6	37	.015	5.00	17	.008	5.89
7	27	.004	6.02	17	.008	7.06

Table 81. Evaluation of Algorithm 2 for thresholds determined from Los Angeles data base (see Table 79). (Continued)

Threshold set	Evaluation on Los Angeles, sensor configuration B data base, $N_I = 35$, $N_F = 8{,}267$			Evaluation on Los Angeles, sensor configuration C data base, $N_I = 35$, $N_F = 6{,}576$		
	Detection rate (%)	False alarm rate (%)	Mean-time-to-detect (minutes)	Detection rate (%)	False alarm rate (%)	Mean-time-to-detect (minutes)
1	86	3.605	1.00	71	3.285	.97
2	71	2.806	2.19	71	2.494	2.77
3	51	1.222	2.70	51	.958	3.24
4	46	.665	3.33	43	.700	3.29
5	37	.302	5.26	29	.289	3.77
6	23	.133	4.21	11	.076	3.75
7	20	.024	4.57	14	.046	3.33

Table 81. Evaluation of Algorithm 2 for thresholds determined from Los Angeles data base (see Table 79). (Concluded)

Evaluation on Minneapolis data base, $N_I = 36$, $N_F = 46{,}247$

Threshold set	Detection rate (%)	False alarm rate (%)	Mean-time-to-detect (minutes)
1	92	1.870	-.18
2	92	1.291	.58
3	72	.374	1.64
4	72	.383	1.10
5	64	.091	1.83
6	50	.024	1.81
7	44	.024	3.06

Table 82. Calibration and evaluation of Algorithm 2 on Minneapolis data base.

$N_I = 36$ $\overline{N}_I = 33$

$N_F = 46{,}247$ $\overline{N}_F = 2{,}429$

Threshold set	Detection rate (%)	False alarm rate (%)	Mean-time-to-detect (minutes)	Thresholds T_1	T_2	T_3
1	92	.785	.94	6.8	.337	.141
2	81	.413	.78	8.6	.353	.141
3	72	.151	1.94	7.1	.606	-.040
4	61	.020	2.68	22.7	.697	-.062
5	50	.011	3.42	29.7	.678	.173
6	42	.004	1.80	25.0	.676	.306
7	36	.004	1.46	28.8	.672	.354
8	25	.003	.94	28.1	.314	.550

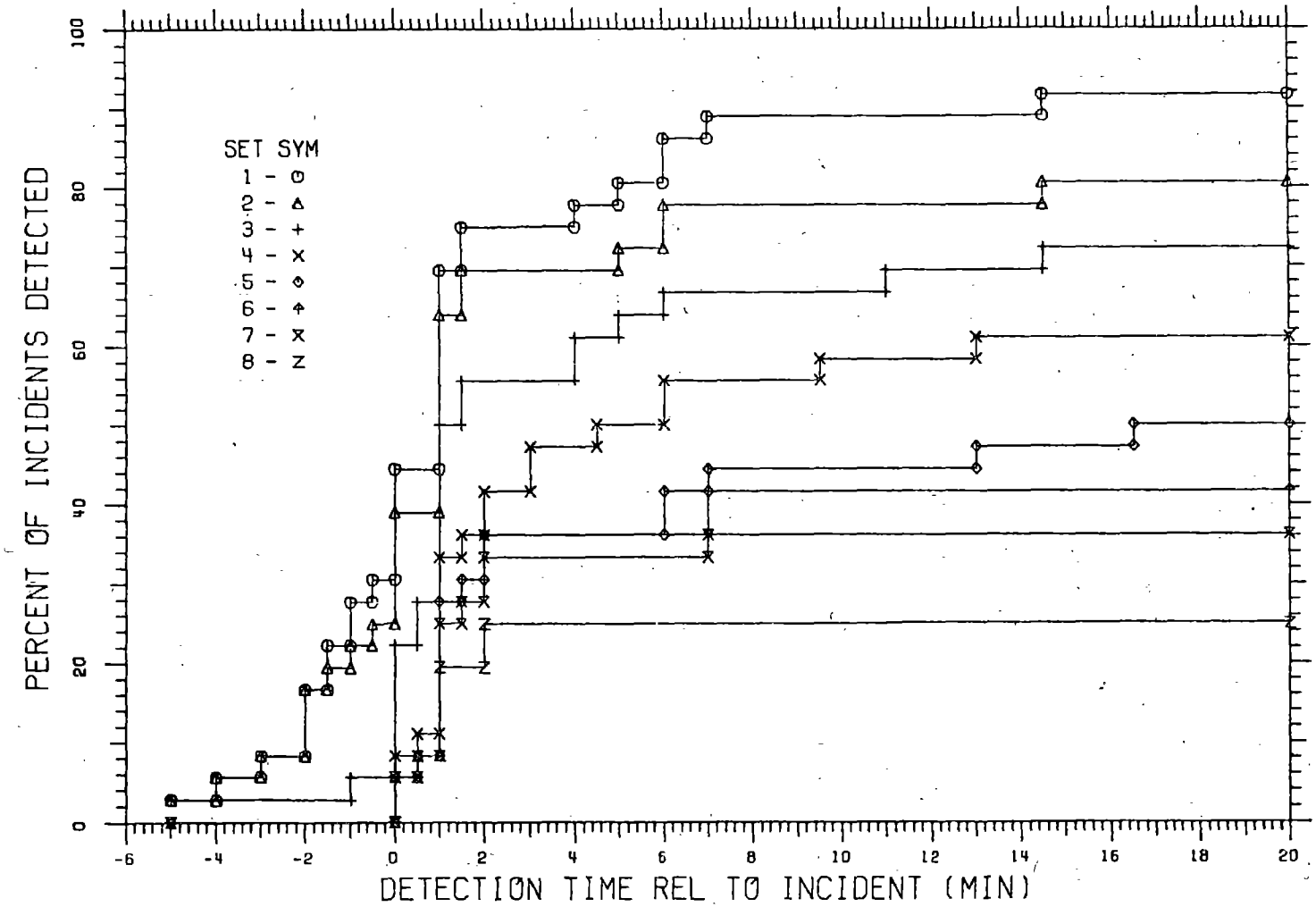

Figure 63. Distribution of times-to-detect for Algorithm 2, Minneapolis data base.

Table 83. Evaluation of Algorithm 2 for thresholds determined from Minneapolis data base (see Table 82).

	Evaluation on Minneapolis clear weather data base, $N_I = 26$, $N_F = 27{,}778$			Evaluation on Minneapolis snowy weather data base, $N_I = 10$, $N_F = 18{,}469$		
Threshold set	Detection rate (%)	False alarm rate (%)	Mean-time to-detect (minutes)	Detection rate (%)	False alarm rate (%)	Mean-time to-detect (minutes)
1	96	.642	1.00	80	.992	.75
2	85	.326	.98	70	.550	.29
3	85	.136	2.23	40	.180	.38
4	69	.029	2.31	40	.005	4.13
5	54	.014	3.21	40	.005	4.13
6	46	.007	2.04	30	0	1.17
7	38	.007	1.55	30	0	1.17
8	31	.004	.94	10	0	1.00

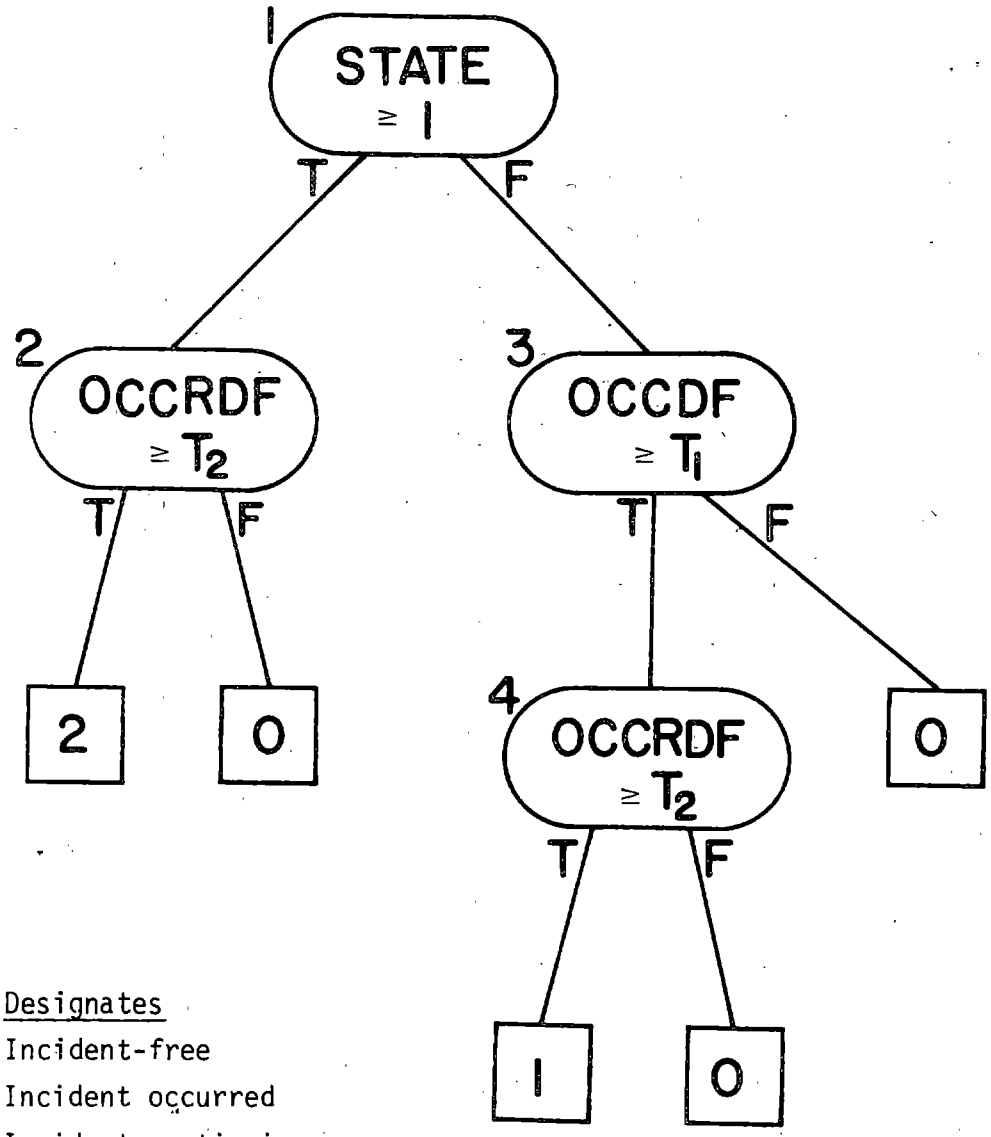

State	Designates
0	Incident-free
1	Incident occurred
2	Incident continuing

Figure 64. Decision tree for Algorithm 3.

Table 84. Coding for Algorithm 3.

Feature No.	Name
1	OCCDF
2	OCCRDF
3	State

Decision Node	NTR	Threshold Vector
1	3,2,3	1
2	2,-2,0	T_2
3	1,4,0	T_1
4	2,-1,0	T_2

Table 85. Calibration and evaluation of Algorithm 3 on Los Angeles data base.

$N_I = 49$ $\overline{N}_I = 40$

$N_F = 104{,}217$ $\overline{N}_F = 3{,}495$

Threshold set	Detection rate (%)	False alarm rate (%)	Mean-time-to-detect (minutes)	Thresholds T_1	T_2
1	82	1.693	.24	5.4	.309
2	71	.945	.88	6.8	.374
3	61	.367	2.73	15.0	.343
4	51	.170	4.87	9.9	.552
5	47	.131	5.23	12.5	.563
6	41	.114	4.17	19.6	.550
7	37	.044	4.70	14.4	.628
8	31	.028	5.11	18.9	.647
9	21	.011	8.82	29.9	.692

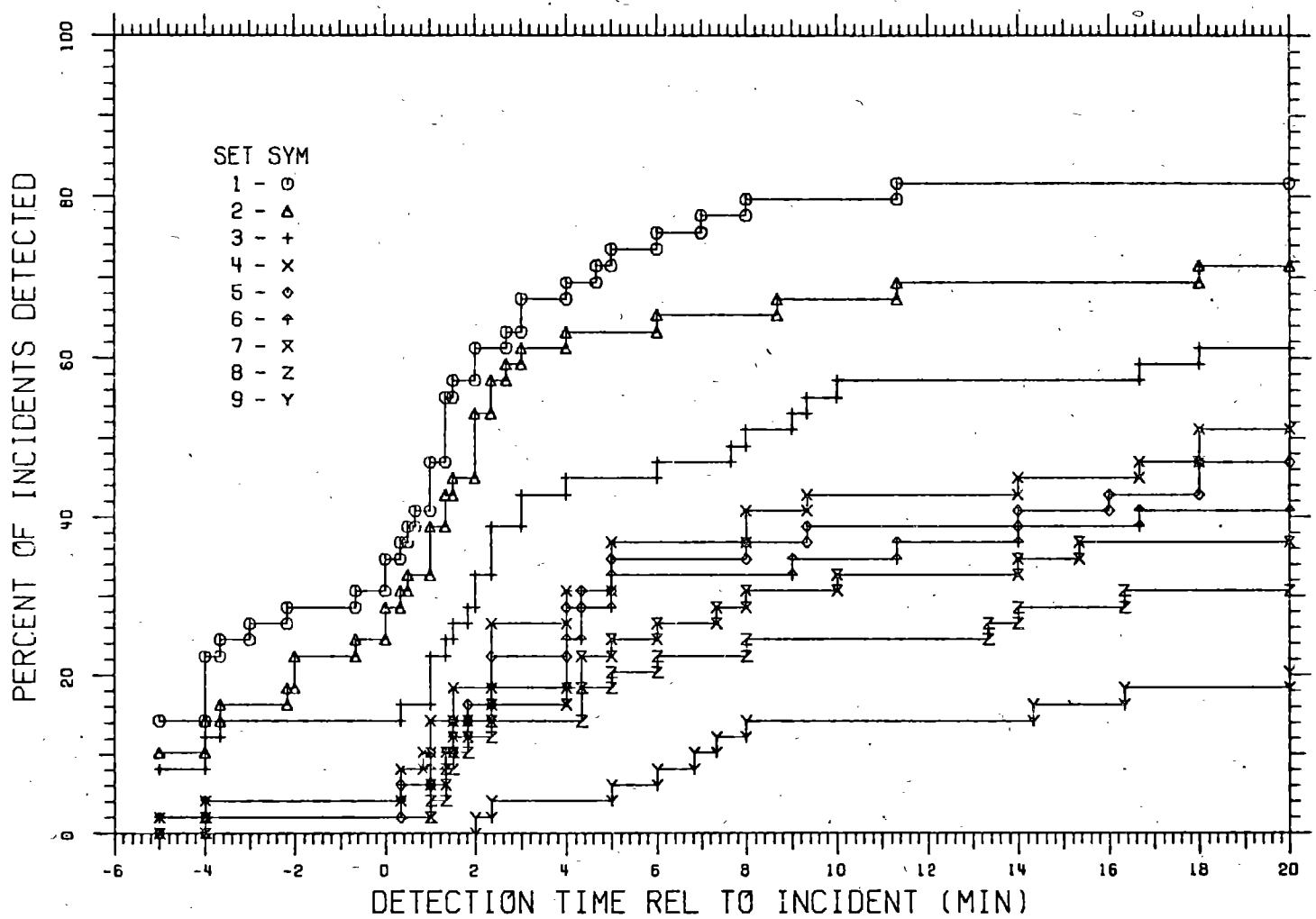

Figure 65. Distribution of times-to-detect for Algorithm 3, Los Angeles data base.

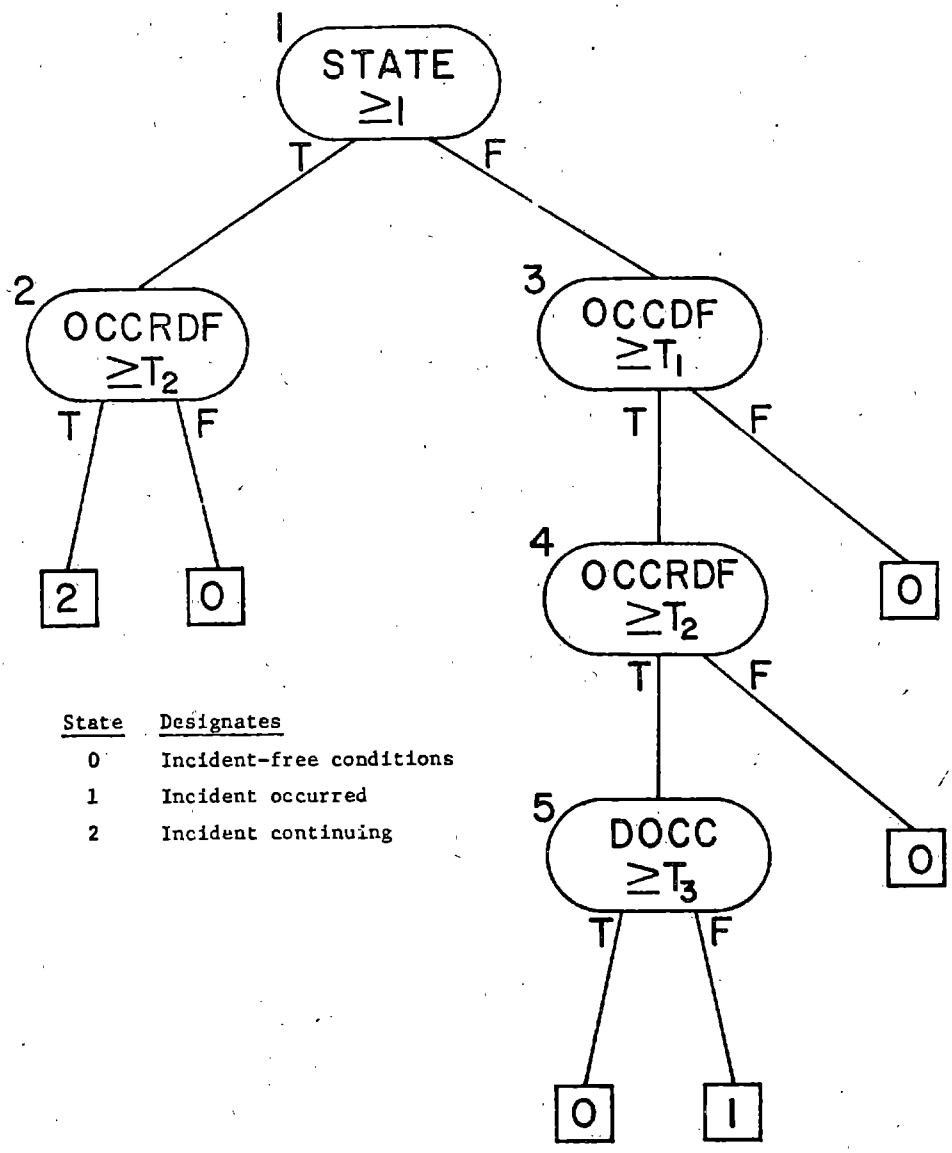

State	Designates
0	Incident-free conditions
1	Incident occurred
2	Incident continuing

Figure 66. Decision tree for Algorithm 4.

Table 86. Coding for Algorithm 4.

Feature No.	Name
1	OCCDF
2	OCCRDF
3	DOCC
4	State

Decision Node	NTR	Threshold Vector
1	4,2,3	1
2	2,-2,0	T_2
3	1,4,0	T_1
4	2,5,0	T_2
5	3,0,-1	T_3

Table 87. Calibration and evaluation of Algorithm 4 on Los Angeles data base.

$N_I = 49$ $\overline{N}_I = 40$

$N_F = 104{,}217$ $\overline{N}_F = 3{,}495$

Threshold set	Detection rate (%)	False alarm rate (%)	Mean-time-to-detect (minutes)	Thresholds T_1	T_2	T_3
1	82	1.577	.64	5.4	.324	26.9
2	71	1.035	.08	6.8	.327	27.0
3	61	.247	2.73	10.9	.501	27.7
4	51	.074	3.43	14.1	.428	16.6
5	41	.035	4.40	16.9	.314	16.2
6	37	.014	5.20	19.6	.394	14.1
7	31	.010	4.64	21.6	.322	14.3
8	29	.009	5.19	22.7	.346	14.0
9	20	.005	8.03	25.8	.332	11.8

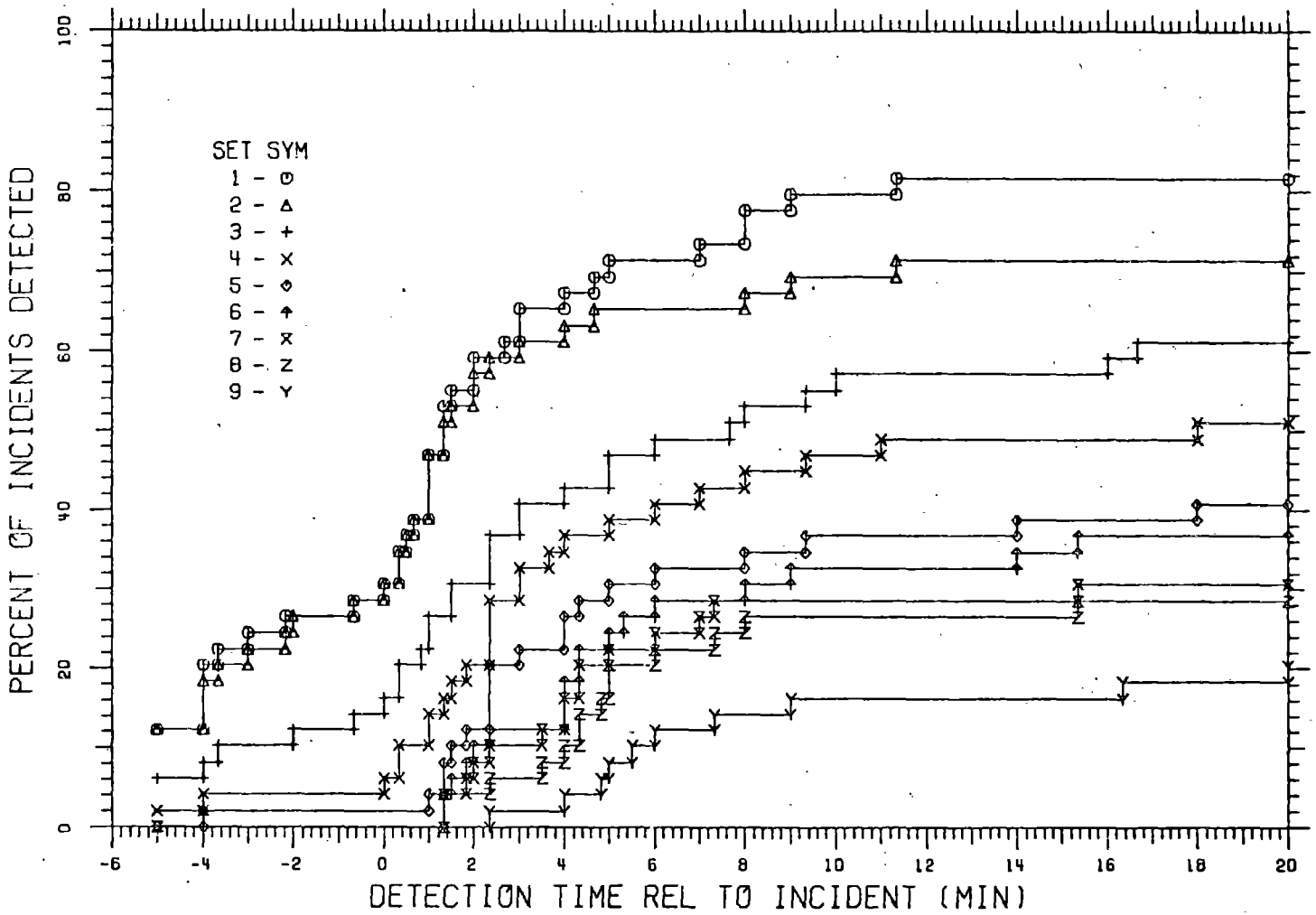

Figure 67. Distribution of times-to-detect for Algorithm 4, Los Angeles data base.

Table 88. Calibration and evaluation of Algorithm 4 on geometrically adjusted Los Angeles data base.

$N_I = 49$ $\overline{N}_I = 40$

$N_F = 108{,}384$ $\overline{N}_F = 2{,}436$

Threshold set	Detection rate (%)	False alarm rate (%)	Mean-time-to-detect (minutes)	Thresholds T_1	T_2	T_3
1	71	.958	1.39	5.8	.325	26.7
2	61	.318	1.86	9.4	.439	26.4
3	51	.068	4.09	13.0	.345	16.5
4	41	.046	5.02	18.8	.488	18.6
5	37	.020	5.98	9.2	.649	16.3
6	31	.019	5.87	8.8	.672	24.4
7	27	.012	5.31	16.4	.656	14.2
8	22	.007	6.52	11.2	.702	12.1

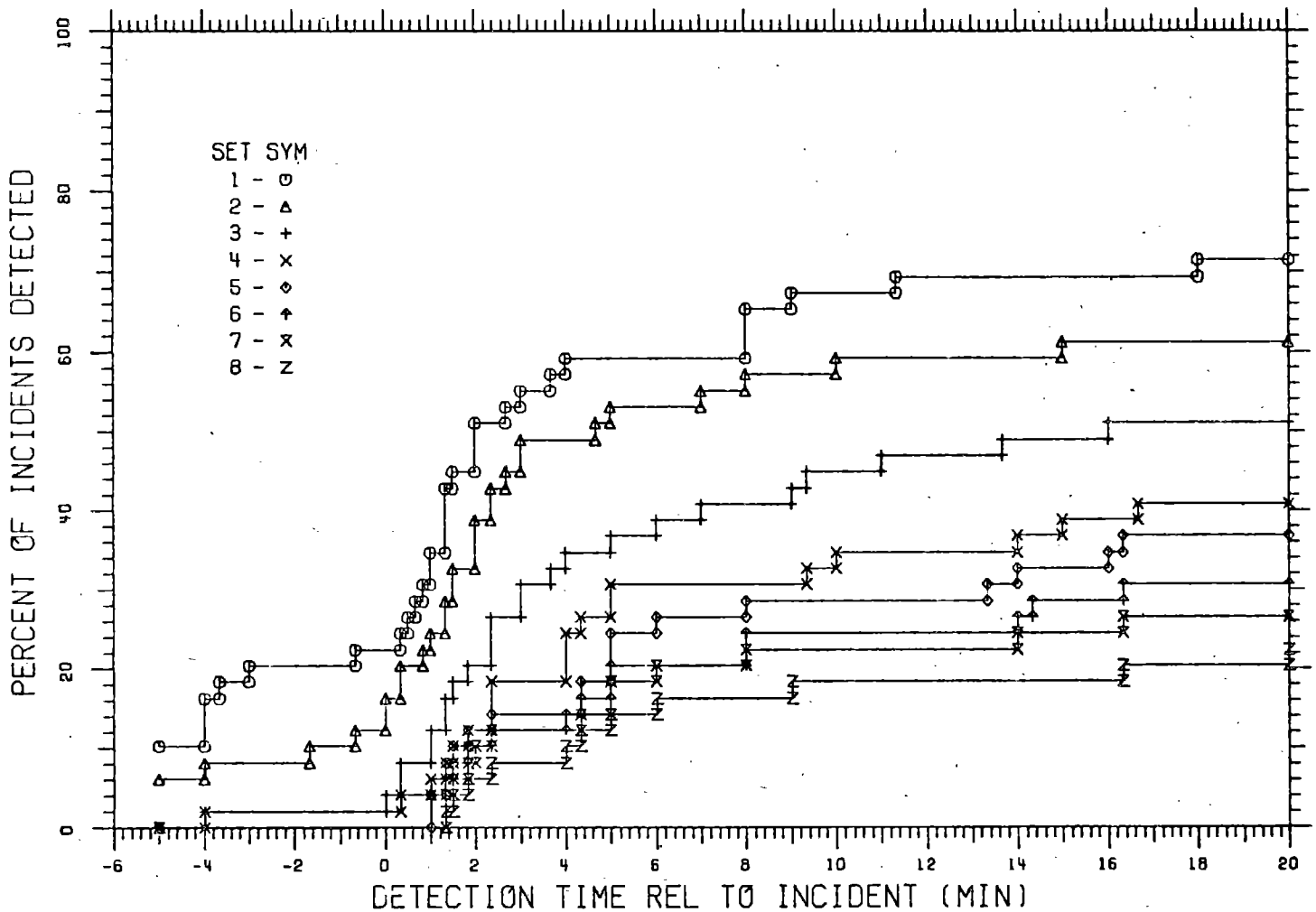

Figure 68. Distribution of times-to-detect for Algorithm 4, geometrically adjusted Los Angeles data base.

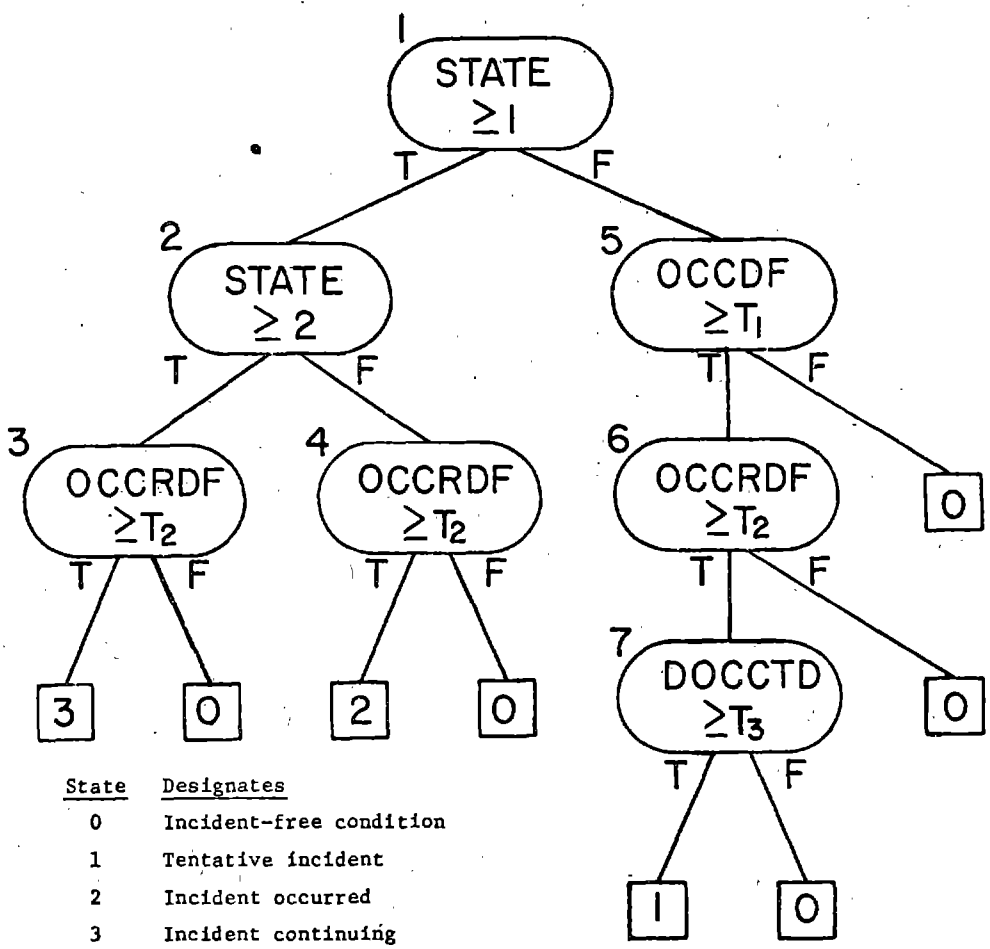

State	Designates
0	Incident-free condition
1	Tentative incident
2	Incident occurred
3	Incident continuing

Figure 69. Decision tree for Algorithm 5.

Table 89. Coding for Algorithm 5.

Feature No.	Name
1	OCCDF
2	OCCRDF
3	DOCCTD
4	State

Decision Node	NTR	Threshold Vector
1	4,2,5	1
2	4,3,4	2
3	2,-3,0	T_2
4	2,-2,0	T_2
5	1,6,0	T_1
6	2,7,0	T_2
7	3,-1,0	T_3

Table 90. Calibration and evaluation of Algorithm 5 on Los Angeles data base.

$N_I = 49$ $\overline{N}_I = 41$

$N_F = 125{,}000$ $\overline{N}_F = 6{,}568$

Threshold set	Detection rate (%)	False alarm rate (%)	Mean-time-to-detect (minutes)	Thresholds T_1	T_2	T_3
1	69	.498	3.07	3.4	.320	.011
2	61	.204	4.24	6.7	.350	.108
3	51	.108	5.04	4.8	.372	.281
4	41	.064	4.95	9.4	.419	.279
5	31	.018	6.00	7.4	.519	.279
6	20	.002	7.43	15.7	.609	.286

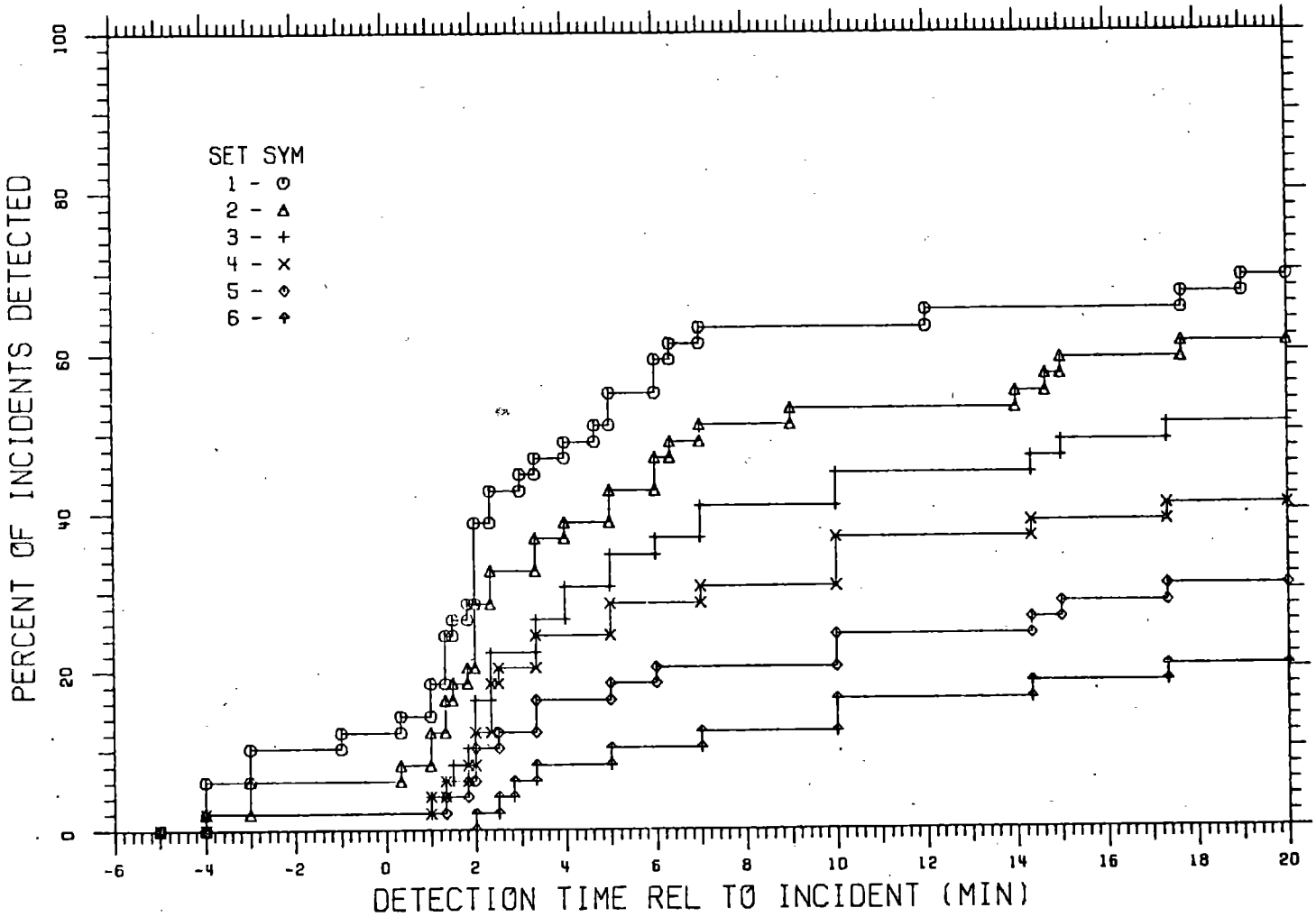

Figure 70. Distribution of times-to-detect for Algorithm 5, Los Angeles data base.

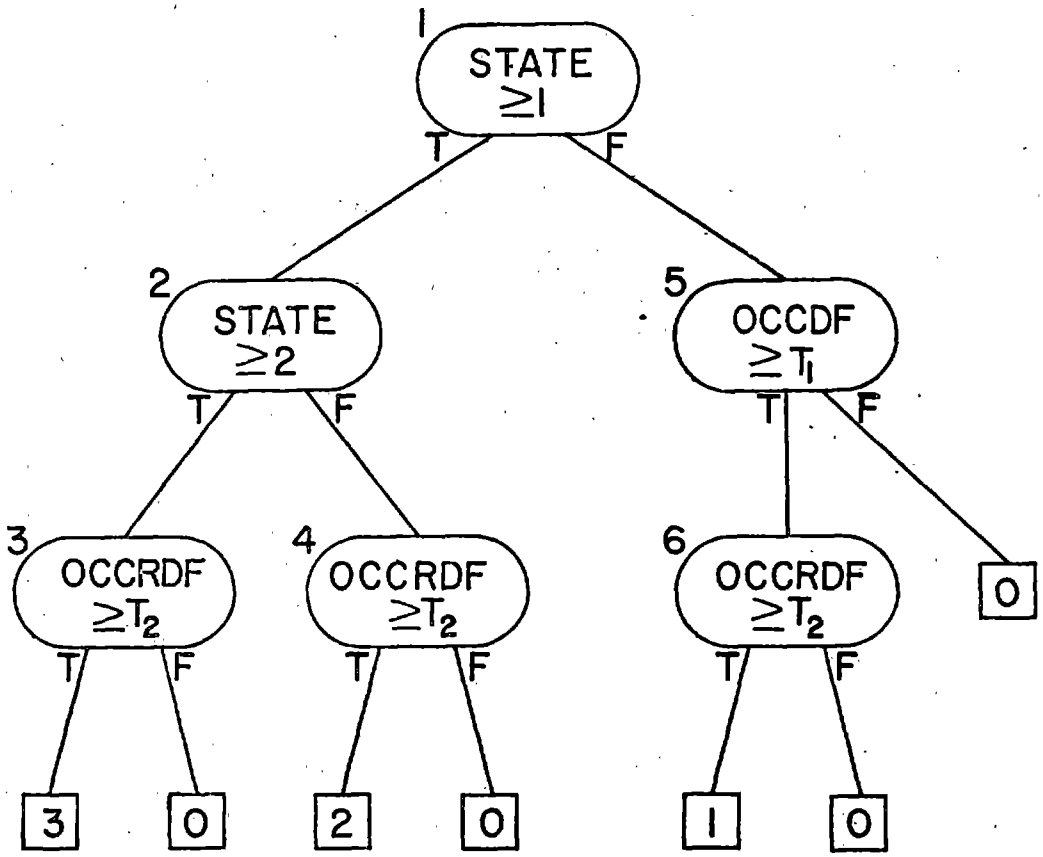

State	Designates
0	Incident-free conditions
1	Tentative incident
2	Incident occurred
3	Incident continuing

Figure 71. Decision tree for Algorithm 6.

Table 91. Coding for Algorithm 6.

Feature No.	Name
1	OCCDF
2	OCCRDF
3	State

Decision Node	NTR	Threshold Vector
1	3,2,5	1
2	3,3,4	2
3	2,-3,0	T_2
4	2,-2,0	T_2
5	1,6,0	T_1
6	2,-1,0	T_2

Table 92. Calibration and evaluation of Algorithm 6 on Los Angeles data base.

$N_I = 49$ $\overline{N}_I = 41$

$N_F = 125{,}000$ $\overline{N}_F = 6{,}568$

Threshold set	Detection rate (%)	False alarm rate (%)	Mean-time-to-detect (minutes)	Thresholds T_1	T_2
1	61	.158	3.84	9.6	.389
2	51	.090	5.53	15.2	.419
3	47	.078	5.46	13.1	.462
4	41	.051	4.53	10.2	.510
5	37	.035	4.70	7.1	.540
6	31	.011	4.73	5.9	.591
7	20	.004	6.93	16.8	.673

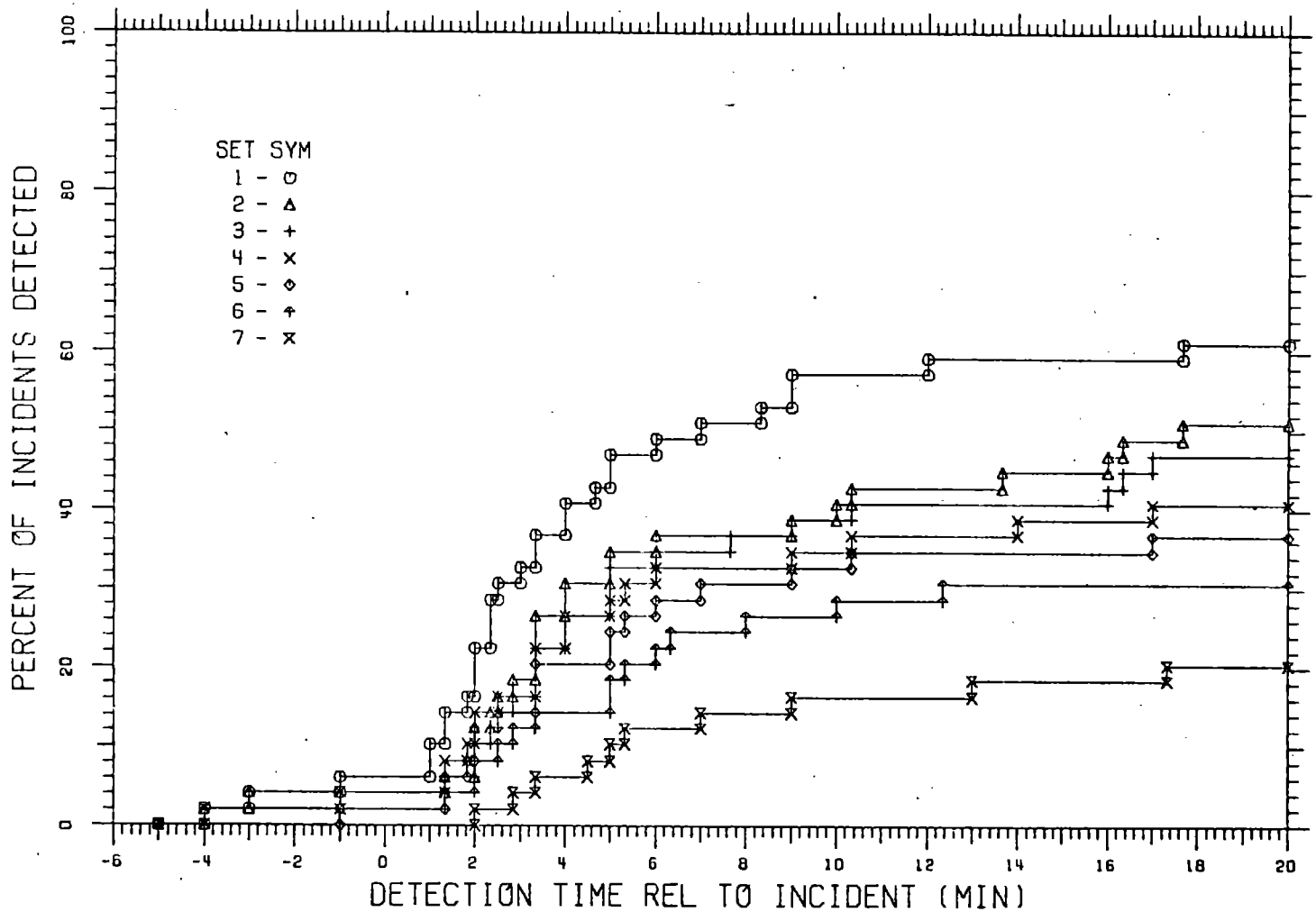

Figure 72. Distribution of times-to-detect for Algorithm 6, Los Angeles data base.

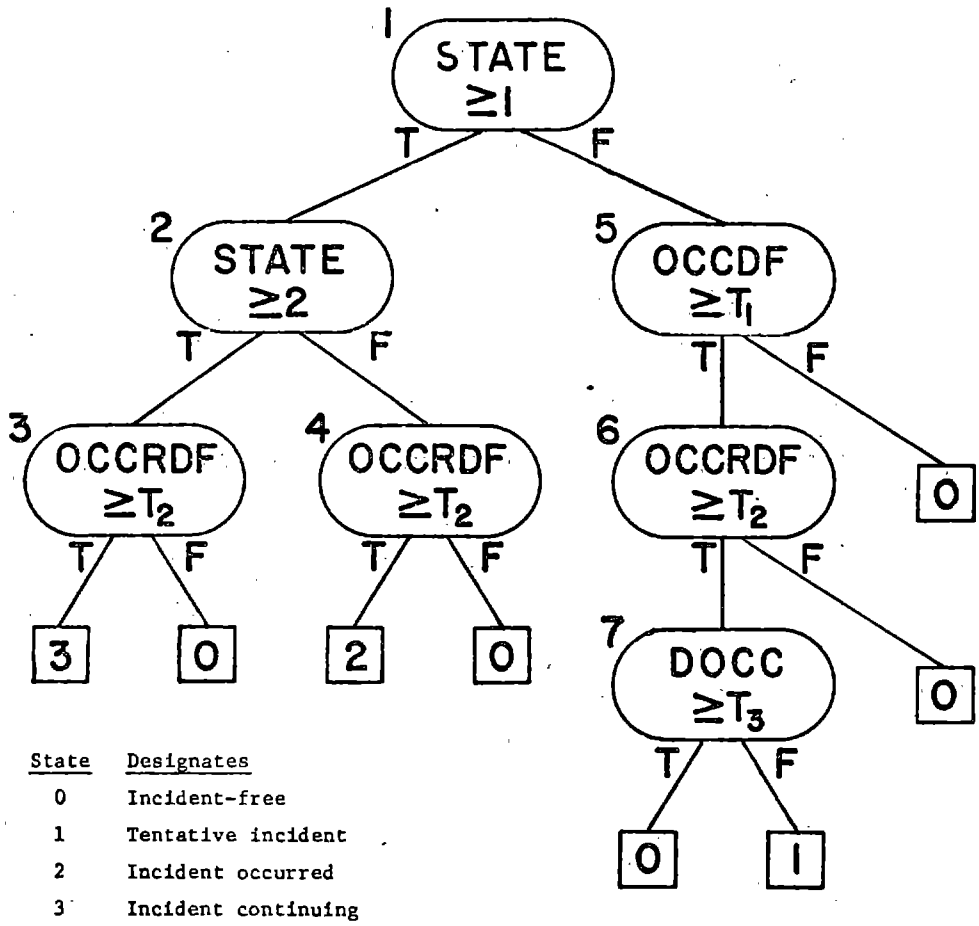

State	Designates
0	Incident-free
1	Tentative incident
2	Incident occurred
3	Incident continuing

Figure 73. Decision tree for Algorithm 7.

Table 93. Coding for Algorithm 7.

Feature No.	Name
1	OCCDF
2	OCCRDF
3	DOCC
4	State

Decision Node	NTR	Threshold Vector
1	4,2,5	1
2	4,3,4	2
3	2,-3,0	T_2
4	2,-2,0	T_2
5	1,6,0	T_1
6	2,7,0	T_2
7	3,0,-1	T_3

State Value	Designates
0	Incident-free
1	Tentative incident
2	Tentative incident
3	Tentative incident
4	Incident confirmed
5	Incident continuing

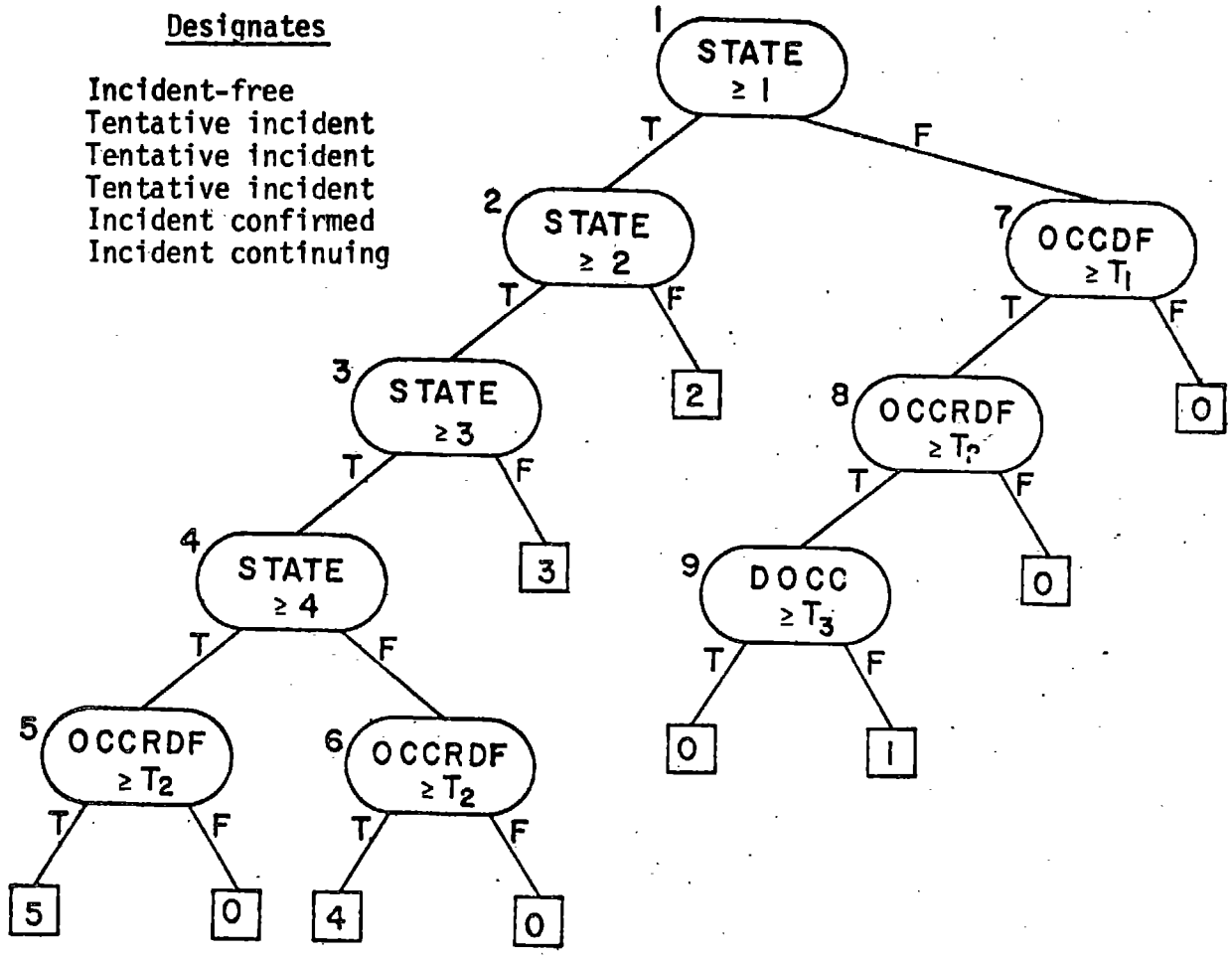

Figure 74. Decision tree for twenty-second update version of Algorithm 7

Table 94. Coding for twenty-second update version of Algorithm 7.

Feature No.	Name
1	OCCDF
2	OCCRDF
3	DOCC
4	State

Decision Node	NTR	Threshold Vector
1	4,2,7	1
2	4,3,-2	2
3	4,4,-3	3
4	4,5,6	4
5	2,-5,0	T_2
6	2,-4,0	T_2
7	1,8,0	T_1
8	2,9,0	T_2
9	3,0,-1	T_3

Table 95. Calibration and evaluation of Algorithm 7 on Los Angeles data base.

$N_I = 49$ $\overline{N}_I = 40$

$N_F = 104,217$ $\overline{N}_F = 3,495$

Threshold set	Detection rate (%)	False alarm rate (%)	Mean-time-to-detect (minutes)	Thresholds T_1	T_2	T_3
1	59	.134	3.25	8.1	.313	16.8
2	51	.050	4.31	12.9	.360	16.6
3	49	.043	4.94	13.1	.358	15.8
4	41	.029	4.85	9.6	.359	12.3
5	37	.017	6.17	13.1	.393	12.5
6	31	.006	5.84	21.6	.301	13.9
7	20	.004	7.73	26.6	.322	13.4

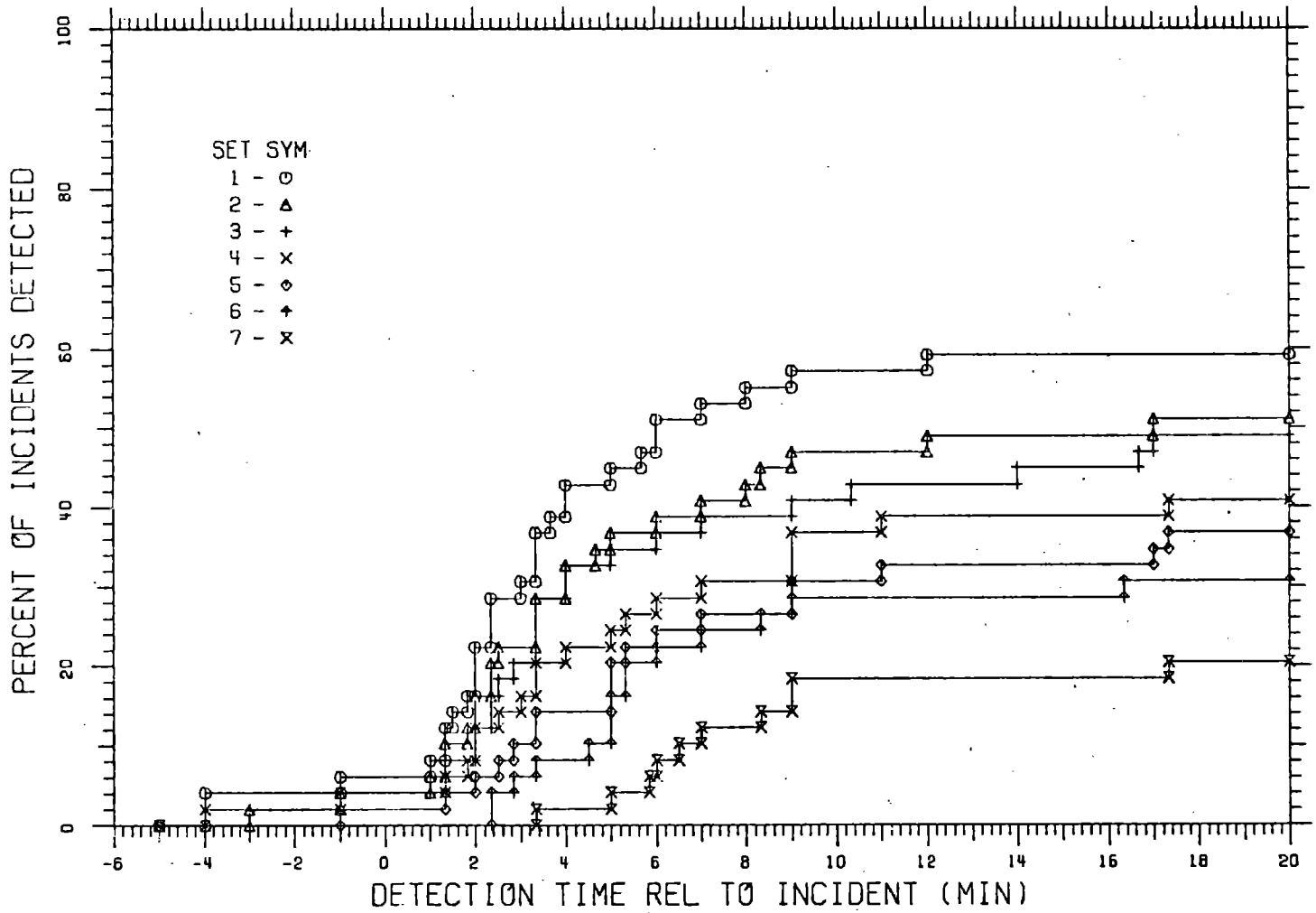

Figure 75. Distribution of times-to-detect for Algorithm 7, Los Angeles data.

Table 96. Evaluation of Algorithm 7 for thresholds determined from Los Angeles data base (see Table 95).

Threshold set	Evaluation on full Los Angeles data base, N_I=111, N_F= 104,217			Evaluation on Los Angeles, sensor configuration A data base, N_I= 35, N_F= 13,357		
	Detection rate (%)	False alarm rate (%)	Mean-time-to-detect (minutes)	Detection rate (%)	False alarm rate (%)	Mean-time-to-detect (minutes)
1	67	.134	2.91	43	.374	2.87
2	59	.050	3.98	37	.180	6.41
3	58	.043	4.26	31	.157	5.67
4	47	.029	4.64	31	.172	4.58
5	43	.017	5.61	29	.075	5.77
6	44	.006	5.14	20	.045	5.57
7	32	.004	6.97	17	.023	7.06

Table 96. Evaluation of Algorithm 7 for thresholds determined from Los Angeles data base (see Table 95). (continued)

Threshold set	Evaluation on Los Angeles, sensor configuration B data base, $N_I = 35$, $N_F = 8{,}267$			Evaluation on Los Angeles, sensor configuration C data base, $N_I = 35$, $N_F = 6{,}576$		
	Detection rate (%)	False alarm rate (%)	Mean-time-to-detect (minutes)	Detection rate (%)	False alarm rate (%)	Mean-time-to-detect (minutes)
1	37	.532	4.56	49	.563	3.61
2	29	.266	4.27	37	.274	3.31
3	29	.230	4.87	37	.228	3.62
4	20	.145	4.29	26	.228	2.04
5	20	.097	4.72	23	.152	1.58
6	23	.048	5.58	26	.122	4.11
7	17	.036	8.39	20	.076	.86

Table 96. Evaluation of Algorithm 7 for thresholds determined from Los Angeles data base (see Table 95) (concluded)

Evaluation on Minneapolis data base, $N_I = 36$, $N_F = 46{,}247$

Threshold set	Detection rate (%)	False alarm rate (%)	Mean-time to-detect (minutes)
1	67	.266	1.29
2	67	.088	1.46
3	67	.069	2.79
4	64	.112	4.28
5	61	.039	4.43
6	61	.017	3.05
7	56	.013	2.68

Table 97. Calibration and evaluation of Algorithm 7 on geometrically adjusted Los Angeles data base

$N_I = 49$ $\overline{N}_I = 40$

$N_F = 108{,}384$ $\overline{N}_F = 2{,}436$

Threshold set	Detection rate (%)	False alarm rate (%)	Mean-time-to-detect (minutes)	Thresholds T_1	T_2	T_3
1	61	.245	3.61	9.9	.316	30.0
2	51	.096	4.29	13.0	.424	24.6
3	47	.030	5.10	10.3	.443	16.6
4	41	.024	5.55	12.3	.464	16.5
5	37	.014	5.52	12.8	.538	17.6
6	31	.007	5.73	21.5	.483	17.7
7	20	.002	7.03	20.8	.669	16.8

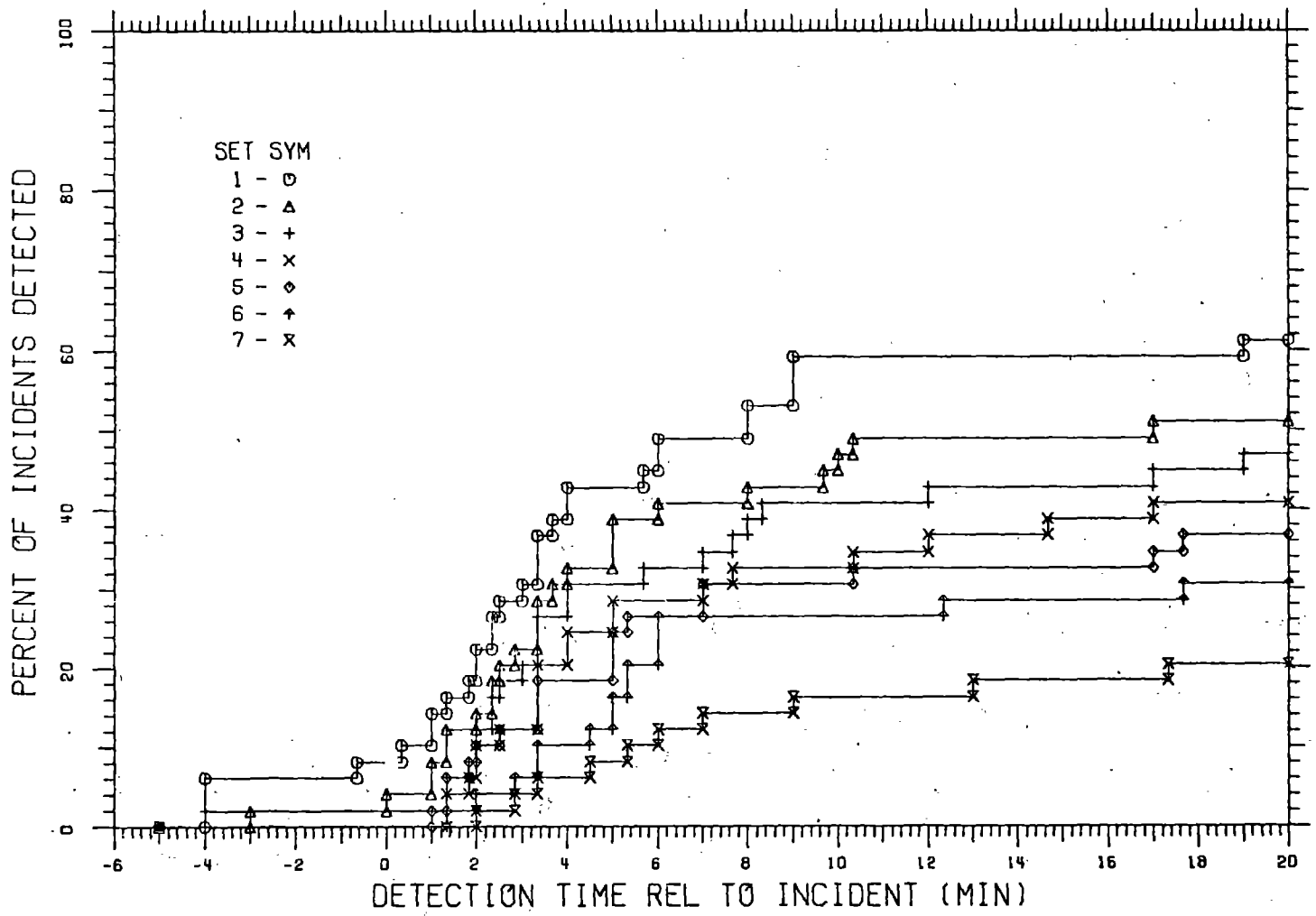

Figure 76. Distribution of times-to-detect for Algorithm 7, geometrically adjusted to Los Angeles data base.

Table 98. Calibration and evaluation of Algorithm 7 on Los Angeles sensor configuration A data base.

$N_I = 35$ $\overline{N}_I = 28$

$N_F = 13{,}357$ $\overline{N}_F = 1041$

Threshold set	Detection rate (%)	False alarm rate (%)	Mean-time-to-detect (minutes)	Thresholds T_1	T_2	T_3
1	51	.457	2.76	7.7	.411	23.6
2	40	.195	3.41	17.6	.454	27.2
3	31	.067	6.12	16.9	.389	16.2
4	20	.030	7.00	22.1	.655	13.7

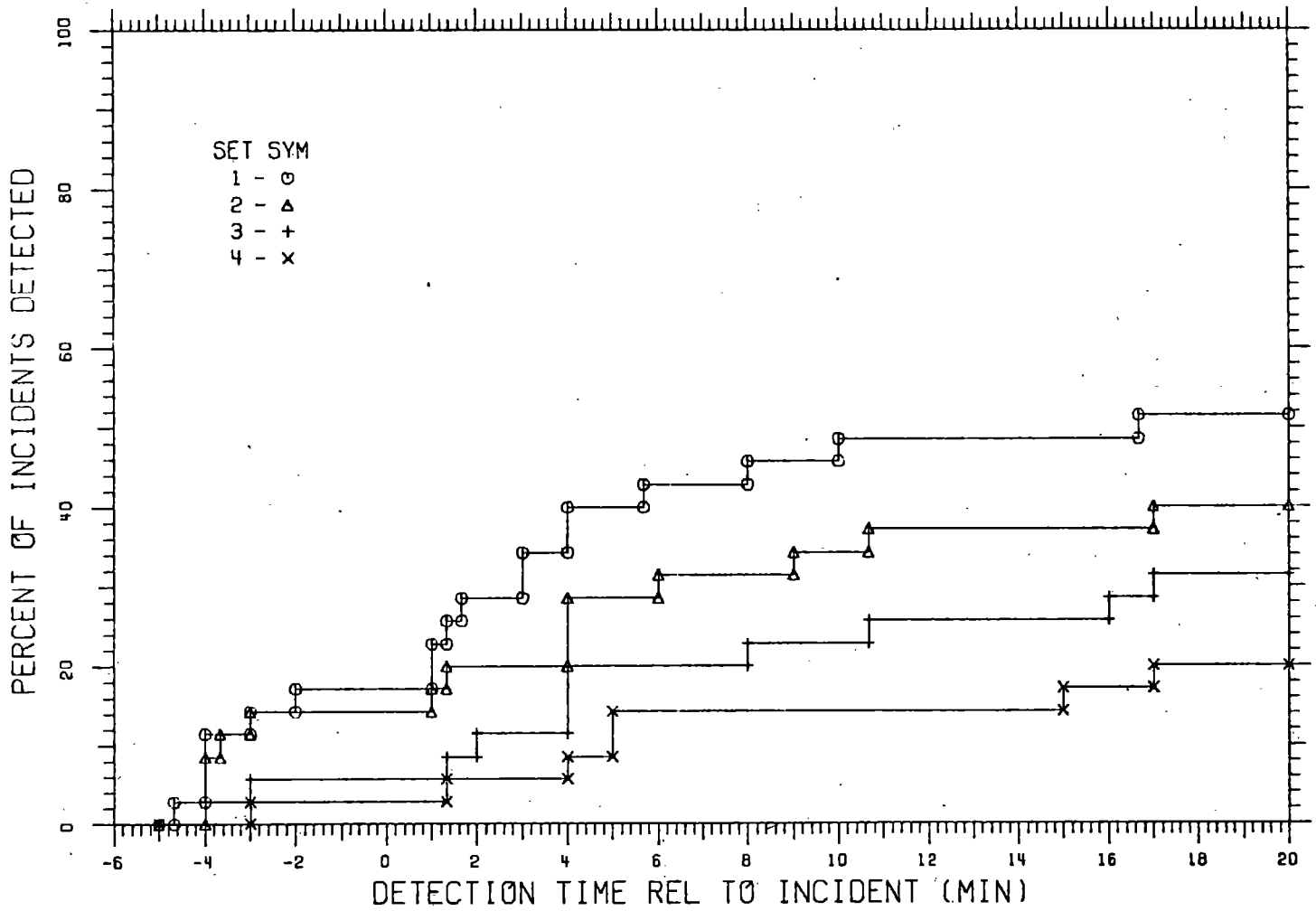

Figure 77. Distribution of times-to-detect for Algorithm 7, Los Angeles, sensor configuration A data base.

Table 99. Calibration and evaluation of Algorithm 7 on Los Angeles sensor configuration B data base.

$N_I = 35$ $\bar{N}_I = 32$

$N_F = 8{,}267$ $\bar{N}_F = 773$

Threshold set	Detection rate (%)	False alarm rate (%)	Mean-time-to-detect (minutes)	Thresholds T_1	T_2	T_3
1	51	.992	4.70	7.7	.348	25.8
2	40	.847	2.00	5.9	.405	28.7
3	31	.109	4.21	5.3	.530	18.8
4	20	.012	7.72	7.6	.676	24.5

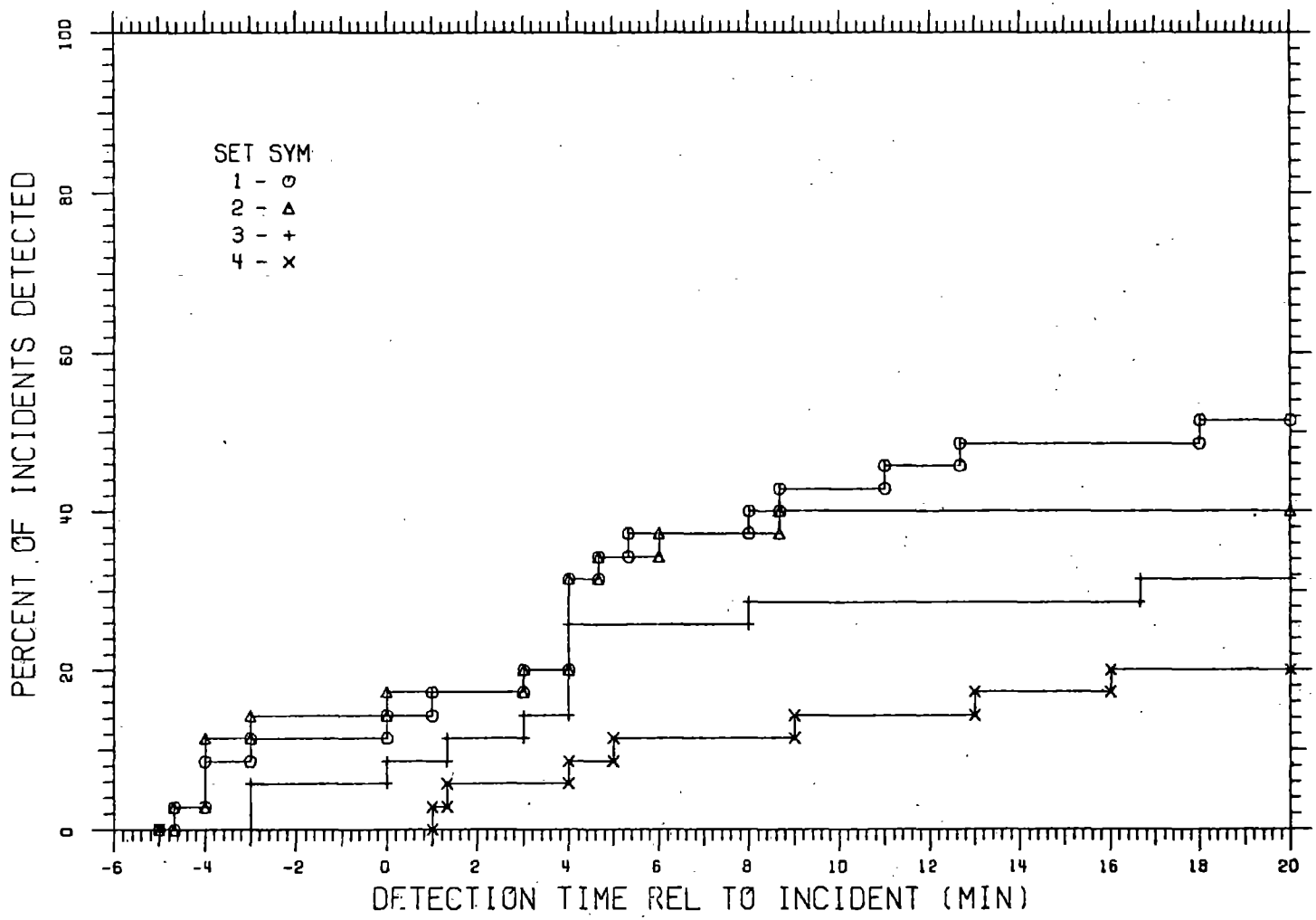

Figure 78. Distribution of times-to-detect for Algorithm 7, Los Angeles, sensor configuration B data base.

Table 100. Calibration and evaluation of Algorithm 7 on Los Angeles sensor configuration C data base.

$N_I = 35$ $\bar{N}_I = 27$

$N_F = 6{,}576$ $\bar{N}_F = 694$

Threshold set	Detection rate (%)	False alarm rate (%)	Mean-time-to-detect (minutes)	Thresholds T_1	T_2	T_3
1	60	1.065	3.29	6.6	.352	29.3
2	51	.578	3.59	7.6	.301	16.1
3	40	.243	4.12	11.6	.341	15.4
4	31	.106	3.33	22.9	.481	16.6
5	20	.030	2.14	29.8	.336	15.1

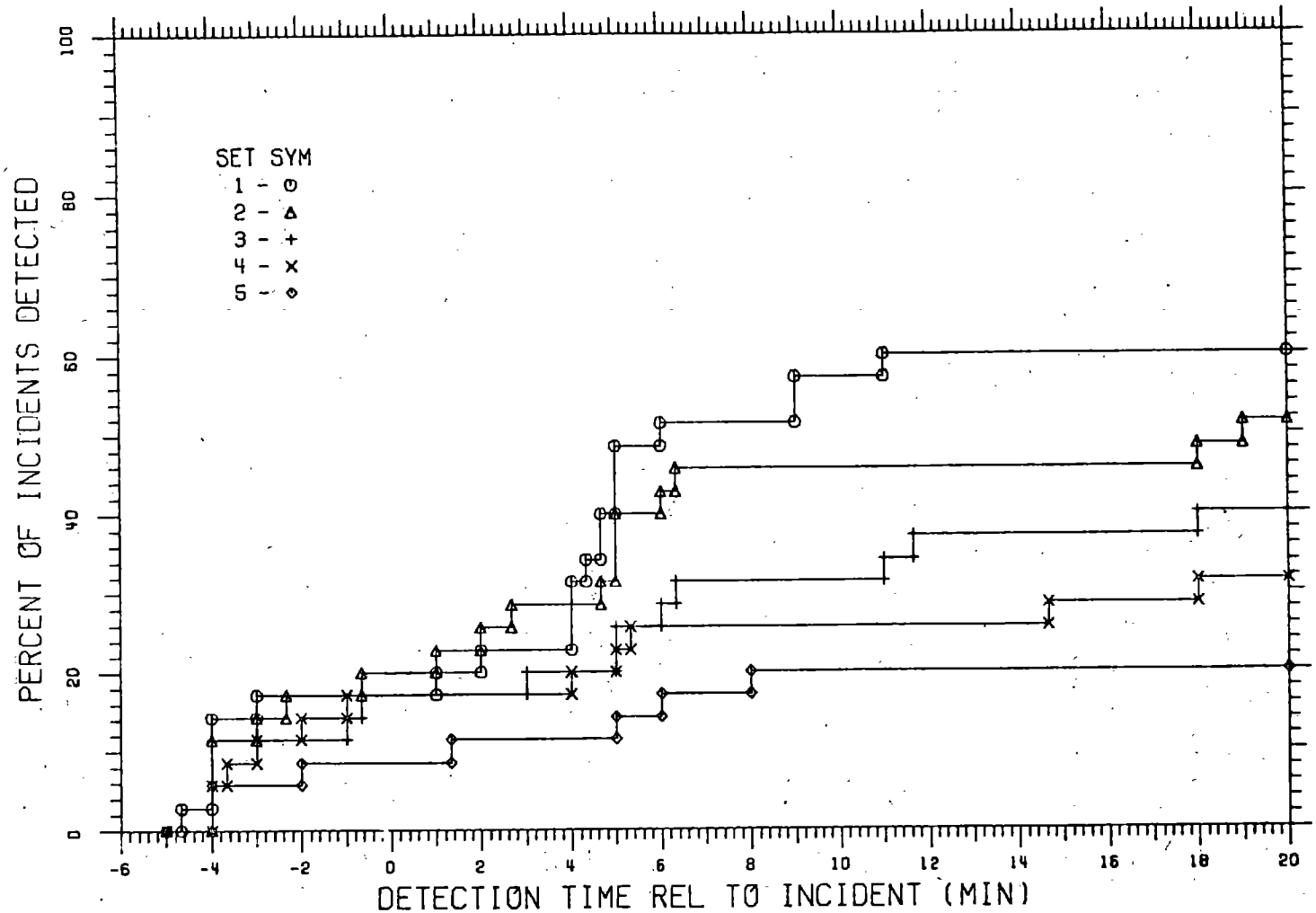

Figure 79. Distribution of times-to-detect for Algorithm 7, Los Angeles, sensor configuration C data base.

Table 101. Calibration and evaluation of Algorithm 7 on Minneapolis data base.

$N_I = 36$ $\overline{N}_I = 33$

$N_F = 46{,}247$ $\overline{N}_F = 2{,}429$

Threshold set	Detection rate (%)	False alarm rate (%)	Mean-time-to-detect (minutes)	Thresholds T_1	T_2	T_3
1	81	.365	1.21	7.4	.306	19.5
2	72	.093	1.10	13.5	.393	21.0
3	61	.013	2.77	21.2	.644	24.5
4	50	.009	4.14	29.3	.667	14.3
5	42	.007	3.60	29.3	.729	16.4
6	39	.007	3.79	26.4	.754	20.7
7	25	.004	4.22	22.1	.812	27.5

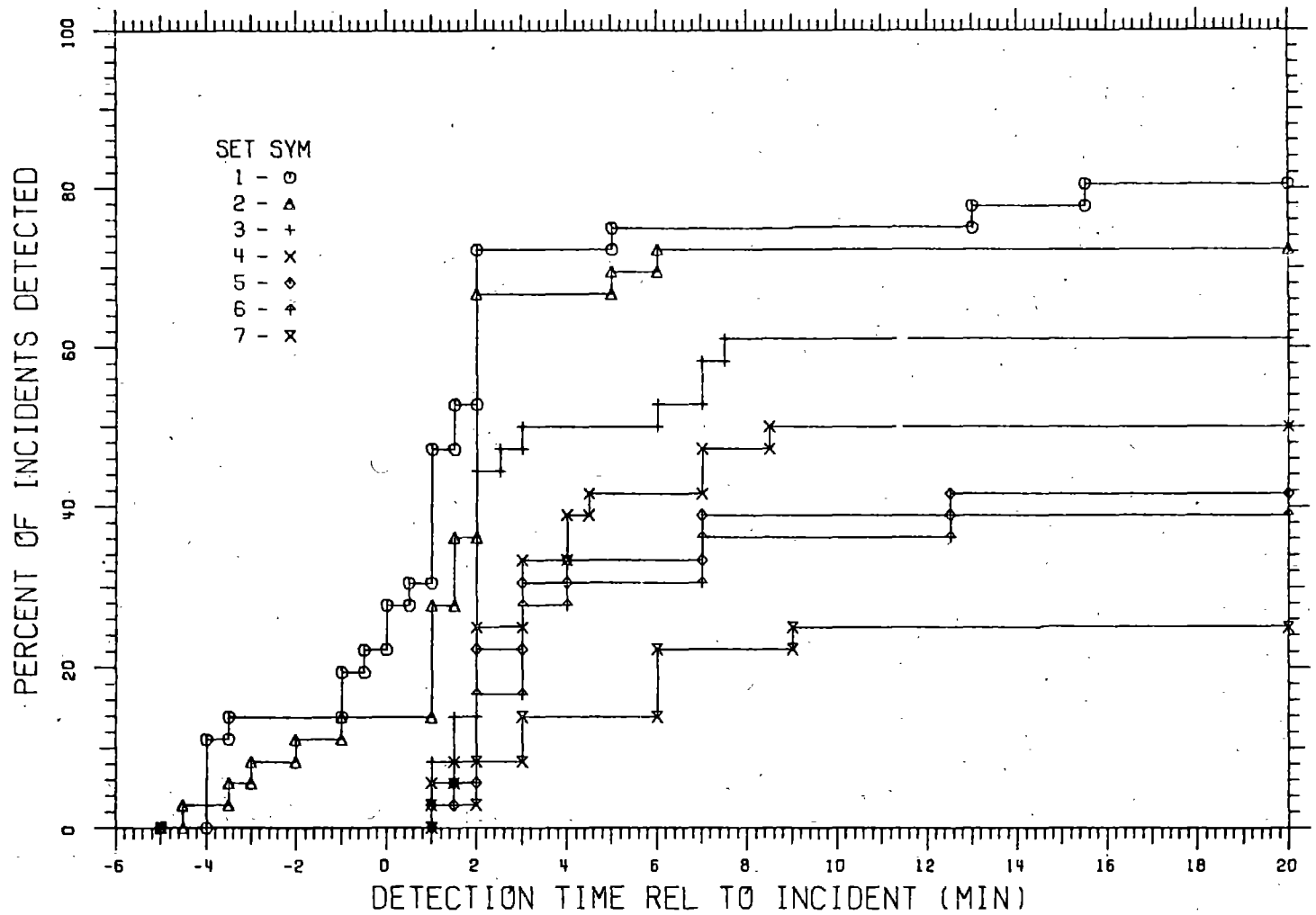

Figure 80. Distribution of times-to-detect for Algorithm 7, Minneapolis data base.

Table 102. Evaluation of Algorithm 7 for thresholds determined from Minneapolis data base (see Table 101).

Threshold set	Evaluation on Minneapolis clear weather data base, $N_I = 26$, $N_F = 27{,}778$			Evaluation on Minneapolis snowy weather data base, $N_I = 10$, $N_F = 18{,}469$		
	Detection rate (%)	False alarm rate (%)	Mean-time-to-detect (minutes)	Detection rate	False alarm rate (%)	Mean-time-to-detect (minutes)
1	89	.351	.92	60	.398	2.50
2	81	.111	1.21	50	.065	.60
3	69	.022	2.36	40	0	4.38
4	58	.014	3.13	30	0	4.17
5	50	.011	3.85	20	0	2.00
6	50	.011	3.92	10	0	2.00
7	31	.007	4.50	10	0	2.00

Table 103. Calibration and evaluation of Algorithm 7 on Minneapolis clear weather data base.

$N_I = 26$ $\bar{N}_I = 25$

$N_F = 27{,}778$ $\bar{N}_F = 1{,}174$

Threshold set	Detection rate (%)	False alarm rate (%)	Mean-time-to-detect (minutes)	Thresholds T_1	T_2	T_3
1	81	.057	3.07	24.5	.322	28.8
2	73	.029	2.76	27.8	.367	20.4
3	65	.018	2.53	23.7	.621	14.2
4	50	.011	4.23	29.8	.729	12.4
5	46	.011	4.38	10.3	.771	22.0
6	31	.007	4.38	6.1	.802	25.2

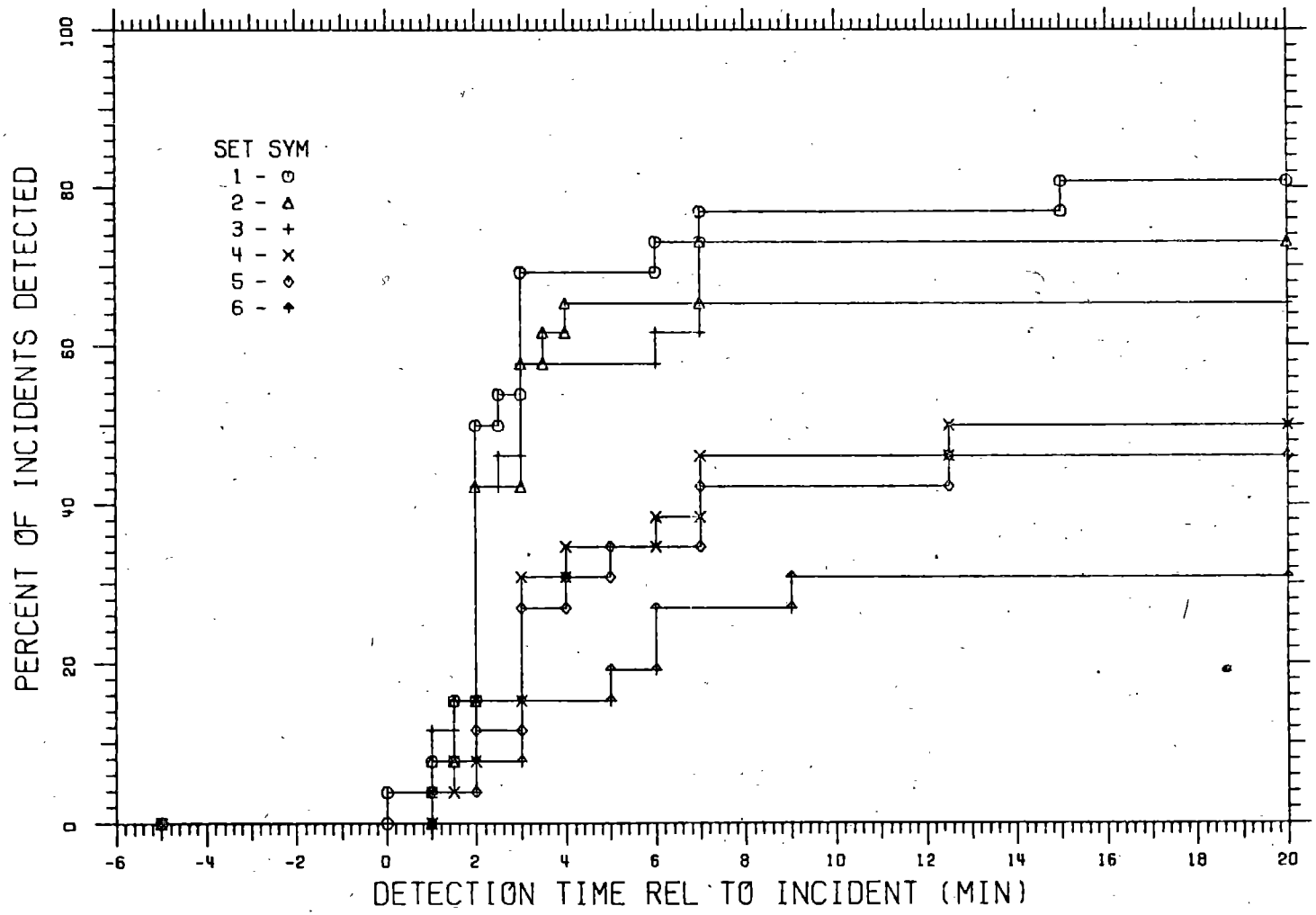

Figure 81. Distribution of times-to-detect for Algorithm 7, Minneapolis clear weather data base.

Table 104. Calibration and evaluation of Algorithm 7 on Minneapolis snowy weather data base.

$N_I = 10$ $\overline{N}_I = 8$

$N_F = 18{,}469$ $\overline{N}_F = 1{,}257$

Threshold set	Detection rate (%)	False alarm rate (%)	Mean-time-to-detect (minutes)	Thresholds T_1	T_2	T_3
1	60	.294	2.17	7.4	.370	19.5
2	50	.065	-.60	13.7	.390	20.2
3	40	0	4.38	24.3	.638	24.0
4	30	0	4.17	26.8	.610	13.4

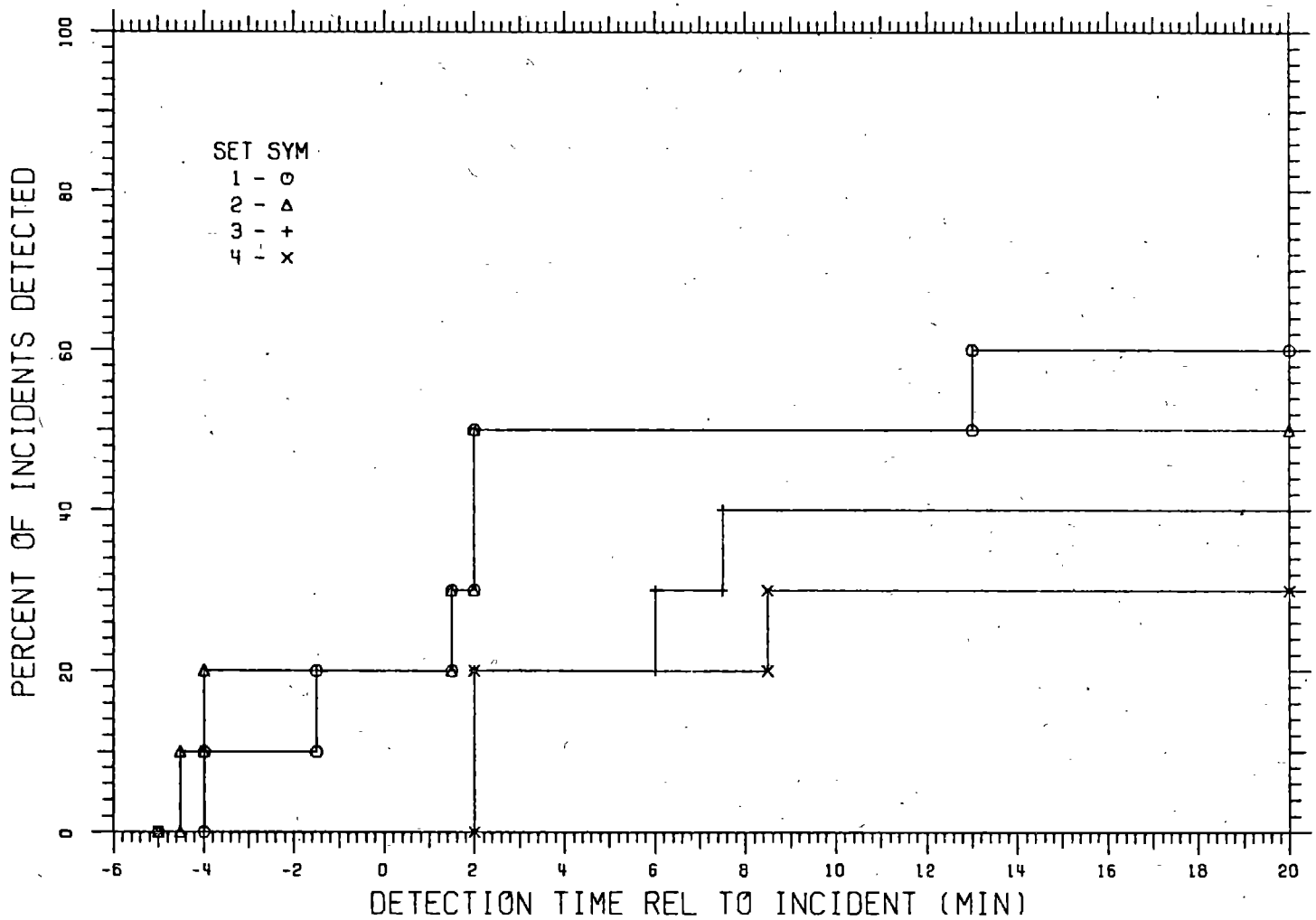

Figure 82. Distribution of times-to-detect for Algorithm 7, Minneapolis snowy weather data base.

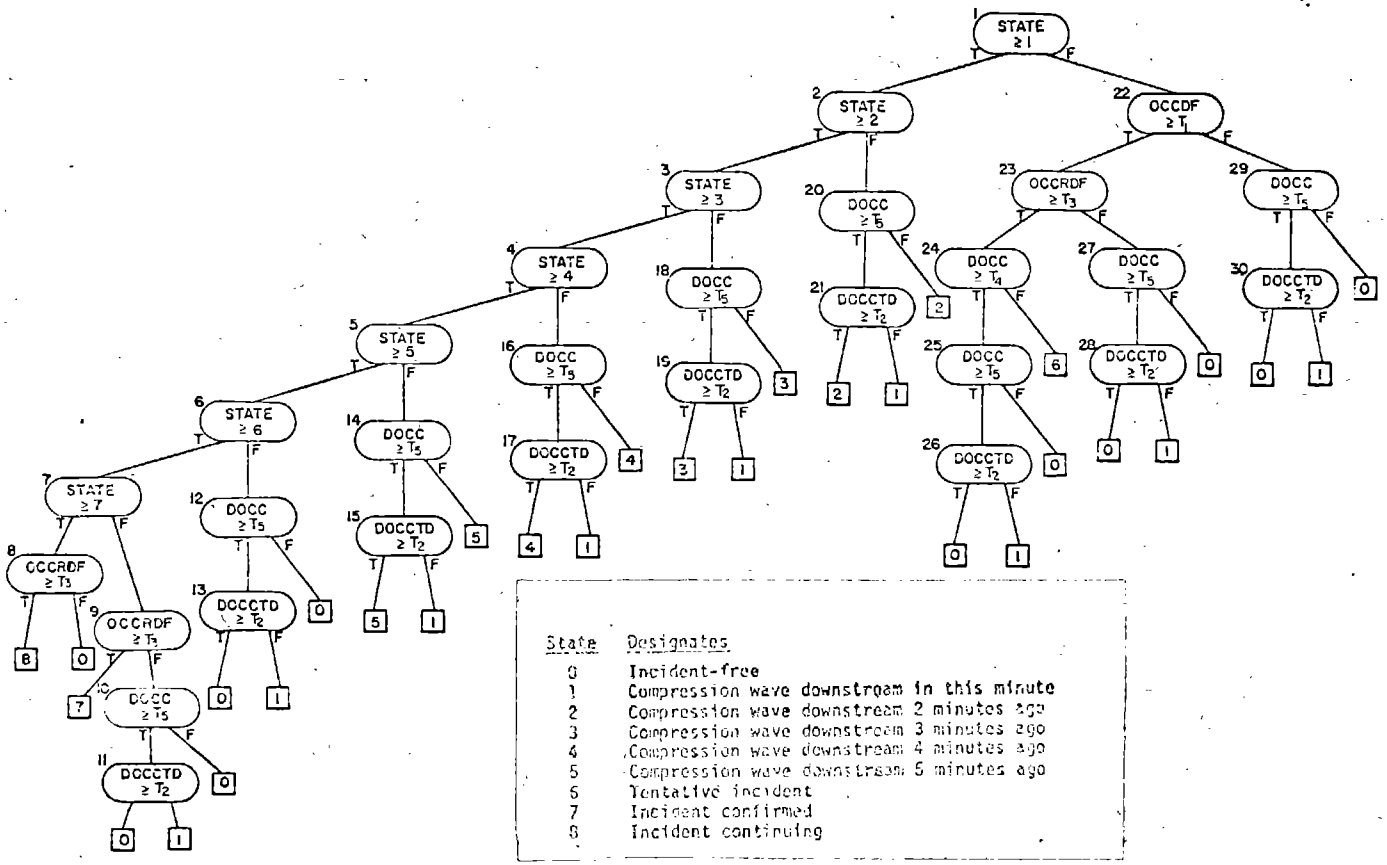

Figure 83. Decision tree for Algorithm 8.

Table 105. Coding for Algorithm 8.

Feature No.	Name
1	OCCDF
2	DOCCTD
3	OCCRDF
4	DOCC
5	State

Decision Node	NTR	Threshold Vector
1	5,2,22	1
2	5,3,20	2
3	5,4,18	3
4	5,5,16	4
5	5,6,14	5
6	5,7,12	6
7	5,8,9	7
8	3,-8,0	T_3
9	3,-7,10	T_3
10	5,11,0	T_5
11	2,0,-1	T_2
12	5,13,0	T_5
13	2,0,-1	T_2
14	5,15,-5	T_5
15	2,-5,-1	T_2
16	5,17,-4	T_5
17	2,-4,-1	T_2
18	5,19,-3	T_5
19	2,-3,-1	T_2
20	5,21,-2	T_5
21	2,-2,-1	T_2

Table 105. Coding for Algorithm 8 (cont.)

Decision Node	NTR	Threshold Vector
22	1,23,29	T_1
23	3,24,27	T_3
24	4,25,-6	T_4
25	5,26,0	T_5
26	2,0,-1	T_2
27	5,28,0	T_5
28	2,0,-1	T_2
29	5,30,0	T_5
30	2,0,-1	T_2

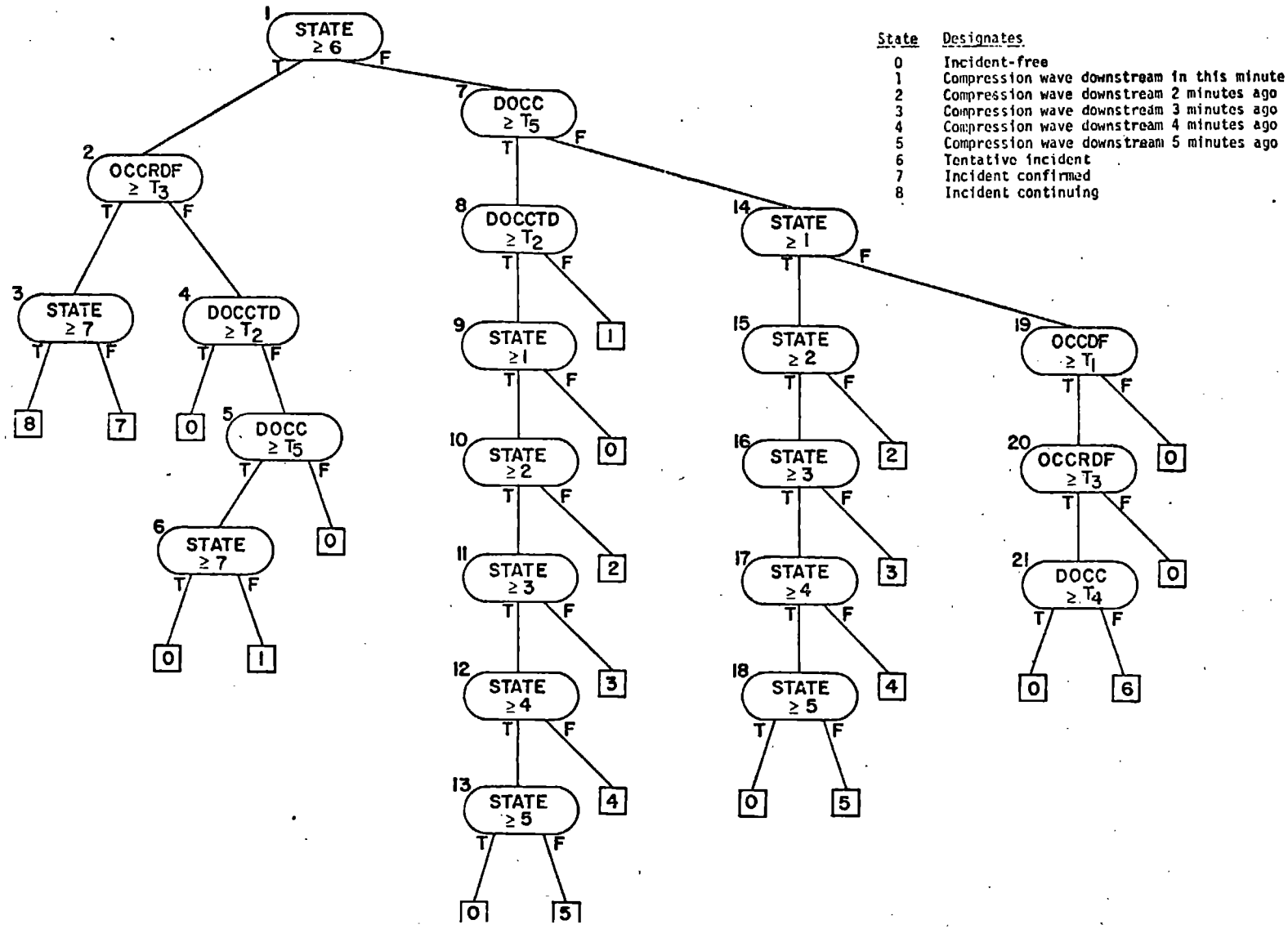

Figure 84. Decision tree for an equivalent form of Algorithm 8.

Table 106. Coding for alternative configuration of Algorithm 8.

Feature No.	Name
1	OCCDF
2	DOCCTD
3	OCCRDF
4	DOCC
5	State

Decision Node	NTR	Threshold Vector
1	5,2,7	6
2	3,3,4	T_3
3	5,-8,-7	7
4	2,0,5	T_2
5	4,6,0	T_5
6	5,0,-1	7
7	4,8,14	T_5
8	2,9,-1	T_2
9	5,10,0	1
10	5,11,-2	2
11	5,12,-3	3
12	5,13,-4	4
13	5,0,-5	5
14	5,15,19	1
15	5,16,-2	2
16	5,17,-3	3
17	5,18,-4	4
18	5,0,-5	5
19	1,20,0	T_1
20	3,21,0	T_3
21	4,0,-6	T_4

Table 107. Calibration and evaluation of Algorithm 8 on Los Angeles data base.

$N_I = 49$ $\bar{N}_I = 42$

$N_F = 103{,}448$ $\bar{N}_F = 5{,}638$

Threshold set	Detection rate (%)	False alarm rate (%)	Mean-time-to-detect (minutes)	Thresholds T_1	T_2	T_3	T_4	T_5^*
1	61	.177	3.88	10.2	-.443	.312	28.8	30
2	51	.038	4.79	13.1	-.296	.309	15.9	30
3	41	.024	5.63	18.1	-.310	.356	18.5	30
4	31	.010	4.93	5.2	-.401	.590	27.9	30
5	20	.003	8.83	24.4	-.392	.579	13.0	30

*Held fixed.

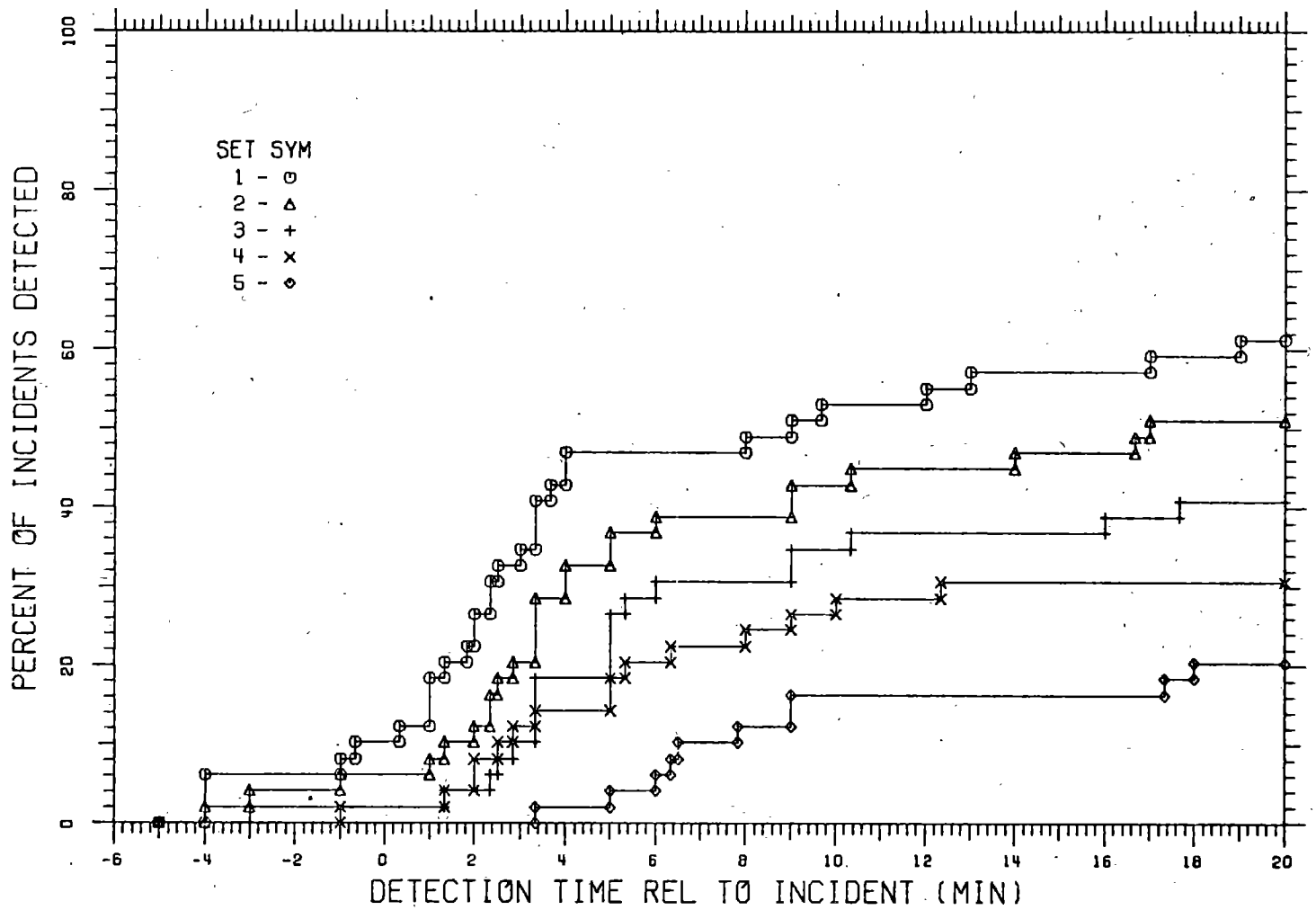

Figure 85 . Distribution of times-to-detect for Algorithm 8, Los Angeles data base.

Table 108. Evaluation of Algorithm 8 for thresholds determined from Los Angeles data base (see Table 107).

Threshold set	Evaluation on full Los Angeles data base, N_I=111, N_F=103,448			Evaluation on Los Angeles, sensor configuration A data base, N_I= 35, N_F= 13,357		
	Detection rate (%)	False alarm rate (%)	Mean-time-to-detect (minutes)	Detection rate (%)	False alarm rate (%)	Mean-time-to-detect (minutes)
1	68	.177	3.04	46	.427	2.02
2	60	.038	4.46	40	.142	6.88
3	53	.024	4.62	31	.090	5.21
4	44	.008	5.00	23	.067	3.83
5	32	.003	6.76	20	.023	7.57

Table 108 Evaluation of Algorithm 8 for thresholds determined from Los Angeles data base (see Table 107). (continued)

	Evaluation on Los Angeles, sensor configuration B data base, N_I=35, N_F=8,267			Evaluation on Los Angeles, sensor configuration C data base, N_I= 35, N_F= 6,576		
Threshold set	Detection rate (%)	False alarm rate (%)	Mean-time-to-detect (minutes)	Detection rate (%)	False alarm rate (%)	Mean-time-to-detect (minutes)
1	40	.605	3.31	46	.532	2.25
2	29	.218	3.57	40	.228	4.69
3	29	.194	4.57	37	.167	3.39
4	23	.048	4.46	29	.198	2.30
5	17	.036	8.22	20	.076	.72

Table 108. Evaluation of Algorithm 8 for thresholds determined from Los Angeles data base (see Table 107). (Concluded)

Evaluation on Minneapolis data base, $N_I = 36$, $N_F = 46{,}257$

Threshold set	Detection rate (%)	False alarm rate (%)	Mean-time-to-detect (minutes)
1	72.2	.270	.37
2	63.9	.082	2.26
3	61.1	.052	1.59
4	63.9	.037	2.83
5	52.8	.009	3.08

Table 109. Calibration and evaluation of Algorithm 8 on Los Angeles data base (T_2 = -.300).

N_I = 49 $\bar{N}_I$ = 42

N_F = 103,448 $\bar{N}_F$ = 5,638

Threshold Set	Detection rate (%)	False alarm rate (%)	Mean-time-to-detect (minutes)	Thresholds T_1	T_2^*	T_3	T_4	T_5^*
1	59	.125	3.46	8.1	-.300	.313	16.8	30
2	51	.044	4.51	12.9	-.300	.360	16.6	30
3	49	.038	5.15	13.1	-.300	.358	15.8	30
4	41	.028	4.95	9.6	-.300	.359	12.3	30
5	37	.016	6.28	13.1	-.300	.393	12.5	30
6	31	.005	5.98	21.6	-.300	.301	13.9	30
7	20	.003	7.93	26.6	-.300	.322	13.4	30

*Held fixed.

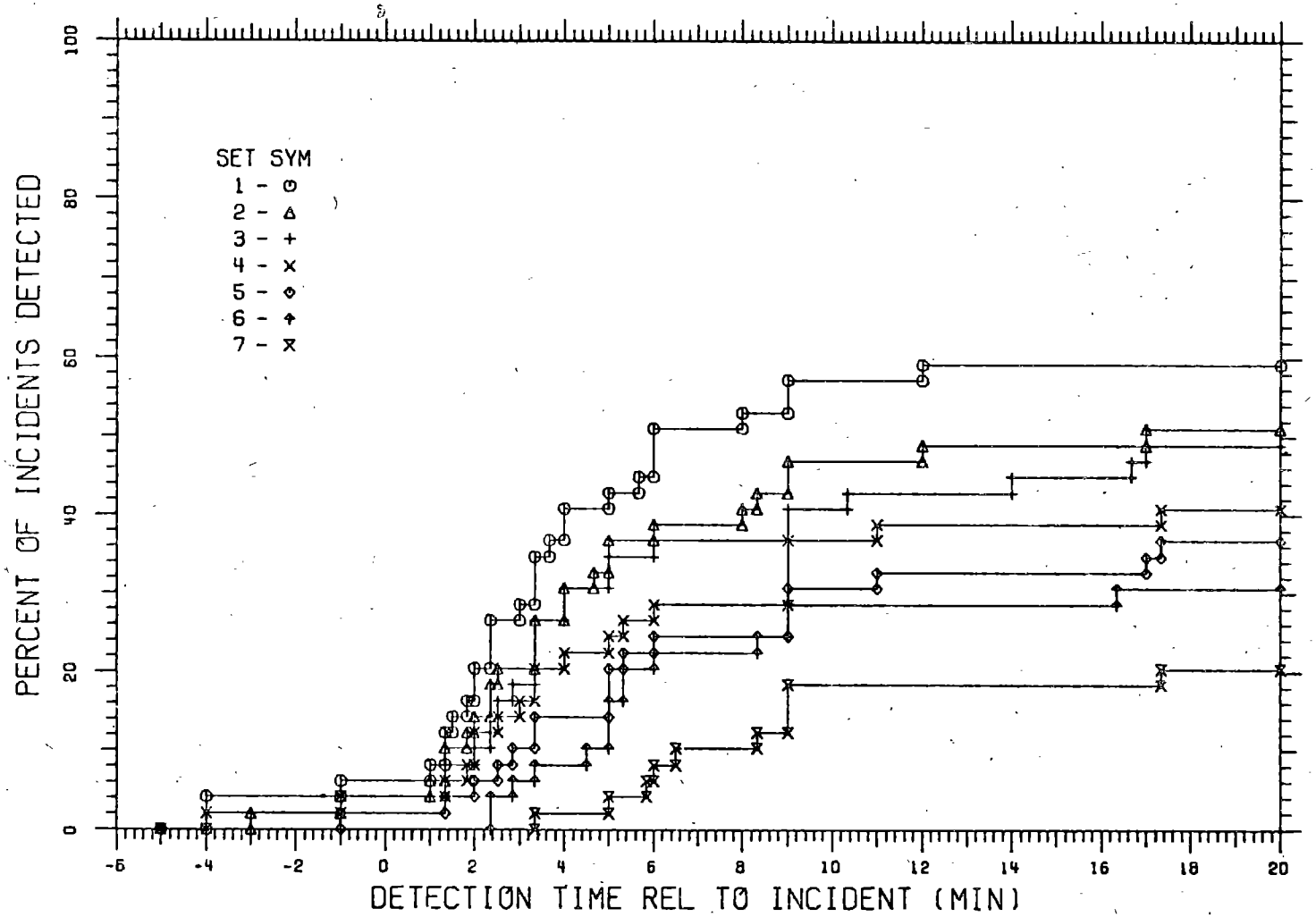

Figure 86. Distribution of times-to-detect for Algorithm 8, Los Angeles data base (T_2= -.300).

Table 110. Calibration and evaluation of Algorithm 8 on geometrically adjusted Los Angeles data base.

$N_I = 49$ $\overline{N}_I = 40$

$N_F = 104{,}217$ $\overline{N}_F = 1{,}248$

Threshold set	Detection rate (%)	False alarm rate (%)	Mean-time to-detect (Minutes)	Thresholds* T_1	T_2	T_2	T_4
1	51	.054	3.97	14.4	-.296	.364	26.9
2	47	.032	5.19	13.0	-.298	.460	24.8
3	41	.023	4.90	14.6	-.311	.439	17.1
4	37	.015	5.48	14.3	-.372	.373	14.1
5	31	.007	4.36	13.7	-.342	.578	18.6
6	27	.003	5.51	21.6	-.266	.599	27.6
7	23	.001	5.94	23.8	-.282	.608	26.3

*T_5 fixed at 30.

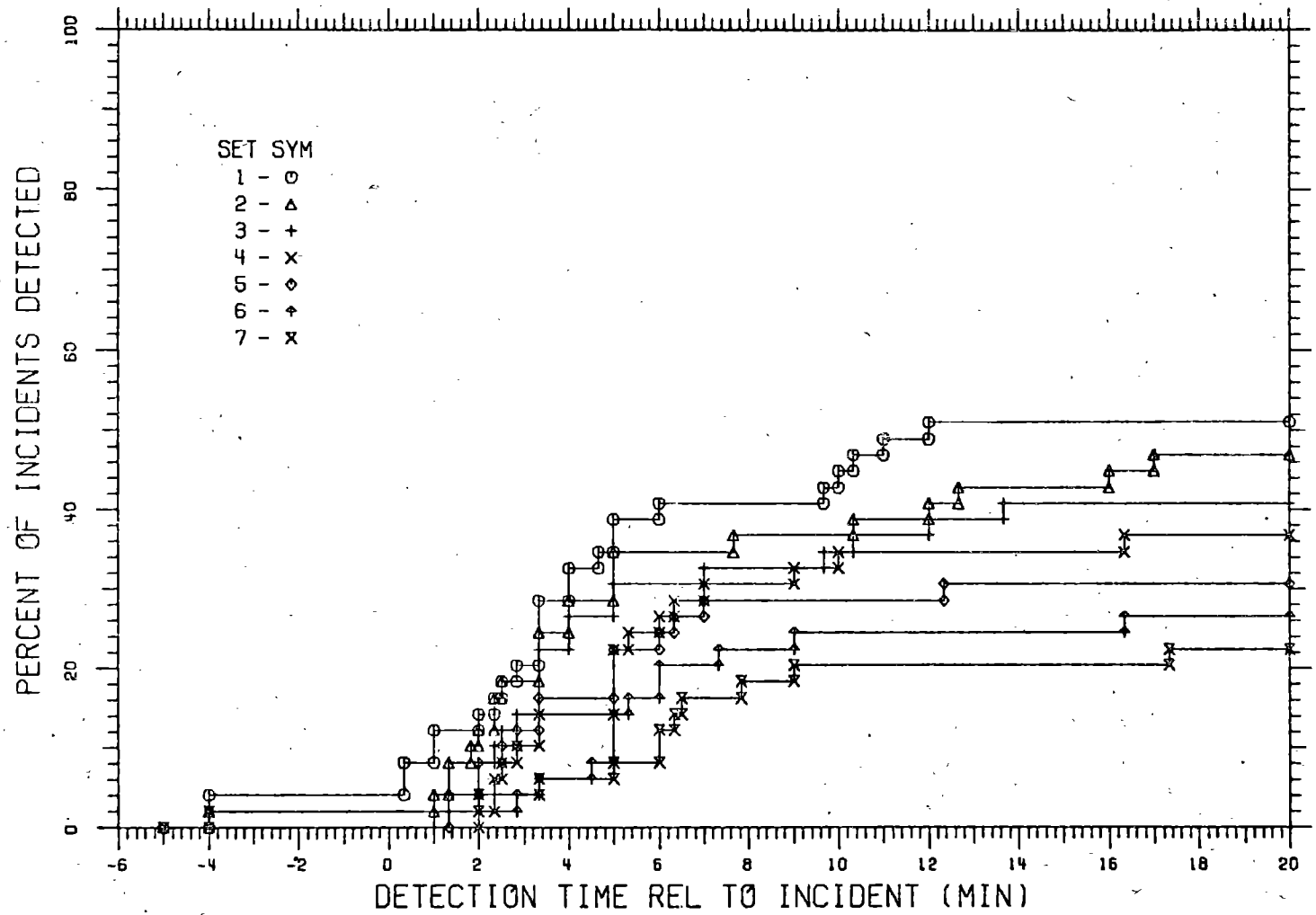

Figure 87. Distribution of times-to-detect for Algorithm 8, geometrically adjusted Los Angeles data base.

Table 111. Calibration and evaluation of Algorithm 8 on Minneapolis data base.

$N_I = 36$ $\bar{N}_I = 34$

$N_F = 46{,}257$ $\bar{N}_F = 3{,}238$

Threshold set	Detection rate (%)	False alarm rate (%)	Mean-time to-detect (Minutes)	Thresholds* T_1	T_2	T_3	T_4
1	80.6	.400	1.35	7.4	-.259	.302	27.3
2	72.2	.065	1.23	17.4	-.649	.391	25.2
3	61.1	.013	3.05	27.8	-.320	.606	28.8
4	55.6	.007	3.10	30.0	-.453	.508	15.4
5	41.7	.004	3.60	30.0	-.677	.724	15.3
6	36.1	.004	3.50	27.8	-.689	.750	11.6
7	27.8	.002	4.00	28.0	-1.084	.792	10.7

*T_5 fixed at 30.

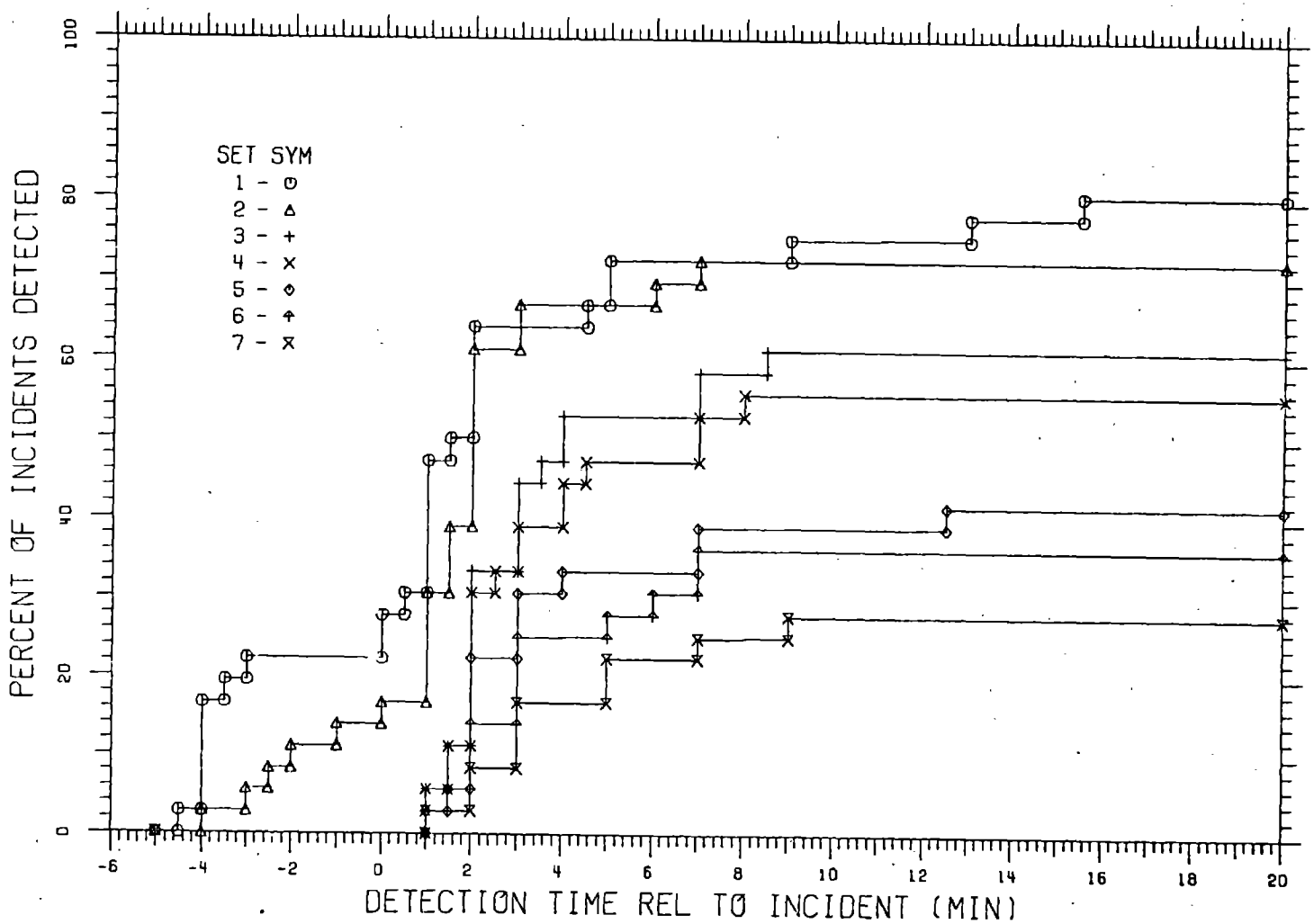

Figure 88. Distribution of times-to-detect for Algorithm 8, Minneapolis data base.

Table 112. Evaluation of Algorithm 8 for thresholds determined from Minneapolis data base (see Table 111).

Threshold set	Evaluation on Minneapolis clear weather data base, $N_I = 26$, $N_F = 27{,}778$			Evaluation on Minneapolis snowy weather data base, $N_I = 10$, $N_F = 18{,}469$		
	Detection rate (%)	False alarm rate (%)	Mean-time-to-detect (minutes)	Detection rate (%)	False alarm rate (%)	Mean-time-to-detect (minutes)
1	85	.348	.91	70	.490	2.86
2	85	.072	1.34	40	.055	.63
3	69	.018	2.81	40	0	4.13
4	65	.011	3.27	30	0	2.17
5	50	.007	3.85	20	0	2.00
6	46	.007	3.63	10	0	2.00
7	35	.004	4.22	10	0	2.00

State	Designates
0	Incident-free
1	Compression wave downstream in this minute
2	Compression wave downstream 2 minutes ago
3	Compression wave downstream 3 minutes ago
4	Compression wave downstream 4 minutes ago
5	Compression wave downstream 5 minutes ago
6	Incident confirmed
7	Incident continuing

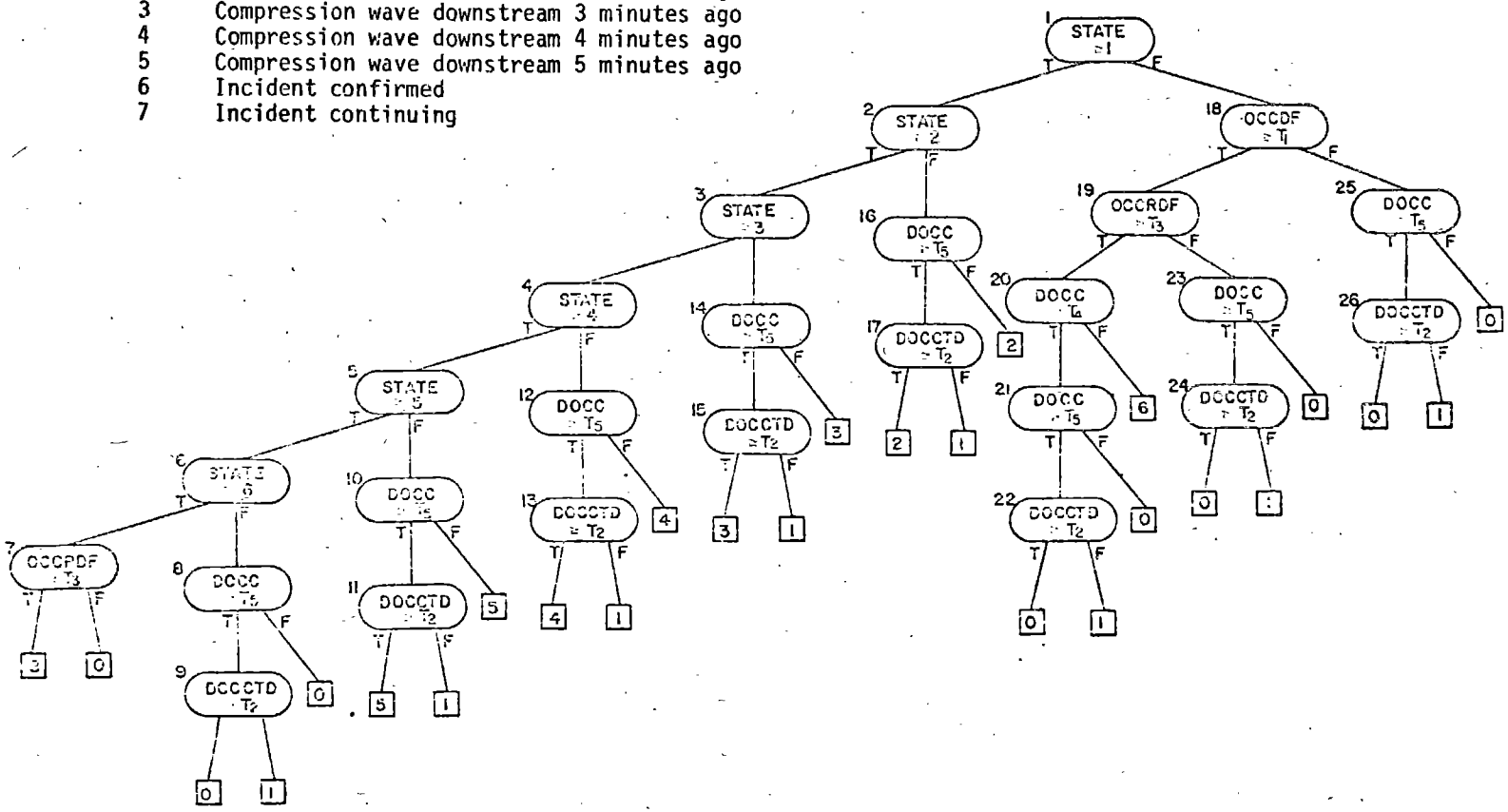

Figure 89. Decision tree for Algorithm 9.

Table 113. Coding for Algorithm 9.

Feature No.	Name
1	OCCDF
2	DOCCTD
3	OCCRDF
4	DOCC
5	State

Decision Node	NTR	Threshold Vector
1	5,2,22	1
2	5,3,20	2
3	5,4,18	3
4	5,5,16	4
5	5,6,14	5
6	5,7,12	6
7	3,-8,0	T_3
12	5,13,0	T_5
13	2,0,1	T_2
14	5,15,-5	T_5
15	2,-5,-1	T_2
16	5,17,-4	T_5
17	2,-4,1	T_2
18	5,19,-3	T_5
19	2,-3,-1	T_2
20	5,21,-2	T_5
21	2,-2,-1	T_2
22	1,23,29	T_1
23	3,24,27	T_3
24	4,25,-6	T_4
25	5,26,0	T_5

Table 113. Coding for Algorithm 9 (cont'd.).

Decision Node	NTR	Threshold Vector
26	2,0,-1	T_2
27	5,28,0	T_5
28	2,0,-1	T_2
29	5,30,0	T_5
30	2,0,-1	T_2

Table 114. Calibration and evaluation of Algorithm 9 on Los Angeles data base.

$N_I = 49$ $\bar{N}_I = 42$

$N_F = 103{,}448$ $\bar{N}_F = 5{,}638$

Threshold set	Detection rate (%)	False alarm rate (%)	Mean-time-to-detect (minutes)	Thresholds T_1	T_2	T_3	T_4	T_5^*
1	78	1.408	.83	5.4	-.306	.308	29.6	30
2	71	1.190	.47	5.8	-.306	.318	29.6	30
3	61	.230	2.08	12.5	-.311	.340	28.7	30
4	51	.070	5.25	17.0	-.277	.332	22.0	30
5	41	.040	4.12	19.6	-.310	.338	22.4	30
6	31	.009	4.98	21.5	-.350	.382	14.0	30
7	20	.004	8.23	26.3	-.322	.376	11.8	30

*Held Fixed

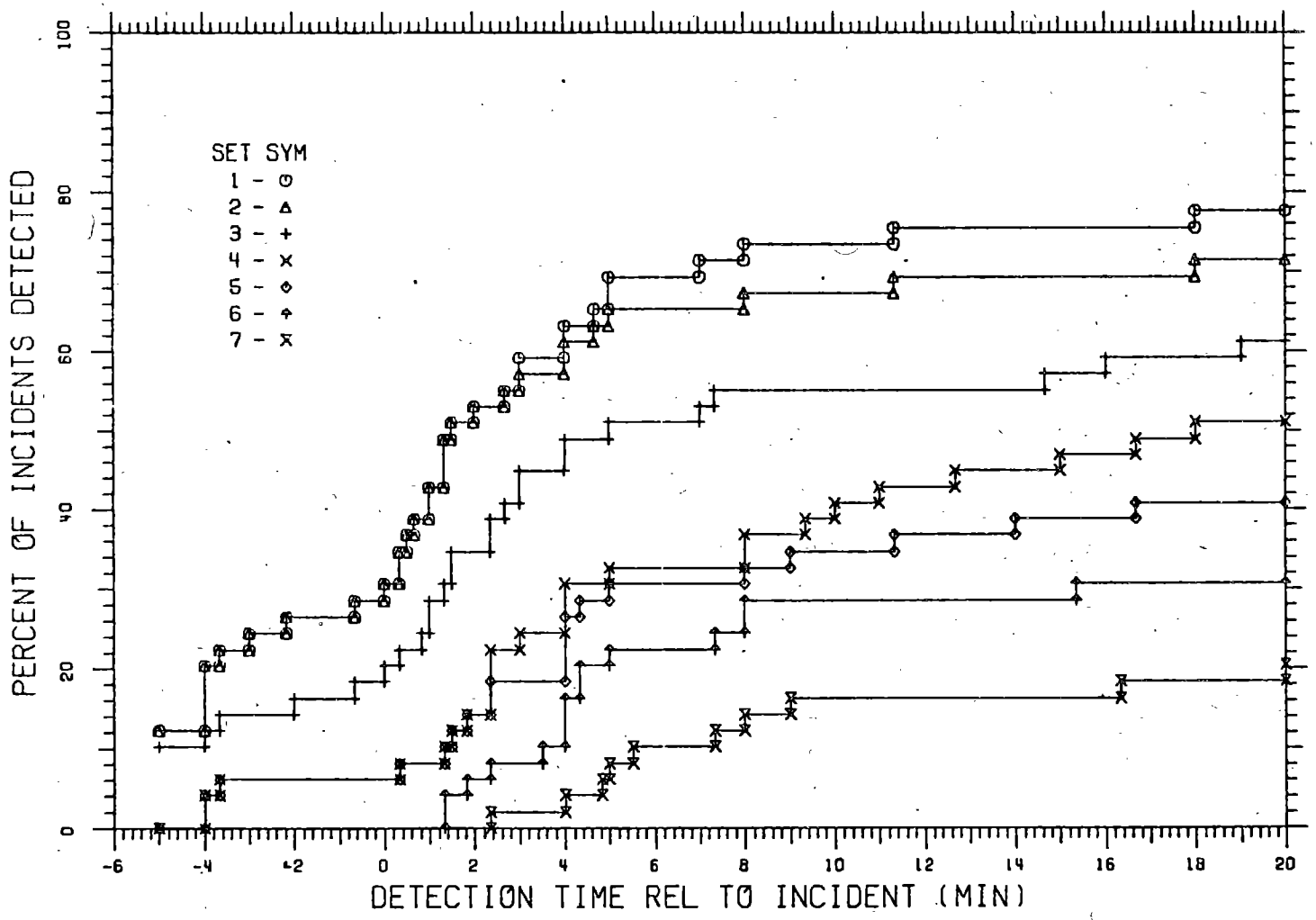

Figure 90. Distribution of times-to-detect for Algorithm 9, Los Angeles data base.

Table 115. Calibration and evaluation of Algorithm 9 on geometrically adjusted Los Angeles data base.

$N_I = 49$ $\overline{N}_I = 40$

$N_F = 104{,}217$ $\overline{N}_F = 1{,}248$

Threshold set	Detection rate (%)	False alarm rate (%)	Mean-time to-detect (Minutes)	Thresholds* T_1	T_2	T_3	T_4
1	71	.979	.93	5.4	-.428	.305	25.4
2	61	.264	2.93	9.9	-.437	.312	21.9
3	51	.080	3.65	9.2	-.543	.535	21.9
4	47	.045	4.44	12.3	-.582	.532	16.1
5	41	.024	5.97	12.6	-.637	.613	17.7
6	37	.019	5.91	14.0	-.584	.642	19.9
7	33	.009	4.67	21.2	-.399	.576	14.2
8	27	.006	5.08	20.8	-.372	.394	12.4
9	20	.003	7.27	23.3	-.440	.419	11.6

*T_5 fixed at 30.

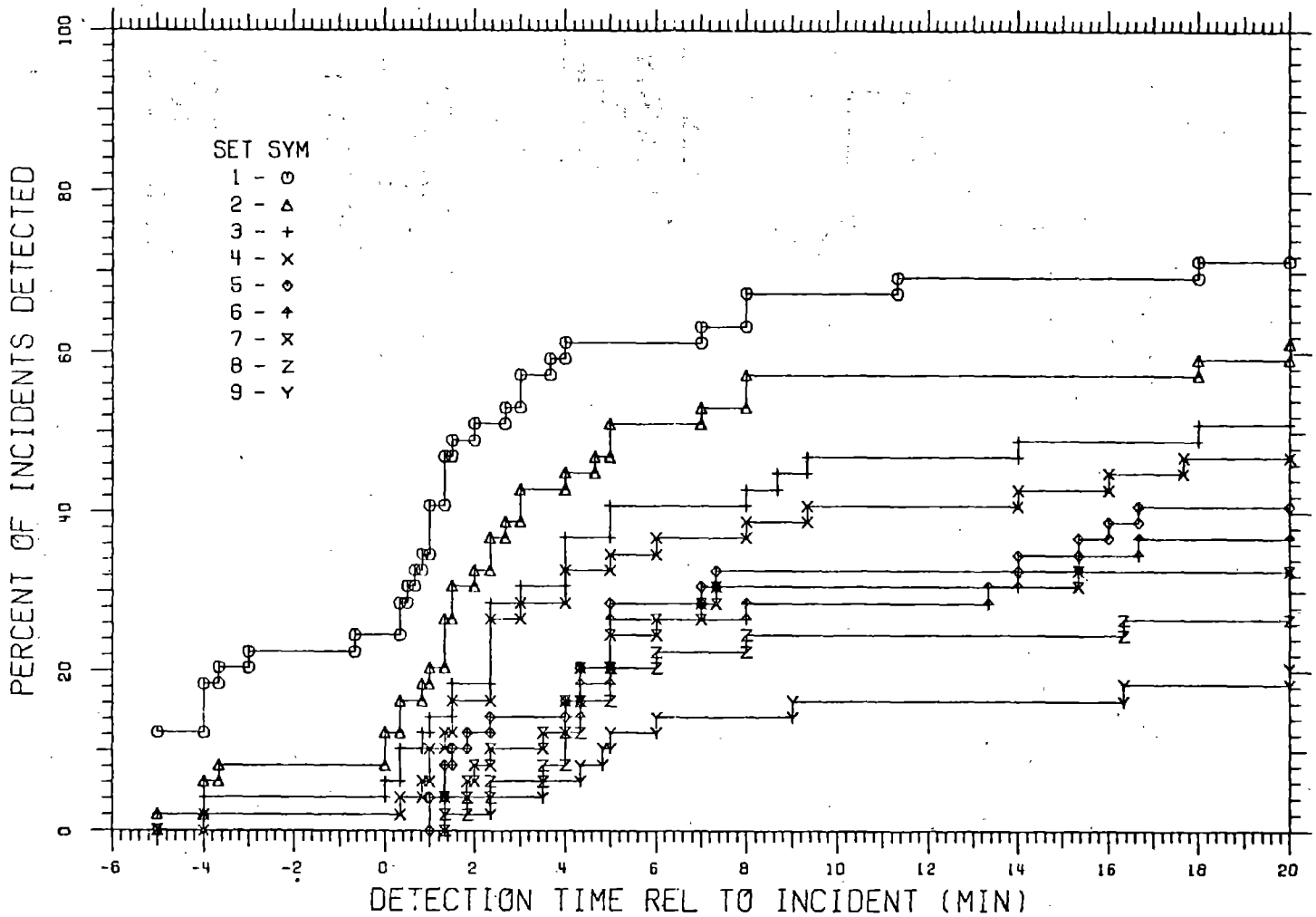

Figure 91. Distribution of times-to-detect for Algorithm 9, geometrically adjusted Los Angeles data base.

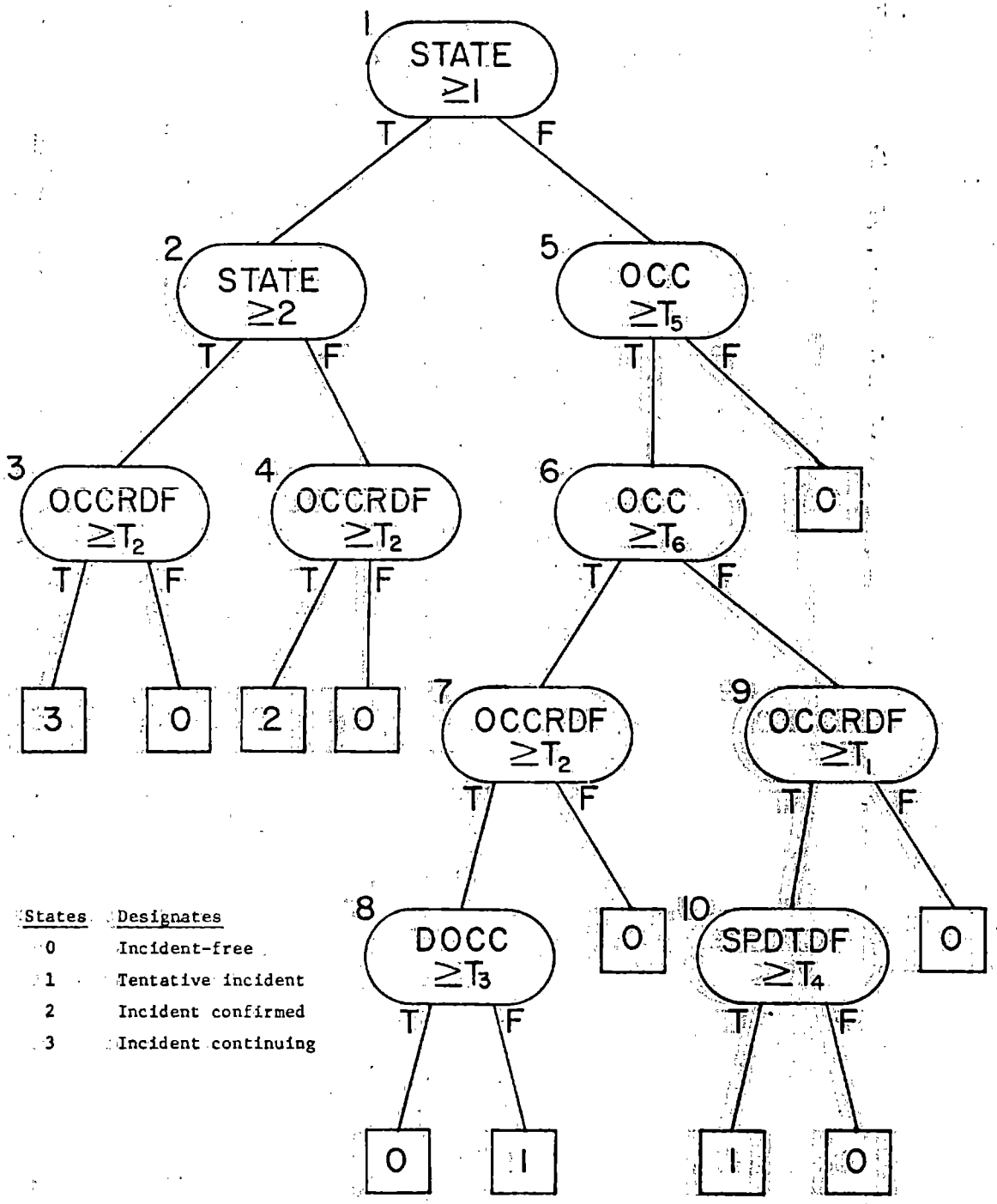

Figure 92. Decision tree for algorithm 10.

Table 116. Coding for Algorithm 10.

Feature No.	Name
1	OCC
2	DOCC
3	OCCRDF
4	SPDTDF
5	State

Decision Node	NTR	Threshold Vector
1	5,2,5	1
2	5,3,4	2
3	3,-3,0	T_2
4	3,-2,0	T_2
5	1,6,0	T_5
6	1,7,9	T_6
7	3,8,0	T_2
8	2,0,-1	T_3
9	3,10,0	T_1
10	4,-1,0	T_4

Table 117. Calibration and evaluation of Algorithm 10 on Los Angeles data base.

$N_I = 49$ $\bar{N}_I = 40$

$N_F = 109{,}090$ $\bar{N}_F = 4{,}650$

Threshold set	Detection rate (%)	False alarm rate (%)	Mean-time-to-detect (minutes)	Thresholds* T_1	T_2	T_3	T_4
1	61	.279	3.88	.319	.340	24.9	.094
2	51	.065	3.59	.450	.310	16.0	.207
3	47	.057	3.73	.497	.353	15.8	.299
4	41	.043	4.98	.612	.451	15.9	.001
5	37	.027	6.57	.553	.510	14.0	.186
6	31	.013	5.07	.449	.588	15.4	.267
7	27	.008	6.36	.720	.588	14.0	.485
8	20	.006	7.93	.620	.676	29.1	.709

*T_5 fixed at 12; T_6 fixed at 25.

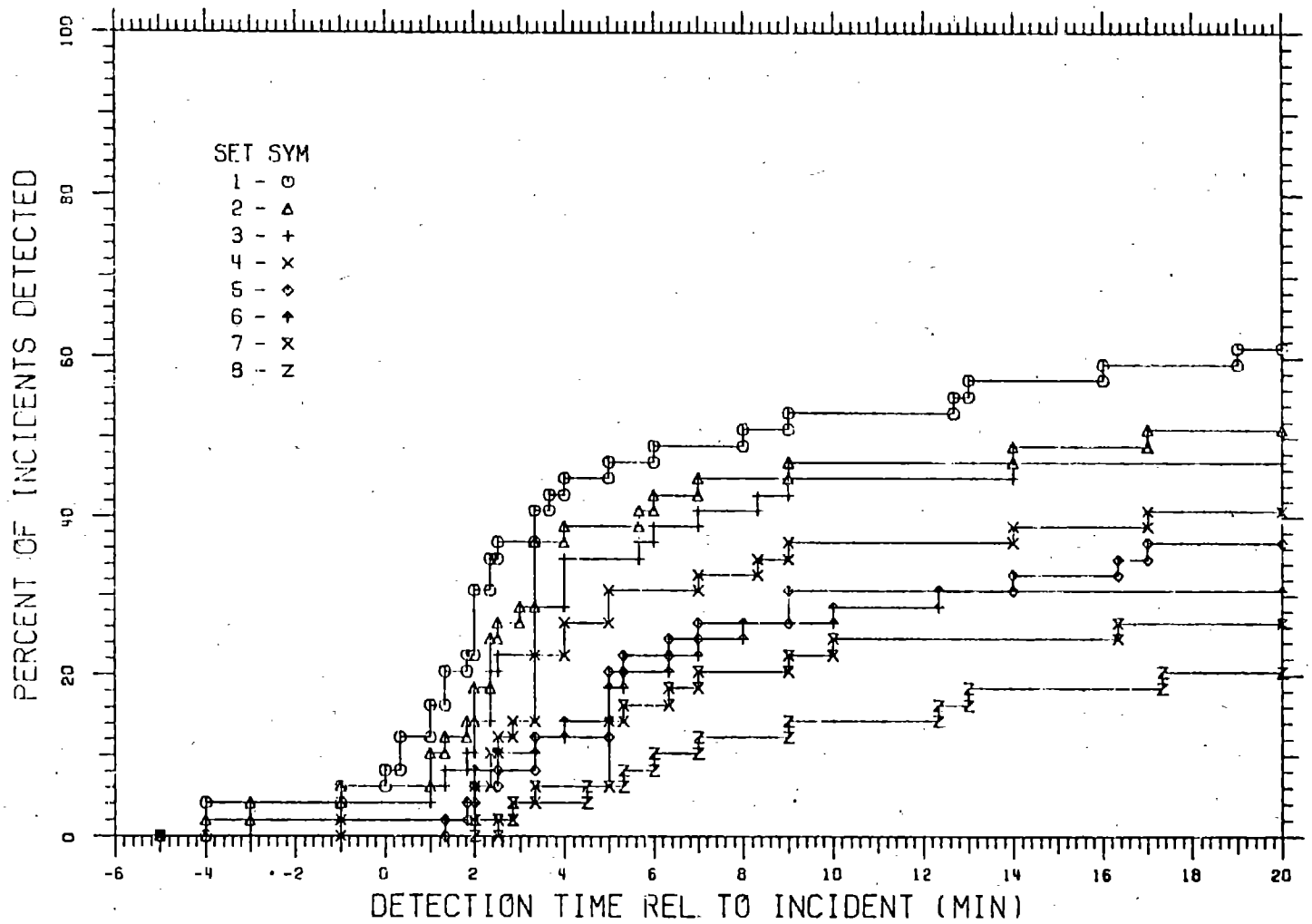

Figure 93. Distribution of times-to-detect for Algorithm 10, Los Angeles data base.

Appendix C

TESTING STATISTICAL SIGNIFICANCE OF DIFFERENCES IN FALSE ALARMS

Preceding page blank

We consider two algorithms with identical detection rates but different false alarm rates. We provide tests for statistical significance of the difference in the false alarms. The basis for the tests is a determination of the probability that two algorithms with identical underlying false alarm rates could have produced, in a finite number of tests, the differences observed.

For the most part, of course, the results of applying two algorithms to data are the same - most tests result in an indication of incident-free conditions. We are particularly interested in those cases for which only one algorithm produced a false alarm, i.e., we exclude from consideration cases for which neither algorithm or both algorithms produced a false alarm. Under the hypothesis that the underlying false alarm rates for the two algorithms are identical, such cases should be equally likely to be associated with each algorithm, i.e., the probability that the first algorithm, say, generated the false alarm for a particular such case is one-half.

Suppose that, of the N such cases, N_1 are associated with the first algorithm, N_2, with the second, and that $N_1 \geq N_2$. The probability that precisely n cases are associated with the first algorithm is given by the Bernoulli distribution with mean one-half, i.e.,

$$p(n) = \binom{N}{n}\left(\frac{1}{2}\right)^N$$

where

$$\binom{N}{n} = \frac{N!}{n!(N-n)!}$$

Then the probability that at least N_1 of the N cases would be associated with one of the algorithms is

$$P(N_1|N) = 2\sum_{n=N_1}^{N} p(n) = 2\sum_{n=N_1}^{N}\binom{N}{n}\left(\frac{1}{2}\right)^N .$$

We say that the difference in the false alarms is significant at the level δ if $\delta \geq P(N_1|N)$.

For large N, $P(N_1|N)$ is well-approximated by the normal distribution. Specifically, for large N,

$$y = \frac{N_1 - \frac{1}{2}N}{\frac{1}{2}\sqrt{N}}$$

is approximately normally distributed, with mean zero and unit standard deviation. Defining

$$F(x) = \frac{1}{\sqrt{2\pi}} \int_{-\infty}^{x} e^{-t^2/2}\, dt \quad ,$$

for large N,

$$P(N_1|N) \approx 1 - F\left(\frac{N_1 - \frac{1}{2}N}{\frac{1}{2}\sqrt{N}}\right)$$

A Simplified Procedure

It is a tedious matter to examine individual cases of false alarms. We now develop a simplified procedure which is based only on false alarm rates and which is conservative, i.e., indicates a level of significance not less than that indicated by the more refined test detailed above.

Suppose we ignore the fact that some false alarms are common cases. Then we can calculate from the false alarm rates, α_1 and α_2, and the total number of incident-free tests, N_F,

$$M_1 = \alpha_1 \cdot N_F/100$$

$$M_2 = \alpha_2 \cdot N_F/100$$

and

$$M = M_1 + M_2$$

and use these in place of the parameters N_1, N_2 and N, respectively. The resultant estimate of the level of significance is conservative. A non-rigorous proof, based on the normal approximation, that this is always the case is easily developed. We need only show that

$$F\left(\frac{M_1 - \frac{1}{2}M}{\frac{1}{2}\sqrt{M}}\right) < F\left(\frac{N_1 - \frac{1}{2}N}{\frac{1}{2}\sqrt{N}}\right)$$

Note that if we designate the number of common false alarm cases by m, then

$$M_1 = N_1 + m$$

$$M_2 = N_2 + m$$

$$M = N + 2m$$

Now

$$\frac{M_1 - \frac{1}{2} M}{\frac{1}{2}\sqrt{M}} = \frac{N_1 + m - \frac{1}{2}[N+2m]}{\frac{1}{2}\sqrt{N + 2m}} = \frac{N_1 - \frac{1}{2} N}{\frac{1}{2}\sqrt{N + 2m}}$$

$$< \frac{N_1 - \frac{1}{2} N}{\frac{1}{2}\sqrt{N}}$$

Montonicity of F yields the desired result.

It is convenient to find an expression in terms of the false alarm rates, as these are directly indicated in tradeoff curves. For this purpose, note that

$$y = \frac{M_1 - \frac{1}{2} M}{\frac{1}{2}\sqrt{M}} = \frac{\alpha_1 - \alpha_2}{\frac{1}{2}\sqrt{(\alpha_1 + \alpha_2)}} \cdot \sqrt{\frac{N_F}{100}}$$

Figures 16 and 17 presented in Section 4.4 provide levels of significance

$$\delta = 2(1 - F(y))$$

for N_F = 45,000 (Minneapolis data base) and N_F = 100,000 (Los Angeles data base), respectively.

GPO 907-289